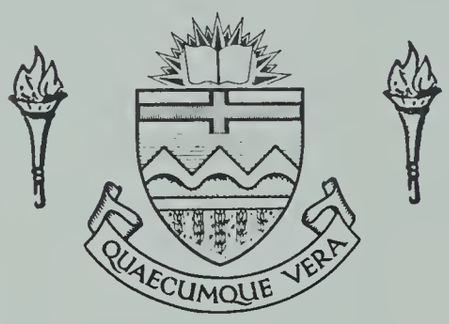
For Reference

NOT TO BE TAKEN FROM THIS ROOM

Ex libris
universitatis
albertaensis



The University of Alberta
Printing Department
Edmonton, Alberta

Digitized by the Internet Archive
in 2020 with funding from
University of Alberta Libraries

https://archive.org/details/Moore1971

THE UNIVERSITY OF ALBERTA

THE SOLUBILITY AND DIFFUSIVITY OF HYDROGEN IN ALIPHATIC AMINES

by



ROBERT GORDON MOORE

A THESIS

SUBMITTED TO THE FACULTY OF GRADUATE STUDIES

IN PARTIAL FULFILMENT OF THE REQUIREMENTS FOR THE DEGREE

OF DOCTOR OF PHILOSOPHY IN CHEMICAL ENGINEERING

DEPARTMENT OF CHEMICAL AND PETROLEUM ENGINEERING

EDMONTON, ALBERTA

SPRING, 1971

UNIVERSITY OF ALBERTA

FACULTY OF GRADUATE STUDIES

The undersigned certify that they have read, and recommend to the Faculty of Graduate Studies for acceptance, a thesis entitled "THE SOLUBILITY AND DIFFUSIVITY OF HYDROGEN IN ALIPHATIC AMINES" submitted by Robert Gordon Moore in partial fulfilment of the requirements for the degree of Doctor of Philosophy.

ABSTRACT

The objectives of this study were: (1) to measure the solubility of hydrogen in ammonia, methylamine, ethylamine, n-propylamine, 1,2-propanediamine and 1,2-ethanediamine and (2) to measure the diffusivity of hydrogen in methylamine.

Solubility data for hydrogen dissolved in ammonia, methylamine, ethylamine and n-propylamine were obtained over the temperature range -70°C to +25°C. Hydrogen solubility data in 1,2-propanediamine and 1,2-ethanediamine were obtained over the temperature range -25°C to +11°C and +25°C to +34°C respectively. The solubility data were obtained at pressures up to 300 psig.

Henry's law was assumed valid for this study and the solubility data were correlated in terms of this law. An equation describing the effect of temperature on Henry's law coefficient was developed for each of the amines considered.

A number of correlations for predicting the solubility of hydrogen in the six amines were reviewed. Those correlations which were derived for polar, nonassociated solvents gave good estimates of the solubility of hydrogen in ethylamine, n-propylamine and 1,2-propanediamine. The predicted hydrogen solubilities in ammonia, methylamine and 1,2-ethanediamine deviated from the experimental values for all the correlations tested.

The measured solubility data were used to extend a correlation proposed by Yen and McKetta. This revised correlation may be used to estimate the solubility of hydrogen in polar, associated amines.

The work described in Part 2 of this project involved the physical absorption of hydrogen in methylamine. This study was conducted in a single sphere absorber and data were obtained over the temperature range $-22^{o}C$ to $-12^{o}C$. An existing mathematical model of the absorption process was utilized for calculating the molecular diffusion coefficients from the rate data.

The accuracy of the diffusion coefficients calculated from the measured rate of hydrogen absorption data is uncertain, as the reliability of the mathematical absorption model is questionable in the allowable range of operating conditions dictated by the requirement of a smooth film on the sphere.

The best estimate of the diffusivity of hydrogen in methylamine at $-20^{o}C$ is $120 \times 10^{-6} \frac{cm.^2}{sec.}$. This value was found to agree, in order of magnitude, with the diffusion coefficients predicted by a number of empirical correlations. However, a firm comparison was not possible due to the uncertainty in the experimental values.

ACKNOWLEDGEMENT

The author wishes to thank Dr. F.D. Otto for his advice and guidance during the course of this study and for his many constructive criticisms and helpful suggestions on the preparation of the manuscript.

Thanks are also due to Mr. Peter Smits and Mr. Harish Kalra for their assistance and advice; to Mr. J. Van Dorn for his guidance on the design of the equipment; to Mr. G.T. Walsh and his staff for their aid in assembling the experimental apparatus; and to the staff of the Fuels and Materials Division of the Atomic Energy of Canada Limited, Chalk River, for their helpful advice.

The author expresses a special thanks to his wife, Carrol, for her encouragement and patience throughout the course of this study.

The financial assistance of the National Research Council and Atomic Energy of Canada Limited is gratefully acknowledged.

TABLE OF CONTENTS

	PAGE
TABLE OF CONTENTS	I
LIST OF TABLES	VI
LIST OF FIGURES	VIII

PART ONE

CHAPTER

1.	INTRODUCTION	1
2.	THEORY	6
	A. Criterion of Equilibrium	6
	B. Ideal Solution Theory	8
	1. General	8
	2. Raoult's Law	10
	3. Ideal Gas Solubility	11
	4. Henry's Law	12
	5. Effect of Temperature on Gas Solubility	14
	6. Effect of Pressure on Gas Solubility	19
	C. Non-Ideal Solution Theory	21
	1. General	21
	2. Regular Solution Theory	25
	3. Other Solution Theories	32
	D. Review of Solubility Coefficients	33
	1. Keunan Coefficient	34
	2. Bunsen Coefficient	35
	3. Ostwald Coefficient	35
	4. Ostwald Coefficient as Used by Horiuti	36
3.	LITERATURE SURVEY	38
	A. Experimental Techniques	38
	B. Available Solubility Data for Hydrogen Dissolved in Liquid Ammonia and Liquid Amines	40
	C. Classification and Nomenclature of Amines	42
	D. Properties of Amines	43

4. EXPERIMENTAL PROCEDURE 48

A. Equipment 48
1. Refrigeration System 48
2. Vacuum System 54
3. Hydrogen Purification Unit 55
4. Amine Purification Unit 55
5. Amine Charge System 55
6. Solubility Cell 56
7. Magnetic Solenoid Pump 57
8. Hydrogen Pre Saturator 62
9. Sampling Section and Sample Cylinder 62
10. Temperature Measurements 63
11. Pressure Measurements 63
12. Solubility Apparatus Valves 63
13. Hydrogen Volumetric Apparatus 64

B. Materials 66

C. Experimental Procedure 67
1. Amine Purification 67
2. Solubility Determinations 69

D. Data Reduction 75

E. Experimental Results 79

F. Reduction of Literature Data on Solubility of Hydrogen in Ammonia 88

5. DISCUSSION OF RESULTS 94

A. The Solubility of Hydrogen in Liquid Ammonia - Comparison of Present Results with Those Tabulated in the Literature 94

B. The Solubility of Hydrogen in Liquid Amines- Comparison of Present Results with Those Calculated from Semi-Empirical Correlations 97

C. General 111

6. CONCLUSIONS AND RECOMMENDATIONS 113

NOMENCLATURE 116

BIBLIOGRAPHY 120

APPENDICES

A1. Experimental Solubility Data

B1. Smoothed Solubility Data

C1. Sample Calculation and Estimation of Errors

D1. Physical Properties

E1. Calibration Data

PART TWO

1. INTRODUCTION 1

2. THEORY 5

A. Hydrodynamic Models of Physical Absorption Processes 5
1. Whitman Film Theory 5
2. Higbie's Penetration Theory 6
3. Danckwerts' Penetration Theory 8
4. Other Surface Renewal Models 10
5. Hydrodynamic Models of Absorption in a Spherical Film 10
(a) Hydrodynamics of the Liquid Film 10
(b) Absorption of a Single Gas in a Liquid Film 10
(1) Lynn, Straatemeier and Kramers 15
(2) Davidson and Cullen 17
(a) Low Depth of Penetration Model 18
(b) High Depth of Penetration Model 19
(3) Olbrich and Wild 21

B. Definition of a Diffusion Coefficient 21

C. Effect of Temperature on Diffusivity 23

D. Effect of Pressure on Diffusivity 24

E. Effect of Concentration on Diffusivity 25

F. Empirical Correlations for Predicting Diffusion Coefficients 25
1. Wilke-Chang Correlation 25
2. Scheibel Correlation 26
3. Sitaraman et al Correlation 26
4. King et al Correlation 26
5. Lusis and Ratcliff Correlation 27

3. LITERATURE SURVEY

A. Experimental Techniques for Measuring Diffusion Coefficients 29
1. Free Diffusional Methods 29

2. Restricted Diffusion Methods 31
3. Steady State Methods 31

B. Experimental Background on the Design of a Single Sphere Absorber 36

C. Experimental Background on the Operation of a Single Sphere Absorber 39

D. Hydrodynamics of the Liquid Film 41

E. Entrance Effects 44

F. Exit Effects 44

G. Interfacial Area Correction Due to the Liquid Film 46

H. Diffusivity Data for Hydrogen Dissolved in Aliphatic Amines 46

4. EXPERIMENTAL APPARATUS AND PROCEDURE 49

A. Description of Apparatus 49
1. Methylamine Feed Tank 52
2. Methylamine Feed System 52
3. Liquid Rotameter 53
4. Liquid Distributor 56
5. Absorption Chamber 57
6. Hydrogen Saturation System 62
7. Outlet Liquid Cooler 64
8. Spent Amine Dump Tank 64
9. Hydrogen Feed System 65
10. Controlled Temperature Chamber 65
11. System Valves 66
12. Temperature Measurement 67
13. Pressure Measurement 67

B. Experimental Procedure 67
1. Methylamine Purification 67
2. Operation of the Single Sphere Absorber 68

C. Data Reduction 71

D. Results 77

5. DISCUSSION OF RESULTS 86

A. Experimental Measurement of Diffusivity 86

B. Comparison of the Experimental Diffusion Coefficients with Estimated Values 89

C. Operating Problems 95
1. Temperature Control 95
2. Measurement of the Methylamine Flow Rate 97
3. Convective Mixing in the Spherical Film 97
4. End Effects 101
5. System Leaks 101
6. Saturation of the Hydrogen Phase 102

D. Operating Characteristics of the Absorber 102
1. Laminar Jet Stability 102
2. Liquid Take-Off Length 103

E. Materials of Construction for Handling Methylamine 105

6. CONCLUSIONS AND RECOMMENDATIONS 106

NOMENCLATURE 111

BIBLIOGRAPHY 115

APPENDICES

A2. Physical Absorption Results

B2. Sample Calculation

C2. Error Analysis

D2. Calibration Section

LIST OF TABLES

TABLE		PAGE
	PART ONE	
1.	Nomenclature for the Amines Considered in This Study	44
2.	Purities of Materials Used in This Study	68
3.	Effect of Temperature on Henry's Law Coefficient - First Degree Fit	86
4.	Effect of Temperature on Henry's Law Coefficient - Best Fit Polynomial	87
5.	Solubility of Hydrogen in Liquid Ammonia - Comparison with Literature Data	95
6.	The Solubility of Hydrogen in Amines at 25°C - Correlation of Prausnitz and Shair	100
7.	Amine Dielectric Constants (25°C) and Dipole Moments	102
8.	The Solubility of Hydrogen in Amines at 25°C - Correlation of Yen and McKetta	104
9.	Amine Polar Characteristic Factors	106
10.	Atomic Parachors	109
11.	The Solubility of Hydrogen in Amines at 20°C - Correlation of Osburn and Markovic	110
	PART TWO	
1.	Coefficients for Series Solution for G. (Olbrich and Wild)	22
2.	Operating Parameters for a Single Sphere Absorber	40
3.	Reynolds Number for Inception of Rippling on a Single Sphere	43
4.	Molecular Diffusion Coefficients for Hydrogen Dissolved in Liquid Ammonia	48
5.	Selected Physical Properties of Hydrogen, Ammonia and Methylamine	89

6.	Diffusion Coefficients for Hydrogen in Ammonia	91
7.	Correction Factors for Diffusion Coefficient Correlations	92
8.	Estimated Diffusion Coefficient for Hydrogen in Methylamine	93
9.	Typical Values of the Dimensionless Flow Parameters	99

LIST OF FIGURES

FIGURE		PAGE
	PART ONE	
1.	Schematic Drawing of the Solubility Apparatus	49
2.	Solubility Cell	51
3.	Schematic Drawing of the Refrigeration System	53
4.	Magnetic Solenoid Pump Valve Cap	58
5.	Schematic Wiring Diagram for the Solenoid Pump	61
6.	Schematic Drawing of Hydrogen Volumetric Apparatus	65
7.	The Solubility of Hydrogen in Ammonia	80
8.	The Solubility of Hydrogen in Methylamine	81
9.	The Solubility of Hydrogen in Ethylamine	82
10.	The Solubility of Hydrogen in n-Propylamine	83
11.	The Solubility of Hydrogen in 1,2-Propanediamine	84
12.	The Solubility of Hydrogen in 1,2-Ethanediamine	85
13.	Polar Characteristic Factors	108
	PART TWO	
1.	Cross Section of Sphere and Liquid Film	10
2.	Schematic Diagram of Single Sphere Absorber	50
3.	Rotameter Viscosity Correction Table	56
4.	Liquid Distributor	58
5.	Schematic Diagram of Absorption Chamber	59
6.	Absorber Base Flange and Take-Off Tube	61
7.	Absorber Top Flange and Laminar Jet	63
8.	Rate of Absorption of Hydrogen in Methylamine at -17°C on the 3/4 Inch Sphere	78

9. Rate of Absorption of Hydrogen in Methylamine at -15°C on the 3/4 Inch Sphere 79

10. Rate of Absorption of Hydrogen in Methylamine at -13°C on the 3/4 Inch Sphere 80

11. Rate of Absorption of Hydrogen in Methylamine at -21°C on the 3/4 Inch Sphere (Kalra (87)) 81

12. Rate of Absorption of Hydrogen in Methylamine at -20°C on the 1 Inch Sphere 82

13. Effect of Temperature on the Diffusivity of Hydrogen in Methylamine 84

14. Effect of Temperature on the Diffusivity of Hydrogen in Ammonia and Methylamine 96

15. Effect of Take-Off Length on Hydrogen Absorption Rate 104

PART ONE

THE SOLUBILITY OF HYDROGEN IN ALIPHATIC AMINES

1. INTRODUCTION

The demand for heavy water has increased rapidly in recent years due to a growing interest in heavy water moderated nuclear reactors as a means of producing electricity. The Canadian nuclear program is based entirely on heavy water moderated reactors which are fuelled by natural uranium, and it is estimated that Canada will require 16,300 tons of heavy water by 1985[1]. The total world's requirement is projected to be 63,300 tons[1] by 1985. As the total world's inventory is currently 4,500 tons[1] and the price of heavy water is set at thirty dollars (U.S.) per pound[2], a strong incentive exists for the development of economic heavy water production processes.

The most attractive processes for large scale heavy water production are based on chemical exchange reactions. Excellent reviews of proposed and existing isotopic exchange reactions have been compiled by Atomic Energy of Canada Limited[3,4,5].

The isotopic exchange reaction which occurs when a hydrogenated liquid LH_n is in equilibrium with a gas GH_m is represented by the general equation

$$LH_n + GH_{m-1}D \underset{k_2}{\overset{k_1}{\rightleftharpoons}} LH_{n-1}D + GH_m \qquad [1.1]$$

This exchange reaction occurs in the liquid phase.

The isotopic exchange of deuterium between gaseous hydrogen sulfide and liquid water is the only exchange process which has been used for large scale heavy water production. This process is known as the GS (Girdler-Sulfide) process[6,7]:

$$H_2O + HDS \underset{k_2}{\overset{k_1}{\rightleftharpoons}} H_2S + HDO \qquad [1.2]$$

A relatively new process, based on the exchange of deuterium between gaseous hydrogen and liquid ammonia in the presence of a homogeneous potassium amide catalyst, has shown potential as an economic competitor of the GS process:

$$NH_3 + HD \underset{k_2}{\overset{k_1}{\rightleftharpoons}} NH_2D + H_2 \qquad [1.3]$$

A prototype H_2/NH_3 plant of 28 tons of D_2O per year capacity is operating in France[8]. This is a monothermal process and is operated in conjunction with a 330 ton per day ammonia synthesis plant.

The main advantage of the hydrogen-ammonia process over the hydrogen-sulfide water process is that the separation factors are larger and are more temperature dependent. The hydrogen-ammonia system can operate at temperatures down to -77°C, whereas the hydrogen sulfide-water process is limited by hydrate formation to cold tower temperatures of +30°C.

The H_2/NH_3 process suffers the disadvantages that a homogeneous catalyst is required, the vapor pressure of ammonia is much greater than that of water and the solubility of hydrogen in liquid ammonia is much lower than the solubility of hydrogen sulfide in water.

A potential improvement over the hydrogen-ammonia exchange may be realized by substituting an aliphatic amine for the ammonia. Aliphatic amines have a lower vapor pressure than ammonia and a study by Bar-Eli and Klein[9] found that the rate of exchange of deuterium

between hydrogen and methylamine or ethylamine was from five to thirty times faster than the corresponding exchange in ammonia. The work of Bar-Eli and Klein[9] was carried out in a shaken flask reactor and the interfacial area of transfer is not recorded. It is therefore impossible to interpret, from their data, the effect of the chemical reaction on the overall transfer rate. The hydrogen-amine exchange is catalyzed by the alkali-substituted amide of the corresponding amine[9].

Two obvious disadvantages of a hydrogen-amine exchange process as opposed to the hydrogen-ammonia system should be noted. Amines are three to twenty times as expensive as ammonia and they have a much larger molecular weight to exchangeable hydrogen ratio. The raw material and equipment handling costs are therefore increased. Also, it should be noted that at present ammonia and amine systems both face a temporary drawback because of the lack of large hydrogen sources. However, these sources will develop as greater volumes of hydrogen are used for ammonia synthesis, space flights and hydrogenation of petroleum products.

To evaluate the economic feasibility of amine-hydrogen exchange reactions as possible heavy water production processes, a fundamental study of the factors affecting the exchange reactions was undertaken by Atomic Energy of Canada Limited. The work reported here represents a portion of that performed under a contract awarded by A.E.C.L. to Dr. F.D. Otto of the Department of Chemical and Petroleum Engineering, The University of Alberta.

The first phase of this project involved the measurement of

hydrogen solubilities in a group of amines which are felt to have economic potential as possible exchange candidates. The economic criteria used in making this selection were low volatility and high exchangeable hydrogen to total weight ratio. The amines chosen were methylamine, ethylamine, n-propylamine, 1,2-propanediamine and 1,2-ethanediamine.

The determination of hydrogen solubilities in the various amines was chosen for the first project as solubility data are required for interpreting further mass transfer studies. In addition, the solubility of hydrogen in a given amine is an important factor for assessing the economic potential of that amine. The exchange rate associated with a particular amine is directly proportional to the hydrogen deuteride solubility (the solubility of hydrogen deuteride in an amine is assumed to equal the solubility of hydrogen in the same amine). As the physical tower size is closely related to the exchange rate, the capital cost involved in building a full scale hydrogen-amine exchange process is dependent on the hydrogen solubility.

The experimental apparatus developed for this study is designed to complement the long range program for measuring amine properties. The complete solubility apparatus may be used for measuring the solubility of hydrogen in amine solutions containing the alkali-substituted amide catalyst. Kinetic equilibrium studies can be performed in the solubility cell as the cell is equipped for continuous circulation of the hydrogen phase. The auxiliary equipment, such as the refrigeration unit, vacuum system and the hydrogen and amine

purification systems, is designed to handle the requirements of a single sphere absorber study and a bubble column study.

Several empirical or semi-empirical correlations are available for predicting the solubility of gases in liquids. A number of these theories have been reviewed in order to ascertain their validity for estimating the solubility of hydrogen in the amines considered in this project.

2. THEORY

The solubility of gases in liquids is described by the thermodynamic equations of phase equilibrium. A number of solution models based on the principle that the liquid phase and vapor phase are in equilibrium have been developed to describe the solubility process. These models differ according to the assumptions used in their derivation. In order to interpret solubility data according to a solution model, it is necessary to understand these underlying assumptions.

The following review presents a discussion of the thermodynamics of phase equilibrium as applied to the solubility of gases in liquids. Various solution models of interest to this study are discussed and also a number of correlations for predicting gas solubilities in liquids are considered.

A. Criterion of Equilibrium

A system is said to be at equilibrium when there is no detectable change in system properties with respect to time. In a closed system consisting of several phases, each of which is at the same temperature and pressure, the thermodynamic criterion of equilibrium is that the free energy change is zero:

$$dF = 0 \qquad [2.1]$$

This law was first deduced by Gibbs[10] in terms of a quantity which he called "the chemical potential". In terms of the chemical potential, equation [2.1] becomes

$$\mu_i' = \mu_i'' = \mu_i''' = \ldots \qquad [2.2]$$

where the subscript i refers to a particular component and the primes refer to the different phases. The chemical potential of a component in a mixture is equivalent to its partial molal free energy:

$$\mu_i = \bar{F}_i \qquad [2.3]$$

The chemical potential of a component is an abstract quantity and somewhat inconvenient to use. G.N. Lewis[11] introduced a related variable known as "fugacity" which is a measure of the thermodynamic escaping tendency of the component. Fugacity can be thought to be an effective gas pressure which has been corrected for deviations from the ideal gas law. The chemical potential and fugacity of a component are related by the following equation:

$$\mu_i = \mu_i^\circ + RT \ln f_i \qquad [2.4]$$

in which the coefficient μ_i° is a function of the temperature and the pure component properties at some reference state. Substituting equation [2.4] into equation [2.2] yields the criterion of equilibrium in terms of fugacity:

$$f_i' = f_i'' = f_i''' \qquad [2.5]$$

For a two phase system as studied in this work, equation [2.5] becomes:

$$f_i^V = f_i^L \qquad [2.6]$$

Therefore, a liquid phase and a vapor phase are in thermodynamic equilibrium when the temperatures of the two phases are equal and when the fugacity of each component in the liquid phase is equal to the fugacity of the same component in the vapor phase.

The fugacity of a component in the vapor phase is related to the

temperature, total pressure, and composition by the following relationship:

$$f_i^V = \phi_i \, y_i \, \pi \qquad [2.7]$$

The liquid phase fugacity is given by:

$$f_i^L = \gamma_i \, x_i \, f_i^{\circ L} \qquad [2.8]$$

The general equation for equilibrium in a two phase (liquid and vapor) system is obtained upon substituting equations [2.7] and [2.8] into equation [2.6]:

$$\phi_i \, y_i \, \pi = \gamma_i \, x_i \, f_i^{\circ L} \qquad [2.9]$$

In order that equation [2.9] may be applied to actual systems, various assumptions concerning the nature of the parameters must be made. The assumptions of interest to this work are discussed in the following pages.

B. Ideal Solution Theory

1. General:

An ideal solution as defined by Hildebrand and Scott[12] is "one in which the activity equals the mole fraction over the entire composition range and over a nonzero range of temperatures and pressures":

$$a_i = \frac{f_i^L}{f_i^{\circ L}} = x_i \quad (0 \leq x_i \leq 1) \qquad [2.10]$$

On comparing equation [2.10] with equation [2.8], it can be seen that for an ideal solution the activity coefficient of the i^{th} component is equal to unity:

$$\gamma_i = 1 \quad (0 \leq x_i \leq 1) \qquad [2.11]$$

The change in free energy associated with the transfer of a mole of component i from pure liquid to an ideal solution is given by:

$$\bar{F}_i - F_i^\circ = RT \ln a_i = RT \ln x_i \qquad [2.12]$$

Hence, the total free energy change when two components form an ideal solution is:

$$\Delta F^m = RT(n_1 \ln x_1 + n_2 \ln x_2) \qquad [2.13]$$

The entropy change on formation of a two component ideal solution is obtained upon differentiating equations [2.12] and [2.13] with respect to temperature when the system pressure and concentration are assumed constant:

$$\bar{S}_i - S_i^\circ = - \left[\frac{\partial[\bar{F}_i - F_i^\circ]}{\partial T}\right]_{\pi,x} = -R \ln x_i \qquad [2.14]$$

For a two component system:

$$\Delta S^m = - \left[\frac{\partial[\Delta F^m]}{\partial T}\right]_{\pi,x} = -R(n_1 \ln x_1 + n_2 \ln x_2) \qquad [2.15]$$

The heat of mixing may be calculated from equations [2.13] and [2.15] since at constant temperature:

$$\Delta H^m = \Delta F^m + T\Delta S^m = 0 \qquad [2.16]$$

The volume change on mixing is, from equation [2.12]:

$$\Delta v^m = \bar{v}_i - v_i^\circ = \left[\frac{\partial[\bar{F}_i - F_i^\circ]}{\partial \pi}\right]_{T,x} = 0 \qquad [2.17]$$

Hence

$$\Delta v^m = 0 \qquad [2.18]$$

Therefore an ideal solution is one in which there is no change in volume and no heat of mixing when pure components are mixed at constant temperature and pressure. The theory implies that there is no solute-solvent interaction due to differences in intermolecular forces of attraction and repulsion or to differences in molecular volume.

2. Raoult's Law:

The general equation of equilibrium (equation [2.9]) for a system in which the liquid phase may be assumed as an ideal solution is:

$$\phi_i \, y_i \, \pi = x_i \, f_i^{\circ L} \qquad [2.19]$$

The reference fugacity ($f_i^{\circ L}$) for the i^{th} pure liquid component is given by[13]:

$$f_i^{\circ L} = P_i^s \, \phi_i^s \exp \int_{P_i^s}^{\pi} \frac{v_i^L \, d\pi}{RT} \qquad [2.20]$$

If the saturated vapor of the component behaves as an ideal gas, then $\phi_i^s = 1$. When the total system pressure is low, the exponential correction or Poynting correction is negligible. The reference fugacity is therefore equal to the saturation pressure of the component:

$$f_i^{\circ L} = P_i^s \qquad [2.21]$$

If the further assumption of ideal gas behavior of the vapor phase in equilibrium with the solution is made, $\phi_i = 1$ in equation [2.19]. Substituting equation [2.21] into equation [2.19] yields

Raoult's law[14,15]:

$$y_i \pi = P_i = x_i P_i^s \qquad [2.22]$$

3. Ideal Gas Solubility:

If Raoult's law is assumed to describe a binary solution consisting of a noncondensable solute and a sub-critical liquid solvent, then for the gaseous solute equation [2.22] becomes:

$$P_2 = x_2 P_2^s \qquad [2.23]$$

The saturation pressure P_2^s of the noncondensable component is found by extrapolating the vapor pressure of the component above its critical temperature. The usual extrapolation procedure involves plotting the logarithm of pressure versus the reciprocal absolute temperature. This method is used for convenience and does not have any physicochemical basis.

This procedure for predicting the saturation pressure for a hypothetical liquid dictates that for a constant partial pressure the solubility of all gases must decrease with increasing temperature. While this is true for most gases, hydrogen is a notable exception. Another obvious drawback of this theory is that it predicts that the solubility of a gas is independent of the solvent.

The ideal solubility theory does, however, give a good estimate of the order of magnitude of the gas solubility. The ideal gas solubility for hydrogen at 1 atm. hydrogen partial pressure is listed by Prausnitz[13] and Hildebrand and Scott[16] to be 8×10^{-4} mole fraction. Grilly[17] has stated that the ideal solubility of

hydrogen at 1 atm. is 25×10^{-4} mole fraction, while Gonikberg[18] presented a value of 65×10^{-4} mole fraction based on the heat of vaporization of hydrogen at 20°C. The ideal solubility of hydrogen as stated by Prausnitz and Hildebrand would appear to be the more plausible value. However, the scatter in the above values indicates the difficulty in obtaining a good value of the hypothetical liquid saturation pressure.

4. Henry's Law:

For a large number of binary solutions involving a gaseous solute and liquid solvent, ideal solution theory may be assumed at very low solute concentrations. Writing equation [2.10] for the liquid solvent:

$$a_1 = \frac{f_1}{f_1^{\circ L}} = x_1 \quad (x_1 \to 1; \quad x_2 \to 0) \qquad [2.24]$$

From equation [2.24] it can be seen that:

$$\frac{\partial \ln a_1}{\partial \ln x_1} = \frac{\partial \ln f_1^{L}}{\partial \ln x_1} = 1 \qquad [2.25]$$

Substituting equation [2.25] into the "Gibbs-Duhem" equation

$$\frac{\partial \ln f_1^{L}}{\partial \ln x_1} - \frac{\partial \ln f_2^{L}}{\partial \ln x_2} = 0 \qquad [2.26]$$

one obtains

$$\frac{\partial \ln f_2^{L}}{\partial \ln x_2} = 1 \qquad [2.27]$$

Integrating the above equation [2.27] gives

$$\ln f_2^L = \ln x_2 + \ln H_2$$

$$f_2^L = H_2 x_2 \qquad [2.28]$$

where H_2 is a constant of integration. If the vapor phase in equilibrium with the solution is assumed to behave as an ideal gas, then from equation [2.9]

$$P_2 = H_2 x_2 \qquad [2.29]$$

which is the form of Henry's law[19]. Henry's law has been found to give excellent approximations when the solubility and partial pressure of the solute are not large. The actual range of applicability is a function of the solvent and solute. Prausnitz[13] gives a rough estimate of 5 to 10 atm. solute partial pressure or approximately 3 mole percent solute concentration in the liquid. Himmelblau[20] states that the solubility of hydrogen in water will obey Henry's law up to a pressure of 100 atmospheres.

Comparing equation [2.28] with equation [2.8], one can see the thermodynamic significance of Henry's law coefficient:

$$f_2^L = H_2 x_2 = \gamma_2 x_2 f_2^{\circ L} \qquad [2.30]$$

$$H_2 = \gamma_2 f_2^{\circ L}$$

The standard state fugacity $f_2^{\circ L}$ depends only on the reference pressure and system temperature. The Henry's law coefficient H_2 is not a function of composition, hence the activity coefficient γ_2 must be concentration independent. Henry's law may be assumed to be valid, therefore, so long as the activity coefficient of the solute is constant. This means that Henry's law can be applied to nonideal

solutions for which the solute concentration is sufficiently dilute. It can be seen from the Gibbs-Duhem equation [2.26] that as long as Henry's law is assumed to apply to a certain degree of approximation, then Raoult's law must apply to the same degree.

5. Effect of Temperature on Gas Solubility:

Hildebrand and Scott[12] relate the temperature coefficient of solubility to the gaseous solute entropy of solution $(\bar{S}_2 - S_2^g)$ using the relationship:

$$\bar{S}_2 - S_2^g = - \left[\frac{\partial[\bar{F}_2 - F_2^g]}{\partial T}\right]_{P,x} \qquad [2.32]$$

The right hand term in equation [2.32] can be transformed using the exact mathematical relationship[21]

$$\left(\frac{\partial x}{\partial z}\right)_y = - \left(\frac{\partial x}{\partial y}\right)_z \left(\frac{\partial y}{\partial z}\right)_x$$

Hence equation [2.32] becomes

$$\bar{S}_2 - S_2^g = + \left[\frac{\partial[\bar{F}_2 - F_2^g]}{\partial \ln x_2}\right]_{P,T} \left(\frac{\partial \ln x_2}{\partial T}\right)_{(\bar{F}_2 - F_2^g),P} \qquad [2.33]$$

where $\left(\frac{\partial \ln x_2}{\partial T}\right)_{(\bar{F}_2 - F_2^g),P}$ is the temperature coefficient of solubility.

The free energy change when a gas at its standard state is dissolved in a solvent is

$$\bar{F}_2 - F_2^g = RT \ln a_2^g \qquad [2.34]$$

where a_2^g is defined as:

$$a_2^g = \frac{f_2^L}{f_2^{\circ g}} \qquad [2.35]$$

Therefore, the first term on the right hand side of equation [2.33] becomes

$$\left[\frac{\partial[\bar{F}_2 - F_2^g]}{\partial \ln x_2}\right]_{P,T} = RT \left(\frac{\partial \ln a_2^g}{\partial \ln x_2}\right)_{P,T} \qquad [2.36]$$

Substituting equation [2.36] into equation [2.33] yields

$$(\bar{S}_2 - S_2^g) = RT \left(\frac{\partial \ln a_2^g}{\partial \ln x_2}\right)_{P,T} \left(\frac{\partial \ln x_2}{\partial T}\right)_{(\bar{F}_2 - F_2^g),P} \qquad [2.37]$$

If the solvent is assumed to be non-volatile such that the gas phase is pure solute at a partial pressure of 1 atmosphere, then

$$f_2^V = f_2^{\circ g} \qquad [2.38]$$

At equilibrium, the fugacity of the gaseous solute is the same in both the liquid and vapor phase:

$$f_2^L = f_2^V = f_2^{\circ g} \qquad [2.39]$$

Substituting equations [2.39] and [2.35] into equation [2.34] yields

$$\bar{F}_2 - F_2^g = RT \ln \frac{f_2^{\circ g}}{f_2^{\circ g}} = 0 \qquad [2.40]$$

which satisfies the constraint of a constant free energy change in equation [2.33].

If Henry's law is assumed to apply,

$$f_2^L = H_2 x_2 \qquad [2.28]$$

then

$$a_2^g = \frac{f_2^L}{f^{\circ g}} = \frac{H_2 x_2}{f^{\circ g}} = K x_2 \qquad [2.41]$$

where

$$K = \frac{H_2}{f^{\circ g}} \qquad [2.42]$$

and

$$\left(\frac{\partial \ln a_2^g}{\partial \ln x_2}\right)_{P,T} = 1 \qquad [2.43]$$

Substituting equation [2.43] into equation [2.37] and neglecting the subscript for constant free energy change yields the desired equation:

$$\bar{S}_2 - S_2^g = RT \left(\frac{\partial \ln x_2}{\partial T}\right)_P = R \left(\frac{\partial \ln x_2}{\partial \ln T}\right)_P \qquad [2.44]$$

The temperature coefficient of solubility may also be related to the enthalpy of solution. At equilibrium

$$\bar{F}_2 = F_2^g \qquad [2.45]$$

hence

$$\bar{h}_2 - T\bar{S}_2 = h_2^g - TS_2^g \qquad [2.46]$$

which upon rearranging becomes

$$\bar{h}_2 - h_2^g = T(\bar{S}_2 - S_2^g) = RT^2 \left(\frac{\partial \ln x_2}{\partial T}\right)_P \qquad [2.47]$$

Equation [2.47] is usually written in the form

$$\bar{h}_2 - h_2^g = -R \left[\frac{\partial \ln x_2}{\partial (1/T)}\right]_P \qquad [2.48]$$

Sherwood and Prausnitz[22] have derived equation [2.44] and [2.48] without making the very stringent assumption of a non-volatile solvent. They have shown the above equations to be valid when the vapor phase density is low.

When the solute partial pressure is 1 atmosphere, and the vapor phase is assumed to behave as an ideal gas, Henry's law becomes:

$$P_2 = H_2 x_2 = 1 \qquad [2.49]$$

hence

$$x_2 = 1/H_2 \qquad [2.50]$$

Substituting equations [2.50] into equations [2.44] and [2.48] gives the effect of temperature on Henry's law coefficient as presented by Denbigh[23]:

$$(\bar{S}_2 - S_2^g) = -R \left[\frac{\partial \ln H_2}{\partial \ln T}\right]_P \qquad [2.51]$$

$$(\bar{h}_2 - h_2^g) = R \left[\frac{\partial \ln H_2}{\partial (1/T)}\right]_P \qquad [2.52]$$

The equations relating the temperature coefficient of solubility to either the entropy of solution or enthalpy of solution of the solvent offer a means of plotting Henry's law coefficient versus temperature. Hildebrand[12] prefers to plot $\ln x_2$ versus $\ln T$ while Himmelblau[20] plots $\ln H_2$ versus $1/T$ to conform to the "van't Hoff" type equation.

Equations [2.44] and [2.48] may be expanded to provide a qualitative estimate of the effect of an increase in temperature on the gas solubility. Consider equation [2.44] written in the following form:

$$\bar{S}_2 - S_2^g = (\bar{S}_2 - S_2^H) + (S_2^H - S_2^g) = RT \left(\frac{\partial \ln x_2}{\partial T}\right)_P \qquad [2.44]$$

where S_2^H is the entropy per mole of the solute considered as a hypothetical pure liquid at the temperature of the solution. The first term on the right hand side is the partial molal entropy of mixing associated with the dissolution of the condensed solute in the liquid solvent. Assuming ideal mixing, this term is given by equation [2.14]:

$$\bar{S}_2 - S_2^H = -R \ln x_2 \qquad [2.53]$$

The second term $(S_2^H - S_2^g)$ represents the entropy change upon condensation of the pure gas to a hypothetical liquid. This term should always be negative as the entropy of the solute in the liquid state is always less than in the pure gas state.

The mole fraction of solute in a given solvent is always less than unity, hence $(\bar{S}_2 - S_2^H)$ is always positive. The smaller the mole fraction, the larger the value of $\ln x_2$, hence the more positive the value of $-R \ln x_2$. If the value of x_2 is such that the entropy of solution is positive, the solubility of the component will increase with rising temperature.

An analogous argument may be applied to the enthalpy of mixing

term. This has been done by Prausnitz[13].

6. Effect of Pressure on Gas Solubility:

Henry's law coefficient has been shown to be independent of composition (equation [2.31] and [2.48]). Experimental data have shown the coefficient to be mildly dependent on pressure also. This dependence can be neglected if the pressure is not large but must be considered at elevated pressures. Kirchevsky and Kasarnovsky[24] and Dodge and Newton[25] independently derived the thermodynamic equations describing the pressure dependence. The effect of pressure on the liquid phase fugacity is given by:

$$\left(\frac{\partial \ln f_2^L}{\partial P}\right)_{T,x} = \frac{\bar{v}_2}{RT} \qquad [2.54]$$

Substituting equation [2.28] into equation [2.54] gives

$$\left(\frac{\partial \ln H_2}{\partial P}\right)_{T,x_2 \to 0} = \frac{\bar{v}_2^{\infty}}{RT} \qquad [2.55]$$

Integrating equation [2.55] from some reference pressure (usually the saturation pressure of the solvent) to the total system pressure yields:

$$\ln(H_2)^{\pi} - \ln(H_2)^{Pr} = \int_{Pr}^{\pi} \frac{\bar{v}_2^{\infty} dP}{RT} \qquad [2.56]$$

Henry's law still applies at the total pressure π:

$$(H_2)^{\pi} = \frac{f_2}{x_2} \qquad [2.57]$$

At conditions far below the critical temperature of the solvent it is reasonable to assume $\bar{v}_2^{\infty}$ to be independent of pressure. Hence equation [2.56] becomes:

$$\ln \frac{f_2}{x_2} = \ln(H_2)^{Pr} + \frac{\bar{v}_2^{\infty} (\pi - Pr)}{RT} \qquad [2.58]$$

which is known as the Krichevsky-Kasarnovsky equation. Various authors[13,20,26,27] have used this equation for correlating solubility data up to 1,000 atmospheres.

The Krichevsky-Kasarnovsky equation may be extended to include those solutions for which the activity coefficient is no longer constant. If the two suffix Margules equation is assumed to describe the activity coefficient of the solvent under its saturation vapor pressure,

$$\ln \gamma_1 = \frac{A}{RT} x_2^2 \qquad [2.59]$$

then the activity coefficient for the solute, γ_2^*, normalized according to the unsymmetric convention, is found from the Gibbs-Duhem equation to be

$$\ln \gamma_2^* = A/RT(x_1^2 - 1) \qquad [2.60]$$

where A is a constant.

An analogous derivation to that presented for the Krichevsky-Kasarnovsky equations yields the Krichevsky-Ilinskaya equation[28]:

$$\ln \frac{f_2}{x_2} = \ln(H_2)^{Pr} + \frac{A}{RT}(x_1^2 - 1) + \frac{\bar{v}_2^{\infty} (\pi - Pr)}{RT} \qquad [2.61]$$

The above equation has a wider range of applicability than that of Krichevsky and Kasarnovsky[24] and has been used by Orentlicher and Prausnitz[29] to correlate hydrogen solubilities in cryogenic solutions where the mole fraction hydrogen may be as large as 20 percent.

C. Non-Ideal Solution Theory

1. General:

The ideal solution concept is a convenient fictional approach to real solution theory and may be considered as a first approximation to the actual state. Deviations from ideal solution behavior may be caused by "physical" forces acting between the molecules of the various components present in the solution or they may be due to "chemical" interactions which result in the formation of a new molecular species. Dolezalek[3] attempted to correlate departures from ideality in terms of chemical reactions between either like or unlike molecules. He postulated that Raoult's law was obeyed for each species present in the solution and the problem was to identify the type and quantity of the various species. This treatment resulted in an oversimplified model for the solution and later investigators have tended to separate the effect of physical and chemical interactions.

Non-ideal solution behavior in solutions of nonelectrolytes is attributed to one or more of the following causes:

(a) Difference in molar volumes of the components. This deviation may be adequately accounted for by using volume fractions rather than mole fractions when calculating the properties of the mixture.

(b) London dispersion forces. London[31,32,33,34] has shown that interactions between the molecules of a solution are caused by the mutual perturbation of the rapidly moving electrons. The instantaneous dipoles which form tend to oscillate in synchronism causing mutual attraction between the component molecules. These forces are short range, additive, non-specific and temperature independent[35].

(c) Dipolar attraction. Electrostatic forces between two permanent dipoles, a permanent dipole and an induced dipole, and a permanent dipole and an ion may cause significant deviations from ideal solution behavior. The interaction energy associated with any one of the above forces is a function of the relative orientation of the permanent dipole or dipoles, the molecular geometry of the interacting molecules and the dipole moment magnitudes. The presence of a polar component may either enhance or reduce the solute solubility as compared to that predicted from ideal solution behavior.

(d) Association. The permanent dipole of a molecule in which hydrogen occurs linked to N, O or F atoms exerts a far greater influence upon another dipole than would be predicted from the magnitude of the dipole itself. This has been attributed to the formation of a hydrogen bond between a hydrogen atom attached to an electronegative atom and an electronegative atom of another molecule. Compounds capable of hydrogen bonding are usually classified as "associated". The term association refers to the aggregation of atoms or molecules into larger units, the forces holding these units together being weaker than those involved in the formation of an ordinary chemical bond.

As associated liquids tend to form weak polymers, they may exist in solution as monomers, dimers, etc. Also, formation of hydrogen bonds interferes with the free rotation of individual molecules, causing a change in the thermodynamic properties of the solution.

If only the liquid solvent is capable of association, then a positive deviation from Raoult's law (reduction in solubility from that of an ideal solution) of the solute will occur. If both the solvent and solute are capable of association, enhanced solubility may occur.

(e) Chemical interactions. The solubility of carbon dioxide or sulfur dioxide in water does not obey Henry's law as the dissolution process is accompanied by the ionization of the solute. As Henry's law accounts for the effect of pressure on the molecular species only, a correction must be applied for that portion of the solute which is in the ionized state. Prausnitz[13] has presented an equation for correlating data on solutions containing an ionized solute.

The solubility of carbon dioxide in aromatic hydrocarbons such as benzene and toluene is enhanced due to Lewis acid-base interaction. A Lewis acid[36] is any substance able to accept without activation energy a lone pair of electrons from another molecule designated as a base. Examples of Lewis acids are I_2, SO_2, CO_2 and BF_3. Typical Lewis bases include ketones, aromatics, esters, olefins, ammonia, and alkyl iodides and sulfides.

(f) Quantum effects. The solubility of hydrogen, helium and neon

is enhanced due to quantum effects[12]. Special consideration must be given these gases when a predictive technique is used to estimate their solubility in a given solvent.

The thermodynamic equations describing a non-ideal solution may be developed in an analogous manner to those of an ideal solution.

The activity of a non-ideal solution is defined as:

$$a_i = \frac{f_i^L}{f_i^{\circ L}} = \gamma_i x_i \qquad (0 \leq x_i \leq 1) \qquad [2.62]$$

The change in free energy of each component when a non-ideal solution is formed is given by:

$$\Delta\bar{F}_i = \bar{F}_i - F_i^\circ = RT \ln a_i = RT \ln x_i + RT \ln \gamma_i \qquad [2.63]$$

Hence, the free energy change per mole of solution when two components are mixed is:

$$\Delta F^m = RT(x_1 \ln x_1 + x_2 \ln x_2) + RT(x_1 \ln \gamma_1 + x_2 \ln \gamma_2) \qquad [2.64]$$

It can be seen from equation [2.13] that the first term on the right hand side of equation [2.64] is the ideal free energy of mixing. The second term represents the "excess" free energy due to non-ideal mixing:

$$\Delta F^E = RT(x_1 \ln \gamma_1 + x_2 \ln \gamma_2) \qquad [2.65]$$

$$\Delta\bar{F}_1^E = RT \ln \gamma_1 \qquad [2.66]$$

$$\Delta\bar{F}_2^E = RT \ln \gamma_2 \qquad [2.67]$$

The excess entropy, enthalpy and volume due to non-ideal mixing are[12]:

$$\Delta\bar{S}_i^E = \bar{S}_i - \bar{S}_i^i = -R \left(\frac{\partial \ln \gamma_i}{\partial \ln T}\right)_{P,x} \qquad [2.68]$$

$$\Delta\bar{h}_i^E = \bar{h}_i - \bar{h}_i^i = RT^2 \left(\frac{\partial \ln \gamma_i}{\partial T}\right)_{P,x} \qquad [2.69]$$

$$\Delta\bar{V}_i^E = \bar{V}_i - \bar{V}_i^i = RT \left(\frac{\partial \ln \gamma_i}{\partial P}\right)_{T,x} \qquad [2.70]$$

It can be observed that the excess enthalpy and volume change on mixing are equal to the actual function changes, since the enthalpy and volume changes on formation of an ideal solution are zero.

It should also be noted that the equations of the preceeding section were developed for sub-critical components. These equations will only apply to a noncondensable component when it is assumed to be in the form of a hypothetical liquid. For this reason, only the symmetric convention for normalization of the activity coefficients has been used.

2. Regular Solution Theory

Hildebrand and Scott[12] define a regular solution as one involving no entropy change when a small amount of one of its components is transferred to it from an ideal solution of the same composition, the total volume remaining unchanged. The concept of a regular solution was first proposed by Hildebrand[37].

Scatchard[38,39,40] and Hildebrand and Wood[41] independently derived what is now known as the Scatchard-Hildebrand equation.

The equation was of the form:

$$\Delta E^M = (x_1 V_1^L + x_2 V_2^L) \left[\left(\frac{\Delta E_1^V}{V_1} \right)^{\frac{1}{2}} - \left(\frac{\Delta E_2^V}{V_2} \right)^{\frac{1}{2}} \right]^2 \psi_1 \psi_2 \qquad [2.71]$$

$$= (x_1 V_1^L + x_2 V_2^L) (\delta_1 - \delta_2)^2 \psi_1 \psi_2$$

The excess free energy of mixing, noting that the excess entropy and total volume change are assumed equal to zero, is equal to the energy of mixing.

$$\Delta F^E \cong \Delta A^E = \Delta E^E - T\Delta S^E = \Delta E^E = \Delta E^M \qquad [2.72]$$

since, for an ideal solution:

$$\Delta E^M = \Delta h^M - P\Delta V^M = 0 \qquad [2.73]$$

The excess free energy change per mole of component 2 is[13]

$$RT \ln \gamma_2 = \left(\frac{\partial (n_1 + n_2) \Delta F^E}{\partial n_2} \right)_{T,P,n_1} \qquad [2.74]$$

which, on substitution of equation (2.71) becomes:

$$RT \ln \gamma_2 = \bar{V}_2^L (\delta_1 - \delta_2)^2 \psi_1^2 \qquad [2.75]$$

The assumptions inherent to the derivation of equation [2.71] are apparent from the definition of a regular solution, however, it is worthwhile summarizing them as an aid to understanding the validity of the theory. The assumptions, as listed by Prausnitz[42] are:

1) No orienting or chemical effects are acting between the molecules of the solution.

2) The entropy of solution at constant volume is equal to that of an ideal solution.

3) The energy of interaction between two molecules of unlike species is given by the geometric mean of the energies of interaction for the two species of like molecules.

4) Mixing at constant temperature and pressure effects no change in the total volume.

The theory of regular solutions cannot be directly applied to the gaseous solute in a liquid solution. This is due to the large decrease in the solute volume associated with the solution process. Also, by definition, the solubility parameter is related to the energy of vaporization of a component. This cannot be readily applied to the noncondensable solute which is above its critical temperature.

In order to apply regular solution theory it is necessary to construct a thermodynamic process in which the solute dissolution occurs at constant volume. It is therefore necessary to include a step in which the gaseous solute is compressed isothermally from the pure solute volume to the partial molar volume of the gas in the solution.

Prausnitz[42] has proposed a three step isothermal thermodynamic process which may be used to describe the mixing process. It is based on the concept of an isometric mixing pressure which is defined as the pressure at which the pure gas has a volume equal to its partial molar volume in solution. The three steps are:

1) Isothermal compression of the pure gas from its partial

pressure and the pure liquid from its vapor pressure to the isometric mixing pressure.

2) Isothermal, isometric, and isopiestic mixing of the pure components at the isometric mixing pressure.

3) Isothermal expansion of the solution from the isometric mixing pressure to its equilibrium pressure.

The free energy change for each of the above steps can be described. Equating the sum of these changes to zero results in the following equation.

$$RT \ln \frac{f_2(P_2)}{x_2 f_2(P_m)} = \bar{V}_2^L (\delta_1 - \delta_2)^2 \psi_1^2 - \int_P^{P_m} \bar{V}_2 \, d\pi \qquad [2.76]$$

where P_2 = partial pressure of the pure gaseous solute in the equilibrium solution (atm.).

π = total pressure of the equilibrium solution (atm.).

P_m = isometric mixing pressure (atm.).

In order to use equation [2.76] parameters must be derived from the pure solute properties. It is not suitable for quantitative work due to difficulties in calculating the mixing pressure P_m and the solute solubility parameter δ_2. However, the thermodynamic framework established in this correlation is useful in understanding the theory underling the more useful correlations of Prausnitz and Shair[43] and Yen and McKetta[44].

Prausnitz and Shair[43] have presented a correlation for predicting the low pressure solubility of nonpolar gases in nonpolar liquids. This correlation is based on a two step isothermal

dissolution process. The pure gas is first isothermally condensed to a hypothetical liquid at 1 atmosphere pressure.

$$\Delta\bar{F}_{2\,I} = RT \ln \frac{f_2^H}{f_2^{\circ g}} \qquad [2.77]$$

The hypothetical liquid is then dissolved in the solvent assuming a constant volume process.

$$\Delta\bar{F}_{2\,II} = RT \ln \gamma_2 x_2 \qquad [2.78]$$

At equilibrium, the sum of the free energy changes for the two steps is zero. Substituting equation [2.75] into equation [2.78] and rearranging results in the equation for gas solubilities at 1 atmosphere solute partial pressure.

$$\frac{1}{x_2} = \frac{f_2^H}{f_2^{\circ g}} \exp \left[\frac{\bar{V}_2^L (\delta_1 - \delta_2)^2 \psi_1^2}{RT} \right] \qquad [2.79]$$

When the gaseous solute is at a partial pressure of 1 atmosphere, it is reasonable to assume $f_2^{\circ g}$ to be unit fugacity. As the solubility of most gases is small at this low pressure, ψ_1^2 may be assumed equal to unity. The fugacity of the hypothetical liquid at a partial pressure of 1 atmosphere must be empirically determined. The significance of this quantity can be seen upon comparing equations [2.79] and [2.76].

$$f_2^H = f_2(P_m) \exp - \left[\frac{\int_1^{P_m} \bar{V}_2^L \, dP}{RT} \right] \qquad [2.80]$$

The parameters δ_1, δ_2, $\bar{V}_2^L$ and f_2^H in equation [2.79] have been compiled by Prausnitz and Shair[43] for a variety of solutes and solvents. The fugacity of the hypothetical liquid f_2^H has been given in a graphical form based on the theorem of corresponding states for all gases other than hydrogen. A separate plot of f_2^H versus the equilibrium temperature has been presented for hydrogen.

The above parameters are temperature dependent however the theory of regular solutions assumes that at constant composition:

$$\ln \gamma_2 \propto \frac{1}{T} \qquad [2.81]$$

From equation [2.75]

$$\ln \gamma_2 = \frac{\bar{V}_2^L(\delta_1 - \delta_2)^2 \psi_1^2}{R} \cdot \frac{1}{T} \qquad [2.75]$$

This implies that $\bar{V}_2^L(\delta_1 - \delta_2)^2 \psi_1^2$ is not temperature dependent. Hence any convenient temperature (usually 25°C) may be chosen for calculating δ_1, δ_2 and $\bar{V}_2^L$.

Yen and McKetta[44] have derived a correlation for predicting the solubility of nonpolar gases in polar, nonassociated liquids. The thermodynamic process considered is identical to that proposed by Prausnitz[42,43], however, the theory of regular solutions was modified to include polar liquids.

The original derivation of regular solution theory as carried out by Hildebrand and Wood[41] assumed the Lennard-Jones potential function to describe the energies between the 1-1, 1-2 and 2-2 components. Yen and McKetta also assumed the Lennard-Jones potential function for the 1-2 and 2-2 energies, however, they introduced the

Stockmayer potential function for the 1-1 or solvent-solvent interaction.

The resulting equation for the solubility of the solute gas when its partial pressure is 1 atmosphere is:

$$\frac{1}{x_2} = \frac{f_2^H}{f_2^{\circ g}} \exp\left[\frac{\bar{V}_2^L(\delta_1^2 + \delta_2^2 - 2\delta_2(\delta_1^2 + \Delta)^{\frac{1}{2}}\psi_1^2}{RT}\right] \qquad [2.82]$$

The parameters δ_1, δ_2, $\bar{V}_2^L$ and f_2^H are the same as the corresponding parameters in the Prausnitz and Shair correlation[43], however, Yen and McKetta redetermined their numerical value using additional data published after the work of Prausnitz and Shair[43]. Solubility data for nonpolar gases in polar solvents were then empirically fit to obtain values of the polar characteristic constant Δ. A general curve of the parameter Δ versus the solvent solubility parameter has been presented by the authors[44].

Hildebrand and Scott[12] have presented a semi-empirical correlation for estimating the solubility of nonpolar gases in nonpolar solvents when the equilibrium temperature is 25°C and the solvent partial pressure is 1 atmosphere.

They found that the solubility data at 25°C for a single gas dissolved in a number of different solvents fell on a unique, continuous curve when the data were plotted as the logarithm of the solute mole fraction versus the solvent solubility parameter (δ_1). The solubility data for twelve gases have been plotted in this manner.

Hildebrand and Scott[12] also found that the solubility data for a number of solutes dissolved in a single solvent could be

correlated by plotting the logarithm of the solute mole fraction versus the solute Lennard-Jones energy parameter $(\frac{\varepsilon}{k})$. Eight curves corresponding to eight different solvents have been presented.

A third plot of the logarithm of the solubility parameter $(-R \ln x_2)$ versus the entropy of solution $(\bar{S}_2 - S_2^g)$ was presented by Hildebrand and Scott[12]. The data were plotted on eight separate curves which correspond to the eight solvents for which the plot was developed. From equation [2.44] the temperature coefficient of solubility is,

$$\bar{S}_2 - S_2^g = R \left(\frac{\partial \ln x_2}{\partial \ln T} \right)_P \qquad [2.44]$$

hence the solubility of a nonpolar gas in a nonpolar liquid can be predicted at temperatures not far removed from the temperature at which the solubility is known. If the solubility has been estimated at 25°C from either of the plots of Hildebrand and Scott[12], then the solubility at temperatures near 25°C may be estimated from the third plot of the above authors[12].

3. Other Solution Theories

A large number of solution models have been proposed in the literature. The preceding section on regular solution theory was presented in considerable detail as this theory has received the most consideration in so far as calculating gas solubilities is concerned. Battino and Clever[45], in a review of the literature on the solubility of gases in liquids have discussed solubility correlations based upon cell potential and cavity models. These solution models, along with the more recent ones of Nakahara and Hirata[46], Miller and Prausnitz[47] and Sadamoto et al[48] have

not been developed to the extent that hydrogen solubilities in polar solvents can be predicted with confidence. Mellan[49] has stated that "The development of new theories of liquids, especially those based upon a simple intermolecular potential energy function and the law of corresponding states has led to a whole series of related theories of solutions which are reasonably satisfactory (better than regular solutions and solubility parameters) when applied to monatomic molecules and to approximately spherical polyatomic molecules, but are otherwise of very limited applicability".

The correlation of Osburn and Markovic[50], which for no better reason than its simplicity of use, is worthwhile mentioning. This correlation is based on the cavity model of Uhlig[51] and Schlapfer[52] who showed that for many gases a plot of the Ostwald coefficient (cc. of gas measured at the equilibrium temperature per cc. of liquid) versus the liquid surface tension at 20°C gave a straight line. The authors[50] developed a nomograph which enables one to estimate the Ostwald coefficient at 20°C from a knowledge of the solvent surface tension at 20°C.

D. Review of Solubility Coefficients

A solubility coefficient is an expression of the amount of solute dissolved in a unit amount of solvent. Either weight, volume or molar units may be used for expressing the amount of solute and solvent. When the amount of solute is expressed in volume units, the reported conditions of temperature and pressure are arbitrary. Most authors prefer to correct the solute volume to standard conditions of 0°C and 760 mm. Hg., however some quote the volume at the saturation conditions.

The saturation pressure may be quoted as the total system pressure or as the partial pressure of the solute in the vapor phase. Care must be exercised when using solubility data to ensure that the assumptions implicit in the use of a particular solubility coefficient are understood.

Various reviews of the commonly used solubility coefficients are available in the literature[20,45,53,54], hence only the more common units and their interconversion will be discussed in this study. The solubility data for a nonideal solution or for a solution which does not conform to the assumptions outlined in the following discussion should be reported simply as a solubility coefficient. This is necessary so as not to confuse the conditions of the experiment with those implied by the use of a specific coefficient.

1. Keunen Coefficient (S)

The Keunen Coefficient, S, is defined as the volume of gas, corrected to 0°C and 760 mm. Hg., dissolved at the reported experimental temperature in a unit weight of solvent under a solute partial pressure of 1 atmosphere.

From Henry's law, equation [2.29], for a solute partial pressure of 1 atmosphere:

$$1(\text{atm.}) = H_2 x_2 \qquad [2.83]$$

But

$$x_2 = \frac{n_2}{n_1 + n_2} \qquad [2.84]$$

On the basis of 1 gm. of solvent:

$$x_2 = \frac{\frac{S}{22414.6}}{\frac{1}{M_1} + \frac{S}{22414.6}} \qquad [2.85]$$

$$x_2 = \frac{1}{\left(\frac{22414.6}{M_1 S}\right) + 1}$$

Therefore, from equation [2.83]

$$H_2 = \frac{1}{x_2} = \left(\frac{22414.6}{M_1 S} + 1\right) \qquad [2.86]$$

which, upon rearranging gives:

$$S = \frac{22414.6}{M_1 (H-1)} \qquad [2.87]$$

Equation [2.86] will be referred to throughout this discussion as all solubility coefficients will be converted to Keunen coefficients. Equation [2.86] can be used to calculate Henry's law coefficients or the mole fraction solute at 1 atmosphere partial pressure.

2. Bunsen Coefficient (α)

The Bunsen coefficient, α, is defined as the volume of gas, corrected to 0°C and 760 mm. Hg., dissolved at the reported experimental temperature in a unit volume of solvent under a solute partial pressure of 1 atmosphere. The Bunsen coefficient is converted to the Keunan coefficient by the relationship:

$$S = \frac{\alpha}{\rho_1} \qquad [2.88]$$

3. Ostwald Coefficient (L)

The Ostwald coefficient, L, is defined as the volume of gas dissolved by a unit volume of solvent, both being measured at

the reported experimental temperature. The Ostwald coefficient is, to a very good approximation, independent of the solute partial pressure so long as Henry's, Boyle's and Dalton's law are assumed valid. As the solute pressure is increased, Henry's law states that the volume of dissolved solute will increase in proportion to the pressure. However, by Boyle's law, the volume will be inversely proportional to pressure. The numerical value of the coefficient will therefore remain the same.

Converting the Ostwald coefficient to the Keunan coefficient yields:

$$S = \frac{273.15\ L}{\rho_1 T} \qquad [2.89]$$

where T is in degrees Kelvin.

The Bunsen coefficient is obtained by equating equations [2.88] and [2.89]

$$\alpha = \left(\frac{273.15}{T}\right) L \qquad [2.90]$$

4. Ostwald Coefficient as Used by Horiuti (γ_H)

The Ostwald coefficient as used by Horiuti[55], γ_H is defined as the volume of gas dissolved by a unit volume of solution, both measured at the reported experimental conditions. The same assumptions are required for this coefficient as were presented for the Ostwald coefficient. A coefficient of dilation by absorption, δ, must be applied when comparing this unit to the previously mentioned coefficients.

$$\delta = \frac{(\text{cc. solution} - \text{cc. solvent})}{\text{cc. gas (STP)}} \qquad [2.91]$$

It can be shown that the Bunsen coefficient is related to the coefficient of Horiuti by the relationship:

$$\alpha = \frac{273.15\ \gamma_H}{(T - 273.15\ \delta\ \gamma_H)} \qquad [2.92]$$

Hence, from equation [2.88], the Keunan coefficient is given by:

$$S = \frac{273.15\ \gamma_H}{\rho_1 (T - 273.15\ \delta\ \gamma_H)} \qquad [2.93]$$

3. LITERATURE SURVEY

A. Experimental Technique

A large variety of experimental techniques have evolved for determining the solubility of gases in liquids. The general approaches may be classified as physical and chemical methods. Physical solubility techniques may be further subdivided into saturation methods and extraction methods. Only the extraction method, that is the procedure in which a representative sample of the previously saturated solution is withdrawn and analyzed for the amount of dissolved gas, will be considered in this study. General reviews of both physical and chemical solubility techniques are available in the literature[45,56,57].

The basic requirement of any solubility determination is to insure effective contacting of the liquid and gas phases so that a true equilibrium is attained. A number of equilibrium cells have been described in the literature. Brainard and Williams[58] designed a cell for which mechanical agitation of the cell contents was provided by a magnetically actuated disc stirrer. Various authors[59,60,61,62] have obtained equilibrium between the gas and liquid phase by shaking the cell assembly. Larson and Black[63] and Thompson and Edmister[64] used "wash bottle' type cells which provided for mixing of the two phases by bubbling the gas phase through the condensed phase on a once through basis. Wash bottle type cells which are equipped for recirculation of one or more of the phases have been described by Aroyan and Katz[65], Fleck and Prausnitz[66] and Eckert and Prausnitz[67]. Magnetic solenoid pumps were used by Aroyan and Katz[65] and Fleck and Prausnitz[66] while Eckert and Prausnitz[76] used a modified peri-

staltic pump which was sealed in a pressure chamber.

Liquid sampling techniques have been discussed by a number of investigators. Brainard and Williams[58] vented a volume of the solution which was approximately twice the volume of the sample line prior to removing samples for analysis. Aroyan and Katz[65] reduced the dead volume of the sample line by introducing a section of Chromel A wire. Prausnitz[66,67] designed liquid sample valves for which the dead volume was negligible.

Pressure maintenance of the equilibrium solution has been carried out by introducing pure gas[63] or mercury[59] into the cell during sampling.

The freeze drying technique for extracting the dissolved gas from a saturated liquid sample has been used by many investigators [58,59,60,61,62,64]. This procedure consisted of trapping the solvent in a liquid nitrogen trap and drawing the released gas, by means of a Toepler pump, into a calibrated burette. This method is very efficient for hydrogen dissolved in light hydrocarbons and liquid ammonia. Dean and Tooke[59] noted some problems when working with dodecane as it tended to freeze into minute particles which became entrained in the effluent hydrogen.

Gas chromatography may be used for extraction of the dissolved gas from the saturated liquid sample[66,67]. This method of analysis is much faster than the volumetric determination based on separation of the light component by freezing of the liquid phase. However, this technique is not suitable for the analysis of samples containing the homogeneous amide catalyst and accurate calibration of the chromatograph is required for each liquid.

General methods for degassing of the solvent have been discussed by Battino and Clever[56]. The amine purification techniques employed in this study were fashioned after those of Fowles et al[68], Eyers et al[69] and Bar-Eli and Klein[70].

B. Available Solubility Data for Hydrogen Dissolved in Liquid Ammonia and Liquid Amines.

The solubility of hydrogen in liquid ammonia was first determined by Schlubach and Ballauf[71]. They reported the solubility at -70°C and one atmosphere pressure to be 0.044 $\frac{\text{cc. } H_2\text{(STP)}}{\text{gm. } NH_3}$.

Larson and Black[63] measured the solubility of a 3:1 hydrogen-nitrogen mixture in liquid ammonia at pressures of 50, 100 and 150 atmospheres. The temperature range of their study was -25°C to +22°C. They released the dissolved hydrogen-nitrogen gas mixture from the liquid ammonia by absorbing the saturated ammonia sample in a previously saturated (gas mixture) solution of 2N sulfuric acid. The liberated gas was collected in a calibrated burette for determination of the total volume and then analyzed for composition by a combustion technique. The amount of ammonia in the sample was measured by titrating aliquot parts of the acid in which it was absorbed. The dissolved volume of hydrogen (STP) divided by the total weight of liquid ammonia was reported as the hydrogen solubility coefficient. Care must be taken to ensure that the correct hydrogen partial pressure is used when the hydrogen solubility coefficients of Larson and Black[63] are compared with those of other investigators.

Hydrogen solubility coefficients at 25°C and total system pressures of 15 atmospheres to 250 atmospheres were reported by

Ipatiew and Teodorowich[72]. They concluded that the solubility of hydrogen in liquid ammonia obeys Henry's law over the pressures investigated.

Extensive data on the solubility of hydrogen in liquid ammonia at total pressures in excess of 50 atmospheres and at temperatures of 0°C, 25°C, 50°C, 75°C, and 100°C have been published by Wiebe and Tremearne[73] and Wiebe and Gaddy[62]. A plot of their data for the first three isotherms versus total pressure indicated that up to approximately 150 atmospheres the solubility increases proportionally with increasing pressure.

Davis[74] has produced a nomograph for interpolating the data of the above authors[73,62].

Reamer and Sage[75] have reported equilibrium ratios for the hydrogen-ammonia system. The authors determined the vapor phase compositions experimentally and used the liquid phase solubilities of Wiebe and Tremearne[73]. A plot of the solubility coefficients as listed by Reamer and Sage[75] result in a series of isothermal curves which do not agree in either shape or magnitude with those of the original authors[73]. The data of Reamer and Sage should therefore be used with caution.

The solubility of hydrogen deuteride in a dilute solution of potassium amide in liquid ammonia has been reported by Bar-Eli and Klein[76]. They list the solubility at two temperatures in the form of a modified Bunsen coefficient.

T°C	$\alpha' \left\{\frac{\text{ml. } H_2 \text{(STP)}}{\text{ml. } NH_3 \text{ atm}}\right\}$
-41.6	0.025 ± 0.0013
-64.0	0.0117 ± 0.0005

The work of Cook et al[77] has shown that the solubility of deuterium, as quoted on a mole fraction basis, is approximately 2.5% greater than that of hydrogen in the eight organic solvents tested. The effect of the dissolved amide is not known, however, the data of Bar-Eli and Klein[76] can probably be used as an estimate of the solubility of hydrogen in ammonia.

Dirian et al[78] have presented an equation for the solubility of hydrogen in liquid ammonia when the hydrogen partial pressure is one atmosphere.

$$\log \tau = -3.74 - \frac{450}{T} \qquad [3.1]$$

$$\tau = \frac{\text{gm. } H_2}{\text{ml. } NH_3}$$

The reliability of this equation is reported[78] as ±20% and no statement is made as to the origin of the data on which the curve is based.

No information on the solubility of hydrogen in the amines chosen for this study was available in the literature.

C. Classification and Nomenclature of Amines

The most important class of organic compounds that show appreciable basicity are the amines. They are formed when one or more of the hydrogen atoms of ammonia are replaced by an alkyl or aryl group. Amines are divided into three subclasses on the basis of the number of hydrocarbon groups attached to the nitrogen atom. The three classes have the general formulae:

RNH_2	Primary
R_2NH	Secondary
R_3N	Tertiary

The properties of the amines in each class depend to a large extent on the number of hydrogen atoms attached to the nitrogen atom.

The common or trivial names for amines are formed by naming the alkyl group or groups attached to the nitrogen atom and following these by the word - amine. The IUPAC (International Union of Pure and Applied Chemistry) system of nomenclature requires the use of the prefix amino followed by the name of the parent structure. The system of numbering isomeric molecules is the same as that used for alkanes. A brief review of the IUPAC system of nomenclature is given in Morrison and Boyd[79]. A third system of nomenclature in common usage is the IUC (International Union of Chemists) system. For this system, the name of the amine function follows the name of the parent chain as the suffix amino. Rules governing the IUC system of nomenclature are found in reference[80].

Table 1 lists the trivial, IUPAC and IUC names of the amines studied. The chemical formulae are also shown.

D. Properties of Amines

Amines, like ammonia, are basic in character and form salts by reaction with acids. They are related to ammonia in the same way that alcohols are related to water. The low molecular weight amines are gaseous at room temperature and have a strong ammoniacal odor. As the molecular weight increases, the amines take on a less

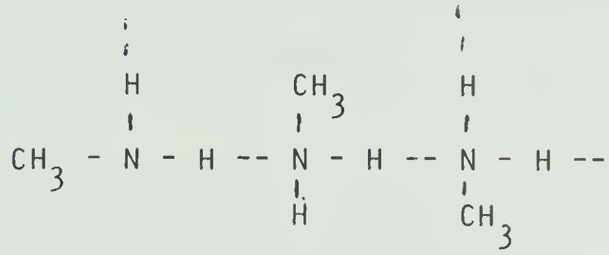
TABLE 1

NOMENCLATURE FOR THE AMINES CONSIDERED IN THIS STUDY

Trivial Name	IUPAC Name	IUC Name	Formula
Methylamine Monomethylamine	Aminomethane	Methane, amino-	$CH_3\ NH_2$
Ethylamine Monoethylamine	Aminoethane	Ethane, amino-	$C_2H_5\ NH_2$
Propylamine N-Propylamine	1-Amino propane	Propane, 1-amino-	$C_3H_7\ NH_2$
1,2-propane diamine	1,2-diaminopropane	Propane, 1,2-diamino-	$H_2N.CH_2.CHNH_2.CH_3$ $C_3H_{10}N_2$
1,2-ethane diamine Ethylene Diamine	1,2-diaminoethane	Ethane,1,2-diamino-	$H_2N.CH_2CH_2NH_2$ $C_2H_8N_2$

strong ammonical odor and develop a pronounced "fishy" smell.

Ammonia and amines are polar compounds due to the presence of the N-H bond. All amines other than those of the tertiary subclass are capable of forming hydrogen bonds.



The ability to associate accounts for the fact that amines have higher boiling points than hydrocarbons of the same molecular weight. The N - H -- N bond is weaker than the H - O -- H or H - F -- H bonds because the electronegativity of nitrogen is less than that of either oxygen or fluorine. Amines therefore have a lower boiling point than the corresponding alcohols.

The simple amines display a large solubility in water. The solubility decreases with an increase in the size of the alkyl group. Amines with alkyl groups of greater than six atoms are almost immiscible with water.

Amine molecules are pyramidal in structure with a nitrogen atom at the apex and either hydrogen or alkyl groups at each corner of the triangular base. In forming amines nitrogen uses sp^3 orbitals directed towards the corners of the tetrahedron. Three of these orbitals overlap orbitals of the hydrogen or alkyl group while the fourth unshared pair of electrons account for the basicity of amines.

Ammonia is more basic than water and amines are more basic than alcohols or ethers. This is due to nitrogen being less electro-

negative than oxygen and as such is more prepared to form a covalent bond with the proton. Aliphatic amines are stronger bases than ammonia as the electron releasing alkyl group or groups tend to stabilize the ammonium ion by dispersing the positive charges. Though amines are strong bases when compared with water, they are weak bases when compared with inorganic bases such as sodium hydroxide.

Selected values of physical property data for the amines considered in this work are listed in Appendix D1. Some of the data were curvefit to enable incorporation in the computer calculation routines.

Vapor pressure data for each amine and ammonia were fit to an equation of the form:

$$\ln P^s = C_1 + \frac{C_2}{T} + C3T + C4 \ln T \qquad [3.2]$$

using the program "Vapfit" of Prausnitz et al[81]. The best fit constants are listed in Table D1-2, Appendix D1.

Density data for ammonia, methylamine and ethylamine were fit to the curve:

$$\rho = A1 + A2T + A3T^2 + A4T^3 \qquad [3.3]$$

using a "Forsythe" orthogonal polynomial fitting routine. Values of the density coefficients are listed in Table D1-3, Appendix D1. The equation for the density of n-propylamine as given in the "International Critical Tables"[82] is presented in the same table.

The methylamine viscosity data of Dye and Dalton[83] were curvefit using a linear least square fitting routine The resulting

equation for the temperature range -70°C to -10°C is:

$$\ln \eta = \frac{741.82}{T} - 4.0524 \qquad [3.4]$$

η = viscosity in centipoise

T = Kelvin degrees

The available viscosity data for ammonia, methylamine, ethylamine, 1,2-propane diamine and 1,2-ethane diamine are presented in Table D1-4 of Appendix D1.

Surface tension data for ammonia, methylamine, ethylamine and propylamine are listed in Table D1-5. The methylamine surface tension data presented in the "Handbook of Chemistry and Physics"[80] were correlated by the method of Othmer[85]. The resulting equation is:

$$\sigma = 23.0 \left(\frac{156.9 - T}{176.9}\right)^{0.96} \qquad [3.5]$$

where: σ = surface tension (dynes/cm.)

T = temperature (°C)

Table D1-6 lists the dielectric constants ($\varepsilon_{vacuum} = 1$) for ammonia, methylamine, ethylamine and 1,2-ethane diamine. No data could be found for n-propylamine and 1,2-propane diamine.

A brief review of hydrogen properties is given in Table D1-7 of Appendix D1.

4. EXPERIMENTAL PROGRAM

A. Equipment

A schematic diagram of the solubility apparatus is shown in Figure 1. The solubility cell was located in a refrigerated bath along with a hydrogen saturator and a solenoid pump. As shown in Figure 2, the solubility cell was equipped with a magnetically coupled stirrer for agitation of the cell contents. The hydrogen phase was continuously circulated through the stirred liquid by the solenoid pump, hence efficient contacting of the cell contents was obtained.

The auxiliary systems which are shown in Figure 1 consisted of a hydrogen purification unit, liquid amine purification unit and a vacuum system. These systems were shared with a single sphere absorption apparatus which will be discussed in Part 2 of this text.

The refrigeration requirements of the solubility apparatus were provided by two low temperature refrigeration units. This refrigeration system was designed to handle the cooling load of a proposed four inch diameter bubble tower, the solubility apparatus and the single sphere absorber.

1. Refrigeration System

A single refrigeration system was designed to handle the cooling requirements of the overall amine exchange study. Two refrigeration units were interconnected in the system. A "Tecumseh" hermetic unit with a rated capacity of 4000 B.T.U./hr. at -40°C provided refrigeration for the higher temperature range. A "York" model F62C-502E, six cylinder, two stage internally compounded refrigerant 502 compressor, with a capacity rating of 7920 B.T.U./hr.

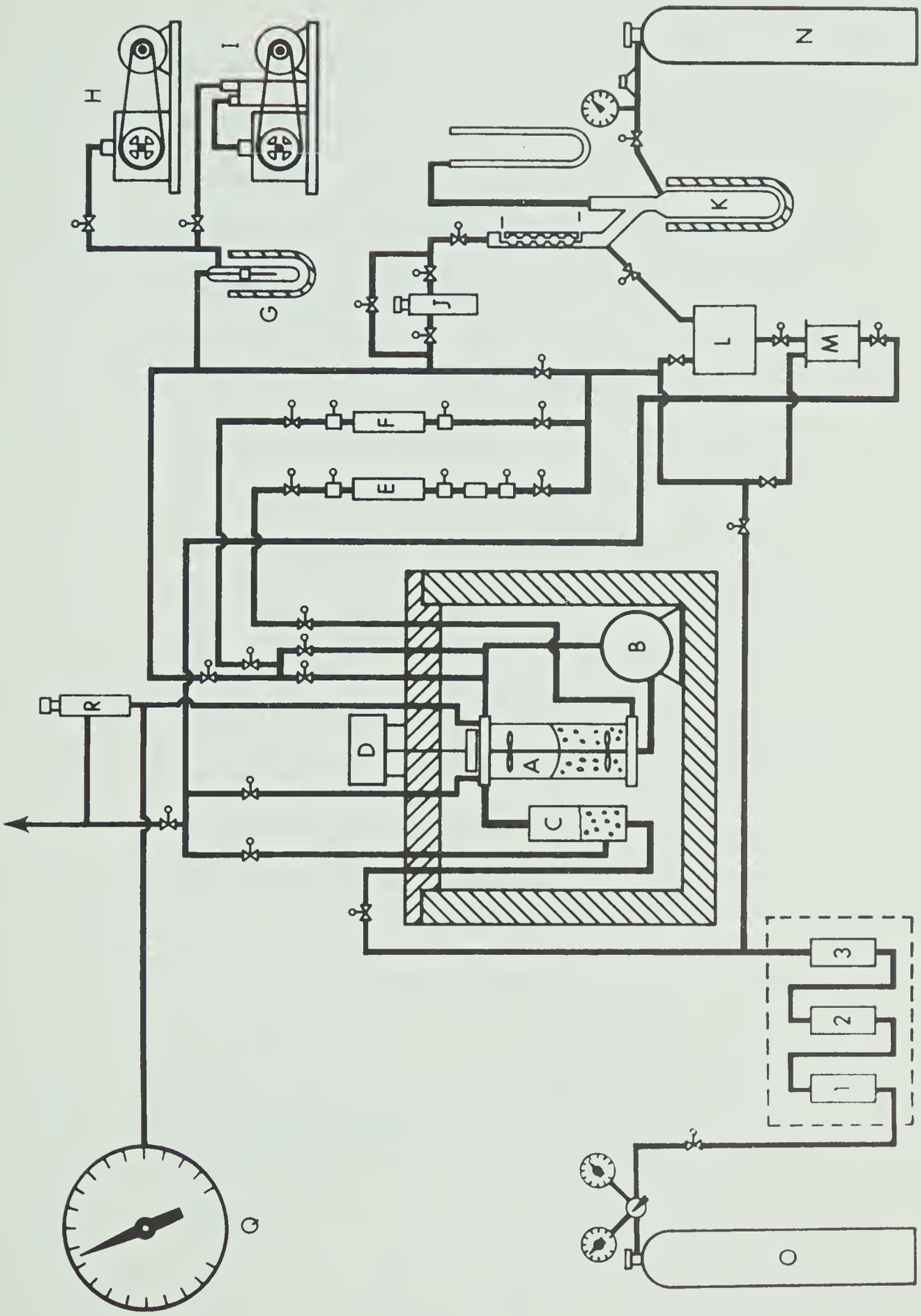


FIG. 1. SCHEMATIC DRAWING OF SOLUBILITY APPARATUS



SYMBOLS FOR FIGURE 1

A	Solubility Cell
B	Solenoid Pump
C	Hydrogen Presaturation Tube
D	Motor Drive for Solubility Cell Stirrer
E	Saturated Liquid Sample Cylinder
F	Saturated Vapor Sample Cylinder
G	Liquid Nitrogen Trap for Vacuum System
H	Mechanical Roughing Pump
I	Mechanical - Diffusion Vacuum Pump
J	Vacuum Manostat
K	Amine Purification Unit
L	Charge Vessel
M	Liquid Charge Measuring Vessel
N	Amine Supply Cylinder
O	Hydrogen Supply Cylinder
P	Hydrogen Purification Unit
	1. Charcoal
	2. Palladium
	3. Silica Gel
Q	Heise Pressure Gauge (0 to 400 psig.)
R	Relief Valve
S	Vent

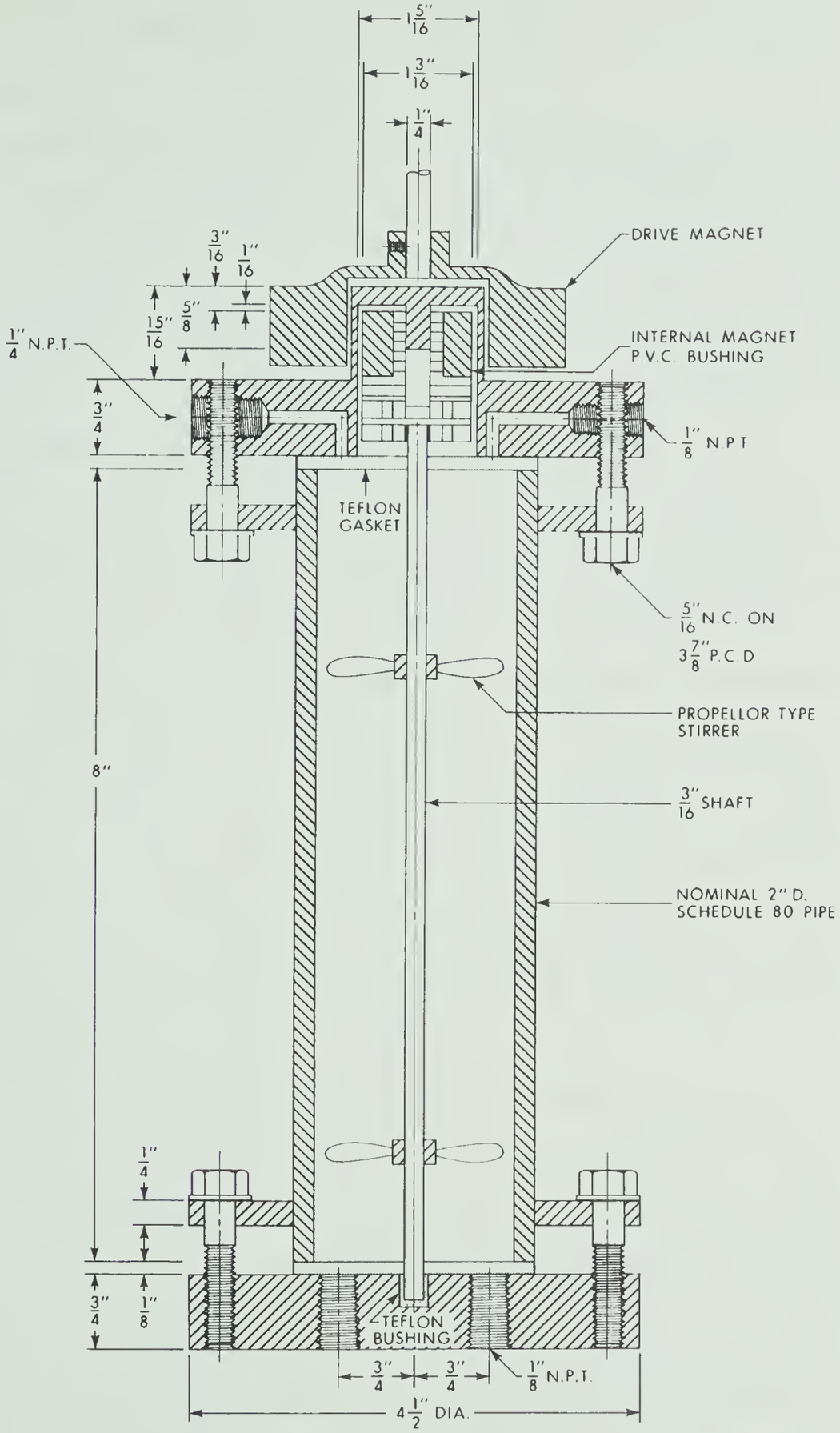


FIG 2. SOLUBILITY CELL

at minus 100°F saturated suction temperature, was used for the low temperature solubility studies.

Denatured ethanol was utilized as the external heat transfer medium. Absorption of moisture and losses due to evaporation were minimized through the use of tight fitting bath lids.

A schematic diagram of the overall refrigeration system is shown in Figure 3. The external piping was either nominal 3/4 inch or 1¼ inch copper pipe insulated with "Armaflex" insulation.

The "Tecumseh" refrigeration unit was equipped with an open bath evaporator thus two circulation pumps were required when this unit was used to refrigerate the solubility apparatus. Level control devices were installed on both baths to guard against a coolant spill due to a pump failure or a misbalance in the flow rates.

The refrigerated bath which housed the solubility cell and associated equipment was constructed of heavy gauge galvanized steel. A four inch layer of styrofoam insulation was sealed between the internal and external sheet metal sides. The internal dimensions of the bath were 30 x 18 x 18 inches.

The bath lid was constructed so as to support all the solubility equipment which required cooling. The frame was formed from two inch channel iron reinforced with ¼ inch flat iron. This was enclosed with galvanized steel and insulated with "Johns Manville 500 Cement". Access ports for the coolant and equilibrium cell piping were installed in the bath lid. These ports were formed by passing copper pipes through the lid and sealing them to the two sides with threaded flanges. Each flow line was provided with a close fitting access

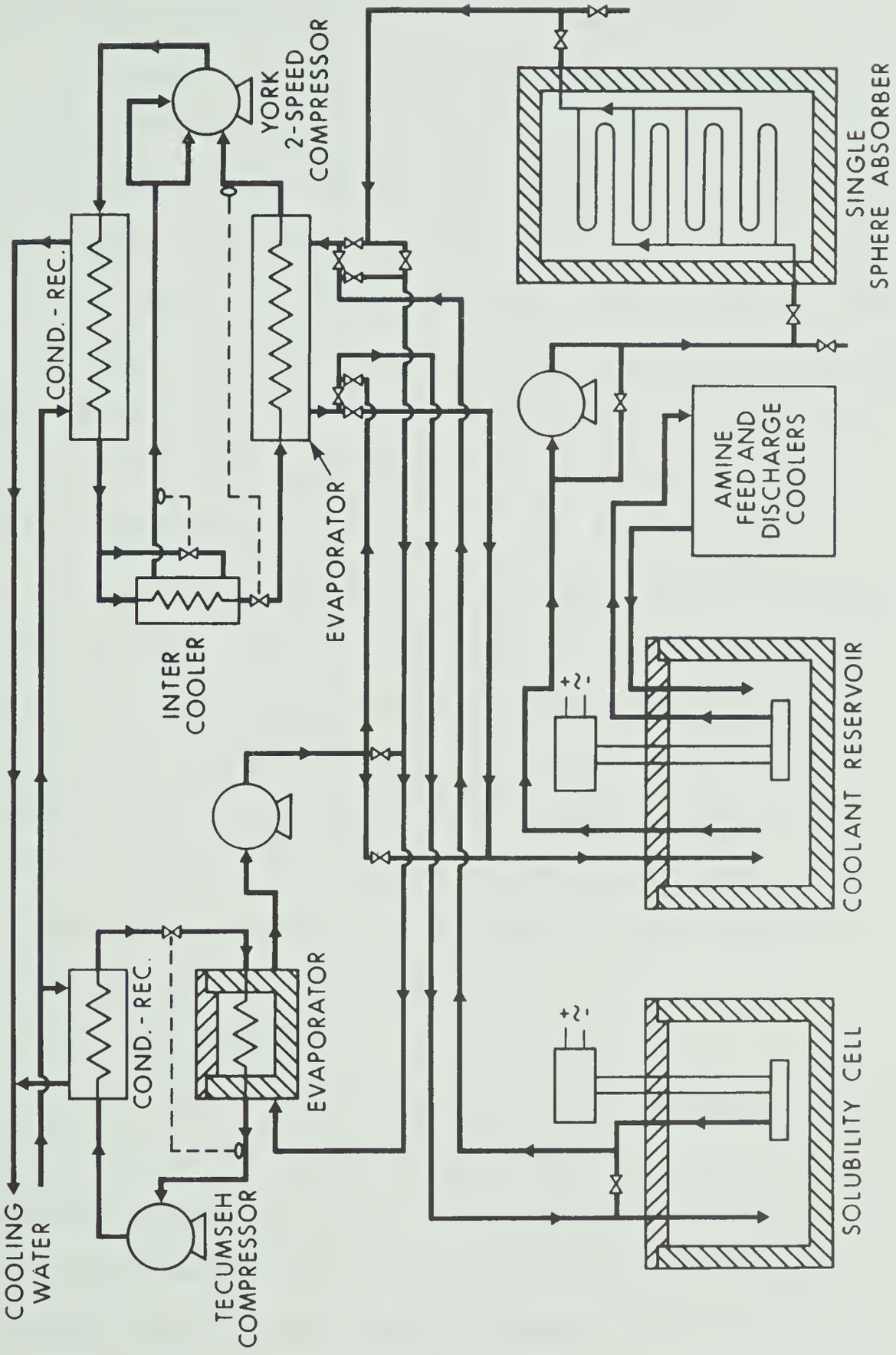


FIG. 3. SCHEMATIC DRAWING OF REFRIGERATION SYSTEM

port. A removable section was built into the lid to enable visual observation and placement of the level control device.

The solubility cell bath was equipped with two 500 watt immersion heaters and an "Aminco" thermo-regulator. The heaters were mounted in removable caps which were threaded to two nominal two inch pipes. These pipes were sealed in the bath lid and extended into the bath to a depth of ten inches. Rubber plugs were inserted in the open end of the two tubes to prevent condensation of moisture. The thermoregulator was located in a depression which was built into the external side of the lid. It was connected through a "Precision" electronic switch to the bath heaters only.

The refrigeration units were provided with built in temperature control schemes. The "Tecumseh" unit was equipped with a "Honeywell Refrigeration Temperature Controller" which enabled variation of the bath temperature from -24°C to the ambient temperature. When the "York" refrigeration unit was used, the temperature of the evaporator was varied by passing hot gas from the second stage suction to the evaporator. An automatic pressure regulating valve controlled the flow of hot gas.

2. Vacuum System

A mechanical roughing pump (Welch Duoseal) and a mechanical roughing-oil diffusion pump (Welch Duoseal - C.V.C.) were separately valved to a common manifold. A liquid nitrogen cold trap was installed in the line between the vacuum manifold and experimental apparatus. A "Nester/Faust" vacuum gauge was connected to the vacuum line immediately downstream from the cold trap.

3. Hydrogen Purification Unit

The hydrogen purification train was composed of three vessels fabricated from nominal one inch steel pipe. The three vessels were packed with activated charcoal (hydrocarbon impurities), palladium supported on alumina (oxygen) and silica gel (water) respectively.

4. Amine Purification Unit

The amine purification unit was a simple flash vacuum distillation apparatus which was used to remove dissolved gases, water and higher boiling amines. The unit construction was similar to that of Ishige[97].

Ethanol was circulated through the amine condenser in a closed circuit. The ethanol was cooled by passing it through a coil immersed in a large dry ice-trichloroethylene bath. The volume of the bath was such that one charge of dry ice would suffice for the complete distillation process. An "Eastern 316 S.S. Type 103" centrifugal pump was used to recycle the coolant.

A "Cartesian Manostat" was employed to regulate the pressure during the distillation. A bypass was installed around the manostat to enable complete evacuation (five microns) of the distillation rig.

5. Amine Charge System

Liquid amine from the purification apparatus was collected in a metal charge vessel. The amine could either be stored in this vessel or charged through a graduated jar to the solubility cell.

The charge vessel was a 300 c.c., type 316 stainless steel vessel which was located in a glass dewar. A hydrogen line was connected to the charge vessel to enable the transfer of liquid amine under a hydrogen pressure.

A graduated glass cylinder was located between the charge vessel and solubility cell. This measuring jar was constructed from a 1½ inch "Q.V.F." glass pipe section mounted between two stainless steel flanges. The jar was calibrated with water and graduated in 25 ml. intervals. Hydrogen pressure was used to force the amine from this graduated cylinder to the solubility cell.

6. Solubility Cell

The solubility cell which had a volume of approximately 400 cc. was provided with a magnetically coupled stirrer. A detailed sketch of the cell is shown in Figure 2.

The radial magnetic coupling and electric motor were obtained from a "Cole-Palmer" magnetic drive centrifugal pump. Both the internal magnet and external or drive magnet were ceramic. The internal magnet was epoxy coated (3M #9 Scotch Cast) to protect against corrosion. A two blade propellor stirrer was located in both the liquid and vapor phase.

The solubility cell was suspended from the lid of the constant temperature refrigerated bath and the motor drive was attached to the external surface of the lid. The length of the drive shaft was eight inches so a sealed bearing was mounted immediately above the external drive magnet to reduce the radial movement of the magnet.

7. Magnetic Solenoid Pump

A magnetic solenoid pump was incorporated into the solubility apparatus to provide contacting of the cell contents in addition to that obtained by the stirrer alone. Efficient circulation of the hydrogen was also important as it would ensure that no concentration gradient existed in the gas phase. A homogeneous gas phase is especially important if vapor phase samples are to be obtained or if kinetic equilibrium studies are to be conducted in the cell.

Magnetic pumps have been utilized by various experimenters (98, 99, 100, 101, 102, 103) for pumping small quantities of gases or liquids. They are desirable as no moving seals are involved. They are self priming and they can be designed for pressures up to 15,000 psi.. Solenoid pumps can be jacketed or immersed in a constant temperature bath, hence heat generation can be controlled. Though commercial solenoid pumps are available (104), the pump used in this study was fabricated in the Department of Chemical and Petroleum Engineering, University of Alberta, machine shop.

The double acting solenoid pump was of stainless steel construction with teflon piston rings, valves, and o-ring seals. A sketch of one half of the pump is shown in Figure 4. The two halves of the pump are identical. The o-ring connector on the pump discharge was ommitted from the drawing.

Both the suction and discharge check valves were formed from teflon discs which were back seated with stainless steel springs. The four external connectors were "Swagelok" ¼ inch o-seal straight

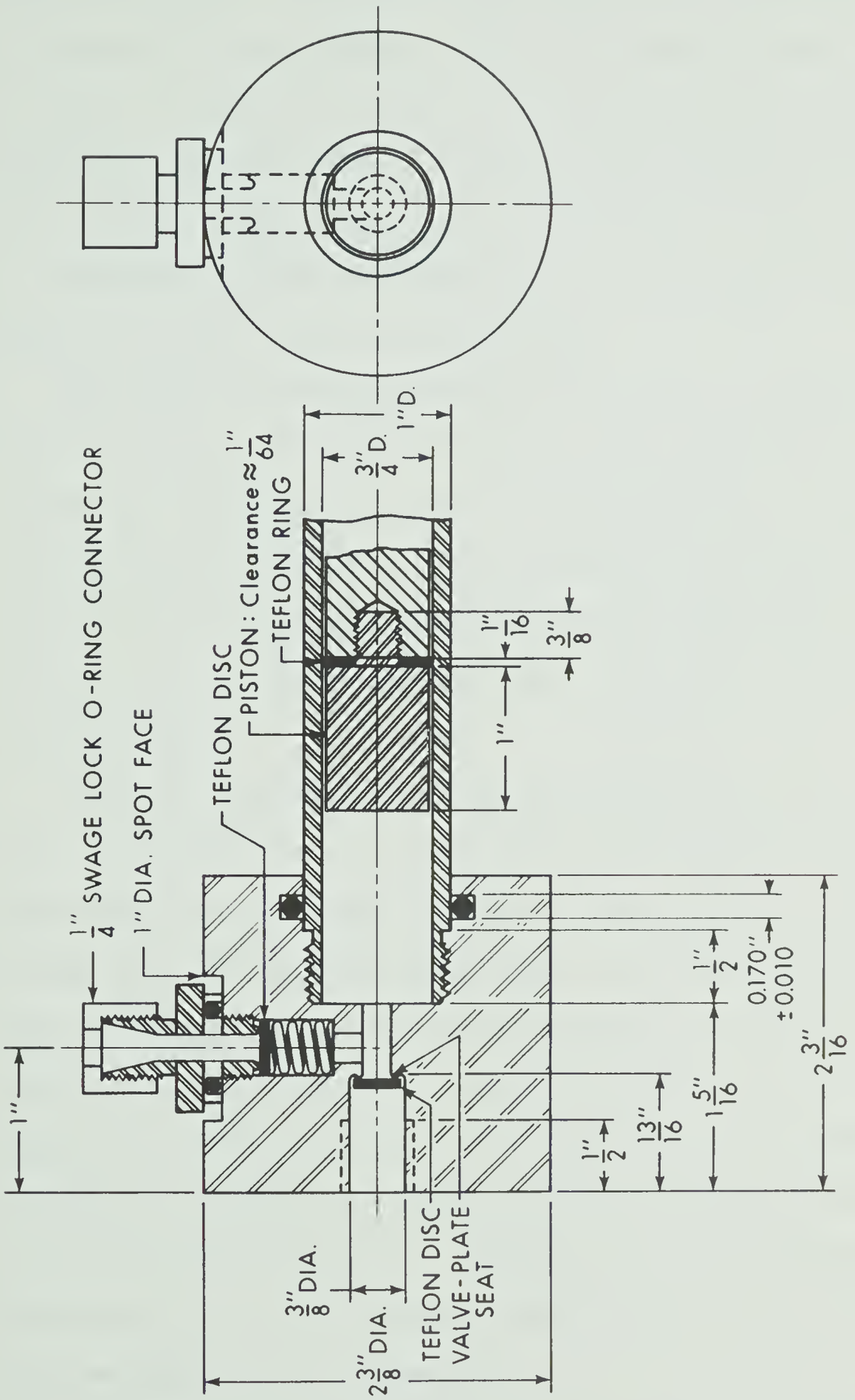


FIG. 4. MAGNETIC SOLENOID PUMP VALVE CAP

thread connectors. The suction valve discs were seated against the threaded end of the connectors. These connectors had been previously machined to provide the valve seat. The discharge valve seats were machined in the pump heads. The check valves appeared to be the most critical components in the design and operation of the pump.

The pump cylinder was formed from one inch stainless steel tubing. Its total length was 13-3/4 inches.

The pump piston was constructed of mild steel. It consisted of three sections (1", 2" 1") which were held together by threaded connections. Two teflon discs were fitted between the sections to act as piston rings. The clearance between the piston rings and cylinder wall could be varied by adjusting the tension with which the three sections were screwed together. The overall piston length was four inches.

Three coils, 3-2/3 inches long and separated by $\frac{1}{4}$ inch fiber discs, were wrapped on the pump cylinder. Each coil had approximately 2300 turns of number 20 enameled copper wire. A variable voltage (9 to 18 volt D.C.) power supply with a maximum current of three amperes was used to excite the solenoids. At the design condition of twelve volts D.C., each coil carried a current of 1.1 amperes resulting in a rating of 2530 ampere-turns. The design of the coils was based on a balance between the number of ampere-turns and the heat generation. Professor D.H. Kelly[105] suggested sizing the coils so that the wire cross-sectional area to current ratio was 800 circular mils/ampere.

The external electronics consisted of the previously mentioned D.C. power source, a repeat cycle multi-gang timer and three switching

relays. The timer was a three gang, single cam assembly driven by a 60 R.P.M. synchronous motor. The two end gangs which controlled the two end solenoids were fitted with one micro switch. The center gang which controlled the middle solenoid was fitted with two opposing switches. The three gangs were timed so that they were sequentially offset by 90 degrees. The pump piston would therefore travel one complete cycle for each revolution of the cam. It should be noted that the three gang timer with four micro switches is equivalent to a four gang timer with four micro switches so long as the cams are offset by 90 degrees.

Figure 5 shows a wiring diagram of the timer and switching relays. Initial tests showed that inductive kick back from the coils burned out the micro switches after a very few hours of operation. To resolve this problem micro switches were wired to activate single throw, three-pole starting relays through a low current circuit. The starting relays were equipped with 50 u.f. capacitors to protect the relay contacts from the induced voltage arcing.

The solenoid pump was enclosed in a sealed mild steel jacket and mounted inside the refrigerated bath. A sealed conduit contained the wires which connected the pump to the external electronics. The pump was mounted horizontally in the refrigerated bath, however, it could equally well have operated in the vertical plane.

The design capacity of the magnetic solenoid pump was 2860 cc./min., but the actual capacity was approximately one half that expected. This reduction was mainly attributed to the check valves.

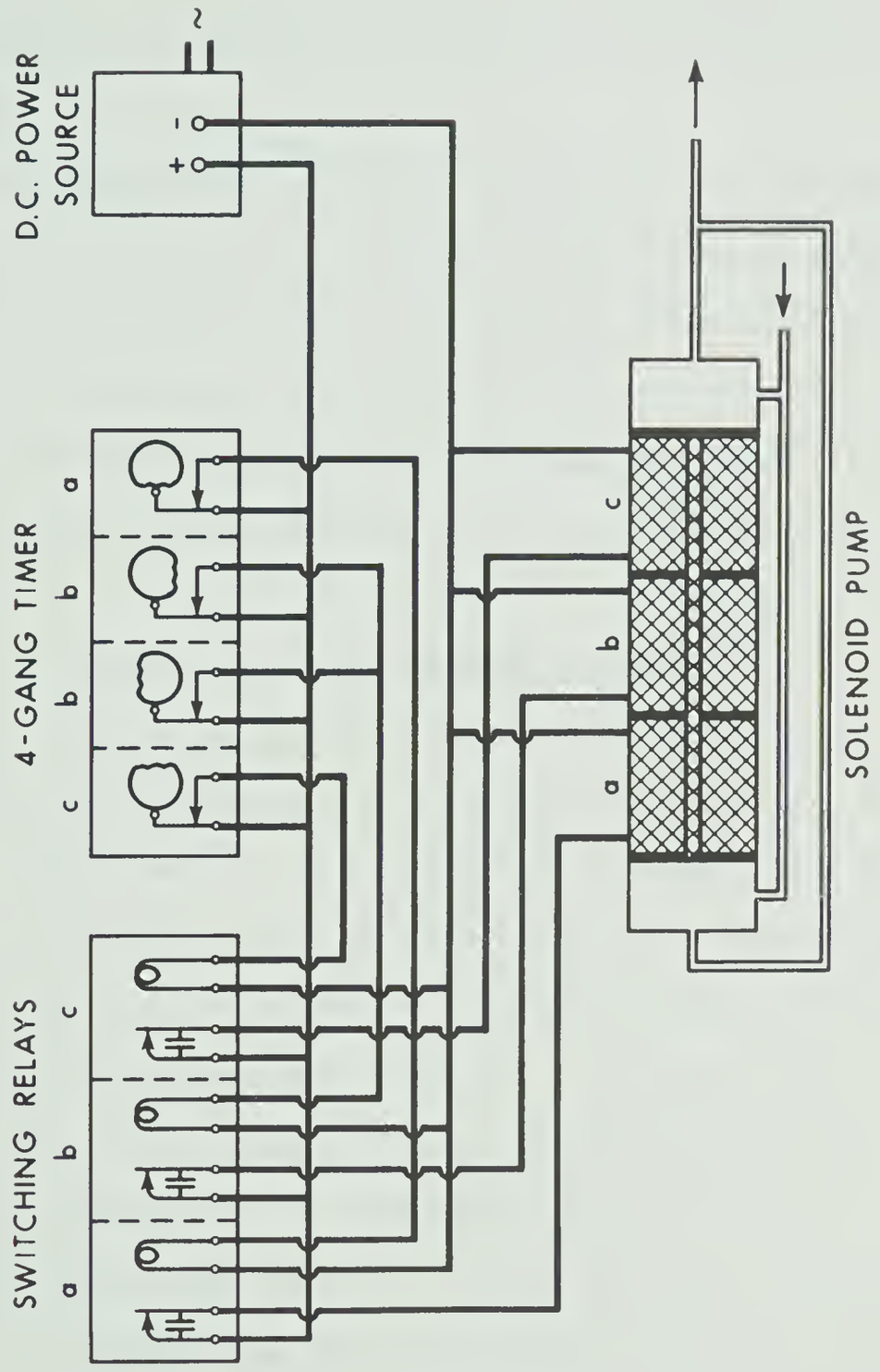


FIG. 5. SCHEMATIC WIRING DIAGRAM FOR THE SOLENOID PUMP

8. Hydrogen Presaturator

A hydrogen saturation chamber was attached to the solubility cell. This vessel was necessary as hydrogen was introduced for pressure maintenance during sampling of the saturated amine sample.

The presaturator was built of type 316 S.S. in two parts. The bottom, or saturation portion consisted of a 50 c.c. chamber for liquid amine while the upper, or liquid disengaging section was packed with steel wool supported on steel mesh screening. A check valve was mounted between the presaturator and solubility cell to prevent the formation of concentration gradients in the cell vapor phase.

9. Sampling Section and Sample Cylinders

Samples of saturated liquid amine were removed by a 1/8 inch stainless steel tube connecting the solubility cell to a sample bomb connector. The sample bomb connector was a machined block fitted with a 1/8 inch N.P.T. female thread for attaching the sample bomb and a 1/8 inch tube on which the shutoff valve was attached with a "Swagelok" connection. A fine bore hole (1/32 inch) was drilled between the two fittings to minimize the dead volume in which expansion of the sample could occur.

The sample bombs were built in two sections to provide an expansion volume when the cold amine sample was warmed. The main bomb volume of 10 c.c. was isolated from an auxiliary volume of 3 c.c. by a valve. Three 1/8 inch "Hoke" miniature forged needle

valves were used on each sample bomb.

Each sample cylinder was equipped with o-ring quick vacuum connectors. A ½ inch vacuum line was provided for evacuation of the cylinders prior to sampling.

10. Temperature Measurement

The temperature of the liquid phase in the solubility cell was measured with a 1/8 inch stainless steel sheathed copper-constantan thermocouple which was sealed in the bottom flange of the vessel by means of a "Swagelok" thermocouple connector. A "Leeds and Northrup" potentiometer was used in conjunction with the thermocouple.

The copper-constantan thermocouple was calibrated against a platinum resistance thermometer. The calibration curve is given in Figure E1-1 of Appendix E1.

11. Pressure Measurement

The equilibrium pressure within the solubility cell was measured with a "Heise" pressure gauge. The pressure range of this gauge was 0 psig. to 400 psig. All internal parts were type 316 stainless steel.

The gauge was calibrated against a dead weight tester and found to be accurate within its specified limits (±0.4 psi.) over the complete pressure range.

12. Solubility Apparatus Valves

The valves on the solubility apparatus were "Whitey" forged body valves. Two valve models were used. The amine feed

and sampling valves were model 0KS2-316 valves equipped with "Kel-F" seats and 1/8 inch "Swagelok" fittings. The hydrogen feed system has 1KS4-316 valves with "Kel-F" seats and $\frac{1}{4}$ inch "Swagelok" fittings. The valves gave good service although periodic replacement of valve stems was necessary due to the deterioration of the "Kel-F" seats.

A "Farris" 2740 series relief valve was connected to the solubility cell. This valve tended to leak and required frequent attention.

13. Hydrogen Volumetric Apparatus

A schematic diagram of the apparatus used to extract the dissolved hydrogen from a given amine sample is shown in Figure 6. The equipment consisted of two liquid nitrogen traps, a Toepler pump, a calibrated burette and a closed-end manometer. A McLeod gauge was also included as a check on the performance of the vacuum pumps.

The two liquid nitrogen traps were of the U-tube design. The main trap had a large collecting bulb (300 c.c.) at the base of the two legs. The auxiliary trap was constructed of 9 mm. tubing and was filled with glass helices.

The Toepler pump was a standard 500 c.c. manually operated pump. Compressed air and vacuum were used for manipulating the mercury level.

Two calibrated burettes were utilized in this study. A 17.07 c.c. burette was installed for low temperature solubility determinations. This was replaced by a 72.67 c.c. burette for the determinations which were conducted above 0°C. Both burettes were of the

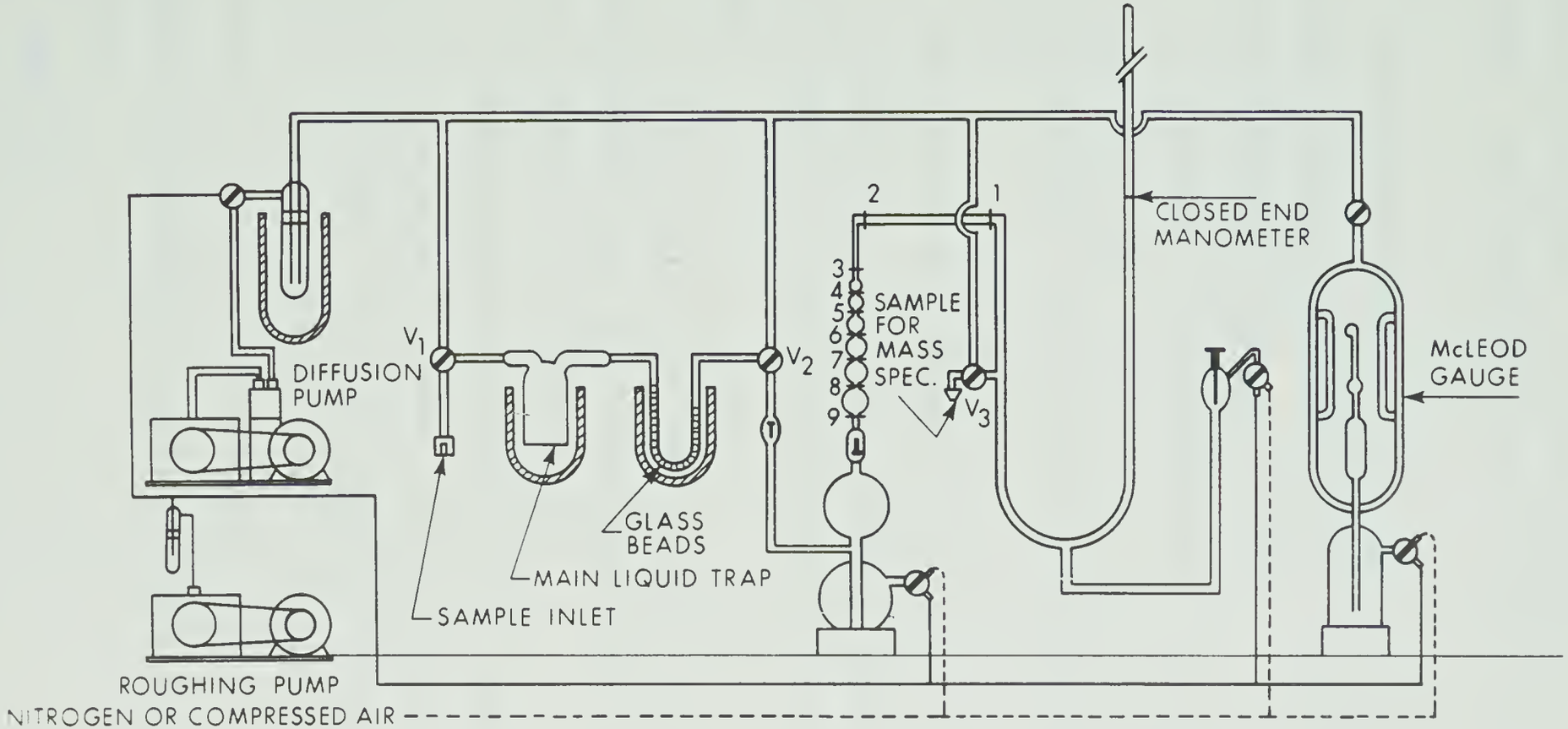


FIG 6. SCHEMATIC DRAWING OF HYDROGEN VOLUMETRIC APPARATUS

composite bulb variety. They were calibrated by a mercury weighing technique. The calibration tables are given in Appendix E1, Table E1-1.

The closed end manometer was formed from barometer tubing and evacuated in situ by the diffusion pump. Provision was made for varying the amount of mercury in the tube.

All stopcocks on the apparatus were of the hollow plug, oblique bore high vacuum type. They were lubricated with "Dow Corning High Vacuum Grease". No problems with hydrogen adsorption were observed.

The sample inlet line consisted of a short section of stainless steel tubing fitted with a quick vacuum connector. A "Kovar" section was used to join the glass tubing to the stainless steel tubing.

A hydrogen sample outlet was attached to the calibrated burettes. Hydrogen samples could then be withdrawn, after the volume was determined, for mass spectrometer analysis.

Two vacuum pumps were committed to the volumetric apparatus. A roughing pump served to remove the degassed amine from the liquid nitrogen traps after the volume determination was completed and to provide vacuum for manipulating the mercury levels in the Toepler pump and McLeod gauge. An oil diffusion pump provided the final evacuation of the complete apparatus prior to a hydrogen volume analysis.

B. Materials

The materials used in this study, along with their supplier,

are listed in Table 2. The purities and major impurities for each amine are also tabulated. The amines, which were of the highest commercially available grades, were dried according to the procedure outlined in the following section.

C. Experimental Procedure

1. Amine Purification

The following procedure was used for purifying ammonia, methylamine, and ethylamine which are normally gases at room temperature. The amine was distilled from the supply cylinder into a liquid nitrogen trap which contained freshly cut metallic lithium for drying. The rate at which the amine flowed from the cylinder to the liquid nitrogen trap was greatly increased by passing the amine through an intermediate condensing coil which was immersed in a dry ice-trichloroethylene bath. When the desired volume of amine had entered the liquid nitrogen trap, which also served as the distilling flask, the supply cylinder valve was closed and a vacuum of approximately five microns was drawn on the complete distillation assembly. The liquid nitrogen dewar was then removed and the amine allowed to melt. The amine was allowed to warm until the solution was a uniform blue color. This blue coloration was used as a criterion of dryness[68]. The time required for the formation of the blue color was dependent on the amount of water in the amines and it could be reduced by totally refluxing the liquid.

The amine was then distilled under a vacuum of approximately six inch of hg. gauge into the solubility cell charge vessel. The

TABLE 2

PURITIES OF MATERIALS USED IN THIS STUDY

Component	Supplier	Purity wt. %	Major Impurities
Ammonia	Matheson	99.95	Water 50 p.p.m. Oil 3 - 5 p.p.m.
Methylamine	Matheson	98.0	Water 0.8% max. Dimethylamine 0.8% max. Trimethylamine 0.6% max.
Ethylamine	Matheson	98.5	Diethyamine 0.5 max. Ammonia 0.6 max. Water 1.2 max.
n-Propylamine	Eastman Organic Chemicals	98.0	Water 1.32%
1,2-Propanediamine	Union Carbide Chemical Company	97.8	Water
1,2-Ethanediamine	Fisher Scientific	98 - 100	Water
Hydrogen	Matheson	Ultra-pure grade	Oxygen < 1 p.p.m. Nitrogen < 5 p.p.m. Dew Point -85°F Total Hydrocarbon As methane 0.2 p.p.m.
Lithium	Fisher Scientific	-	-
Molecular Sieves (4A)	Fisher Scientific		

initial and final portions of the liquid charge were destroyed.

N-propylamine, 1,2-ethanediamine and 1,2-propanediamine which are liquids at room temperature were initially dried by contacting with type 4A molecular sieves. The molecular sieves had been previously conditioned by heating (200°C) under vacuum for approximately 24 hours. The dried liquid amine was then poured into the distilling flask which contained freshly cut metallic lithium. The distilling flask was immersed in liquid nitrogen and the procedure described above for the lighter amines followed.

2. Solubility Determinations

Liquid amine was transferred from the charge vessel to the graduated cylinder. A known volume of liquid was then introduced to the hydrogen presaturator (25 ml.) and the solubility cell (175 ml.). The amine was forced from the charge vessel and graduated cylinder by introducing low pressure hydrogen gas to these vessels.

Purified hydrogen was introduced to the cell through the presaturation chamber. The hydrogen pressure was brought to the desired level (as set on the regulator) and the magnetic stirrer and solenoid pump started. The cell pressure would decline initially as the hydrogen was absorbed in the amine. Hydrogen was added after approximately 2 hours to restore the pressure to the value set on the regulator. It was important that the cell pressure correspond to the regulator pressure since hydrogen was introduced to the cell to maintain the pressure when liquid samples were obtained. The system was then left for approximately 8 hours to ensure equil-

ibrium of the cell contents.

The solenoid pump was turned off approximately 2 hours prior to the time of sampling. The pump would produce heat, hence this procedure was developed to ensure that the temperature of the cell contents was equal to that of the refrigerated bath. The magnetic stirrer was stopped approximately ½ hour before the liquid samples were obtained.

The procedure followed for obtaining a liquid sample was:

1) A weighed sample bomb was attached to the sample cylinder and the bomb and chamber were evacuated for approximately 20 minutes.

2) The pressure and temperature in the solubility cell were recorded.

3) The bottom two sample cylinder valves were closed and a liquid sample was introduced into the 10 c.c. chamber. (Ammonia and methylamine samples which were obtained at low equilibrium pressures required cooling of the sample bombs by either immersion in a dry ice-alcohol bath or by spraying with liquid nitrogen. This procedure was necessary as these amines would produce a pressure in the warm sample cylinders which prevented the withdrawal of a representative liquid sample.)

4) Hydrogen gas was introduced into the cell as the sample was being withdrawn.

5) The inlet sample cylinder valve was closed and the center valve opened immediately.

6) The first sample taken was released to the vacuum pump to ensure that no error arose due to the concentration gradient in the sample line. The sample cylinder was then re-evacuated and a sample obtained in the above manner.

7) The cell pressure was again recorded.

8) A second sample bomb was then connected and a liquid sample was obtained in the same manner except that no liquid was vented.

9) The sample cylinders were prepared for weighing. Care was taken to ensure that all "Teflon" sealing tape was removed from the threads and that no amine remained in the external valve ports.

10) Each sample bomb was weighed and the mass of the amine sample obtained by subtracting the mass of the empty cylinder. A "Mettler model B5C7000" analytic balance was used for all measurements.

11) A sample bomb was connected to the hydrogen volumetric apparatus.

12) The sample inlet line connecting the sample bomb and hydrogen volumetric apparatus was evacuated through valves V1 and V2 of Figure 3. The Toepler pump and collecting burette were isolated during this step.

13) When the pressure reading on the McLeod gauge was approximately 0.001 micron, valve V2 was rotated to connect the inlet sample line and cold traps to the Toepler pump.

14) The Toepler pump was operated for approximately 15 pumping strokes to draw any residual gas volume from the cold trap section and to collect it in the calibrated burette.

15) Mercury was forced from the Toepler pump into the calibrated burette. The mercury meniscus in the confining leg of the closed end manometer was constantly adjusted to maintain its position near reference mark 1 (Figure 3).

16) The mercury level in the calibrated burette was approximately set at the calibration mark corresponding to the smallest calibrated volume.

17) The mercury levels were adjusted to the calibration marks and the height of the mercury legs in the closed end manometers read with a cathetometer.

18) The temperature of the room was recorded and assumed equal to that of the enclosed gas.

19) The mercury level in the confining leg of the manometer was then lowered to a level slightly above the connection to valve V3. The mercury in the calibrated burette was lowered into the Toepler pump.

20) Liquid nitrogen dewars were placed around the cold traps.

21) The sample cylinder valve was slowly opened to control the rate of vaporization of the amine sample into the cold traps. It was necessary to apply external heat to the sample bomb when analyzing n-propylamine, 1,2-ethanediamine and 1,2-propanediamine.

22) The Toepler pump was operated for approximately 15 strokes to draw the released hydrogen into the collecting burette.

23) Valve V2, Figure 3 was then closed to isolate the cold traps from the Toepler pump. The two liquid nitrogen dewars

were removed to allow the solidified amine to melt.

24) Mercury was forced from the Toepler pump into the calibrated hydrogen burette. The mercury miniscus in the confining leg of the closed end manometer was constantly adjusted to maintain its position near reference mark 1 (Figure 3).

25) The mercury miniscus in the calibrated burette was set approximately at that calibration mark for which the enclosed hydrogen volume gave the highest readable pressure.

26) The two mercury levels were adjusted to the desired reference marks and the height of the mercury legs in the closed end manometer read with a cathetometer.

27) The temperature of the room was noted and assumed equal to that of the enclosed hydrogen. This assumption was checked by allowing a large amount of time between two sets of readings on the same volume. No change in the pressures with time was noted providing the room temperature remained constant.

28) The mercury level in the confining leg of the U-tube was then lowered and the mercury level in the calibrated burette drawn back into the Toepler pump. The hydrogen sample was retained in the calibrated burette by the Toepler pump check valve.

29) The large cold trap was immersed in liquid nitrogen. When it appeared that the amine had collected in this trap, liquid nitrogen was applied to the second trap.

30) Valve V2 was again opened to the Toepler pump and approximately 15 pumping strokes performed.

31) The mercury was again forced from the Toepler pump into the composite burette. The mercury level in the confining leg of the U-tube was again held near reference mark 1.

32) Steps (18), (19) and (20) were repeated.

33) The volume of hydrogen, corrected to S.T.P., dissolved in the weighed amount of amine was calculated from the last set of readings. If an abnormal variation of more than approximately 0.5 per cent was apparent in the two sets of readings, a third thawing and pumping operation was performed.

34) When the hydrogen volume determinations were complete, valves V1 and V2 were adjusted to connect the cold traps to the vacuum manifold.

35) The diffusion pump was isolated and the roughing pump connected, through a liquid nitrogen trap, to the manifold.

36) The liquid nitrogen dewars were removed from the amine sample traps. The amine was allowed to distill into the vacuum pump trap.

37) When no amine remained in the sample traps, the roughing pump was isolated and the diffusion pump connected to the vacuum manifold.

38) The mercury level in the calibrated burette was drawn into the Toepler pump and the mercury level in the closed end manometer was withdrawn to a level below valve V3.

39) Valve V3 was then opened to the vacuum manifold and valve V2 rotated so that the sample cold traps and Toepler pump were

connected.

40) The complete system was allowed to evacuate for approximately two hours in preparation for another volume determination. The vacuum cold trap was cleaned before or during this last step.

D. Data Reduction

The following section outlines the method used to reduce the experimental measurements to solubility units which are useful for industrial design calculations and suitable for comparison with data presented in the literature.

The solubility of hydrogen in a given amine for equilibrium conditions corresponding to a temperature T and total system pressure π was firstly expressed as the solubility coefficient

$$S^P = \frac{V_2}{W_1} \left(\frac{\text{c.c. } H_2 \text{(STP)}}{\text{gm. amine}} \right) \qquad [4.1]$$

where the superscript P refers to the hydrogen partial pressure at the equilibrium conditions.

The volume of hydrogen corrected to standard conditions of 0°C and 76.0 cm. Hg. hydrogen partial pressure (V_2) was calculated from the measurements on the hydrogen volumetric apparatus.

$$V_2 = \frac{273.15}{76.0} \left\{ \frac{V^f_{cal} \; P^f_{cor}}{T^f_k} - \frac{V^r_{cal} \; P^r_{cor}}{T^r_k} \right\} \qquad [4.2]$$

The superscripts r and f refer to the residual gas volume measurement and the final gas volume measurement as outlined in

steps (17) and (18) and steps (26) and (27) of the previous section. The volume of hydrogen which was present in the sample bomb prior to sampling was considered to be negligible. The subscript cor on the pressure measurements indicates that a correction was applied for the capillary rise in the two legs of the closed end manometer. (See Appendix C1).

The mass of the liquid amine (W_1), in which the corrected hydrogen volume (V_2) was dissolved, was calculated by subtracting the mass of the dissolved hydrogen from the mass of solution.

$$W_1 = W_s - W_2 \qquad [4.3]$$

$$W_2 = \frac{2.016\ V_2}{22414.6} \qquad [4.4]$$

The mole fraction dissolved hydrogen corresponding to the solubility coefficient S^P was calculated from the relationship:

$$x_2^P = \frac{1}{\left(\frac{22414.6}{M_1 S^P} + 1\right)} \qquad [4.5]$$

The solubility of hydrogen in the various amines was assumed to obey Henry's law at the temperatures and pressures of this study. Hence, at a given temperature T

$$P_2 = H_2\ x_2^P \qquad [4.6]$$

where the hydrogen partial pressure is given by:

$$P_2 = \pi - P_1^s(1 - x_2^P) \qquad [4.7]$$

Henry's law coefficient was obtained by substituting equation [4.7] into equation [4.6].

$$H_2 = \frac{\pi - P_1^s(1 - x_2^P)}{x_2^P} \qquad [4.8]$$

A sample calculation based on the above procedure is given in Appendix C1. An error analysis corresponding to the experimental conditions of the sample calculation is also presented.

The experimentally determined Henry's law coefficients were correlated with temperature in the manner suggested by Hildebrand[12].

$$\ln H_2 = f\left(\frac{1}{T}\right) \qquad [4.9]$$

The form of equation [4.9] used by Hildebrand[12] and Himmelblau[20] (limited temperature range) was:

$$\ln H_2 = A + \frac{B}{T} \qquad [4.10]$$

The experimental data were fit to an equation of this form using a linear least square fitting routine. A first order equation describing the temperature dependence of the Henry's law coefficient was desirable for ease in using the data for future calculations.

It was apparent, however, that for some of the amines there was a slight curvature in the plot of the logarithm of Henry's law coefficient versus the reciprocal of absolute temperature. This behavior was consistent with the observation of Prausnitz and Chueh[106], who used a fifth degree polynomial to represent the solubility of hydrogen in various solvents.

$$\ln H_2 = A_0 + \frac{A_1}{T} + \frac{A_2}{T^2} + \frac{A_3}{T^3} + \frac{A_4}{T^4} + \frac{A_5}{T^5} \qquad [4.11]$$

A best fit equation of degree five or less was therefore obtained using a "Forsythe" fitting routine. The best fit equation was determined from the minimum standard deviation which was defined as:

$$\sigma = \sqrt{\frac{\sum_{i=1}^{N} (d_i)^2}{N - M - 1}} \qquad [4.12]$$

where $d_i = (\ln H_2)_{exp} - (\ln H_2)_{cal}$

N = number of data points

M = degree of polynomial

The best fit polynomials were used to calculate smoothed values of Henry's law coefficient over the temperature range of this study. In addition to the calculation of Henry's law coefficient, the mole fraction hydrogen, which would exist at the same temperature if the hydrogen partial pressure was one atmosphere, and the Keunan coefficient were also calculated.

$$x_2' = \frac{1}{H_2} \qquad [4.13]$$

$$S = \frac{22414.6}{M_1 (H_2 - 1)} \qquad [4.14]$$

These latter two solubility coefficients are useful for comparison with other data and for hand calculations since:

$$x_2^P = x_2' P_2 \qquad [4.15]$$

$$S^P \cong S\ P_2 \qquad [4.16]$$

E. Experimental Results

The results of the experimental determination on the solubility of hydrogen in ammonia, methylamine, ethylamine, n-propylamine, 1,2-propanediamine and 1,2-ethanediamine are listed in Tables A1-1 to A1-6, respectively in Appendix A1. The individual determinations for each amine have been arranged according to the date of sampling. The experimental data are presented as a solubility coefficient (S^P), mole fraction dissolved hydrogen (x^P) and Henry's law coefficient (H_2). The temperature, total pressure and hydrogen partial pressure of the solubility cell contents at the time of sampling are also listed. The hydrogen partial pressure was calculated from equation [4.7].

A plot of the logarithm of the experimentally determined Henry's law coefficient versus the reciprocal of absolute temperature is given for each of the amines in Figures 7 to 12. The coefficients determined for a first degree fit of the individual curves are presented in Table 3.

The experimental data for the solubility of hydrogen in ammonia, methylamine, ethylamine and n-propylamine as plotted in Figures 7 to 12 can be seen to display a slight departure from linearity. The best fit equations, for each of the above mentioned amines are summarized in Table 4.

It can be seen that a considerable reduction in the standard deviation for the individual components is obtained by correlating the data with a polynomial of degree greater than one. The range

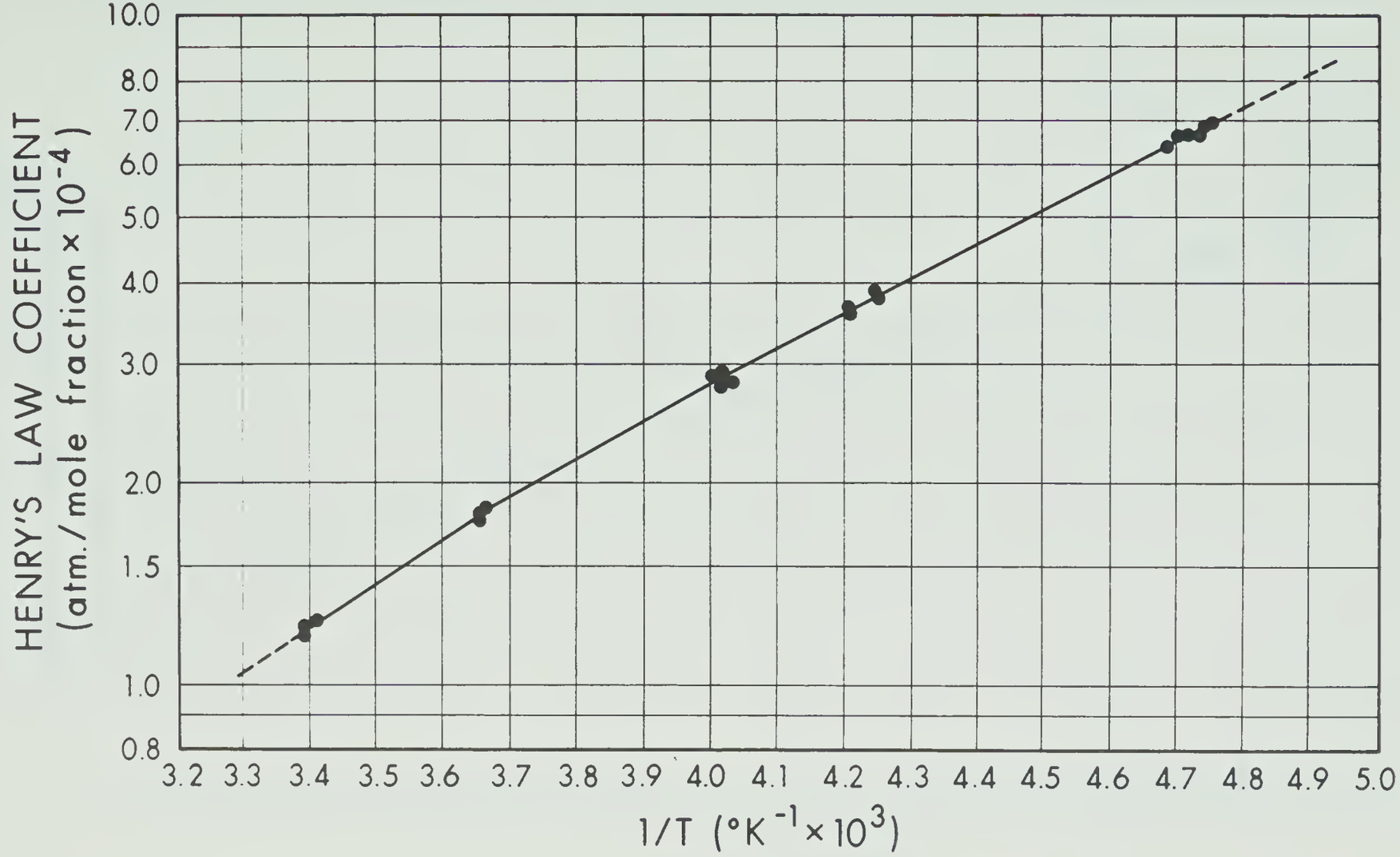


FIG. 7. THE SOLUBILITY OF HYDROGEN IN AMMONIA

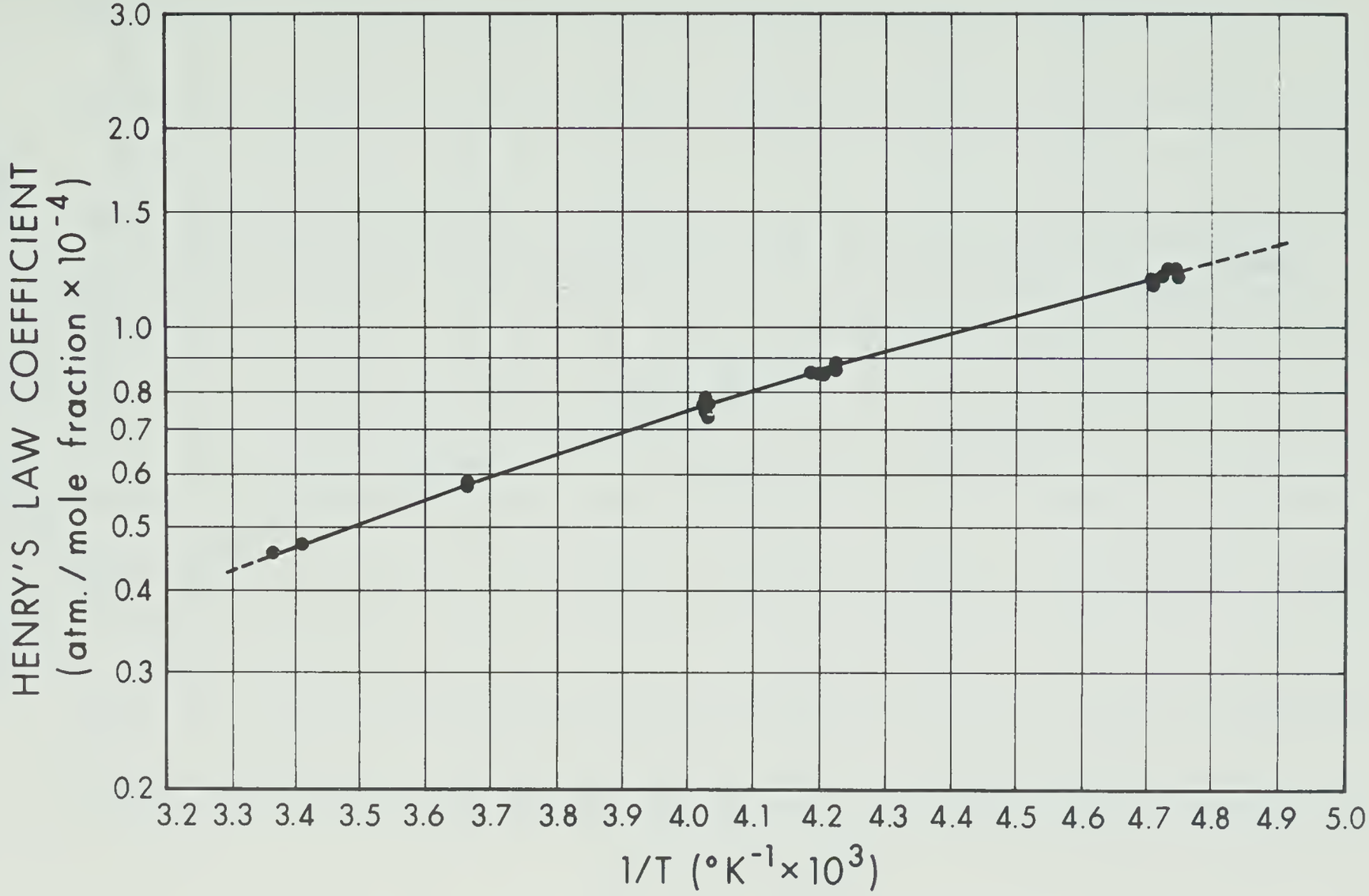


FIG. 8. THE SOLUBILITY OF HYDROGEN IN METHYLAMINE

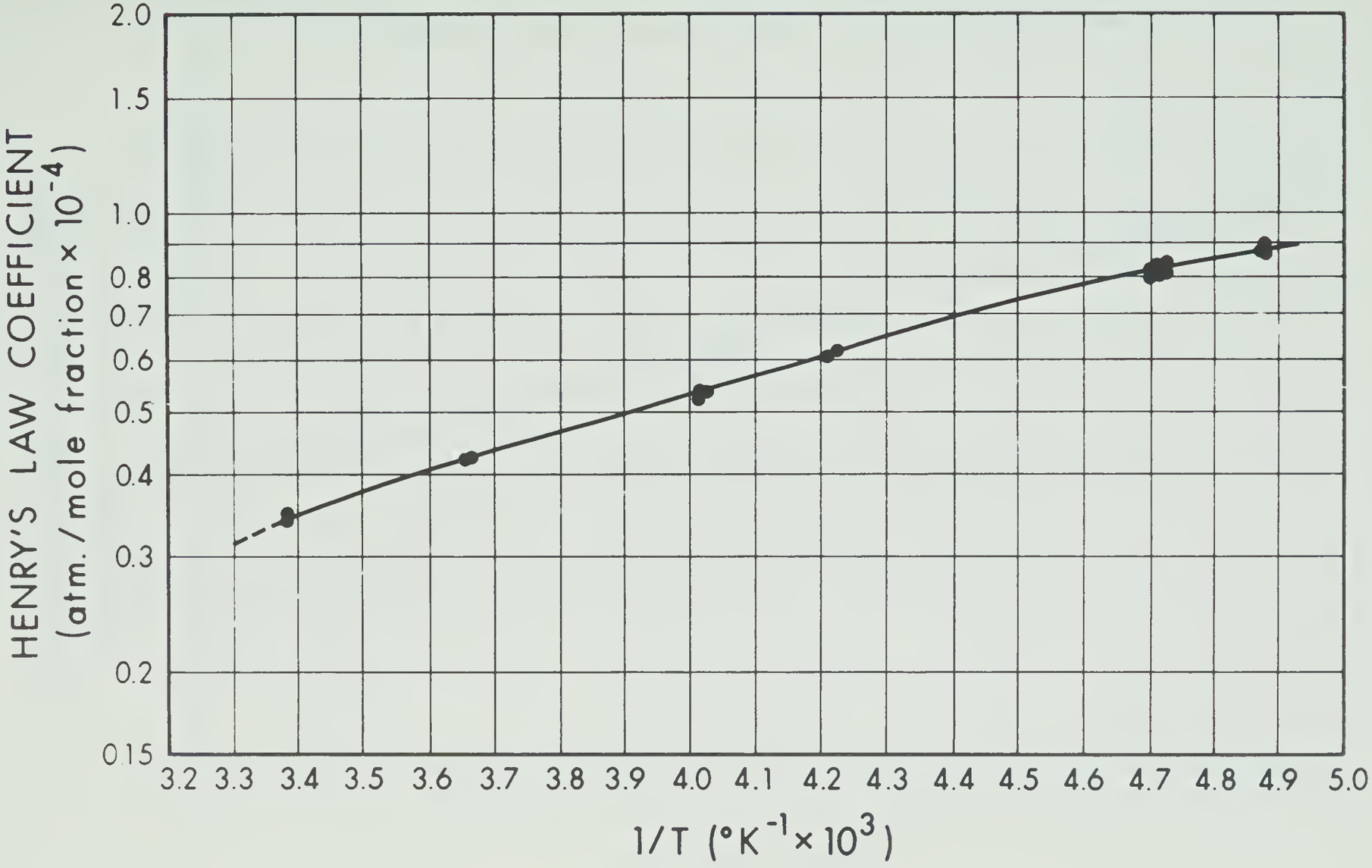


FIG. 9. THE SOLUBILITY OF HYDROGEN IN ETHYLAMINE

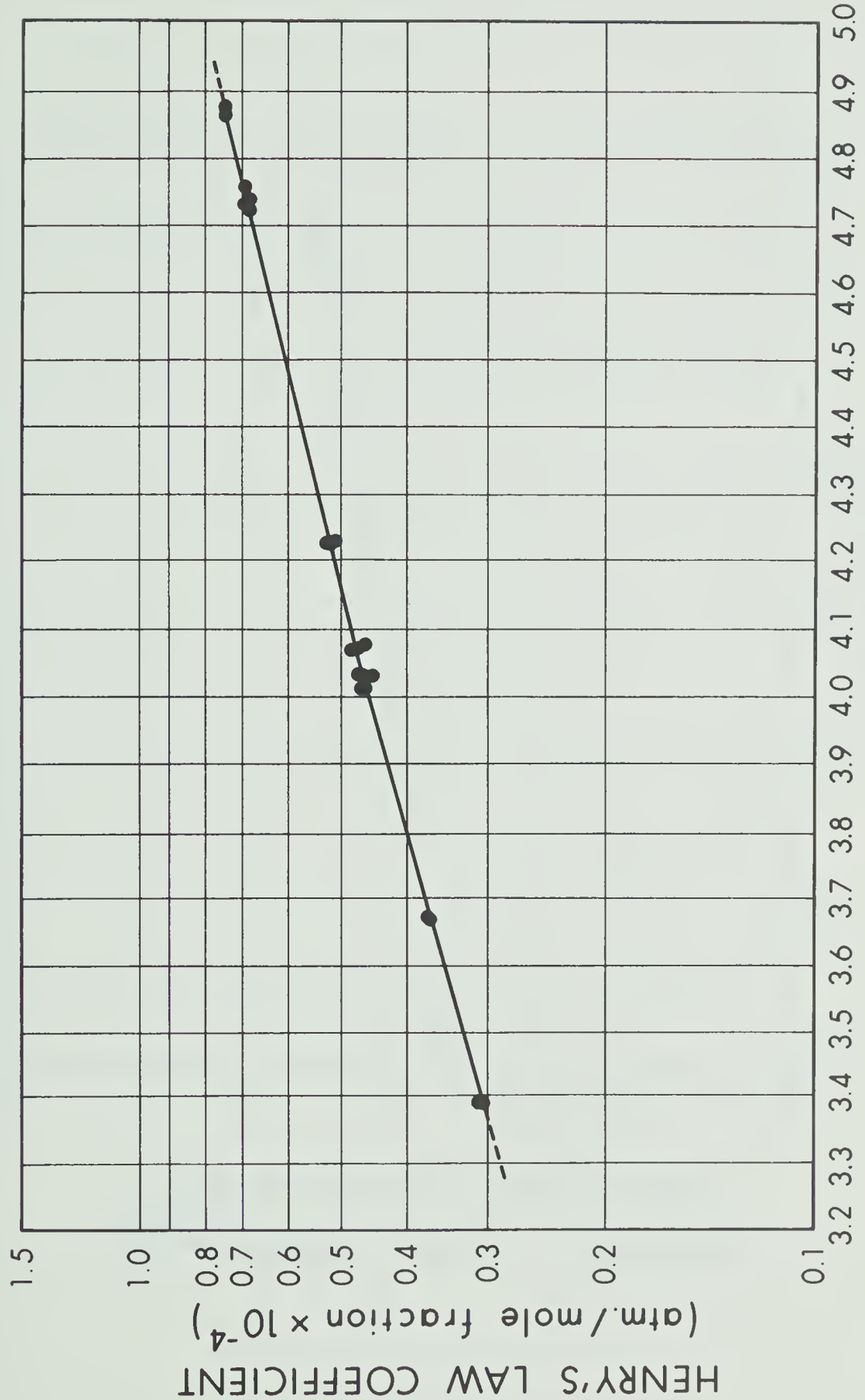


FIG. 10. THE SOLUBILITY OF HYDROGEN IN N-PROPYLAMINE

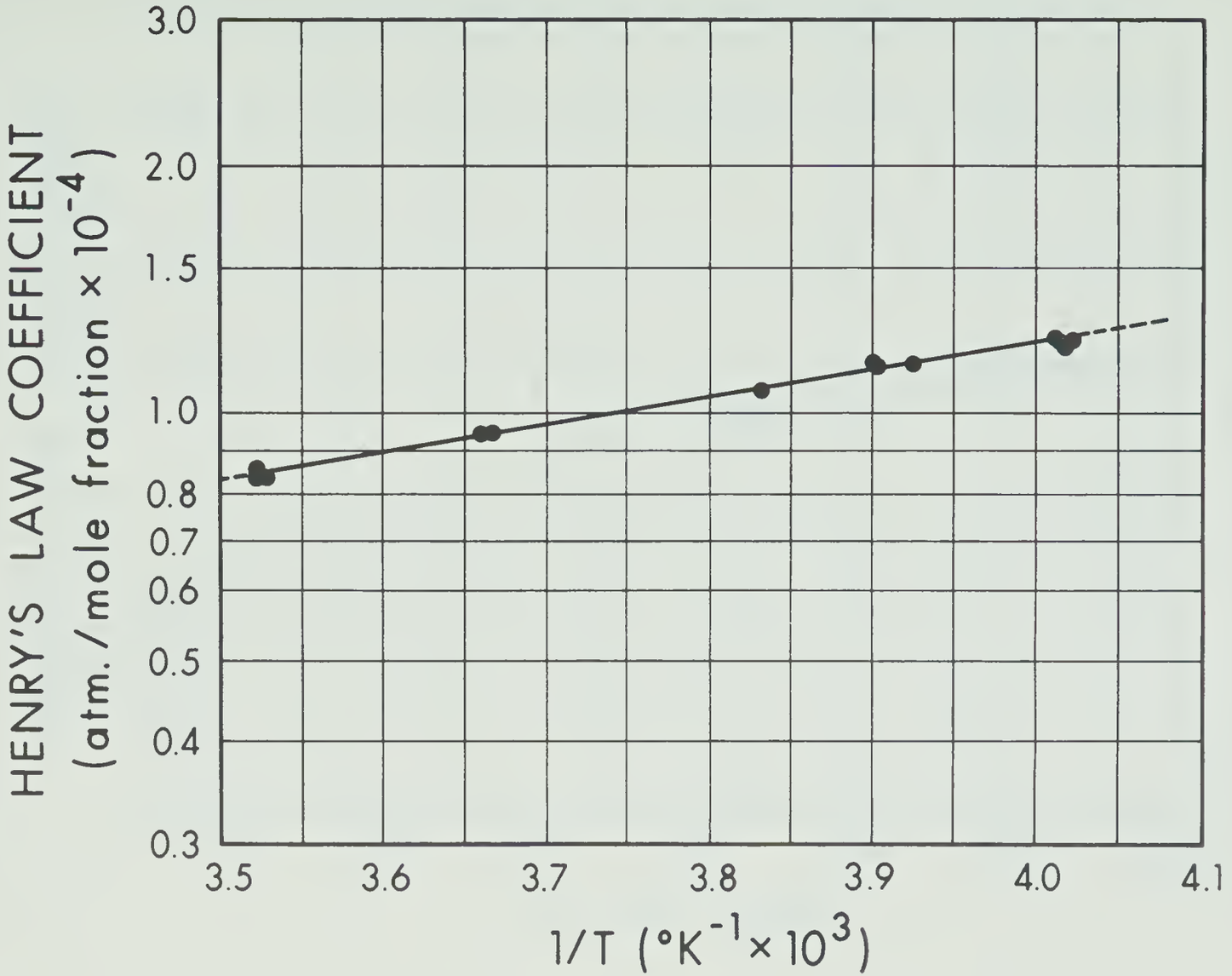


FIG. 11. THE SOLUBILITY OF HYDROGEN IN 1,2-PROPANEDIAMINE

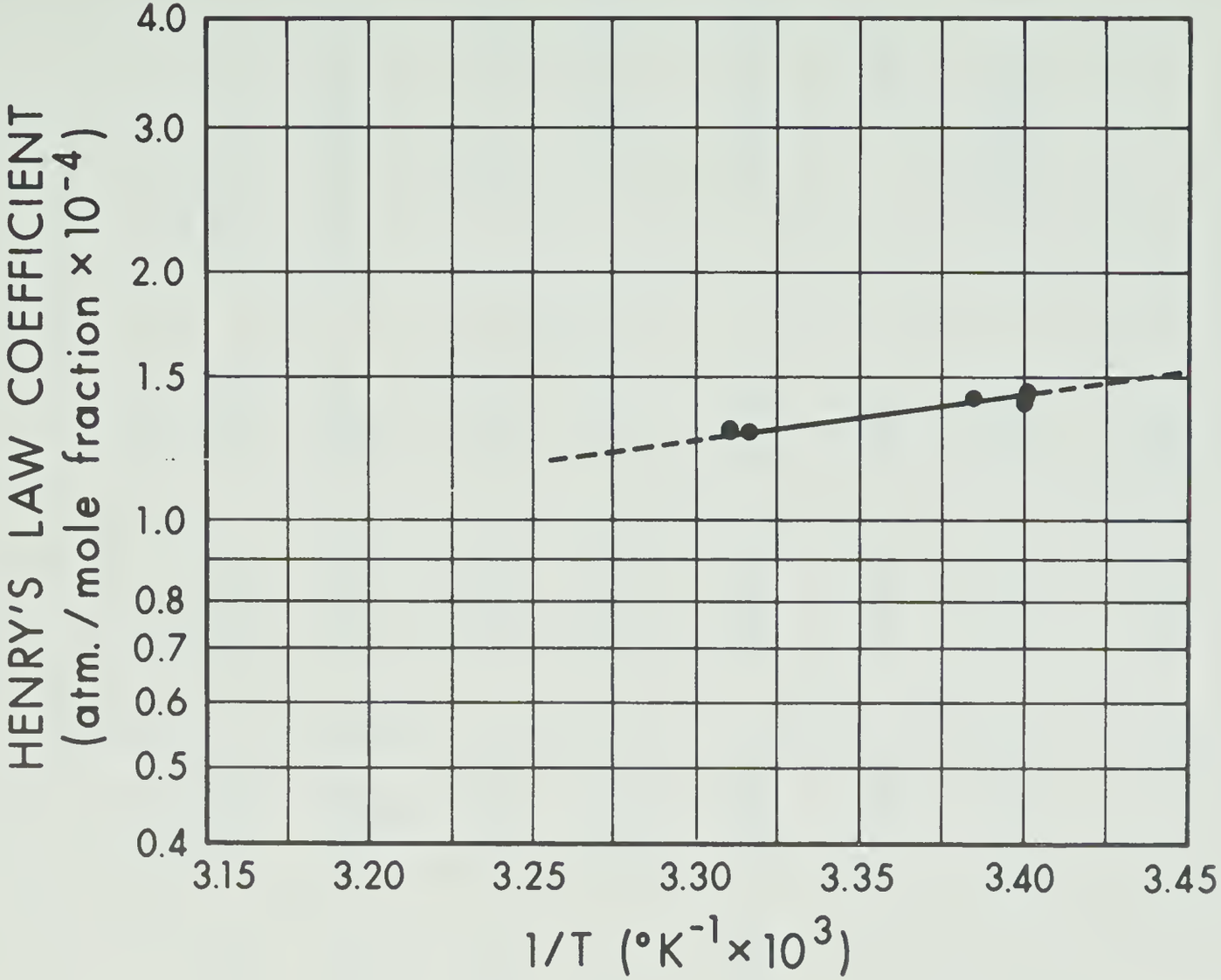


FIG. 12. THE SOLUBILITY OF HYDROGEN IN 1,2-ETHANEDIAMINE

TABLE 3

EFFECT OF TEMPERATURE ON HENRY'S LAW COEFFICIENT

$$\ln H_2 = A + \frac{B}{T}$$

Component	A	B	σ	Temperature Range
Ammonia	5.1981	125.40	0.02941	-62°C to +22°C
Methylamine	6.1092	700.95	0.02542	-62°C to +23°C
Ethylamine	6.0640	622.87	0.01989	-68°C to +23°C
N-propylamine	6.1058	581.55	0.01635	-68°C to +22°C
1,2-propanediamine	6.3524	765.38	0.01342	-25°C to +11°C
1,2-ethanediamine	5.5842	1186.74	0.00775	+25°C to +34°C

TABLE 4

EFFECT OF TEMPERATURE ON HENRY'S LAW COEFFICIENT

BEST FIT POLYNOMIAL

$$\ln H_2 = A_0 + A_1 \beta + A_2 \beta^2 + A_3 \beta^3 + A_4 \beta^4 + A_5 \beta^5$$

$$\beta = \frac{10000.0}{T}$$

Component	A_0	A_1	A_2	A_3	A_4	A_5	σ
Ammonia	-4.7907	8.1917	-1.5872	0.1196			0.01554
Methylamine	4.1403	1.6612	-0.1160				0.01324
Ethylamine	-480.0271	587.8376	-282.3599	67.5366	-8.0334	0.3801	0.01133
N-Propylamine	5.0287	1.0975	-0.0612				0.01240

of temperatures over which the solubilities were measured have been ommitted from Table 4 as the values correspond with those listed in Table 3.

Smoothed data for the solubility of hydrogen in ammonia, methylamine, ethylamine, n-propylamine, 1,2-propanediamine and 1,2-ethanediamine are presented in Tables B1-1 to B1-6, Appendix B1. These data were generated by a computer program based on the best fit equation for each amine. The smooth curve drawn through the experimental data points in Figures 7 to 12, represents the best fit polynomial for the given amine.

F. Reduction of Literature Data on Solubility of Hydrogen in Ammonia

The solubility of hydrogen in ammonia has been measured by several investigators. In order to compare the data obtained in this study with that presented in the literature, it was necessary to reduce all the data to a common basis. The unit of solubility chosen for the purpose of comparison was Henry's law coefficient. The inverse of Henry's law coefficient, or the mole fraction hydrogen which would be dissolved in liquid ammonia under a hydrogen partial pressure of one atmosphere, was also calculated.

A variety of solubility coefficients have been used by the various authors. The coefficients differ not only in terms of the quoted units but also in the reported conditions of the equilibrium mixture. A brief discussion is therefore given as to the pro-

cedure used in reducing the data of the various authors. The basic assumptions applied to all the data were:

1) The vapor phase behaves as an ideal gas.

2) Poynting's correction is negligible.

3) Henry's law is obeyed.

a) Wiebe and Tremearne[73]

Their data on the solubility of hydrogen in liquid ammonia at 25°C and at total pressures of 25, 50, 75, 100 and 150 atmospheres were analyzed in the following manner.

1) The solubility coefficient $S^P \left(\frac{\text{c.c. } H_2 \text{ (STP)}}{\text{gm. } NH_3} \right)$ was converted to mole fraction hydrogen.

$$x^P = \frac{1}{\frac{22414.6}{17.03\ S^P} + 1} \qquad [4.17]$$

2) The hydrogen partial pressure was calculated.

$$P_2 = \pi - P_1^s(1 - x_2^P) \qquad [4.18]$$

The mole fraction hydrogen was then plotted versus the hydrogen partial pressure, the curve passing through the origin. The slope of this curve at the origin was taken as Henry's law coefficient. The mole fraction hydrogen at one atmosphere partial pressure was:

$$x_2^1 = \frac{1}{H_2} \qquad [4.19]$$

b) Wiebe and Gaddy[62]

The solubility coefficient for hydrogen in liquid ammonia

at 0°C and total pressures of 50 and 100 atmospheres were converted to Henry's law coefficients and mole fraction hydrogen at one atmosphere hydrogen partial pressure in the manner outlined above.

c) Ipatiew and Teodorowich[72]

Ipatiew and Teodorowich measured the solubility of hydrogen in liquid ammonia at 25°C and at pressures up to 250 atmospheres. Their data were presented as cubic centimeters of hydrogen at S.T.P. per 100 c.c. of liquid ammonia.

1) The solubility coefficient was converted to the form of Wiebe and Tremearne[73].

$$S^P = \frac{\alpha''}{100\ \rho_l} \left(\frac{\text{c.c. } H_2 \text{(STP)}}{\text{gm. } NH_3} \right) \qquad [4.20]$$

where α'' is the solubility coefficient of Ipatiew and Teodorowich.

The mole fraction hydrogen was then calculated from equation [4.17]. A plot of the mole fraction dissolved hydrogen versus the listed pressures of 15, 100, 200 and 250 atmospheres resulted in a curve which passed through the origin. As the vapor pressure of ammonia at 25°C is 10.2 atmospheres, it was apparent that the quoted equilibrium pressures were hydrogen partial pressures rather than total pressures. Henry's law coefficient was determined from the slope of the plotted curve at the origin and the mole fraction hydrogen at one atmosphere hydrogen partial pressure was determined according to equation [4.19].

d) Larson and Black[63]

The solubility coefficients presented by Larson and

Black for hydrogen dissolved in liquid ammonia were determined by analyzing the total volume and concentration of gas dissolved when a 3:1 hydrogen-nitrogen mixture was contacted with liquid ammonia. The procedure used to obtain Henry's law coefficients for hydrogen dissolved in liquid ammonia was:

1) The solubility coefficient S_P, as quoted for hydrogen, was converted to mole fraction hydrogen using equation [4.17]

2) The hydrogen partial pressure was calculated.

In the vapor phase

$$Y_2 = 3Y_3 \qquad [4.21]$$

where the subscripts 2 and 3 refer to hydrogen and nitrogen respectively.

From Dalton's law:

$$Y_2 \pi + Y_3 \pi = \pi - P_1^s(1 - x_2 - x_3) \qquad [4.22]$$

Equation [4.21] was substituted into equation [4.22] yielding:

$$Y_2 = \frac{3}{4}\left\{\frac{\pi - P_1^s(1 - x_2 - x_3)}{\pi}\right\} \qquad [4.23]$$

The hydrogen partial pressure was therefore:

$$P_2 = Y_2 \pi = \frac{3}{4}\{\pi - P_1^s(1 - x_2 - x_3)\} \qquad [4.24]$$

Subscript 1 refers to the liquid ammonia. The data of Larson

and Black[63] were presented at total pressures of 50, 100 and 150 atmospheres and at various temperatures in the range -25°C to +22°C. Henry's law coefficients were calculated for each determination and plotted as the natural logarithm of Henry's law coefficient versus the reciprocal of absolute temperature. The values calculated at total pressures of 50 and 100 atmospheres were found to lie on one curve, but the values determined from the 150 atmosphere measurements were consistently above the line. The 150 atmosphere values were therefore discarded and the values of Henry's law coefficient as presented in Table (5-1) were based on the data of the two remaining isobars.

e) Bar-Eli and Klein[76]

Bar-Eli and Klein measured the solubility of hydrogen deuteride in a solution of potassium amide dissolved in liquid ammonia. The data were presented for temperatures of -41.6°C and -64.0°C in the form of a modified Bunsen coefficient (ml. H_2(STP)/ml. NH_3/atm.). Assuming a hydrogen partial pressure of one atmosphere, the solubility coefficient of Bar-Eli and Klein[76] was converted to a Keunan coefficient (S) and the mole fraction hydrogen at one atmosphere partial pressure calculated from equation [2.85].

$$S = \frac{\alpha''' \times 1 \text{ atm.}}{\rho_1} \qquad [4.25]$$

$$x_2^1 = \frac{1}{\frac{22414.6}{17.03\ S} + 1} \qquad [2.85]$$

Henry's law coefficient is the inverse of the mole fraction hydrogen at one atmosphere partial pressure.

f) Dirian et. al.[78]

The equation of Dirian was used to calculate the mole fraction hydrogen at one atmosphere hydrogen partial pressure and Henry's law coefficients for temperatures of 25°C, 0°C, -20°C, -41.6°C and -64°C. The solubility coefficient used by Dirian et al[78] was grams of hydrogen per milliliter of liquid ammonia. The hydrogen partial pressure was one atmosphere. This coefficient was converted to a Keunan coefficient and the mole fraction hydrogen at one atmosphere hydrogen partial pressure and Henry's coefficient were calculated from equation [2.85] and [2.86].

$$S = \frac{22414.6}{2.016 \times 1.000028} \left(\frac{\tau}{\rho_l}\right) \qquad [4.26]$$

5. DISCUSSION OF RESULTS

A. The Solubility of Hydrogen in Liquid Ammonia - Comparison of Present Results with Those Tabulated in the Literature

In the present study the solubility of hydrogen in liquid ammonia was measured at total pressures up to 300 psig. and at various temperatures in the range -62°C to +22°C. These data were reduced to Henry's law coefficients and correlated with respect to temperature. The best fit equation describing the solubility of hydrogen in liquid ammonia (Table 4) was used to calculate Henry's law coefficients at temperatures for which literature values are available. The calculated values, along with the reduced literature values are summarized in Table 5. The per cent deviation has been defined as:

$$\% \text{ deviation} = \left\{ \frac{(H_2)_1 - (H_2)_2}{(H_2)_2} \right\} 100 \qquad [5.1]$$

where the subscripts 1 and 2 refer to the literature value and the value measured in this study respectively.

The solubility data of Larson and Black[63] are in good agreement with the data obtained in this study over the complete temperature range of their work (-22°C to +25°C). The solubility of hydrogen in liquid ammonia at 25°C, as measured by Wiebe and Tremearne[73], agrees well with the value determined in the present study but a discrepancy is apparent when comparing the above two values with that measured by Ipatiew and Teodorowich[72]. The Henry's law coefficient determined at 0°C in this study is in

TABLE 5

SOLUBILITY OF HYDROGEN IN LIQUID AMMONIA

COMPARISON WITH LITERATURE DATA

Temperature	This Study		Literature		% Deviation	Reference
°C	$x_i \times 10^4$	$H_i \times 10^{-4}$	$x_i \times 10^4$	$H_i \times 10^{-4}$		
25	.8755	1.142	0.8680	1.152	+ 0.85	Wiebe and Tremearne [73]
25	.8755	1.142	0.8156	1.226	+ 6.84	Ipatiew and Teodorowich [72]
25	.8755	1.142	0.8621	1.16	+ 1.53	Larson and Black [63]
25	.8755	1.142	0.7956	1.257	+ 9.12	Dirian et al [78]
0	.5565	1.7968	.5429	1.842	+ 2.44	Wiebe and Gaddy [62]
0	.5565	1.7968	.5618	1.78	- 0.95	Larson and Black [63]
0	.5565	1.7968	.5466	1.829	+ 1.78	Dirian et al [78]
-20	.3808	2.6258	.3774	2.65	+ 0.89	Larson and Black [63]
-20	.3808	2.6258	.3881	2.577	- 1.92	Dirian et al [78]
-41.6	.2447	4.087	.2549	3.923	- 4.17	Dirian et al [78]
	.2447	4.087	.2743	3.646	-12.10	Bar-Eli & Klein [76]
-64.0	0.1415	7.069	.1521	6.574	- 7.50	Dirian et al [78]
	0.1415	7.069	.1238	8.080	+12.50	Bar-Eli and Klein [76]

fair agreement with the corresponding value as measured by Wiebe and Gaddy[62].

Henry's law coefficients calculated from the high pressure data of the above authors[62,63,72,73] could tend to be too high if the pressures at which the data were determined fall outside the region in which Henry's law could be assumed valid. As a graphical extrapolation technique is very dependent on the points in the immediate vicinity of the extrapolation, the slope of the extrapolated curve depends on the nature of the line connecting the origin with those data points which were measured at the lowest pressures. If the lowest pressure points are outside Henry's law region, the net effect is an increase in Henry's law coefficient. This effect was noted in the data of all the investigators when the experimental pressure was above 200 atmospheres.

The agreement between the Henry's law coefficients measured in this study with those calculated from the equation of Dirian et al[78] is satisfactory in the temperature region -20°C to 0°C. Significant deviations are apparent at the temperature extremes. Dirian[78] does not list the source of the data used in developing his equation and it is likely that the observed difference in the temperature dependence of his equation and the present results is due to solubility data being available to him for a limited temperature range.

The solubility coefficients as determined by Bar-Eli and Klein[76] display a significant deviation from the values obtained in this study. Their results could be expected to deviate somewhat due to

the nature of their system (HD dissolved in a solution of potassium amide in liquid ammonia), however, the very strong temperature dependence of their data is not consistent with the observations of this study or the observations of Larson and Black[63].

B. The Solubility of Hydrogen in Liquid Amines - Comparison of Present Results with those Calculated from Semi-Empirical Correlations

Several empirical or semi-empirical correlations are available for predicting the solubility of gases in liquids. As the theory of solutions is still not well understood, many of the correlations have been developed for nonpolar liquids. One would not expect their correlations to be satisfactory for predicting the solubility of hydrogen in polar, associated liquids such as the amines studied in this work.

The two initial predictive methods considered were based on the regular solution theory of Hildebrand[12]. The use of these methods required the calculation of a solubility parameter δ_1 for each of the six liquids studied. The temperature chosen for the comparisons was 25°C.

Hildebrand and Scott[12] have summarized the various methods for calculating the liquid solubility parameters. They indicate that it is a waste of effort to seek high precision in the evaluation of δ_1 as the energy of mixing theory is only approximate. However, they stress that it is important that the solubility parameters be calculated in a consistent manner at the same reference temperature.

Calorimetrically determined heat of vaporization data were available at 25°C for ammonia, methylamine and ethylamine. The solubility parameters for the above amines were calculated from the following relationship[12].

$$\delta_1 = \left[\frac{\Delta H - RT}{V_1^L}\right] \qquad [5.2]$$

No heat of vaporization data for n-propylamine, 1,2-propanediamine and 1,2-ethanediamine were available at the reference temperature of 25°C. The Clausius - Clapeyron equation was used to estimate ΔH from the vapor pressure data.

$$\frac{\partial \ln P_1^s}{\partial T} = \frac{\Delta H}{RT^2} \qquad [5.3]$$

The liquid molar volume at 25°C for each amine was calculated from the pure component density and molecular weight.

$$V_1^L = \frac{M_1}{\rho_1} \qquad [5.4]$$

The solubility coefficient for each amine was calculated and these coefficients are listed in Tables 6 and 8.

The correlation of Prausnitz and Shair[43] was first used to estimate the solubility of hydrogen in the various amines. The mole fraction hydrogen dissolved in the amine when the hydrogen partial pressure is one atmosphere is given by

$$\frac{1}{x_2} = H_2 = \frac{f_2^H}{f_2^{\circ g}} \exp\left[\frac{\bar{V}_2^L(\delta_1 - \delta_2)^2 \psi_1^2}{RT}\right] \qquad [2.79]$$

The assumptions underlying this correlation are summarized in Chapter 2.

The hypothetical liquid fugacity f_2^H is an empirically determined quantity. Its value at 25°C was read from Figure 2 of the paper by Prausnitz[43]. The solubility parameter and molar volume of the dissolved hydrogen were determined by Prausnitz and Shair[43] to be:

$$\delta_2 = 3.25 \left(\frac{\text{cal.}}{\text{c.c.}}\right)^{\frac{1}{2}}$$

$$\bar{V}_2^L = 31.0 \left(\frac{\text{c.c.}}{\text{gm. mole}}\right) \qquad [5.5]$$

The solvent volume fraction (ψ_1) was assumed equal to unity due to the very low concentration of hydrogen in the liquid phase.

A summary of the calculated (Equation [2.79]) and experimental hydrogen mole fractions at one atmosphere hydrogen partial pressure is given in Table 6. The best fit equation was used to calculate the experimental value for each amine. Dielectric constants at 25°C and one atmosphere pressure are also listed for the six amines.

The agreement between the calculated solubilities and the experimental coefficients is poor. This is due to the fact that equation [2.79] was derived for nonpolar liquids. The magnitude of the percent deviations (see equation [5.1] for the definition of the percent deviation) appears to be related to the magnitude of the dielectric constant. This same behavior was noted by Gjaldbaek[107] who studied the solubility of hydrogen, oxygen and carbon monoxide in a series of polar solvents. Gjaldbaek explained the phenomena by assuming that the molecules of the solvent induce moments in

TABLE 6

THE SOLUBILITY OF HYDROGEN IN AMINES AT 25°C

CORRELATION OF PRAUSNITZ AND SHAIR

f_2^H = 620 atm. $f_2^{\circ g}$ = 1 atm.

Component	δ_r	Mole frac. x 10^4 Eqn. [2.79]	Mole frac. x 10^4 This Study	% Deviation	ε
Ammonia	12.14	0.2673	0.8755	-69.5	16.26
Methylamine	10.45	1.073	2.231	-51.9	9.4
Ethylamine	9.34	2.318	2.990	-22.5	6.1
N-propylamine	9.1	2.666	3.284	-18.8	5.5
1,2-propanediamine	10.6	0.9518	1.338	-28.9	-
1,2-Ethanediamine	12.3	0.2230	0.7030	-68.3	13.7

the molecule of the solute gas, which results in an increased attraction between the solute and solvent. The solubility of the solute in the polar solvent is therefore enhanced as compared to its solubility in a nonpolar solvent which has the same solubility parameter.

Yen and McKetta[44] extended the work of Prausnitz and Shair[43] to include the solubility of nonpolar gases in polar, nonassociated liquids. In order to determine if any of the amines studied in the present work could be considered as polar, nonassociated liquids, Pauling's criterion as presented by Yen and McKetta[44] and Gjaldbaek and Anderson[108] was used. Yen and McKetta have presented a plot of the dielectric constant at 25°C and one atmosphere pressure versus the dipole moment (gas phase) for a number of polar liquids. The polar liquids which were nonassociated fell on a smooth, continuous curve while those which were capable of association fell above the curve.

The following values of the dielectric constant and dipole moment for the amines, along with the curve of Yen and McKetta[44] were used to determine which amines were nonassociated.

It was concluded that only ethylamine and n-propylamine (assuming value of ε for iso-propylamine is representative of value for n-propylamine) could be considered as nonassociated liquids. The solubility of hydrogen in these amines should therefore agree with that predicted by the Yen and McKetta[44] correlation. Ammonia, 1,2-ethanediamine and methylamine were the most highly associated

TABLE 7

AMINE DIELECTRIC CONSTANTS (25°C) AND DIPOLE MOMENTS

Component	ε (25°C)	μ (debye)
Ammonia	16.26	1.47
Methylamine	9.4	1.31
Ethylamine	6.1	1.3
N-propylamine	5.5[a]	1.4
1,2-propanediamine	-	1.95[b]
1,2-ethanediamine	13.7	1.92

[a] Value of ε quoted is that of iso-propylamine @ 20°C[88]

[b] value of μ quoted is that of 1,3-propanediamine[87]

amines and were expected to display a large deviation from the correlation of the above authors. Unfortunately, no data on the dielectric constant of 1,2-propanediamine could be found..

The semi-empirical correlation developed by Yen and McKetta[44] is of the form:

$$\frac{1}{x_2} = H_2 = \frac{f_2^H}{f_2^{\circ g}} \exp\left[\frac{\bar{V}_2^L(\delta_1^2 + \delta_2^2 - 2\delta_2(\delta_1^2 + \Delta)^{\frac{1}{2}}\ \psi_1^2}{RT}\right] \qquad [2.82]$$

Equation [2.82] differs from equation [2.79] of Prausnitz and Shair[43] by the inclusion of the polar characteristic factor $\Delta\left(\frac{cal.}{c.c.}\right)$. Values of Δ have been presented by Yen and McKetta in graphical form as a function of the solvent solubility parameter (δ_1). The empirical parameters f_2^H, δ_2, and $\bar{V}_2^L$ were re-evaluated by Yen and McKetta. The values of f_2^H corresponded closely with those of Prausnitz and Shair[43], however the values of δ_2 and $\bar{V}_2^L$ were calculated to be:

$$\delta_2 = 3.83 \left(\frac{cal.}{c.c.}\right)^{\frac{1}{2}}$$

$$\bar{V}_2^L = 37.3 \frac{c.c.}{gm.\ mole} \qquad [5.6]$$

The hypothetical liquid hydrogen fugacity was determined from Figure 2 of Yen and McKetta's paper. The value of Δ for four of the amines was obtained from Figure 5 of the same paper. As values of Δ were presented for solvents having a solubility parameter between $7.5\left(\frac{cal.}{c.c.}\right)^{\frac{1}{2}}$ and $11.5\left(\frac{cal.}{c.c.}\right)^{\frac{1}{2}}$, it was not possible to calculate the

TABLE 8

THE SOLUBILITY OF HYDROGEN IN AMINES AT 25°C

CORRELATION OF YEN AND McKETTA[44]

f_2^H = 620 atm. $f_2^{\circ g}$ = 1 atm.

Component	δ_1	Δ	Mole Frac. x 10^4 Eqn.[2.82]	Mole Frac. x 10^4 This Study	% Deviation
Methylamine	10.45	20	1.569	2.231	-29.7
Ethylamine	9.34	6	2.775	2.990	- 7.2
n-propylamine	9.1	5.5	3.224	3.284	- 1.8
1,2-propanediamine	10.6	22	1.420	1.338	+ 6.1

solubility of hydrogen in ammonia or 1,2-ethanediamine.

The predicted solubilities are compared with the experimental values (calculated from best fit equation) in Table 8.

The agreement between the predicted and experimental solubilities is good for ethylamine, n-propylamine and 1,2-propanediamine. It also appears that 1,2-propanediamine can be considered as a non-associating liquid along with ethylamine and n-propylamine. The dielectric constant of 1,2-propanediamine, as estimated from the graph of Yen and McKetta[44], is approximately 9. This value agrees with the general trend of percent deviation versus dielectric constant as shown in Table 6. As is expected, the agreement between the calculated and experimental solubility of hydrogen in methylamine is poor.

The success of the Yen and McKetta correlation in predicting the solubility of hydrogen in ethylamine, n-propylamine, and 1,2-propanediamine indicates that equation [2.82] is useful for predicting the solubility of hydrogen in other amines. This is expecially true for those amines which are, by Pauling's criterion, considered nonassociated.

In order to determine if the correlation of Yen and McKetta[44] may be modified to predict the solubility of hydrogen in polar, associated amines, polar characteristic factors were calculated from the solubility data determined in this study. The empirical solute parameters δ_2, $\bar{V}_2^L$, and f_2^H as determined by Yen and McKetta were assumed to apply and the liquid solubility parameters (δ_1), given in Table 6 were used.

TABLE 9

AMINE POLAR CHARACTERISTIC FACTORS

$f_2^{\circ g}$ = 1 atm. f_2^H = 620 atm. $\delta_2 = 3.82 \left(\frac{\text{cal.}}{\text{c.c.}}\right)^{\frac{1}{2}}$ $\bar{V}_2^L = 37.3 \frac{\text{c.c.}}{\text{gm. mole}}$

Component	$\delta_1 \left(\frac{\text{cal.}}{\text{c.c.}}\right)^{\frac{1}{2}}$	$\Delta \left(\frac{\text{cal.}}{\text{c.c.}}\right)$
Ammonia	12.14	81.0
Methylamine	10.45	36.4
Ethylamine	9.34	8.9
n-Propylamine	9.1	6.0
1,2-propanediamine	10.6	18.1
1,2-ethanediamine	12.3	78.8

The resulting values of the polar characteristic factor (Δ) are shown in Table 9.

The above values of the polar characteristic factor (Δ)are plotted in Figure 13 along with the original points of Yen and McKetta. It can be seen that two curves may be used to represent the data obtained in this study. The lower curve, which is the same as that of the original authors[44], is suitable for those amines which are nonassociated. The upper curve passes through the values of Δ calculated for the associated amines of this study. This curve should be used with caution as the basic assumption of additivity of the energies of molecular pairs is violated for associated liquids.

The solubility of hydrogen in ammonia, methylamine, ethylamine, n-propylamine, 1,2-propanediamine and 1,2-ethanediamine were also estimated from the nomograph of Osburn and Markovic[50]. The physical property required for estimating the solubility was the amine surface tension at 20°C.

Surface tension data at 20°C were available for ammonia, methylamine, ethylamine, and n-propylamine. The surface tension of 1,2-propanediamine and 1,2-ethanediamine was estimated by the method of Gambill[109]. Values of σ for the other four amines were also determined by this method for the sake of comparison.

$$\sigma = \left(\frac{[P]}{V_1^L}\right) \qquad [5.7]$$

[P] = Sugden parachor

V_1^L = molar volume of the amine

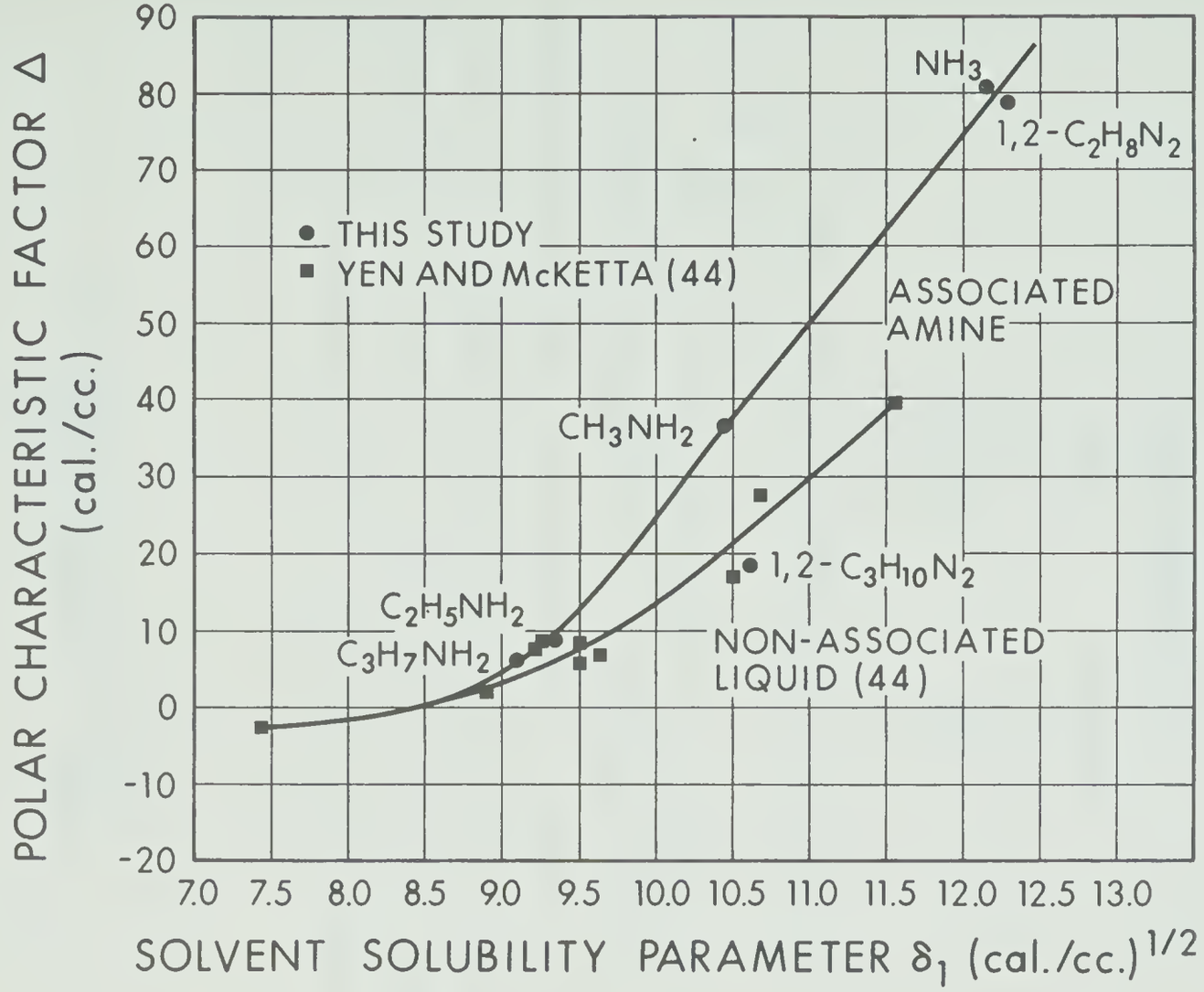


FIG. 13. POLAR CHARACTERISTIC FACTORS

The Sugden parachors [P] were calculated from the atomic parachors as summarized by Osburn and Markovic[50]. The required values are shown in Table 10.

TABLE 10

ATOMIC PARACHORS[50]

ATOM	PARACHOR
Carbon	9.2
Hydrogen	15.4
Nitrogen	17.5

The Sugden parachor for methylamine ($CH_3 NH_2$), as calculated from the above values is:

$$[P] = (1 \times 9.2) + (5 \times 15.4) + (1 \times 17.5) = 103.7 \qquad [5.8]$$

The Ostwald coefficient (c.c. of hydrogen at 20°C per c.c. of liquid amine at 20°C) was obtained from the solubility nomograph (Figure 3) of the paper by Osburn and Markovic[50]. The Ostwald coefficient (L) was then converted to mole fraction hydrogen at 20°C and one atmosphere hydrogen partial pressure using the relationship:

$$x_2 = \frac{1}{\frac{22414.6(293.15)}{273.15\ L\ V_1^L} + 1} \cong \frac{L\ V_1}{24056} \qquad [5.9]$$

Values of the mole fraction hydrogen at 20°C as estimated by the above method are compared with those determined in this study in Table 11. The solubilities of hydrogen in ammonia, methylamine,

TABLE 11

THE SOLUBILITY OF HYDROGEN IN AMINES AT 20°C

CORRELATION OF OSBURN AND MARKOVIC[50]

P = 1 atm.

Component	V_1^L	[P]	σ	L	H_2	Mole Frac. x 10^4 Calculated	Mole Frac. x 10^4 This Study	% Deviation
Ammonia	27.88	-	21.5[a]	0.105	8218	1.217	0.8007	+52.0
Ammonia	27.88	63.7	27.2	0.079	10923	0.916	0.8007	+14.3
Methylamine	46.84	-	19.90[a]	0.112	4586	2.180	2.122	+ 2.7
Methylamine	46.84	103.7	24.0	0.092	5583	1.791	2.122	-15.6
Ethylamine	65.91	-	19.9[a]	0.112	3260	3.068	2.826	+ 8.6
Ethylamine	65.91	143.7	22.6	0.098	3725	2.684	2.826	- 6.7
n-Propylamine	82.41	-	22.4[a]	0.100	2920	3.424	3.158	+ 8.4
n-Propylamine	82.41	183.7	24.7	0.090	3244	3.082	3.158	- 2.4
1,2-Propanediamine	85.80	216.6	40.6	0.043	6521	1.533	1.280	+19.8
1,2-Ethanediamine	66.81	176.6	48.8	0.028	12860	0.777	0.657	+18.3

[a] Experimental surface tension

ethylamine and n-propylamine, as predicted from the measured and estimated values of surface tension, are listed.

It is apparent from the above table that the correlation of Osburn and Markovic[50] is able to predict the solubility of hydrogen in the amines within ±20 percent. A significant portion of this uncertainty may be due to errors in reading the nomograph. The solubility of hydrogen in ammonia, as predicted from the experimental surface tension data, displays a deviation which is considerably larger than the ±20% uncertainty. This error is reduced when the estimated surface tension is used, and it is quite possible that the value of the experimental surface tension at 20°C is in error.

Reid and Sherwood[93] state that no reliable method is available for estimating the surface tension of polar materials. The use of reliable surface tension data for the amines would probably reduce the degree of uncertainty to approximately ±10 percent. However, in spite of the rather large degree of uncertainty (±20%) associated with the Osburn and Markovic[50] correlation, based on estimated surface tension values, the correlation provides a good initial estimate of the hydrogen solubility at 20°C in an amine for which no data are available.

C. General

The overall performance of the solubility apparatus was satisfactory after the initial operating problems were overcome. Some of the problems which required corrective action were:

1) The length of unsupported shaft between the motor drive and the external drive magnet on the solubility cell was too long.

The radial movement of the magnet was such that the magnet rubbed on the cell housing. The magnet disintegrated after very few hours of operation. A guide bearing mounted immediately above the drive magnet corrected this problem.

2) The solenoid pump proved to be a dependable experimental device for which the only drawback was heat generation. This trouble was overcome by deactivating the pump approximately two hours prior to the time of sampling. The magnetic stirrer was operated for an additional hour after stopping the pump.

3) Extreme care was required to ensure that all the amine was removed from the cell upon completion of a set of determinations. A small amount of 1,2-propanediamine was present in the cell during solubility tests on ethylamine. The measured solubility of hydrogen in ethylamine was considerably reduced due to the presence of diamine. The solubility data for each amine were listed in chronological order to enable the identification of a given amine charge. A sudden change in solubility for a complete amine charge would indicate the presence of a contaminant or a system leak.

An operating problem for which no solution was found was a slight drift in the cell temperature (±0.2°C) over a twenty-four hour period. In addition to this, it was very difficult to set the temperature at a given desired value.

6. CONCLUSIONS AND RECOMMENDATIONS

The solubility of hydrogen in ammonia, methylamine, ethylamine, n-propylamine, 1,2-propanediamine and 1,2-ethandiamine was measured over the temperature range -70°C to +25°C at total system pressures up to 300 psig.. On a mole fraction basis, the relative ability of the amines to dissolve hydrogen, arranged in order of decreasing hydrogen solubility is: n-propylamine, ethylamine, methylamine, 1,2-propanediamine, ammonia, and 1,2-ethanediamine.

The solubility of hydrogen in the above amines obeyed Henry's law for the pressure range of this study. The data for each amine were correlated versus pressure with Henry's law. The logarithm of Henry's law coefficients were correlated versus the reciprocal of the absolute system temperatures.

The solubility data were measured by a physical extraction technique coupled with a freeze-drying separation of the dissolved hydrogen from the amine solvent. This technique was time consuming but it enjoyed the advantage that no separate calibration of the apparatus was necessary for each amine. Another advantage is the suitability of the freeze-drying technique for measuring the solubility of hydrogen in amide solutions.

The experimental determinations on the solubility of hydrogen in liquid ammonia are in good agreement with the data presented in the literature. No data were available on hydrogen solubility in the five amines.

The semi-empirical correlation of Prausnitz and Shair[43] is unsatisfactory for predicting the solubility of hydrogen in any of

the amines considered. However, the percent deviation between the experimental and predicted solubilities appeared to be related to the magnitude of the dielectric constant of the amine.

Yen and McKetta's[44] correlation provided a good estimate of the solubility of hydrogen in ethylamine, n-propylamine, and 1,2-propanediamine. The predicted solubility of hydrogen in methylamine was low and no estimate was possible for the solubility of hydrogen in ammonia and 1,2-ethanediamine.

A polar characteristic factor, or the coefficient in the equation of Yen and McKetta[44] which accounts for the effect of the polar solvent molecule, was calculated for each amine from the experimental solubility coefficients. The polar characteristic factor (Δ) for the associated solvents ammonia, methylamine, and 1,2-ethanediamine fall on a curve which is above the nonassociated solvent curve of the original authors[44]. This modified curve can be used to obtain the polar characteristic factor of an associated amine for which no solubility data are available.

The correlation of Osburn and Markovic[50] provided a rough estimate (±20%) of the solubility of hydrogen in each of the amines considered. This correlation could be considered when an initial estimate of the solubility of hydrogen in an amine is required.

Recommendations for additional experimental work are as follows:

(1) It would be useful to have information on the vapor phase compositions of the various hydrogen-amine systems to check on the assumptions used in fitting the solubility coef-

ficients. Such data are also of industrial importance for tower humidification calculations.

(2) The effect of the amide on the hydrogen solubility is not known, and since the exchange reaction involves an amide solution, the measurement of the solubility of hydrogen in amine solutions containing the alkali-substituted amide would be worthwhile.

(3) Data on the solubility of hydrogen deuteride in the amide solutions may be of interest, however the solubility would not be expected to be significantly different from that of hydrogen.

NOMENCLATURE

The nomenclature in use throughout this paper is given in the following list. Special symbols are defined where they occur.

English Letter Symbols

A Helmholtz free energy of the system (cal.)

A_i Helmholtz free energy per mole of i^{th} component (cal./mole)

$\bar{A}_i$ Partial molal Helmholtz free energy of i^{th} component (cal./mole)

a_i Activity of the i^{th} component

E Internal energy of the system (cal.)

E_i Internal energy per mole of the i^{th} component (cal./mole)

$\bar{E}_i$ Partial molal internal energy of the i^{th} component (cal./mole)

F Gibbs free energy of the system (cal.)

F_i Gibbs free energy per mole of i^{th} component (cal./mole)

$\bar{F}_i$ Partial molal free energy of the i^{th} component (cal./mole)

f_i Fugacity of pure i^{th} component (atm.)

$f_i^{\circ L}$ Fugacity of pure liquid i at some reference pressure and the temperature of the system (atm.)

$f_i^{\circ g}$ Fugacity of pure gas i at latm. pressure and the temperature of the system (atm.)

H_2 Henry's law coefficient for dissolved solute $\left(\frac{\text{atm.}}{\text{mole fraction}}\right)$

h Enthalpy of system (cal.)

h_i Enthalpy per mole of i^{th} component (cal./mole)

$\bar{h}_i$ Partial molal enthalpy of i^{th} component (cal./mole)

L Ostwald Coefficient $\left(\frac{\text{c.c. solute @ T,P}}{\text{c.c. solvent}}\right)$

M_i Molecular weight (gm./gm. mole)

n_i Number of moles of i^{th} component

P_i Partial pressure of i^{th} component (atm.)

P Partial pressure of solute (implies hydrogen partial pressure) (atm.)

P_r Reference pressure

P_i^s Saturation or vapor pressure of pure i^{th} component (atm.)

R Ideal gas constant = $1.9872 \frac{cal}{K^\circ - mole} = 82.0567 \frac{c.c.atm.}{K^\circ\ mole}$

S^P Solubility coefficient when the hydrogen partial pressure is P atmospheres. $\left(\frac{c.c.\ H_2\ (STP)}{gm.\ solvent}\right)$

S Keunan Coefficient $\left(\frac{c.c.\ solute\ (STP)}{gm.\ solvent}\right)$

S Entropy of system $\left(\frac{cal.}{K^\circ}\right)$

S_i Entropy per mole of i^{th} component $\left(\frac{cal.}{mole - K^\circ}\right)$

$\bar{S}_i$ Partial molal energy of i^{th} component $\left(\frac{cal.}{mole - K^\circ}\right)$

T System temperature (Kelvin degrees)

V Total volume of system (c.c.)

V_2 Volume of hydrogen corrected to standard conditions of 0°C and 760 mm. Hg.

V_i Molar volume of ith component $\left(\frac{c.c.}{mole}\right)$

$\bar{V}_i$ Partial molal volume of i^{th} component $\left(\frac{c.c.}{mole}\right)$

W_i Mass of i^{th} component (gms.)

x_i Mole fraction of i^{th} component in the liquid phase

Y_i Mole fraction of i^{th} component in the vapor phase

x_2^P Hydrogen mole fraction when hydrogen partial pressure is P atmospheres

x_2' Hydrogen mole fraction when hydrogen partial pressure is one atmosphere

Greek Letter Symbols

α Bunsen coefficient $\frac{\text{c.c. solute (STP)}}{\text{c.c. solvent}}$

α' Modified Bunsen coefficient as used by Bar-Eli and Klein[63] $\left(\frac{\text{c.c. solute (STP)}}{\text{c.c. solvent atm.}}\right)$

α'' Modifien Bunsen coefficient as used by Ipatiew and Teodorwich[72] $\left(\frac{\text{c.c. } H_2 \text{ (STP)}}{100 \text{ c.c. } NH_3}\right)$

γ_i Activity coefficient of i^{th} component in the liquid phase (symmetric convention)

γ_i^* Activity coefficient of i^{th} component in the liquid phase (unsymmetric convention)

γ_H Horiuti coefficient $\left(\frac{\text{c.c. solute @ T,P}}{\text{c.c. solution}}\right)$

Δ Polar characteristic factor (Eqn. [2.82]) (cal./cc)

δ_i Solubility parameter of i^{th} component $(\text{cal./cc})^{\frac{1}{2}}$

μ_i Chemical potential of i^{th} component (cal./mole)

π Total system pressure (atm.)

ρ_i Density of i^{th} component (gms./cc.)

σ Surface tension (dynes/cm.)

τ Dirian's solubility coefficient $\left(\frac{\text{gm. } H_2}{\text{ml. } NH_3}\right)$

ϕ_i Fugacity component of i^{th} component in vapor phase

ψ_i Volume fraction of i^{th} component in solution

$\left(\frac{\varepsilon}{K}\right)$ Lennard-Jones energy parameter (Kelvin degrees)

Subscripts

i Component

1 Solvent

2 Solute

3 Solution

Superscripts (Process)

E	Excess
M	Mixing

Superscripts (State)

g	Gas or solute
H	Hypothetical liquid
i	Ideal
L	Liquid
o	Pure component
P	Hydrogen partial pressure
P_r	Reference pressure
s	Standard state
v	Vapor
π	Total pressure
1	Hydrogen partial pressure of one atmosphere
∞	Infinite dilution

BIBLIOGRAPHY

(1) Feature Article, Chemistry in Canada, 21, No. 10, 36, (1969).

(2) Feature Article, Chemical Engineering, 77, No. 3, 56, (1970).

(3) Rae, H.K., "A Review of Heavy Water Production Processes", Atomic Energy of Canada Limited, Report AECL-2503, 1965.

(4) Rae, H.K., "Chemical Exchange Processes for Heavy Water", Atomic Energy of Canada Limited, Report AECL-2555, 1966.

(5) Bancroft, A.R., "The Canadian Approach to Cheaper Heavy Water (1967)", Atomic Energy of Canada Limited, Report AECL-3044, 1968.

(6) Bebbington, W.P., and Thayer, V.R., Chem. Eng. Progr., 55, No. 10, 70, (1959)

(7) Proctor, J.F., and Thayer, V.R., Chem. Eng. Progr., 58, No. 4, 53, (1962).

(8) Elliwood, P., Chem. Eng., 75, No. 4, 56, (1968).

(9) Bar-Eli, K., and Klein, F.S., J. Chem. Soc. (London), 36 3083, (1962).

(10) Gibbs, J.W., "Collected Works", Vol. I, p.p. 55-354, Longmans, Green & Co., Inc., New York, N.Y., 1931.

(11) Lewis, G.N., and Randall, M., "Thermodynamics and the Free Energy of Chemical Substances", McGraw-Hill Book Company, Inc., New York, N.Y., 1923.

(12) Hildebrand, J.H., and Scott, R.L., "Regular Solutions", Prentice-Hall, Inc., Englewood Cliffs, New Jersey, 1962.

(13) Prausnitz, J.M., "Molecular Thermodynamics of Fluid-Phase Equilibria", Prentice-Hall, Inc., Englewood Cliffs, New Jersey, 1969.

(14) Raoult, F.M., Comptes Rendus, 104, 1430, (1887).

(15) Raoult, F.M., Z. physik. Chem., 2, 353, (1888).

(16) Hildebrand, J.H., and Scott, R.L., "The Solubility of Non-electrolytes", 3rd Edition, Dover Publications, Inc., New York, 1964.

(17) Grilly, E.R., J. Am. Chem. Soc., 73, 843, (1951).

(18) Gonikberg, M.G., J. Phys. Chem. (U.S.S.R.), 14, 582, (1940).

(19) Henry, W., Phil. Trans. Roy. Soc., (London), 29, 274, (1803).

(20) Himmelblau, D.M., Journal of Chem. and Eng. Data, 5, No. 1, 10, (1960).

(21) Van Wylen, G.J., and Sonntag, R.E., "Fundamentals of Classical Thermodynamics", 2nd Printing, Chapter 10, John Wiley and Sons, Inc., New York, 1966.

(22) Sherwood, A.E., and Prausnitz, J.M., A.I.Ch.E.J., 8, 519, (1962).

(23) Denbigh, K., "The Principles of Chemical Equilibrium", 2nd Edition, p.p. 586, Cambridge University Press, Great Britain, 1966.

(24) Krichevsky, I.R., and Kasarnovsky, J.S., J. Am. Chem. Soc., 57, 2168, (1935).

(25) Dodge, B.F., and Newton, R.H., Ind. Eng. Chem., 29, 718, (1937).

(26) Wiebe, R., and Gaddy, V.L., J. Am. Chem. Soc., 61, 315, (1939).

(27) Kobayashi, R., and Katz, D.L., Ind. Eng. Chem., 45, 440, (1953).

(28) Krichevsky, I.R., and Ilinskaya, A.A., Zh. fiz. Khim. U.S.S.R., 19, 621, (1945).

(29) Orentlicher, M., and Prausnitz, J.M., Chem. Eng. Sci, 19, 775, (1964).

(30) Dolezalek, F.Z., Z. physik. Chem., 64, 727, (1908).

(31) Eisenschitz, R., and London, F., Z. physik, 60, 491, (1930).

(32) London, F., Ibid, 63, 245, (1930).

(33) London, F., Z physik. Chem., B11, 222, (1930).

(34) London, F., Trans. Faraday Soc., 33, 8, (1937).

(35) Hildebrand, J.H., and Rotariu, G.J., Anal. Chem., 24, 770, (1952).

(36) Lewis, G.N., "Valence and the Structure of Atoms and Molecules", Chemical Catalog Co., New York, 1923.

(37) Hildebrand, J.H., J. Am. Chem. Soc., 51, 66, (1929).

(38) Scatchard, G., Chem. Rev., 8, 321, (1931).

(39) Scatchard, G., J. Am. Chem. Soc., 56, 995, (1934).

(40) Scatchard, G., Trans. Faraday Soc., 33, 160, (1937).

(41) Hildebrand, J.H., and Wood, S.E., J. Chem. Phys., 1, 817, (1933).

(42) Prausnitz, J.M., A.I.Ch.E.J., 4, 269, (1958).

(43) Prausnitz, J.M., and Shair, F.H., A.I.Ch.E.J., 7, 682, (1961).

(44) Yen, L.C., and McKetta Jr., J.J., A.I.Ch.E.J., 8, 501, (1962).

(45) Battino, R., and Clever, H.L., Chem. Rev., 66, 395, (1966).

(46) Nakahara, T., and Hirata, M., J. Chem. Eng. of Japan, 2, 137, (1969).

(47) Miller, R.C., and Prausnitz, J.M., I.&E.C. Fundamentals, 8, 449, (1969).

(48) Sadamoto, S., Mitsudomi, H., and Yorizane, M., Kagaku Kōgaku, 33, 867, (1969).

(49) Mellan, I., "Compatibility and Solubility", Noyes Development Corporation", Park Ridge, New Jersey, 1968.

(50) Osburn, J.D., and Markovic, P.L., Chem. Eng., 76, No. 18, 105, (1969).

(51) Uhlig, H.H., J. Phys, Chem., 41, 1215, (1937).

(52) Schlapfer, P., Audykowski, T., and Bukowiecki, A., Schweiz Arch. Angew. Wiss. Tech., 15, 299, (1949).

(53) Markham, A.E., and Kobe, K.A., Chem. Rev., 28, 519, (1941).

(54) Friend, L., and Adler, S.B., Chem. Eng. Progr., 53, 452, (1957).

(55) Horiuti, J., Sci. Papers Inst. Phys. Chem. Research (Tokyo), 17, 125 (1931).

(56) Cook, M.W., and Hanson, D.N., Rev. Sci. Instr., 28, 370, (1957).

(57) Nader, W.J., Vold, R.D., and Vold, M.J., "Physical Methods of Organic Chemistry", 3rd ed., pt. 1, Vol. 1, p.p. 677, Inter-Science Publishers Inc., New York. 1959.

(58) Brainard, A.J., and Williams, G.B., A.I.Ch.E.J., 13, 60, (1967).

(59) Dean, R., and Tooke, J.W., Ind. Eng. Chem., 29, 346, (1946).

(60) Wiebe, R., and Tremearne, T.H., J. Am. Chem. Soc., 55, 975, (1933).

(61) Ibid, 56, 2357, (1934).

(62) Wiebe, R., and Gaddy, V.L., Ibid, 59, 1984, (1937).

(63) Larson, A.T., and Black, C.A., Ind. Eng. Chem., 17, 715, (1925).

(64) Thompson, R.E., and Edmister, W.C., A.I.Ch.E.J., 11, 457, (1965).

(65) Aroyan, H.J., and Katz, D.L., Ind. Eng. Chem., 43, 185, (1951).

(66) Fleck, R.N., and Prausnitz, J.M., I.&E.C. Fund., 7, 174, (1968).

(67) Eckert, C.A., and Prausnitz, J.M., A.I.Ch.E.J., 11, 886, (1965).

(68) Fowles, G.W.A., McGregor, W.R., and Symons, M.C.R., J. Chem. Soc. (London), 3329, (1957).

(69) Eyers, E.C., Young II, A.E., and Panson, A.J., J. Am. Chem. Soc., 79, 5118, (1957).

(70) Bar-Eli, K., and Klein, F.S., J. Chem. Soc. (London), 36, 1378, (1962).

(71) Schlubach, H.H., and Ballauf, F., Ber., 54, 2825, (1921).

(72) Ipatiew, V.V., and Teodorowich, V.P., J. Gen. Chem. (U.S.S.R.), 2, 305, (1932).

(73) Wiebe, R., and Tremearne, T.H., J. Am. Chem. Soc., 56, 2357, (1934).

(74) Davis, D.S., Ind. Eng. Chem., 33, 1454, (1941).

(75) Reamer, H.H., and Sage, B.H., J. Chem. Eng. Data, 4, 152, (1959).

(76) Bar-Eli, K., and Klein, F.S., J. Chem. Phys., 35, 1915, (1961).

(77) Cook, M.W., Hanson, D.N., and Alder, B.J., J. Chem. Phys., 26, 748, (1957).

(78) Dirian, G., Botter, F., Ravoire, J., and Grandcollot, P., J. Chim. Physique, 60, 139, (1963).

(79) Morrison, R.T. and Boyd, R.N., "Organic Chemistry", p.p. 108, Allyn and Bacon, Inc., Boston, 1962.

(80) Handbook of Chemistry and Physics, 49th. Ed., The Chemical Rubber Co., Cleveland, Ohio, 1968.

(81) Prausnitz, J.M., Eckert, C.A., Orye, R.V. and O'Connell, J.P., "Multicomponent Vapor-Liquid Equilibria", Prentice-Hall, Inc., Englewood Cliffs, N.J., 1967.

(82) International Critical Tables, McGraw-Hill Book Company, Inc., New York, N.Y., 1933.

(83) Dye, J.L., and Dalton, L.R., J. Phys. Chem., 71, 184, (1967).

(84) Swift Jr., E., and Calkins, C.R., J. Am. Chem. Soc., 65, 2415, (1943).

(85) Perry, J.H., "Chemical Engineers' Handbook", 4th Ed., p.p. 3-223, McGraw-Hill Book Company, Inc., New York, N.Y., 1963.

(86) Matheson Gas Data Book, 4th. ed., The Matheson Company, Inc., Herst Litho Inc., New York, N.Y., 1966.

(87) Lang, N.A., "Handbook of Chemistry", 10th. Ed., McGraw-Hill Book Company, Inc., New York, N.Y., 1967.

(88) Encyclopaedia Britannica, Vol. 1, p.p. 795, Encyclopaedia Britannica, Inc., Chicago, 1967.

(89) API 44-TRC, "Selected Data on Thermodynamics and Spectroscopy", The Thermodynamics Research Center, Dept. of Chemistry, Texas A & M University, College Station, Texas, 1968.

(90) Alkyl and Alkylene Amines, Union Carbide Chemicals Company, New York, N.Y., 1961.

(91) Atomic Energy of Canada Ltd. Memorandum, "Summary of Amine Properties", Private Communication.

(92) Propylene Diamine, Union Carbide Chemicals, Product Bulletin Number F-40669A, Union Carbide Chemicals Company, New York, N.Y., 1966.

(93) Reid, R.C., and Sherwood, T.K., "The Properties of Gases and Liquids", 2nd. Ed., p.p. 508, McGraw Hill Book Company, New York, N.Y., 1966.

(94) Smyth, C.P., "Dielectric Constants and Molecular Structure", Appendix I, The Chemical Catalog Company Inc., New York, 1931.

(95) Wesson, L.G., "Tables of Electric Dipole Moments", The Technology Press, Cambridge Massachusettes, 1948.

(96) Berns, D.S., Evers, C.E., and Frank Jr., P.W., J. Am. Chem. Soc., 82, 310, (1960).

(97) Ishige, T., M. Sc. Thesis, Department of Chemical and Petroleum Engineering, University of Alberta, Edmonton, Alberta, 1968.

(98) Livingston, R., J. Phys. Chem., 33, 954, (1929).

(99) Murthy, A., Vasudeva, R., and Rao, B. Sanjive, Proc. Indian Acad. Sci., 34A, 283, (1951).

(100) Rosen, F.D., Rev. Sci. Instruments, 24, 1061, (1953).

(101) Exline, P.G., and EnDean, H.J., Trans. Am. Soc. Mech. Engrs., 70, 279, (1948).

(102) Sterner, C.J., Rev. Sci. Instruments, 31, 1159, (1960).

(103) Fleck, R.N., and Prausnitz, J.M., I.&E.C. Fundamentals, 7, 174, (1968).

(104) Cimco Magnetic Pump, Coleman Tulsa Company, 4208 So. 74th. E. Ave., Tulsa, Okla.

(105) Kelly, D.H., private communication, University of Alberta, Edmonton, Alberta.

(106) Prausnitz, J.M. and Chueh, P.L., "Computer Calculations for High Pressure Vapor - Liquid Equilibria", Prentice-Hall, Inc., Englewood Cliffs, N.J., 1968.

(107) Gjaldbaek, J.C., Acta. Chemica Scandinavica, 6, 623, (1952).

(108) Gjaldbaek, J.C., and Anderson, E.K., Ibid, 8, 1398, (1954).

(109) Gambill, W.R., Chem. Eng., 72, n.7, 146, (1958).

APPENDIX A1

EXPERIMENTAL SOLUBILITY DATA

The experimental determinations of the solubility of hydrogen in ammonia, methylamine, ethylamine, n-propylamine, 1,2-propanediamine, and 1,2-ethanediamine are listed in Tables A1-1 to A1-6. The data for each amine have been listed in chronological order to enable a check of the reproducability of the data for different charges of the same amine. The headings "Sol. (c.c./gm.)" and "Mole fraction" correspond to the solubility coefficients "S^P" and mole fraction "x^P" respectively. The remainder of the headings are self-explanatory.

TABLE A1-1

SOLUBILITY OF HYDROGEN IN AMMONIA

DATE	PRESSURE (ATM) TOTAL	PRESSURE (ATM) HYDROGEN	TEMP.(C)	SOL.(GC/GM)	MOLE FRAC.	HENRYS CONS. IDEAL
10/17/68	7.55	6.06	-25.01	0.2837	0.2155E-03	28116.
10/18/68	7.54	6.01	-24.50	0.2843	0.2159E-03	27835.
10/18/68	7.59	6.06	-24.53	0.2756	0.2094E-03	28958.
10/21/68	16.36	14.81	-24.31	0.6660	0.5064E-03	29247.
10/21/68	16.35	14.36	-24.95	0.6935	0.5266E-03	29209.
10/22/68	14.42	12.90	-24.67	0.5907	0.4486E-03	28754.
10/24/68	14.64	13.10	-24.39	0.5996	0.4553E-03	28772.
10/24/68	14.57	13.01	-24.11	0.5977	0.4539E-03	28673.
10/25/68	14.51	12.93	-23.83	0.5857	0.4448E-03	29066.
10/28/68	16.60	15.06	-24.39	0.7101	0.5393E-03	27931.
10/28/68	16.58	15.04	-24.39	0.6885	0.5228E-03	28775.
2/25/69	13.99	13.10	-35.61	0.4820	0.3660E-03	35773.
2/25/69	13.99	13.10	-35.61	0.4777	0.3628E-03	36100.
2/26/69	18.07	17.20	-38.07	0.5904	0.4484E-03	38552.
2/26/69	18.07	17.20	-38.07	0.6053	0.4597E-03	37604.
3/ 4/69	15.66	7.23	19.89	0.7634	0.5797E-03	12476.
3/ 4/69	15.66	7.23	19.89	0.7621	0.5787E-03	12496.
3/ 6/69	17.02	16.90	-59.83	0.3472	0.2637E-03	63710.
3/ 7/69	18.17	18.06	-60.46	0.3823	0.2903E-03	65207.
3/11/69	17.19	17.01	-62.16	0.3333	0.2535E-03	67082.
3/11/69	17.19	17.01	-62.16	0.3303	0.2509E-03	67785.
3/12/69	17.37	17.19	-62.29	0.3332	0.2531E-03	67895.
3/13/69	18.62	18.44	-62.04	0.3696	0.2808E-03	65682.
3/14/69	15.70	15.53	-61.09	0.3093	0.2353E-03	65344.
6/11/69	15.76	11.50	0.19	0.8378	0.6361E-03	18071.
6/12/69	21.52	17.25	0.19	1.2692	0.9634E-03	17909.
6/12/69	21.52	17.25	0.19	1.2625	0.9583E-03	18004.
6/13/69	18.93	14.67	0.13	1.0732	0.8147E-03	18011.
6/13/69	18.93	14.68	0.11	1.0725	0.8142E-03	18028.
6/16/69	17.74	3.74	21.96	0.9459	0.7175E-03	12177.
6/16/69	17.74	3.74	21.96	0.9595	0.7285E-03	11993.

TABLE A1-2
SOLUBILITY OF HYDROGEN IN MONOMETHYLAMINE

DATE	PRESSURE (ATM) TOTAL	PRESSURE (ATM) HYDROGEN	TEMP.(C)	SOL.(CC/GM)	MOLE FRAC.	HENRYS COEF. IDEAL
10/31/68	4.17	3.77	-24.67	0.3473	0.4811E-03	7331.
11/ 1/68	9.42	9.01	-24.73	0.8543	0.1183E-02	7613.
11/ 1/68	9.42	9.01	-24.73	0.8533	0.1181E-02	7632.
11/ 3/68	9.41	9.01	-24.95	0.8332	0.1153E-02	7815.
11/ 4/68	17.43	17.02	-24.70	1.5722	0.2174E-02	7831.
11/ 4/68	17.45	17.04	-24.70	1.5326	0.2188E-02	7737.
11/ 5/68	17.41	17.01	-24.95	1.5985	0.2210E-02	7692.
11/ 5/68	17.40	17.00	-24.95	1.6226	0.2243E-02	7575.
11/ 6/68	17.40	17.00	-24.81	1.5960	0.2207E-02	7702.
11/ 7/68	10.29	9.89	-24.95	0.9435	0.1306E-02	7574.
1/29/69	7.84	7.30	-60.49	0.4824	0.6630E-03	11670.
1/30/69	7.87	7.33	-60.49	0.4787	0.6629E-03	11311.
1/30/69	13.93	13.39	-61.30	0.8250	0.1147E-02	12105.
1/30/69	13.93	13.39	-61.52	0.8265	0.1144E-02	12140.
1/31/69	20.07	20.03	-61.67	1.1671	0.1615E-02	12404.
1/31/69	20.07	20.03	-61.61	1.1766	0.1628E-02	12305.
2/ 3/69	16.70	16.67	-62.16	0.9767	0.1352E-02	12332.
2/ 3/69	16.70	16.67	-62.16	0.9734	0.1347E-02	12373.
2/ 4/69	15.39	15.35	-62.35	0.9652	0.1336E-02	11942.
2/ 7/69	10.79	10.58	-36.51	0.8773	0.1214E-02	8713.
2/ 7/69	10.79	10.58	-36.51	0.8502	0.1177E-02	8990.
2/12/69	11.50	11.27	-35.12	0.9534	0.1319E-02	8543.
2/18/69	8.32	8.60	-35.24	0.7149	0.9836E-03	8690.
2/18/69	8.62	8.60	-35.24	0.7154	0.9904E-03	8683.
2/19/69	14.40	14.17	-34.60	1.1894	0.1645E-02	8610.
2/19/69	14.40	14.17	-34.66	1.1782	0.1630E-02	8692.
2/20/69	19.03	18.79	-34.02	1.5744	0.2177E-02	8632.
2/20/69	19.03	18.79	-34.02	1.5712	0.2173E-02	8648.
6/ 4/69	14.04	12.72	-0.21	1.5700	0.2171E-02	5858.
6/ 4/69	14.04	12.72	-0.21	1.5758	0.2179E-02	5837.
6/ 5/69	20.96	19.65	-0.37	2.4257	0.3350E-02	5867.
6/ 5/69	20.96	19.65	-0.37	2.4373	0.3366E-02	5839.
6/ 6/69	17.65	14.69	20.14	2.2523	0.3111E-02	4721.
6/ 9/69	21.07	17.31	22.75	2.8281	0.3901E-02	4565.
6/ 9/69	21.07	17.31	22.75	2.8058	0.3873E-02	4593.

TABLE A1-3
SOLUBILITY OF HYDROGEN IN MONOETHYLAMINE

DATE	PRESSURE (ATM) TOTAL	PRESSURE (ATM) HYDROGEN	TEMP.(C)	SOL.(CC/GM)	MOLE FRAC.	HENRYS COEF. IDEAL
1/ 1/69	11.34	11.21	-24.11	1.0720	0.2152E-02	5209.
1/ 9/69	11.34	11.21	-24.11	1.0561	0.2120E-02	5287.
1/10/69	14.76	14.63	-24.53	1.3688	0.2746E-02	5328.
1/10/69	14.75	14.61	-24.53	1.3563	0.2721E-02	5371.
1/13/69	17.84	17.70	-24.23	1.6553	0.3319E-02	5334.
1/13/69	17.84	17.70	-24.28	1.6502	0.3309E-02	5350.
1/15/69	10.56	10.42	-24.00	0.9911	0.1990E-02	5236.
1/15/69	10.56	10.42	-24.00	0.9748	0.1957E-02	5324.
1/16/69	14.30	14.16	-24.11	1.3388	0.2686E-02	5273.
3/19/69	11.44	11.43	-61.39	0.7063	0.1419E-02	8058.
3/20/69	13.68	13.67	-61.76	0.8347	0.1676E-02	8157.
3/20/69	13.68	13.68	-61.76	0.8083	0.1623E-02	8424.
3/25/69	18.35	18.34	-69.01	1.0480	0.2104E-02	8718.
3/26/69	17.26	17.25	-68.17	0.9882	0.1984E-02	8697.
3/26/69	17.26	17.25	-68.17	0.9906	0.1989E-02	8676.
3/27/69	17.67	17.67	-68.17	1.0112	0.2030E-02	8703.
3/27/69	17.67	17.67	-68.17	0.9806	0.1969E-02	8975.
4/ 1/69	17.29	17.27	-61.03	1.0729	0.2153E-02	8022.
4/ 1/69	17.23	17.27	-61.03	1.0359	0.2080E-02	8307.
4/ 2/69	17.69	17.68	-60.84	1.0887	0.2185E-02	8091.
4/ 2/69	17.69	17.68	-60.84	1.0395	0.2087E-02	8085.
4/ 3/69	15.14	15.13	-61.06	0.9393	0.1887E-02	8018.
4/ 3/69	15.14	15.13	-61.06	0.9242	0.1856E-02	8153.
4/ 7/69	18.08	18.06	-60.62	1.1250	0.2258E-02	8000.
4/ 7/69	18.08	18.06	-60.62	1.0991	0.2206E-02	8188.
4/ 8/69	17.33	17.26	-35.64	1.4336	0.2876E-02	6003.
4/ 8/69	17.33	17.26	-35.64	1.4207	0.2850E-02	6058.
4/ 9/69	15.90	15.83	-35.12	1.3062	0.2621E-02	6040.
4/ 9/69	15.90	15.83	-35.12	1.3169	0.2642E-02	5991.
4/10/69	13.99	13.93	-35.54	1.1307	0.2269E-02	6137.
6/20/69	20.66	20.17	0.11	2.3784	0.4752E-02	4236.
6/23/69	17.93	17.45	-0.29	2.0514	0.4110E-02	4247.
6/23/69	17.92	17.45	-0.29	2.0601	0.4127E-02	4229.
6/24/69	16.37	15.13	22.42	2.1873	0.4331E-02	3448.
6/25/69	20.92	19.55	22.65	2.8407	0.5682E-02	3440.
6/25/69	20.92	19.55	22.65	2.8538	0.5708E-02	3424.
6/26/69	18.21	16.92	22.90	2.4654	0.4935E-02	3428.

TABLE A1-4
SOLUBILITY OF HYDROGEN IN N-PROPYLAMINE

DATE	PRESSURE (ATM) TOTAL	PRESSURE (ATM) HYDROGEN	TEMP.(C)	SOL.(CC/GM)	MOLE FRAC.	HENRYS COEF. IDEAL
11/13/68	4.20	4.17	-24.61	0.3374	0.8891E-03	4689.
11/15/68	11.14	11.11	-24.67	0.9211	0.2423E-02	4587.
11/15/68	11.14	11.11	-24.67	0.9171	0.2413E-02	4606.
11/15/68	11.09	11.06	-24.67	0.8955	0.2356E-02	4696.
11/17/68	13.94	13.92	-27.34	1.1345	0.2983E-02	4666.
11/18/68	17.26	17.23	-24.67	1.3981	0.3673E-02	4690.
11/18/68	17.26	17.23	-24.67	1.3923	0.3658E-02	4709.
12/16/68	10.58	10.54	-23.29	0.8584	0.2259E-02	4669.
12/16/68	10.53	10.54	-23.29	0.8498	0.2236E-02	4716.
12/17/68	14.11	14.08	-23.34	1.1336	0.2994E-02	4702.
12/17/68	14.11	14.08	-23.34	1.1281	0.2966E-02	4745.
12/18/68	17.18	17.15	-24.67	1.3885	0.3648E-02	4702.
12/18/68	17.18	17.15	-24.67	1.3796	0.3625E-02	4732.
4/15/69	16.65	16.65	-61.79	0.8949	0.2354E-02	7071.
4/15/69	16.65	16.65	-61.79	0.9170	0.2412E-02	6901.
4/16/69	18.42	18.42	-61.42	1.0095	0.2655E-02	6936.
4/16/69	18.42	18.42	-61.42	1.0031	0.2638E-02	6980.
4/17/69	15.39	15.39	-62.01	0.8717	0.2293E-02	6928.
4/18/69	17.41	17.41	-62.73	0.9430	0.2481E-02	7019.
4/22/69	18.44	18.44	-67.92	0.9300	0.2447E-02	7539.
4/23/69	17.59	17.59	-67.23	0.8904	0.2343E-02	7508.
4/23/69	17.49	17.49	-67.23	0.8841	0.2326E-02	7517.
4/24/69	13.86	13.84	-35.23	1.3766	0.3617E-02	5209.
4/25/69	13.86	13.84	-36.28	1.3811	0.3629E-02	5192.
4/28/69	12.23	12.23	-36.16	0.8778	0.2309E-02	5315.
4/28/69	12.29	12.23	-36.16	0.8791	0.2313E-02	5307.
4/28/69	12.29	12.27	-36.22	0.8801	0.2316E-02	5301.
4/29/69	16.91	16.93	-27.20	1.3431	0.3529E-02	4784.
4/29/69	16.91	16.88	-27.20	1.3196	0.3468E-02	4869.
4/30/69	13.93	13.90	0.11	1.4063	0.3695E-02	3736.
4/30/69	13.93	13.90	0.11	1.4091	0.3702E-02	3729.
7/ 2/69	20.73	20.69	0.03	2.0965	0.5498E-02	3747.
7/ 2/69	20.73	20.69	0.03	2.1044	0.5519E-02	3733.
7/ 3/69	15.27	14.92	21.87	1.8117	0.4755E-02	3138.
7/ 3/69	15.27	14.92	21.87	1.8227	0.4784E-02	3119.

TABLE A1-5
SOLUBILITY OF HYDROGEN IN 1,2-PROPANEDIAMINE

DATE	PRESSURE (ATM) TOTAL	PRESSURE (ATM) HYDROGEN	TEMP.(C)	SOL.(CC/GM)	MOLE FRAC.	HENRYS COEF. IDEAL
11/21/68	7.54	7.54	-23.89	0.1811	0.5987E-03	12591.
11/22/68	10.44	10.44	-24.14	0.2566	0.8479E-03	12309.
1/20/69	13.35	13.85	-24.45	0.3456	0.1142E-02	12135.
1/20/69	13.79	13.79	-24.78	0.3400	0.1123E-02	12275.
1/21/69	18.92	18.92	-24.45	0.4610	0.1522E-02	12366.
5/ 1/69	17.56	17.56	-17.06	0.4590	0.1516E-02	11534.
5/ 1/69	17.56	17.56	-17.06	0.4585	0.1514E-02	11596.
5/ 2/69	16.00	16.00	-18.41	0.4160	0.1374E-02	11643.
5/ 2/69	16.00	16.00	-18.41	0.4189	0.1384E-02	11561.
5/ 5/69	13.17	13.17	-12.08	0.3701	0.1222E-02	10773.
5/ 6/69	16.65	16.65	0.11	0.5236	0.1745E-02	9540.
5/ 6/69	16.65	16.65	0.11	0.5296	0.1748E-02	9521.
5/ 7/69	18.16	18.15	-0.43	0.5735	0.1893E-02	9590.
5/ 7/69	18.16	18.15	-0.43	0.5724	0.1889E-02	9609.
5/12/69	13.27	13.27	10.74	0.4755	0.1570E-02	8451.
5/12/69	13.27	13.27	10.74	0.4670	0.1542E-02	8604.
5/13/69	17.18	17.18	10.41	0.6131	0.2024E-02	8489.
5/13/69	17.18	17.18	10.41	0.6110	0.2017E-02	8513.
5/14/69	18.48	18.48	10.56	0.6640	0.2191E-02	8432.
5/14/69	18.48	18.48	10.56	0.6634	0.2189E-02	8440.
5/15/69	17.71	17.71	10.36	0.6373	0.2105E-02	8411.

TABLE A1-6
SOLUBILITY OF HYDROGEN IN 1,2-ETHANEDIAMINE

DATE	PRESSURE (ATM) TOTAL	PRESSURE (ATM) HYDROGEN	TEMP.(C)	SOL.(CC/GM)	MOLE FRAC.	HENRYS COEF. IDEAL
7/ 8/69	14.46	14.44	26.38	0.3849	0.1031E-02	14006.
7/ 8/69	14.46	14.44	26.38	0.3845	0.1030E-02	14021.
7/ 9/69	18.01	17.99	25.43	0.4735	0.1268E-02	14185.
7/14/69	21.20	21.18	25.88	0.5613	0.1503E-02	14095.
7/14/69	21.20	21.18	25.88	0.5670	0.1518E-02	13952.
7/16/69	21.69	21.65	33.13	0.6355	0.1701E-02	12730.
7/16/69	21.69	21.65	33.13	0.6338	0.1697E-02	12764.
7/17/69	18.11	18.08	33.61	0.5250	0.1406E-02	12862.
7/17/69	18.11	18.08	33.61	0.5263	0.1409E-02	12831.

APPENDIX B1

SMOOTHED SOLUBILITY DATA

Smoothed solubility data for hydrogen in ammonia, methylamine, ethylamine, n-propylamine, 1,2-propanediamine and 1,2-ethanediamine are listed in Tables B1-1 to B1-6. The data presented in each table were generated from the best fit equation, which was developed for each amine from the experimental data. The Henry's law coefficient, mole fraction hydrogen at one atmosphere hydrogen partial pressure and Keunan coefficient are presented for each temperature.

TABLE B1-1
SOLUBILITY OF HYDROGEN IN AMMONIA
SMOOTHED SOLUBILITY CURVE. DEGREE OF FIT=3

TEMP(C)	HENRYS COEF.	X (1ATM.P.P.)	KRUMAN COEF.
-75.00	99319.	0.1010E-04	0.0133
-70.00	84395.	0.1185E-04	0.0156
-65.00	72864.	0.1372E-04	0.0181
-60.00	63569.	0.1573E-04	0.0207
-55.00	55937.	0.1788E-04	0.0235
-50.00	49565.	0.2018E-04	0.0266
-45.00	44173.	0.2264E-04	0.0298
-40.00	39552.	0.2528E-04	0.0333
-35.00	35551.	0.2813E-04	0.0370
-30.00	32057.	0.3119E-04	0.0411
-25.00	28982.	0.3450E-04	0.0454
-20.00	26258.	0.3808E-04	0.0501
-15.00	23834.	0.4196E-04	0.0552
-10.00	21666.	0.4616E-04	0.0608
-5.00	19720.	0.5071E-04	0.0667
0.0	17968.	0.5565E-04	0.0733
5.00	16388.	0.6102E-04	0.0803
10.00	14959.	0.6685E-04	0.0880
15.00	13664.	0.7319E-04	0.0963
20.00	12489.	0.8007E-04	0.1054
25.00	11422.	0.8755E-04	0.1152
30.00	10453.	0.9567E-04	0.1259
35.00	9570.	0.1045E-03	0.1375

TABLE B1-2

SOLUBILITY OF HYDROGEN IN MONOMETHYLAMINE

SMOOTHED SOLUBILITY CURVE. DEGREE OF FIT=2

TEMP(C)	HENRYS COEF.	X (1ATM.P.P.)	KFUNAN COEF.
-90.00	17222.	0.5807E-04	0.0419
-85.00	16223.	0.6164E-04	0.0445
-80.00	15260.	0.6553E-04	0.0473
-75.00	14341.	0.6973E-04	0.0503
-70.00	13468.	0.7425E-04	0.0536
-65.00	12645.	0.7909E-04	0.0571
-60.00	11871.	0.8424E-04	0.0608
-55.00	11147.	0.8971E-04	0.0647
-50.00	10470.	0.9551E-04	0.0689
-45.00	9833.	0.1016E-03	0.0734
-40.00	9250.	0.1081E-03	0.0780
-35.00	8703.	0.1149E-03	0.0829
-30.00	8194.	0.1220E-03	0.0881
-25.00	7722.	0.1295E-03	0.0935
-20.00	7282.	0.1373E-03	0.0991
-15.00	6874.	0.1455E-03	0.1050
-10.00	6495.	0.1540E-03	0.1111
-5.00	6142.	0.1628E-03	0.1175
0.0	5814.	0.1720E-03	0.1241
5.00	5508.	0.1815E-03	0.1310
10.00	5224.	0.1914E-03	0.1382
15.00	4959.	0.2016E-03	0.1456
20.00	4712.	0.2122E-03	0.1532
25.00	4482.	0.2231E-03	0.1611
30.00	4266.	0.2344E-03	0.1692
35.00	4065.	0.2460E-03	0.1776

TABLE B1-3
SOLUBILITY OF HYDROGEN IN MONOETHYLAMINE
SMOOTHED SOLUBILITY CURVE. DEGREE OF FIT=5

TEMP(C)	HENRYS COEF.	X (1 ATM. P.P.)	KEENAN COEF.
-80.00	10659.	0.9382E-04	0.0466
-75.00	9578.	0.1044E-03	0.0519
-70.00	8947.	0.1118E-03	0.0556
-65.00	8484.	0.1177E-03	0.0585
-60.00	8083.	0.1237E-03	0.0615
-55.00	7676.	0.1303E-03	0.0649
-50.00	7249.	0.1379E-03	0.0686
-45.00	6820.	0.1466E-03	0.0729
-40.00	6413.	0.1559E-03	0.0775
-35.00	6029.	0.1659E-03	0.0825
-30.00	5675.	0.1762E-03	0.0876
-25.00	5362.	0.1866E-03	0.0928
-20.00	5033.	0.1987E-03	0.0988
-15.00	4833.	0.2069E-03	0.1029
-10.00	4614.	0.2167E-03	0.1078
-5.00	4417.	0.2264E-03	0.1126
0.0	4237.	0.2360E-03	0.1174
5.00	4066.	0.2460E-03	0.1223
10.00	3894.	0.2568E-03	0.1277
15.00	3722.	0.2687E-03	0.1336
20.00	3539.	0.2826E-03	0.1405
25.00	3344.	0.2990E-03	0.1487
30.00	3132.	0.3192E-03	0.1587
35.00	2906.	0.3442E-03	0.1712

TABLE B1-4
SOLUBILITY OF HYDROGEN IN N-PROPYLAMINE
SMOOTHED SOLUBILITY CURVE. DEGREE OF FIT=2

TEMP(C)	HENRYS COEF.	X (1ATM.P.P.)	KEUNAN COEF.
-80.00	8695.	0.1150E-03	0.0436
-75.00	8176.	0.1223E-03	0.0464
-70.00	7696.	0.1299E-03	0.0493
-65.00	7252.	0.1379E-03	0.0523
-60.00	6842.	0.1462E-03	0.0554
-55.00	6463.	0.1547E-03	0.0587
-50.00	6113.	0.1636E-03	0.0620
-45.00	5788.	0.1728E-03	0.0655
-40.00	5488.	0.1822E-03	0.0691
-35.00	5210.	0.1920E-03	0.0728
-30.00	4951.	0.2020E-03	0.0766
-25.00	4711.	0.2123E-03	0.0805
-20.00	4488.	0.2228E-03	0.0845
-15.00	4281.	0.2336E-03	0.0886
-10.00	4087.	0.2446E-03	0.0928
-5.00	3907.	0.2559E-03	0.0971
0.0	3739.	0.2675E-03	0.1015
5.00	3581.	0.2792E-03	0.1059
10.00	3434.	0.2912E-03	0.1105
15.00	3296.	0.3034E-03	0.1151
20.00	3167.	0.3158E-03	0.1198
25.00	3045.	0.3284E-03	0.1246
30.00	2931.	0.3412E-03	0.1294
35.00	2824.	0.3541E-03	0.1343

TABLE B1-5

SOLUBILITY OF HYDROGEN IN 1,2-PROPANEDIAMINE

SMOOTHED SOLUBILITY CURVE. DEGREE OF FIT=1

TEMP(C)	HENRYS COEF.	X (1 ATM.P.P.)	KEUNAN COEF.
-35.00	14274.	0.7006E-04	0.0212
-30.00	13362.	0.7484E-04	0.0226
-25.00	12540.	0.7974E-04	0.0241
-20.00	11799.	0.8475E-04	0.0256
-15.00	11128.	0.8986E-04	0.0272
-10.00	10519.	0.9507E-04	0.0287
-5.00	9963.	0.1004E-03	0.0304
0.0	9456.	0.1058E-03	0.0320
5.00	8992.	0.1112E-03	0.0336
10.00	8565.	0.1168E-03	0.0353
15.00	8173.	0.1224E-03	0.0370
20.00	7811.	0.1280E-03	0.0387
25.00	7476.	0.1338E-03	0.0405
30.00	7166.	0.1395E-03	0.0422
35.00	6879.	0.1454E-03	0.0440

TABLE B1-6

SOLUBILITY OF HYDROGEN IN 1,2-ETHANEDIAMINE

SMOOTHED SOLUBILITY CURVE. DEGREE OF FIT=1

TEMP(C)	HENRYS COEF.	X (1ATM.P.P.)	KEENAN COEF.
11.00	17338.	0.5768E-04	0.0215
16.00	16130.	0.6200E-04	0.0231
21.00	15043.	0.6648E-04	0.0248
26.00	14062.	0.7111E-04	0.0265
31.00	13174.	0.7591E-04	0.0283
36.00	12368.	0.8085E-04	0.0302

APPENDIX C1

SAMPLE CALCULATION AND ESTIMATION OF ERRORS

A. Calculation Routine

The amount of hydrogen dissolved in a unit weight of amine under the temperature and pressure conditions of the solubility cell is given by:

$$S^P = \frac{V_2}{W_1} \qquad [C1\text{-}1]$$

where: S^P = solubility coefficient $\left\{\frac{\text{c.c. } H_2 \text{ (STP)}}{\text{gm. amine}}\right\}$

V_2 = volume of dissolved hydrogen corrected to standard conditions of 0°C and 760 m.m. hg. (c.c.)

M_1 = mass of liquid amine (gm.)

The corrected volume of hydrogen, as determined in the hydrogen volumetric apparatus, is given by:

$$V_2 = \frac{273.15}{76.0}\left\{\frac{V^f_{cal}\ P^f_{cor}}{T^f_K} - \frac{V^r_{cal}\ P^r_{cor}}{T^f_K}\right\} = (V_f - V_r) \qquad [C1\text{-}2]$$

where: $P^f_{cor} = P^f_m - P_{cap}$ [C1-3]

$P^r_{cor} = P^r_m - P_{cap}$ [C1-4]

V^f_{cal} = calibrated volume of gas burette occupied by total hydrogen sample. (c.c.)

V^r_{cal} = calibrated volume of gas burette occupied by residual hydrogen volume. (c.c.)

P^f_{cor} = corrected pressure of the total hydrogen sample when the burette volume is V^f_{cal}. (cm. Hg.)

P^r_{cor} = corrected pressure of the residual hydrogen sample when the burette volume is V^r_{cal}. (cm. Hg.)

P^f_m = measured pressure of the total hydrogen sample when the burette volume is V^f_{cal}. (cm. Hg.)

P^r_m = measured pressure of the residual hydrogen sample when the burette volume is V^r_{cal}. (cm. Hg.)

P_{cap} = capillary correction for the closed-end manometer. (cm. Hg.)

T^f_K = temperature of total hydrogen sample (K°)

T^r_K = temperature of residual hydrogen sample (K°)

The mass of amine, as determined by weighing the sample cylinders when empty and full, is:

$$W_1 = W_f - W_e - W_2 = W_s - W_2 \qquad [C1\text{-}5]$$

$$W_2 = \frac{2.016\ V_2}{22414.6} \qquad [C1\text{-}6]$$

where: W_1 = mass of amine. (gm.)

W_f = mass of sample bomb plus amine solution (gm.)

W_e = mass of sample bomb empty. (gm.)

W_s = mass of amine solution. (gm.)

W_2 = mass of dissolved hydrogen. (gm.)

The mole fraction hydrogen at the equilibrium conditions of the saturated solution prior to sampling is:

$$x_2^P = \frac{1}{\frac{22414.6}{M_1 S^P} + 1} \qquad [C1\text{-}7]$$

where: M_1 = molecular weight of the amine. $\left(\frac{\text{gm.}}{\text{gm. mole}}\right)$

Henry's law coefficient is:

$$H_2 = \frac{P_2}{x_2^P} \qquad [C1\text{-}8]$$

The hydrogen partial pressure (P_2) is calculated assuming Dalton's law and Raoult's law to be valid.

$$P_2 = \pi - P_1^s(1 - x_2^P). \qquad [C1\text{-}9]$$

$$\pi = P_g + P_{bar}. \qquad [C1\text{-}10]$$

π = absolute cell pressure at equilibrium. (atm.)

P_1^s = saturation temperature of the amine at the equilibrium temperature T. (atm.)

P_g = cell pressure as measured on gauge prior to sampling. (atm.)

P_{bar} = barometric pressure. (atm.)

B. Estimation of Errors

Substituting equation [C1-5] and equation [C1-6] into equation [C1-1] yields:

$$S^P = \left\{\frac{1}{\frac{W_s}{V_2} - \frac{2.0}{22414.6}}\right\} \qquad [C1\text{-}11]$$

The change in the value of the solubility coefficient (ΔS^P) corresponding to differential changes ΔV_2 and ΔW_s in the measured values V_2 and W_s respectively is:

$$\Delta S^P = \left|\left(\frac{\partial S^P}{\partial V_2}\right)\right| |\Delta V_2| + \left|\left(\frac{\partial S^P}{\partial W_s}\right)\right| |\Delta W_s| \qquad [C1\text{-}12]$$

Substituting the required partial derivatives from equation [C1-11] into equation [C1-12] gives:

$$\frac{\Delta S^P}{S^P} = \frac{\Delta V_2}{V_2} + \frac{2.0}{22414.6}\ \frac{\Delta V_2}{W_1} + \frac{\Delta W_s}{W_1} \qquad [C1\text{-}13]$$

The differential change in the corrected hydrogen volume (ΔV_2) is obtained from equation [C1-2]

$$\Delta V_2 = \left|\left(\frac{\partial V_2}{\partial V^f_{cal}}\right)\right| |\Delta V^f_{cal}| + \left|\left(\frac{\partial V_2}{\partial P^f_{cor}}\right)\right| |\Delta P^f_{cor}| + \left|\left(\frac{\partial V_2}{\partial T^f_K}\right)\right| |\Delta T^f_K|$$

$$+ \left|\left(\frac{\partial V_2}{\partial V^r_{cal}}\right)\right| |\Delta V^r_{cal}| + \left|\left(\frac{\partial V_2}{\partial P^r_{cor}}\right)\right| |\Delta P^r_{cor}| + \left|\left(\frac{\partial V_2}{\partial T^r_K}\right)\right| |\Delta T^r_K| \qquad [C1\text{-}14]$$

Substituting the required partial derivatives yields:

$$\Delta V_2 = V_f \left\{\frac{\Delta V^f_{cal}}{V^f_{cal}} + \frac{\Delta P^f_{cor}}{P^f_{cor}} + \frac{\Delta T^f_K}{T^f_K}\right\} + V_r \left\{\frac{\Delta V^r_{cal}}{V^r_{cal}} + \frac{\Delta P^r_{cor}}{P^r_{cor}} + \frac{\Delta T^r_K}{T^r_K}\right\} \qquad [C1\text{-}15]$$

The estimated error in the solubility coefficient is obtained from equations [c1-15] and [C1-13]. The estimated error in the mole fraction hydrogen equals:

$$\frac{\Delta x_2{}^P}{x_2{}^P} = \frac{\Delta S^P}{S^P}\ (1 - x_2{}^P) \qquad [C1\text{-}16]$$

The estimated error in Henry's law coefficient equals:

$$\frac{\Delta H_2}{H_2} = \frac{\Delta P}{P} + \frac{\Delta x_2^P}{x_2^P} \qquad [C1\text{-}17]$$

where ΔP is obtained from equation [C1-10]

$$\Delta P = \Delta\pi + \Delta P_1^s \qquad (1 >> x_2^P) \qquad [C1\text{-}18]$$

$$\Delta\pi = \Delta P_g + \Delta P_{bar} \qquad [C1\text{-}19]$$

The range of uncertainty in the experimental measurements were estimated to be:

1) Calibrated Volume: $\Delta V_{cal} = 0.05\%\ V_{cal}$ $\Delta V_{cal} = \pm 0.0005\ V_{cal}$

2) Corrected Pressure: $\Delta P_m = \Delta P_{cap} = 2 \times 0.005$ cm.

$\Delta P_{cor} = \pm 0.020$ cm.

3) Hydrogen Temperature: $\Delta T_K^f = \Delta T_K^r = \pm 0.10$ °K

4) Sample Mass: $\Delta W_f = \Delta W_e = 0.0001$ gm. $\Delta W_s = \pm 0.0002$ gm.

5) Total Pressure: $\Delta P_g = \pm 0.40$ psig.

6) Barometric Pressure: $\Delta P_{bar} = 0.02$ cm. Hg.

7) Amine Vapor Pressure: $\Delta P_1^s = \pm 0.01\ P_1^s$

Sample Calculation

Date of determination: June 4/69 Sample Bomb A

Amine studied: Methylamine

Weight determination

1) Sample and bomb = W_f = 254.8893 gm.

2) Bomb empty = W_e = 247.7555 gm.

3) Sample weight = W_s = 7.1338 gm.

Barometric pressure = P_{bar} = 69.88 cm. Hg. = 13.51 psi.

Barometer temperature = 24°C

Cell temperature = -0.007 m.v. = -0.21°C

Cell pressure before bleed = 192.75 psig.

Cell pressure after bleed = 192.75 psig.

Cell pressure after sample = 192.75 psig.

Absolute system pressure = = 192.75 + 13.51 = 206.26 psia. = 14.03 atm.

Date of analysis: June 4/69

1) Calculation of residual volume:

Calibrated volume = 1 - 3 Measured 41.400 Corrected P_{m_r} = .545

= 0.4911 c.c. Pressure 40.855 Pressure P_{cap} = .450

Burette temperature = 24.0°C P_{m_r} 0.545 cm. P_{cor_f} = .095

$$\text{Residual volume} = V_r = \frac{0.4911 \times 0.095 \times 273.15}{76.0 \times 297.15} = 0.0006 \text{ c.c. (STP)}$$

2) Calculation of total volume before melt:

Calibrated volume = 1 - 6 Measured 67.515 Corrected P_{m_f} = 26.660

= 35.3312 c.c. Pressure 40.855 Pressure P_{cap} = 0.450

Burette temperature = 24.1°C P_{m_f} 26.660 P_{cor_f} = 26.210 cm.

Total volume hydrogen before melt =

$$\frac{35.3312 \times 26.210 \times 273.15}{76.0 \times 297.25} = 11.1967 \text{ c.c. (STP)}$$

3) Calculation of total volume after melt:

Calibrated volume = 1 - 6 Measured 67.520 Corrected P_{m_f} = 26.665

= 35.3312 c.c. Pressure 40.855 Pressure P_{cap} = 0.450

Burette temperature = 24.1°C P_{m_f} 20.665 P_{cor_f} = 26.215

Total volume of hydrogen after melt = V_f =

$$\frac{35.3312 \times 26.215 \times 273.15}{76.0 \times 297.25} = 11.1989 \text{ c.c. (STP)}$$

Volume of hydrogen corrected to 0°C and 760 m.m. Hg. pressure is:

$$V_2 = V_f - V_r = 11.1989 - 0.0006 = 11.1983 \text{ c.c. } H_2(\text{STP})$$

Therefore the solubility coefficient for hydrogen dissolved in methylamine at -0.21°C and 14.03 atm. absolute pressure is given by equation [C1-1]

$$S^P = \frac{11.1983}{(7.1338 - \frac{2.0}{22414.6} \times 11.1983)} = \frac{11.1983}{7.1328} = 1.5700 \frac{\text{c.c. } H_2(\text{STP})}{\text{gm. amine}}$$

The mole fraction hydrogen is, from equation [C1-7]

$$x_2^P = \frac{\frac{1.5700}{22414.6}}{\frac{1.5700}{22414.6} + \frac{1.0}{31.06}} = 0.002171 \frac{\text{moles } H_2}{\text{total moles}}$$

Henry's law coefficient is, from equation [C1-8]

$$H_2 = \frac{P_2}{x_2^P} = \frac{-P^s}{(x_2^P)} = \frac{(14.04 - 1.32) \text{ atm.}}{0.002171 \text{ moles fraction } H_2} = \frac{12.72}{0.002171}$$

$$= 5858 \frac{\text{atm.}}{\text{mole fraction } H_2}$$

Estimate of Errors

Solubility Coefficient

From equation [C1-13]

$$\frac{\Delta S^P}{S^P} = \frac{\Delta V_2}{V_2} + \frac{2.0}{22414.6} \frac{\Delta V_2}{M_1} + \frac{\Delta W_s}{W_1} \qquad [C1-13]$$

$$\Delta V_2 = V_f \left\{ \frac{\Delta V^f_{cal}}{V^f_{cal}} + \frac{\Delta P^f_{cor}}{P^f_{cor}} + \frac{\Delta T^f_K}{T^f_K} \right\} + V_r \left\{ \frac{\Delta V^r_{cal}}{V^r_{cal}} + \frac{\Delta P^r_{cor}}{P^r_{cor}} + \frac{\Delta T^r_K}{T^r_K} \right\} \qquad [C1\text{-}14]$$

$$= 11.1983 \left\{ 0.0005 + \frac{0.020}{26.215} + \frac{0.10}{297.25} \right\} + (\text{negligible})$$

$$= 11.1983\{0.0005 + 0.0008 + 0.0003\} = 11.1983(0.0016) = 0.0179$$

$$\frac{\Delta V_2}{V_2} = 0.0016$$

The error in the solubility coefficient S^P is obtained from equation [C1-13] to be:

$$\frac{\Delta S^P}{S^P} = 0.0016 + \frac{2.0}{22414.6} \left(\frac{0.0179}{7.1328} \right) + \frac{0.0002}{7.1328} \qquad [C1\text{-}15]$$

$$= 0.0016 + 0.00002 + 0.00003$$

$$= 0.0017$$

$$\Delta S^P = \pm 0.0027$$

$$S^P = 1.5700 \pm 0.0027 \left(\frac{\text{c.c. } H_2 \text{(STP)}}{\text{gm. amine}} \right)$$

The error in the hydrogen mole fraction is:

$$\frac{\Delta x_2{}^P}{x_2{}^P} = 0.0017(1.000 - 0.0022) = 0.0017 \qquad [C1\text{-}16]$$

$$\Delta x_2{}^P = \pm 0.000004$$

$$x_2{}^P = 0.002171 \pm 0.000004$$

The expected error in Henry's law coefficient is:

$$\frac{\Delta H_2}{H_2} = \frac{\Delta P}{P} + 0.0017 \qquad [C1\text{-}17]$$

$$\Delta P = \Delta P_g + \Delta P_{bar} + \Delta P_s \qquad [C1\text{-}18] \text{ \& } [C1\text{-}19]$$

$$= 0.162 \text{ atm.}$$

$$\frac{\Delta H_2}{H_2} = \frac{0.0162}{12.72} + 0.0017$$

$$= 0.0030$$

$$\therefore \Delta H_2 = \pm 18$$

$$H_2 = 5858 \pm 18$$

It can therefore be seen from the error analysis that the last two digits quoted for S^P, x_2^P and H_2 are uncertain. The values of the solubility coeficient, S^P, and hydrogen mole fraction are expected to be within ±0.2% due to errors in the experimental measurements. Henry's law coefficient is expected to be within ±0.30 per cent depending on the solubility of the amine vapor pressure data.

APPENDIX D1

PHYSICAL PROPERTIES

A summary of the physical property data for the five amines considered in this hydrogen solubility study, together with the properties for ammonia, are listed in Tables D1-1 to D1-6 inclusive. Generalized properties of hydrogen are given in Table D1-7. The number of the reference from which each property was obtained has been listed along side the value. The data were presented in this manner to indicate the value chosen from the somewhat conflicting results of the various investigators. The data presented were felt to be the best available at the time of this study.

TABLE D1-1

PROPERTY	NAME OF AMINE											
	AMMONIA		METHYLAMINE		ETHYLAMINE		n-PROPYLAMINE		1,2-ETHANEDIAMINE		1,2-PROPANEDIAMINE	
Mol. wt.	17.03	(86)	31.06	(86)	45.09	(86)	59.11	(90)	60.10	(90)	74.13	(90)
B. Pt. °C @ 760 m.m.	-33.35	(80)	-6.33	(89)	16.58	(86)	48.5	(89)	116.9	(90)	120.9	(90,92)
F. Pt. °C	-77.7	(80)	-93.46	(89)	-81.0	(86,90)	-83.0	(90)	10.8	(90)	-37.2	(92)
Crit. temp. °C	132.9	(86)	156.9	(86)	183.2	(86)	223.8	(91)				
Crit. Pres. atm.	111.3	(86)	73.6	(86)	55.54	(86)	46.8	(93)				
Crit. density gm/cc	0.235	(86)	0.216	(86)	0.2434	(86)	0.254	(93)				
Latent heat of vaporization at B. Pt. (cal./gm. mole)	5581	(88)	6210	(86)	6495	(86)	7159	(90)	9650	(90)	9184	(90)
Specific gravity 20°/20°	0.6097	(86)	0.6616	(89)	0.6817	(89)	0.7160	(89)	0.8995	(90)	0.8640	(90)
of liquid 25°/20°	0.6023	(86)	0.6558	(89)	0.6757	(89)	0.7108	(89)			0.8569	(80)
Electric dipole Moment for molecule in gas phase (debye)	1.47	(80)	1.31	(80)	1.3	(87)	1.4	(86)	1.92	(95)		
Number of H exchangeable H atoms	3		2		2		2		4		4	
Wt/exch. H atom	5.7		15.5		22.5		29.6		15.0		18.5	

TABLE D1-2

POLYNOMIAL FIT OF THE AMINE VAPOR PRESSURE

$$\ln P = C1 + \frac{C2}{T} + C3T + C4 \ln T$$

P - Vapor Pressure (atmospheres)

T - Temperature (Kelvin degrees)

Amine	C_1	C_2	C_3	C_4	Temperature Range	Reference
Ammonia	75.655967	-4615.475709	0.015718	-10.981819	-60°C to 110.0°C	(86)
Methylamine	100.905535	-5716.325059	0.022480	-15.300000	-74.1°C to 9.5°C	(89)
Ethylamine	88.898194	-5931.336179	0.014278	-12.800000	-61.3°C to 50.0°C	(86)
n-Propylamine	5.890836	-4195.511650	-0.009992	1.800000	-36°C to 68.0°C	(89)
1,2-Ethanediamine	7196.745477	-209915.971130	1.854607	-1237.280901	19°C to 116.9°C	(90)
1,2-Propanediamine	4033.076448	-121729.318450	1.014114	-690.000000	8°C to 120.9°C	(90)

TABLE D1-3

POLYNOMIAL FIT OF AMINE DENSITIES

$$\rho = A1 + A2T + A3T^2 + A4T^3$$

ρ - Density $\left(\frac{gm.}{c.c.}\right)$

T - Temperature (Kelvin degrees)

Amine	A_1	A_2	A_3	A_4	Temperature Range	Reference
Ammonia	1.06365	-2.64191×10^{-3}	7.26592×10^{-6}	-1.20124×10^{-8}	-51°C to +51°C	(86)
Methyalmine	0.90580	-4.00947×10^{-4}	-1.45769×10^{-6}		-50°C to +30°C	(86)
Ethylamine	0.95690	-7.00075×10^{-4}	-7.85493×10^{-7}		-50°C to +50°C	(86)

$$\rho = B1 + B2T + B3T^2$$

ρ - Density $\left(\frac{gm.}{ml.}\right)$

T - Temperature (Degrees Celsius)

Amine	B_1	B_2	B_3	Temperature Range	Reference
n-Propylamine	0.7344	-6.133×10^{-4}	8.4×10^{-6}	0°C to 15°C	(82)

TABLE D1-4

AMINE VISCOSITY

Ammonia

T°C	μ(C.P.)	Ref.
-69.0	0.475	(80)
-50.0	0.317	(80)
-40.0	0.276	(80)
-33.5	0.255	(80)
20	0.180	(91)

Methylamine

T°C	μ(C.P.)	Ref.
-80	0.829	(83)
-78.3	0.9120	(96)
-69.7	0.665	(83)
-63.3	0.6704	(96)
-59.7	0.552	(83)
-50.0	0.480	(83)
-40.0	0.422	(83)
-34.9	0.400	(83)
-30.0	0.372	(83)
-22.8	0.3532	(96)
-20.0	0.331	(83)
-14.4	0.300	(83)
-10.0	0.291	(83)
-10.0	0.285	(83)
0.0	0.236	(83)
0.0	0.2742	(96)

Ethylamine

T°C	μ(C.P.)	Ref.
-55.7	0.800	(83)
-50.0	0.771	(83)
-50.0	0.780	(83)
-40.0	0.588	(83)
-33.5	0.437	(83)
-30.0	0.467	(83)
-20.0	0.415	(83)
-10.0	0.370	(83)
-10.0	0.343	(83)
0.0	0.328	(83)
10.0	0.299	(83)
16.0	0.276	(83)
23.2	0.259	(83)
23.2	0.250	(83)

1,2-Ethanediamine

T°C	μ(C.P.)	Ref.
20	1.6	(90)

1,2-Propanediamine

T°C	μ(C.P.)	Ref.
0	2.9	(92)
20	1.6	(92)
40	1.1	(92)

TABLE D1-5

AMINE SURFACE TENSION

Ammonia				Methylamine				Ethylamine				Propylamine			
T°C.	IN CONTACT WITH	σ (dynes/cm.)	Ref.	T°C.	IN CONTACT WITH	σ (dynes/cm.)	Ref.	T°C.	IN CONTACT WITH	σ (dynes/cm.)	Ref.	T°C.	IN CONTACT WITH	σ (dynes/cm.)	Ref.
11.1	vapor	23.4	(80)	-70	nitrogen	29.2	(80)	-74.0	nitrogen	28.9	(87)	10	air	23.5	(82)
34.1	vapor	18.1	(80)	-20	vapor	23.0	(80)	-21.5	nitrogen	23.2	(87)	20	air	22.4	(82)
59.0	vapor	13.0	(87)	-12	nitrogen	22.2	(80)	0	nitrogen	21.3	(87)	45	air	19.4	(82)
				15	vapor	20.60	(84)	9.9	nitrogen	20.4	(80)				
				25	vapor	19.19	(84)	15	vapor	20.56	(86)				
				35	vapor	17.65	(84)								

TABLE D1-6

DIELECTRIC CONSTANT OF LIQUID AMINE

($\varepsilon_{vacuum} = 1$)

Ammonia			Methylamine			Ethylamine			1,2-Ethanediamine		
T°C.	ε	Ref.	T°C.	ε	Ref.	T°C.	ε	Ref.	T°C.	ε	Ref.
-77.2	25.0	(80)	-10.0	11.4	(80)	10	6.94	(82)	18	16.0	(82)
-60.0	26.7	(88)	25.0	9.4	(80)	21	6.3	(87)	20	14.2	(87)
-33.4	22.4	(80)				25	6.1	(87)	25	13.7	(87)
5.0	18.9	(88)									
15.0	17.8	(80)									
25.0	16.9	(80)									
35.0	16.3	(80)									

TABLE D1-7

GENERALIZED PROPERTIES OF HYDROGEN

Molecular Weight	2.016
Normal Boiling Point	20.39°K
Normal Freezing Point	13.96°K
Critical Temperature	33.3°K
Critical Pressure	12.8 atm.
Critical Molar Volume	65 $cm.^3$/gm. mole
Critical Compressibility Factor	0.304
Latent Heat of Vaporization at B. Pt.	0.216 Kcal./gm.mole
Latent Heat of Fusion at F. Pt.	0.028 Kcal./gm.mole

APPENDIX E1

CALIBRATION DATA

The thermocouple calibration curve is given in Figure E1-1. This curve was obtained by calibrating the cell thermocouple against a platinum resistance thermometer. The emf. as measured from the thermocouple was compared with the standard emf. as given in the "Leeds and Northrop" conversion book at the temperature indicated by the platinum resistance thermometer. The equation for the deviation of the thermocouple was found to be:

$$\varepsilon_s = \frac{(\varepsilon_A - 0.001)}{0.989} \qquad [E1\text{-}1]$$

ε_s - standard emf. as determined in tables.

ε_A - measured emf.

The standard emf. versus temperature tables were stored in tabular form in a computer routine. The cell temperature was obtained by interpolation of this table for the corrected voltage as given by equation [E1-1]

The volumes of the two composite bulb gas burettes used in this study are listed in Table [E1-1]. These volumes were obtained by a mercury weighing technique. The tabulated mean percent error was obtained by averaging the deviations from the mean of all the measurements performed on a given volume. The average deviation was divided by the mean value to yield the percent error.

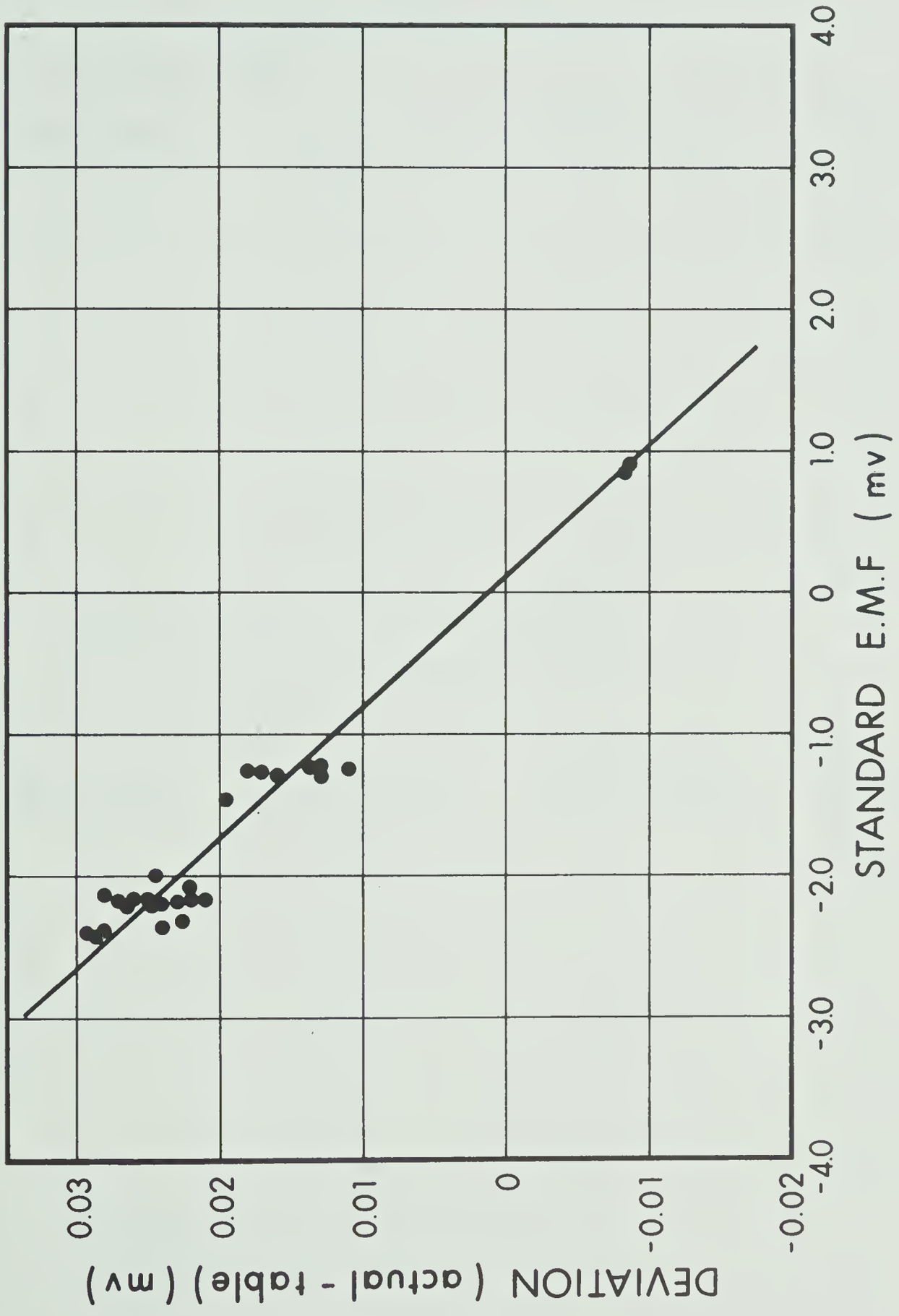


FIG. E1-1 CALIBRATION OF CELL THERMOCOUPLE



TABLE E1-1

CALIBRATION CURVE FOR GAS BURETTES

A) Gas burette number 1.

Volume Number	Volume (c.c.)	Number of Determinations	Mean % Error
1 - 2	0.35077	4	0.507
1 - 3	0.66158	3	0.28
1 - 4	0.97361	4	0.16
1 - 5	1.72945	3	0.023
1 - 6	2.60871	3	0.052
1 - 7	4.45152	4	0.045
1 - 8	8.83279	2	0.018
1 - 9	17.07259	3	0.032

Burette calibrated with mercury at 22.0°C

Estimated Accuracy of calibration = ±0.05%

B) Gas burette number 2.

Volume Number	Volume (c.c.)	Number of Determinations	Mean % Error
1 - 2	0.0732	4	0.92
1 - 3	0.4911	4	0.0086
1 - 4	8.2386	4	0.015
1 - 5	21.4575	4	0.012
1 - 6	35.3312	4	0.0088
1 - 7	48.9761	3	0.0029
1 - 8	72.6722	3	0.0027

Burette calibrated with mercury at 22.5°C

Estimated accuracy of calibration = ±0.02%

PART TWO

THE DIFFUSIVITY OF HYDROGEN IN METHYLAMINE

1. INTRODUCTION

Isotopic exchange reactions are, at present, the most economic means of enriching a deuterium source to the concentration where reactor grade heavy water may be produced. A brief review of some of the existing and proposed exchange reactions was presented in Part 1 of this thesis. The isotopic exchange of hydrogen deuteride between gaseous hydrogen and a liquid aliphatic amine appears to have economic potential as a future heavy water production process, with the most promising aliphatic amine being methylamine[1].

The exchange of isotopic hydrogen with methylamine in the region of low deuterium concentration can be described by the following reversible reaction.

$$HD + CH_3NH_2 \rightleftharpoons CH_3NHD + H_2 \qquad [1.1]$$

which occurs in the presence of the homogeneous catalyst potassium methylamide.

The equilibrium constant for the reaction is:

$$K' = \frac{P(H_2)\ C(CH_3NHD)}{P(HD)\ C(CH_3NH_2)} \qquad [1.2]$$

and if the solubility of HD is assumed to equal that for H_2, then equation [1.1] can be written as:

$$K' = \frac{C(H_2)\ C(CH_3NHD)}{C(HD)\ C(CH_3NH_2)} \qquad [1.3]$$

A study by Bourke and Lee[2] of the analogous exchange reaction for ammonia-hydrogen showed that the exchange rate can be assumed to be first order with respect to both the concentration of HD

and of NH_2D. Assuming the methylamine-hydrogen exchange is also first order in both the concentration of HD and CH_3NHD and that the concentration of dissolved H_2 and CH_3NH_2 are essentially constant, then equation [1.1] simplifies to the following form:

$$HD \underset{k_2}{\overset{k_1}{\rightleftharpoons}} CH_3NHD \qquad [1.4]$$

The equilibrium constant for the above reaction is:

$$K = \frac{C(CH_3NHD)}{C(HD)} = K' \frac{C(CH_3NH_2)}{C(H_2)} \qquad [1.5]$$

Bourke and Lee[2] quoted a value of K for the ammonia-hydrogen exchange as 3.26×10^4 at a hydrogen partial pressure of eight atmospheres and a temperature of -30°C. If the equilibrium constant for the methylamine-hydrogen exchange is of the same order of magnitude, then the exchange as represented by equation [1.4] can be considered to be irreversible.

$$HD \overset{k_1}{\rightarrow} CH_3NHD \qquad [1.6]$$

The rate of absorption of HD in methylamine may be expressed by the general equation:

$$G = k_L\, a(C_i - C_o) \qquad [1.7]$$

The chemical absorption coefficient k_L is in general a function of the molecular diffusion coefficient of the dissolved solute (D) and the kinetic velocity constant (k_1). For example, in the fast reaction regime, the chemical absorption coefficient for the reaction described by equation [1.6] is given by the expression:

$$k_L = \sqrt{Dk_1} \qquad [1.8]$$

The chemical absorption coefficient can be evaluated from absorption studies in various experimental absorbers for which the interfacial area of transfer (a) is known. If the molecular diffusion coefficient (D) is also known, the kinetic velocity constant (k_1) can be determined from equation [1.8].

The objective of the work outlined in this portion of the thesis is to initiate a program for measuring the kinetic velocity constant (k_1) for the hydrogen-methylamine exchange reaction. As a knowledge of the molecular diffusion coefficient is necessary for evaluation of this parameter, the first step in the program is the measurement of the diffusivity of hydrogen in methylamine.

The apparatus chosen for this study is the single sphere absorber. This absorber has been successfully employed by a number of investigators[3,4,5,6,7] for absorption with chemical reaction studies. A number of papers[8,9,10,11,12] are also available regarding the use of a single sphere absorber for measuring the diffusivity of various gases in water.

The single sphere absorber is one of a group of laboratory absorbers for which the hydrodynamics are known to the extent that rigorous calculations of the diffusion time (Astarita (7)) and surface area can be made. Other absorbers which fit in this category are the wetted wall column, laminar jet, annular jet and rotating drum. For the purpose of this study, the reasons for choosing the single sphere absorber are as follows:

(a) The end effects, both entrance and exit, are reported to be less than those of a wetted wall column.

(b) Various authors[5,9] have stated that relatively high liquid flow with the absence of surface ripples is possible.

(c) The diffusion times are in the order of 0.1 sec. to 1 sec. as compared to diffusion times of 0.01 sec. to 0.1 sec. for the laminar jet. A large diffusion or contact time is desirable for operation in the fast reaction regime as defined by Astarita[7,13].

(d) The surface area ranges from 10 $cm.^2$ to 40 $cm.^2$ as opposed to 0.3 $cm.^2$ to 10 $cm.^2$ for the laminar jet. The rate of absorption of the slightly soluble hydrogen deuteride solute would be difficult to measure for an interfacial area of the magnitude generated in a laminar jet.

(e) The liquid flow rate required for a laminar jet is in general much greater than the flow required for a single sphere absorber.

The work described in this portion of the thesis is concerned with the single sphere absorber design and its utilization for physical absorption studies involving hydrogen gas and liquid methylamine. Various models describing the physical absorption process associated with a single sphere absorber are discussed. A brief review of some of the methods for determining diffusion coefficients, and a number of empirical correlations for predicting diffusion coefficients are presented.

2. THEORY

A. Hydrodynamic Models of Physical Absorption Process

A number of hydrodynamic models of the interface between a gas phase and a liquid film have been presented in the literature. Some of the better known models describing the physical absorption process will be described below. The absorption of a single gas in a liquid film which is flowing over a sphere will also be discussed.

1. Whitman Film Theory[14]:

The liquid close to the gas-liquid interface is assumed to be in laminar flow parallel to a plane while the liquid below a depth x_L is assumed to be in turbulent motion. The dissolved solute concentration in the bulk of the phase (turbulent region) is assumed to be constant so that the rate of absorption is determined by the molecular diffusion in the stagnant surface film of thickness x_L. The thickness of the stagnant film is assumed to be small, hence, the diffusion process is assumed to be at steady state.

The average rate of physical absorption is defined by the steady state equation:

$$\bar{G}^\circ = -D\left(\frac{\partial C}{\partial x}\right)_{x=0} \qquad [2.1]$$

with the following boundary conditions.

$$x = 0; \quad C = C_i \qquad [2.2]$$

$$x = x_L; \quad C = C_o \qquad [2.3]$$

The liquid depth (x) is measured from the interface.

The concentration gradient at the interface may be approximated by the expression:

$$-\left(\frac{\partial C}{\partial x}\right)_{x=0} = \frac{(C_i - C_o)}{x_L} \qquad [2.4]$$

The absorption coefficient for physical absorption is defined as:

$$K_L^\circ = \frac{\bar{G}^\circ}{(C_i - C_o)} \qquad [2.5]$$

which, upon substituting equations [2.1] and [2.4] in equation [2.6] becomes:

$$K_L^\circ = \frac{D}{x_L} \qquad [2.6]$$

The first order dependence of the physical absorption coefficient on the diffusivity as predicted by the Whitman Film Theory[14] is in contradiction with experimental findings which indicate that the absorption coefficient is proportional to the square root of the diffusivity. Another drawback of this theory is the fact that the stagnant film thickness (x_L) is unknown. The Whitman Film Theory has, however, been extensively used for predicting the behaviour of absorption experiments.

2. Higbie's Penetration Theory (Systematic Surface Renewal)[15]:

A hydrodynamic model proposed by Higbie[15] in 1935 assumes the gas-liquid interface is made up of a number of fluid elements which are continually being brought to the surface by the motion of

the fluid. While the element of fluid remains at the interface, gas is absorbed by unsteady state molecular diffusion. The absorption process is described by the following differential equation.

$$D \frac{\partial^2 C}{\partial x^2} = \frac{\partial C}{\partial t} \qquad [2.7]$$

where the time t is measured from the moment the element arrives at the interface. The associated boundary conditions are:

$$t = 0; \quad x \geq 0, \quad C = C_o \qquad [2.8]$$

$$t > 0; \quad x = 0, \quad C = C_i \qquad [2.9]$$

$$t > 0; \quad x \to \infty, \quad C \text{ is bounded} \qquad [2.10]$$

Equation [2.7] can be used to describe the absorption process when the following conditions are fulfilled[4].

(a) The diffusion coefficient is constant.

(b) Heat effects are negligible.

(c) Mass transfer into the element occurs by molecular diffusion only.

(d) The contact time is short, so that the liquid element may be assumed to be infinitely deep.

(e) There is negligible diffusion in the direction of flow.

Equation [2.7] is easily solved with the aid of Laplace transform theory to yield the concentration profile.

$$(C - C_o) = (C_i - C_o) \operatorname{erfc} \left\{ \frac{x}{2\sqrt{Dt}} \right\} \qquad [2.11]$$

The instantaneous absorption rate of solute gas into the element is:

$$G^\circ = -D\left(\frac{\partial C}{\partial x}\right)_{x=0} = (C_i - C_o)\sqrt{\frac{D}{\pi t}} \qquad [2.12]$$

and the average absorption rate over the total life of an element t*, where each element is assumed to have the same life, is therefore:

$$\bar{G} = \frac{1}{t^*}\int_0^{*t} G^\circ \, dt = 2(C_i - C_o)\sqrt{\frac{D}{\pi t^*}} \qquad [2.13]$$

The physical absorption coefficient, as defined by equation [2.5] is:

$$K_L^\circ = 2\sqrt{\frac{D}{\pi t^*}} \qquad [2.14]$$

Equation [2.14] has been confirmed by experimental measurements of absorption in bubbles of medium size[7], absorption in a wetted wall column[16,17,18,19] and absorption in a laminar jet[20,21].

3. Danckwerts' Penetration Theory (Random Surface Renewal)[22,23]

Random surface renewal theory is an extension of the penetration theory as derived by Higbie[15]. Danckwerts[22,23] rejected the assumption of equal life for each surface element in favor of a random age distribution which assumes that the chance of an element being submerged is independent of age. The average rate of absorption is given by the following equation:

$$\bar{G}^\circ = \int_0^\infty \sqrt{\frac{D}{\pi t}}\,(C_i - C_o)\,\psi(t)\,dt \qquad [2.15]$$

where $\psi(t)$ is the distribution function of surface ages and $\psi(t)\,dt$ is the fraction of surface elements whose age is between t and

t + dt. The distribution function must satisfy the condition:

$$\int_0^\infty \psi(t)\, dt = 1 \qquad [2.16]$$

The form of the age-distribution function presented by Danckwerts is:

$$\psi(t) = se^{-st} \qquad [2.17]$$

where s is the rate of surface renewal.

The average absorption rate, assuming the age-distribution function of Danckwerts[22,23] is given by the expression:

$$\bar{G}^\circ = (C_i - C_o)\sqrt{Ds} \qquad [2.18]$$

It can be seen that the form of the age-distribution function for Higbie's[15] systematic renewal theory is of the form:

$$\psi(t) = \frac{1}{t^*} \qquad 0 < t < t^*$$
$$\psi(t) = 0 \qquad t^* < t < \infty \qquad [2.19]$$

The physical absorption coefficient, assuming Danckwerts' age-distribution, is obtained from equation [2.5] to:

$$K_L^\circ = \sqrt{Ds} \qquad [2.20]$$

Astarita[7] drops the distinction between Higbie's and Danckwerts' model, and defines an equivalent diffusion time by the equation:

$$t_D = \frac{D}{K^{\circ 2}} \qquad [2.21]$$

The physical meaning of equivalent diffusion time is that it is the average life of a surface element.

4. Other Surface Renewal Models

A number of surface renewal models can be found in the literature[24,25,26]. These models differ from the Higbie and Danckwerts models in the form of the age-distribution function and in the specified boundary conditions.

5. Hydrodynamic Models of Absorption in a Spherical Film

(a) Hydrodynamics of Liquid Film

Consider a vertical section of a sphere over which liquid is flowing in a laminar film with no surface rippling (Figure 1). It has been determined[3,4,6,8,9] that the velocity profile along a radial line OP can be described by the equation for flow down an inclined plane. The angle between the vertical plane and equiv-

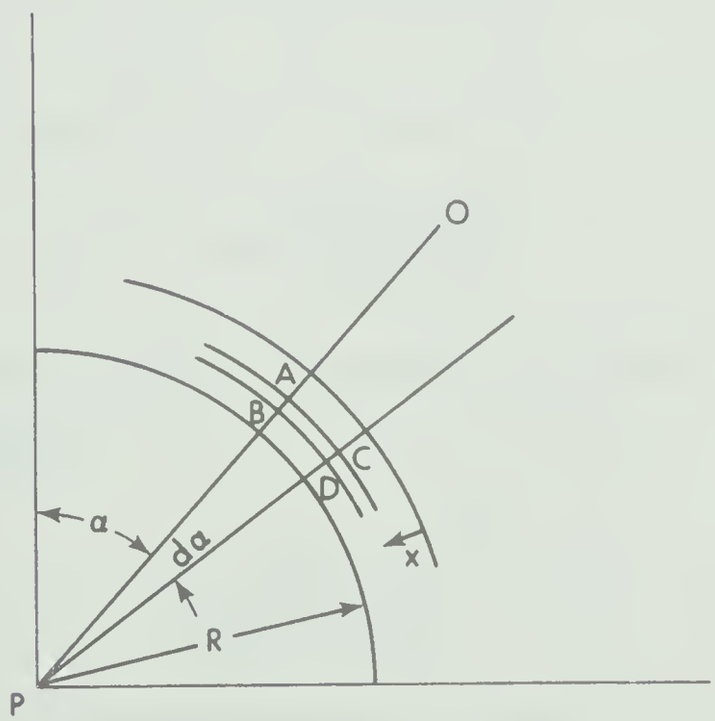


FIG. 1: CROSS SECTION OF SPHERE AND LIQUID FILM

alent inclined plane (α) is continuously changing. The width of the equivalent flow channel ($2\pi R \sin \alpha$) varies with latitude on the sphere, hence, the film thickness is also continuously changing. Utilizing the solution of Nusselt[27] for flow down an inclined plane yields the following equation for the velocity along a streamline.

$$V_\psi = \frac{g \Delta^2 \sin \alpha}{2\nu} \left[1 - \left(\frac{x}{\Delta}\right)^2\right] \qquad [2.22]$$

The velocity of the surface film (x=0) is then equal to:

$$V_o = \frac{g \Delta^2 \sin \alpha}{2\nu} \qquad [2.23]$$

and

$$V_\psi = V_o \left[1 - \left(\frac{x}{\Delta}\right)^2\right] \qquad [2.24]$$

The average or bulk velocity $\bar{V}_\psi$, as obtained from equation [2.24] is:

$$\bar{V}_\psi = \frac{g \Delta^2 \sin \alpha}{2\nu} = \frac{2}{3} V_o \qquad [2.25]$$

The volumetric liquid flow rate is given by the expression:

$$L = \frac{g \Delta^3 2\pi R \sin^2 \alpha}{3\nu} \qquad [2.26]$$

Rearranging equation [2.26] yields the film thickness at any latitude of the sphere.

$$\Delta = \left\{\frac{3L\nu}{2\pi R\, g \sin^2 \alpha}\right\}^{1/3} = \frac{\Gamma_\nu}{\bar{V}_\psi} \qquad [2.27]$$

The volumetric liquid flow rate, per unit length of wetted perimeter, in obtained from equations [2.25] and [2.27].

$$\Gamma_v = \frac{L}{2\pi R \sin \alpha} \qquad [2.28]$$

The surface velocity of the liquid film as given by equation [2.23] can be expressed in terms of the system parameters upon the substitution of equation [2.27] for Δ.

$$V_o = \left(\frac{9g}{32\nu\ \pi^2}\right) L^{1/3}\ R^{-2/3}\ \sin^{-1/3}\ \alpha \qquad [2.29]$$

The age of an element of area on the free film surface, at any latitude of the sphere, can be obtained from the above equations.

$$t = \int_0^\alpha \frac{R\ d\ \alpha}{V_o} = \left(\frac{9g}{32\ \pi^2\ \nu}\right)^{-1/3} L^{-2/3}\ R^{5/3} \int_0^\alpha \sin^{1/3}\ \alpha\ d\ \alpha \qquad [2.30]$$

Therefore, the diffusion time, or time available for absorption as an element of area flows over the sphere, is equal to:

$$t^* = \left(\frac{9g}{32\ \pi^2\ \nu}\right)^{-1/3} L^{-2/3}\ R^{5/3} \int_0^\pi \sin^{1/3}\ \alpha\ d\ \alpha \qquad [2.31]$$

where:
$$\int_0^\pi \sin^{1/3}\ \alpha\ d\ \alpha = \frac{\Gamma\left[\frac{2}{3}\right]\ \Gamma\left[\frac{1}{2}\right]}{\Gamma\left[\frac{7}{6}\right]} = 2.58 \qquad [2.32]$$

The dimensionless groups for laminar flow of a liquid over the single sphere absorber, as evaluated at the equator of the sphere, are:

(1) Reynolds Number

$$R_e = \frac{\text{Inertial Forces}}{\text{Viscous Forces}} = \frac{4L}{2\pi R \sin \alpha} = \frac{4\Gamma_v}{\nu} \qquad [2.33]$$

(2) Froude Number

$$F_r = \frac{\text{Inertial Forces}}{\text{Gravity Forces}} = \frac{L}{24\ \pi\ R\ \nu} = \frac{\Gamma_v^{\,2}}{4g\ \Delta^3} \qquad [2.34]$$

$$F_r = \frac{R_e}{48} \qquad [2.35]$$

(3) Weber Number

$$W_e = \frac{\text{Inertial Forces}}{\text{Surface Forces}} = \frac{4\rho\ \Gamma_v^{\,2}}{\Delta\sigma} \qquad [2.36]$$

(4) Bond Number

$$B_o = \frac{\text{Gravity Forces}}{\text{Surface Forces}} = \frac{16\rho g}{\sigma}\ \Delta^2 \qquad [2.37]$$

$$B_o = \frac{W_e}{F_r} \qquad [2.38]$$

(b) Absorption of a Single Gas in a Liquid Film

Consider the liquid volume element ABCD as shown in Figure 1. The element is bounded by two streamlines AC and BD and two radial lines AB and CD. Under steady state conditions the transfer of solute by diffusion across the radial lines AB and CD is negligible compared to the mass transfer by convection. The reverse is true for mass transfer across the streamlines where the convective term is neglected.

The net transport of material across the radial lines is equal to:

$$2\pi R \sin\alpha\ V_\psi \left(\frac{\partial C}{\partial \alpha}\right)_\psi\ dx\ d\alpha \qquad [2.39]$$

The net material transferred by diffusion across the streamlines is:

$$2\pi D \sin\alpha \left\{ R^2 \left(\frac{\partial^2 C}{\partial x^2} \right)_\alpha - 2R \left(\frac{\partial C}{\partial x} \right)_\alpha \right\} dx\, d\alpha \qquad [2.40]$$

At steady state conditions a mass balance about the element will yield the differential equation describing the steady state absorption of a solute gas in the liquid film. This equation, obtained by equating equations [2.39] and [2.40] is:

$$\left(\frac{\partial^2 C}{\partial x^2} \right)_\alpha - \frac{2}{R} \left(\frac{\partial C}{\partial x} \right)_\alpha = \frac{V_\psi}{RD} \left(\frac{\partial C}{\partial \alpha} \right)_\psi \qquad [2.41]$$

The relevant boundary conditions are:

(1) $t = 0;\ x \geqslant 0,\ C = C_o$ [2.42]

i.e. at the point of entry of the liquid on the sphere, the liquid concentration is uniform.

(2) $t > 0;\ x = 0;\ C = C_i$ [2.43]

i.e. the surface in contact with the soluble gas is assumed to be saturated.

(3) $t \geqslant 0;\ x = \Delta;\ \frac{\partial C}{\partial x} = 0$ [2.44]

i.e. no gas crosses the surface of the sphere.

A fourth boundary condition which is applicable for low depth of solute penetration or for a low percent saturation of the exit liquid is:

(4) $t \geqslant 0;\ x = \infty;\ C = C_o$ [2.45]

Various analytic and numerical solutions of equation [2.41] have been reported in the literature. A brief review of the assumptions

and boundary conditions employed by various authors is given in the following section.

(1) Lynn, Straatemeier and Kramers[8]

Lynn et al[8] assumed that the second term on the left hand side of equation [2.41] is negligible compared to the first term.

$$\left(\frac{\partial^2 C}{\partial x^2}\right)_\alpha >> \frac{2}{R}\left(\frac{\partial C}{\partial x}\right) \qquad [2.46]$$

Hence, equation [2.41] becomes:

$$\left(\frac{\partial^2 C}{\partial x^2}\right)_\alpha = \frac{V_\psi}{RD}\left(\frac{\partial C}{\partial \alpha}\right)_\psi \qquad [2.47]$$

The age of an element of area (t) located on a streamline is related to the latitude of the sphere by the equation:

$$dt = \frac{R\ d\ \alpha}{V_\psi} \qquad [2.48]$$

or upon rearranging:

$$\left(\frac{\partial t}{\partial \alpha}\right)_\psi = \frac{R}{V_\psi} \qquad [2.49]$$

Since,

$$\left(\frac{\partial C}{\partial \alpha}\right)_\psi = \left(\frac{\partial C}{\partial t}\right)_\psi \left(\frac{\partial t}{\partial \alpha}\right)_\psi = \frac{R}{V_\psi}\left(\frac{\partial C}{\partial t}\right)_\psi \qquad [2.50]$$

equation [2.47] becomes:

$$D\left(\frac{\partial^2 C}{\partial x^2}\right)_\alpha = \left(\frac{\partial C}{\partial t}\right)_\psi \qquad [2.51]$$

The boundary conditions used for the solution of the above equation are:

(1) $t = 0;\ x > 0;\ C = C_o$ [2.42]

(2) $t > 0;\ x = 0;\ C = C_i$ [2.43]

(3) $t > 0;\ x = \infty;\ C = C_o$ [2.45]

The solution of equation [2.51] with the associated boundary conditions is the same as the solution of Higbie's penetration theory (equation [2.11]).

$$(C - C_o) = (C_i - C_o)\ \text{erfc}\left\{\frac{x}{2\sqrt{Dt}}\right\} \qquad [2.11]$$

$$\simeq (C_i - C_o)\left[1 - \frac{2}{\sqrt{\pi}}\left(\frac{x}{2\sqrt{Dt}}\right)\right] \qquad [2.52]$$

The total rate of absorption G of gas in the spherical film is given by:

$$G = D \int_{\alpha_0}^{\alpha_2} -2\pi R^2 \sin\alpha \left(\frac{\partial C}{\partial x}\right)_{x=0} d\alpha \qquad [2.53]$$

Substituting equation [2.52] into equation [2.53], and noting that the age of the element, t, is given by equation [2.30], yields:

$$G = \left[\frac{18g\ \pi}{\nu}\right]^{1/6} L^{1/3}\ R^{7/6}\ D^{1/2} \int_0^{\pi} \frac{\sin\alpha\ d\alpha}{\left[\int_0^{\alpha} \sin^{1/3}\alpha\ d\alpha\right]^{\frac{1}{2}}} (C_i - C_o) \qquad [2.54]$$

The limits of the integral were taken as $\alpha_o = 0°$ and $\alpha_2 = \pi$. The true limits are approximately $\alpha_0 = 4°$ and $\alpha_2 = 176°$, however, the error in the overall absorption rate is negligible.

Lynn et al[8] determined the integral to be:

$$\int_0^{\pi} \frac{\sin \alpha \, d\alpha}{\left[\int_0^{\alpha} \sin^{1/3} \alpha \, d\alpha\right]^{\frac{1}{2}}} = 2.33 \qquad [2.55]$$

however, Astarita[7] integrated the same function and found:

$$\int_0^{\pi} \frac{\sin \alpha \, d\alpha}{\left[\int_0^{\alpha} \sin^{1/3} \alpha \, d\alpha\right]^{\frac{1}{2}}} = 2.10 \qquad [2.56]$$

The work of Goettler and Pigford[5] would indicate that the value presented by Lynn et al is the correct value.

(2) Davidson and Cullen[9]

The analysis of Lynn et al[8] neglected the effect of the stretching of the surface film, and the resulting distortion of the concentration gradient. The concentration gradient in the upper half of the sphere is increased due to the film stretching while the concentration gradient on the lower half is reduced. Davidson and Cullen[9] introduced a dimensionless length, $y = \frac{x}{\Delta}$, into the differential equation of Lynn et al[8]. Equation [2.41] is transformed, with the above substitution, to the following form:

$$\left(\frac{\partial^2 C}{\partial y^2}\right)_{\alpha} = \frac{V_{\psi} \, \Delta^2}{RD} \left(\frac{\partial C}{\partial \alpha}\right)_{\psi} \qquad [2.57]$$

which, upon substitution of equation [2.24] for V_{ψ} becomes:

$$\left(\frac{\partial^2 C}{\partial y^2}\right)_{\alpha} = \frac{V_0 (1 - y^2) \, \Delta^2}{RD} \left(\frac{\partial C}{\partial \alpha}\right)_{\psi} \qquad [2.58]$$

Davidson and Cullen[9] introduced a stream function ψ which is a function of y only.

$$\psi = \int_0^x V_\psi \, 2\pi(R + \Delta - x) \sin \alpha \, d\alpha \qquad [2.59]$$

Hence

$$\psi = \frac{3}{2}L\left(y - \frac{y^3}{3}\right) \qquad [2.60]$$

and

$$\left(\frac{\partial C}{\partial \alpha}\right)_\psi = \left(\frac{\partial C}{\partial \alpha}\right)_y \qquad [2.61]$$

By definition

$$\left(\frac{\partial \phi}{\partial \alpha}\right)_y = \frac{R}{V_0 \Delta^2} \qquad [2.62]$$

Substituting equations [2.62] and [2.61] into equation [2.58] results in the transformed differential equation.

$$D\left(\frac{\partial^2 C}{\partial y^2}\right)_\phi = (1 - y^2)\left(\frac{\partial C}{\partial \phi}\right)_y \qquad [2.63]$$

(a) Low Depth of Penetration Model

For very low depths of penetration, $y^2 << 1$, and equation [2.63] becomes:

$$D\left(\frac{\partial^2 C}{\partial y^2}\right)_\phi = \left(\frac{\partial C}{\partial \phi}\right)_y \qquad [2.64]$$

The associated boundary conditions, in terms of the transformed variables y and ϕ are:

(1) $\phi = 0;\ y \geq 0;\ C = C$ [2.42a]

(2) $\phi > 0;\ y = 0;\ C = C_i$ [2.43a]

(3) $\phi > 0;\ y = \infty;\ C = C_o$ [2.45a]

Equation [2.64] is of the same form as Higbie's penetration theory equation (equation [2.11]), hence the solution is:

$$(C - C_o) = (C_i - C_o)\ \text{erfc}\left\{\frac{y}{2\sqrt{D\phi}}\right\} \qquad [2.65]$$

The total rate of absorption of gas on the spherical film (equation [2.53]), written in terms of the transformed variables is:

$$G = \frac{3}{2}LD \int_0^{\phi_2} -\left(\frac{\partial C}{\partial y}\right) d\phi \qquad [2.66]$$

Substituting equation [2.65] into equation [2.66], and transforming the variable ϕ, as defined in equation [2.62], to the original system parameters yields the final form of the equation describing the total absorption rate of solute gas.

$$G = (12 \times 1.68)^{\frac{1}{2}} \left(\frac{2\pi g}{3\nu}\right)^{1/6} R^{7/6}\ L^{1/3}\ D^{\frac{1}{2}}\ (C_i - C_o) \qquad [2.67]$$

The physical absorption coefficient, as defined by equation [2.5] is:

$$K_L^\circ = \frac{\frac{G}{A}}{(C_i - C_o)} = 2.08\sqrt{\frac{D}{\pi t^*}} \qquad [2.68]$$

where the diffusion time t^* is defined by equation [2.31].

Equation [2.67] corresponds to equation (16) of the paper by Davidson and Cullen[9].

(b) <u>High Depth of Penetration Model</u>

If the degree of saturation of the liquid film is such that the liquid can no longer be assumed to be infinitely deep, then the

y^2 term in equation [2.63] can not be neglected.

$$D\left(\frac{\partial^2 C}{\partial y^2}\right)_\phi = (1 - y^2)\left(\frac{\partial C}{\partial \phi}\right)_y \qquad [2.63]$$

Davidson and Cullen[9] and Olbrich and Wild[28] have solved the above equation with the following boundary conditions.

(1) $\phi = 0;\ y > 0;\ C = C_o$ [2.42a]

(2) $\phi = 0;\ y = 0;\ C = C_i$ [2.43a]

(3) $\phi > 0;\ y = 1;\ \frac{\partial C}{\partial y} = 0$ [2.44a]

Davidson and Cullen[9] adapted the solution of Pigford[29] and Vyazovov[30] for gas absorption in a liquid film flowing down a wetted wall column. The solution for the single sphere and wetted wall column are equivalent so long as the value of ϕ_2 is the same for the two equations. The expression for ϕ_2, as defined by equation [2.62], for a single sphere is:

$$\phi_2 = \frac{2}{3} \times 1.68\pi \left(\frac{2\pi g}{3\nu}\right)^{1/3} \frac{R^{7/3}}{L^{4/3}} \qquad [2.69]$$

The total rate of absorption of a soluble gas into a laminar liquid film formed by passing a liquid over a sphere, when the depth of penetration is high is:

$$G = L(C_i - C_o)[1 - 0.7857 \exp(-3.414\ \alpha) - 0.1001 \exp(-26.21\ \alpha) - 0.03599 \exp(-70.43\ \alpha) - 0.01811 \exp(-136.5\ \alpha)....] \qquad [2.70]$$

where:
$$\alpha = 2 \times 1.68\pi \left(\frac{2\pi g}{3\nu}\right)^{1/3} \frac{R^{7/3}}{L^{4/3}} D = \frac{3}{2} D\ \phi_2 \qquad [2.71]$$

Davidson and Cullen[9] recommend using equation [2.70] when the outlet liquid saturation exceeds 40%.

(3) Olbrich and Wild[28]

Olbrich and Wild[28] extended the solution of Davidson and Cullen[9] so that it may be used for both low depth of penetration and high depth of penetration cases. Their solution is of the same form as equation [2.70], however, it contains ten terms.

$$G = L(C_i - C_o)\left[1 - \sum_{n=1}^{10} B_n \exp(-\beta_n \alpha)\right] \qquad [2.72]$$

The coefficients for equation [2.72] are listed in Table 1.

The calculated absorption rate corresponding to liquid saturations in excess of 40% is almost identical when calculated from equation [2.70] or equation [2.72].

B. Definition of a Diffusion Coefficient

The diffusion coefficient is defined by equation [2.1] as the proportionality constant in the rate equation for unidirectional mass transfer.

$$\bar{G}^\circ = -D\left(\frac{\partial C}{\partial x}\right)_{x=0} \qquad [2.1]$$

A number of theories concerning molecular diffusion of dissolved gases in liquids have been postulated[21,31,32], but the theoretical models cannot be relied upon to predict the value of the diffusion coefficient. However these theoretical models have served as the basis for a number of empirical and semi-empirical correlations for predicting the diffusion coefficient of dissolved gases. A few of the more useful correlations will be discussed in a subsequent section of this chapter.

TABLE 1

COEFFICIENTS FOR SERIES SOLUTION FOR G.

(Olbrich and Wild[28])

n	B_n	β_n
1	0.7897026	3.414446
2	0.09725511	26.440559
3	0.03609362	70.832821
4	0.01868637	136.57071
5	0.011401760	223.64880
6	0.007675970	332.06472
7	0.005517943	421.81720
8	0.004157034	612.90545
9	0.003243974	785.32896
10	0.002601795	979.08735

C. Effect of Temperature on Diffusivity

The temperature variation of the diffusion coefficient has been expressed in a number of ways.

Eyring[33] suggested that diffusion is a rate process which varies with the exponential function of temperature. Hence

$$D = A_1 \exp \frac{-E_d}{RT} \qquad [2.73]$$

or

$$\ln D = \frac{-E_d}{RT} + \ln A_1 \qquad [2.74]$$

Eyring[33] further postulated that the mechanism for diffusion and viscosity are similar and in a dilute solution the energy of activation for diffusion (E_d) is equal to the energy of activation for viscosity (E_v).

$$\ln \mu_1 = \frac{-E_v}{RT} + \ln A_2 \qquad [2.75]$$

The theory of Eyring[33] would therefore predict that a plot of the natural logarithm of the diffusion coefficient versus the reciprocal absolute temperature would result in a straight line, the slope of which is equal to the slope of the curve for liquid viscosity when plotted in the same manner. The work of Othmer and Thakar[34] indicates that the ratio of $\frac{E_d}{E_v}$ for a number of solvents varies between 1.07 and 1.15. The average value of the ratio may be taken as 1.1.

Himmelblau[21] favors plotting the logarithm of the diffusion coefficient versus the Othmer temperature scale[35]. This method

involves plotting logarithmically the property of one material against the same property or vapor pressure of a reference material.

Einstein[36,37] and Sutherland[38] proposed independently that the diffusivity of a dissolved solute could be correlated by an equation of the form:

$$\frac{D\,\mu_1}{T} = C_1 (V_2)^{-1/3} \qquad [2.76]$$

The Stokes-Einstein equation (equation [2.76]) indicates that for a given solvent, the group $\frac{D\,\mu_1}{T}$ is dependent on the solute molar volume but is independent of temperature. The most recent version of Eyring's theory[39], as discussed by Himmelblau[21,40] suggests that the same group $\frac{D\,\mu_1}{T}$ is not independent of temperature. Himmelblau[40] found experimentally that for hydrogen and helium in water, $\frac{D\,\mu_1}{T}$ tended to decrease with increasing temperature.

The exact effect of temperature on diffusion coefficients will not be known until better data are available for a number of solute-solvent pairs.

D. Effect of Pressure on Diffusivity

The exact effect of pressure on diffusion coefficients is not well understood and requires more detailed investigation.

An increase in pressure is however known to cause a decrease in the diffusion coefficient. This is to be expected as the molecular spacing is reduced with increasing pressure, causing a decrease in the solute mobility.

E. Effect of Concentration on Diffusivity

Himmelblau[21] states that under normal conditions, the concentration of a sparingly soluble solute in a liquid solvent is very low and does not appreciably alter the viscosity of the solution from that of the pure solvent. The diffusivity should therefore not be appreciably altered by concentration changes.

Bolles and Fair[41] have reviewed various recent articles on this subject. It is apparent from their review that concentration does effect diffusivity if the solution is non-ideal.

F. Empirical Correlations for Predicting Diffusion Coefficients

The theory of liquids is not yet developed to the stage where theoretical predictions of diffusion coefficients may be made with confidence. The existing correlations for predicting diffusion coefficients are based on empirical correlations of experimental data. A number of empirical correlations have been developed. These methods are reviewed by Himmelblau[21], Bolles and Fair[41], Reid and Sherwood[42], Hu and Wood[43], and Wilke et al[44]. The correlations reviewed below were felt to have some validity for predicting the diffusion coefficients of sparingly soluble gases which are dissolved in nonaqueous solvents.

1. Wilke-Chang Correlation[45]

The empirical form of this correlation is:

$$\frac{D \mu_1}{T} = 7.4 \times 10^{-8} \frac{(a M_1)^{\frac{1}{2}}}{V_2^{0.6}} \qquad [2.77]$$

where a is an "association parameter" to define the effective molecular weight of the solvent. The "association parameter" must be

determined from experimental diffusivity data for the solvent in question. Wilke and Chang[45] list a value of 2.6 for water, 1.9 for methanol, 1.5 for ethanol and 1.0 for non-associated solvents.

2. Scheibel Correlation[46]

The Scheibel[46] correlation is similar to the Wilke-Chang correlation, however, it does not require an "association parameter". The Scheibel equation is of the form:

$$\frac{D \mu_1}{T} = \frac{K}{V_2^{1/3}} \qquad [2.78]$$

When $V_2 < 2.5\ V_1$, Scheibel[46] recommends that the constant K be equal to:

$$K = 17.5 \times 10^{-8} \qquad [2.79]$$

3. Sitaraman et al Correlation[47]

The empirical equation of Sitaraman et al[47] is of the form:

$$D = 5.4 \times 10^{-8} \left(\frac{M_1^{\frac{1}{2}}\ \Delta H_1^{*1/3}\ T}{\mu_1\ V_2^{\frac{1}{2}}\ \Delta H_2^{*0.3}} \right)^{0.93} \qquad [2.80]$$

The parameters ΔH_1^* and ΔH_2^* are the latent heat of vaporization $\left(\frac{\text{cal.}}{\text{gm.}}\right)$ at the normal boiling point of the solvent and solute respectively.

4. King et al Correlation[48]

The correlation of King et al[48] is of a similar form to that of Sitaraman et al[47].

$$\frac{D\,\mu_1}{T} = 4.4 \times 10^{-8} \left(\frac{V_1}{V_2}\right)^{1/6} \left(\frac{\Delta H_1}{\Delta H_2}\right)^{\frac{1}{2}} \qquad [2.81]$$

The latent heats of vaporization at the normal boiling point for the solvent (ΔH_1) and solute (ΔH_2) are in calories per gram mole. King et al[48] limit the range of applicability of the above equation to values of $\frac{D\,\mu_1}{T}$ less than 1.5×10^{-7} $\frac{cp.\ cm.^2}{K^\circ\ sec.}$.

5. Lusis and Ratcliff Correlation[49]

The Lusis and Ratcliff correlation is of the form:

$$\frac{D\,\mu_1}{T} = 8.52 \times 10^{-8}\ (V_1)^{-1/3} \left[1.40 \left(\frac{V_1}{V_2}\right)^{1/3} + \left(\frac{V_1}{V_2}\right)\right] \qquad [2.82]$$

The above equation has general applicability for the entire range of solute and solvent molar volumes.

The utility of the above mentioned correlations for predicting the diffusivity of hydrogen in methylamine is somewhat in question. A significant lack of diffusivity data exists for temperatures below 0°C, hence, the applicability of these equations for low temperature predictions is not certain. A second consideration, as discussed by Himmelblau[40] and Nakanishi et al[50], is the presence of quantum effects associated with the diffusion of hydrogen in liquids with high internal pressures. Ferrell and Himmelblau[40] have developed an equation which takes account of the quantum effects, however, this equation is valid for water only.

Reid and Sherwood[42] used some of the above correlations for predicting the diffusivity of hydrogen in water. They[42] found

that the Wilke-Chang[45] correlation predicted a value which was 29% low and that the Scheibel[46] correlation predicted a value which was 34% low. Reid and Sherwood[42] recommend that the Scheibel[46] equation be used for non aqueous solutions. They state that for temperatures between 10°C and 30°C, the estimation should never be in error by more than 50%. The magnitude of this error indicates the difficulty associated with estimating the diffusivity of hydrogen in a non aqueous solvent.

3. LITERATURE SURVEY

A. Experimental Techniques for Measuring Diffusion Coefficients

The accurate measurement of molecular diffusion coefficients is one of the most difficult tasks facing experimentalists. The methods for measuring diffusion coefficients are usually classified in three categories[31,51]. These categories are free diffusion, restricted diffusion and steady state methods. Free diffusion and restricted diffusion techniques are often classified simply as unsteady state methods.

Suitable mathematical models are required for evaluating the diffusion coefficients from the measured rate of diffusion data. These models are not presented in this work but they are found in the references presented for each technique.

1. Free Diffusion Methods

For this method a sharp interface is formed between two phases in a vertical column and mutual diffusion across this interface causes a change in the concentration of the two phases. Free diffusion is assumed to occur so long as the concentration at the extremes of the two phases furthest from the interface retain their initial value.

Free diffusion methods are usually used for determining mutual diffusion coefficients of two liquid components. For this type of system, the large concentration gradients can be measured by optical techniques based on the refractive index of the solution[31,51]. Diffusion coefficients for dissolved gases may be obtained by measuring the rate of transfer of the solute gas across an interface between two solutions of different concentration. This method may involve

measuring the concentration gradient by interferometric techniques[21] or by measuring the average concentration of the two solutions after a set time period[52,53,54]. Convective mixing is the greatest source of error associated with this technique. In an attempt to prevent this some workers[53,54] have added colloids to the liquid, however, the effect of gels on molecular diffusion is uncertain.

The measurement of the rate of transfer of a gas across an interface between a pure liquid and saturated gas has been used by a number of workers[55,56,57,58,59] to determine diffusion coefficients. The amount of gas dissolved is measured by observing the change in volume, at constant pressure, of the gas phase. The experiment is carried out in a capillary tube to eliminate convection.

An unsteady state technique has been used by Ferrel and Himmelblau[40] for measuring the diffusivity of hydrogen and helium in water. This method is based on the technique of Taylor[60,61] and involved imposing a step change in the concentration of the solute gas in water which was flowing through a long (20 foot) capillary. The diffusion coefficients were calculated from the measurements of the laminar dispersion in the capillary (Laminar dispersion obtained from the bulk concentration versus time data as measured at the exit of the capillary). This method enjoys the advantage that gas solubility data are not required. However, maintaining a 20 foot section of capillary tubing in a constant temperature, vibration free state, could present large experimental problems when sub-ambient temperatures are involved.

2. Restricted Diffusion Methods

Restricted diffusion is a continuation of the free diffusion process to the extent that the concentration of the total volume of the two phases begin to change. If restricted diffusion is allowed to continue until steady state is attained, the concentration in the column will become uniform.

Restricted diffusion methods are not easily adapted to measuring molecular diffusion coefficients of gases in liquids and will not be further discussed in the work.

3. Steady State Methods

Diffusion is allowed to occur in a solution in such a way that a time invariant state is attained in the system. Upon attainment of steady state, the concentration of the solution, concentration gradient, and mass flux are constant at any given point.

Steady state methods may be divided into two general categories based on the condition of the interface between the two phases. The categories are quiescent interface methods and mobile interface methods. Quiescent surface cells (Northrop-Anson[62]) have been extensively used for measuring diffusion coefficients. Absorption experiments on mobile interfaces are gaining in popularity as a means for determining diffusion coefficients.

(a) Quiescent Surface Methods

The Northrop-Anson[62] or diaphragm cell method is the most common steady state technique for obtaining diffusion coefficients. The design and operation of diaphragm cells have been reviewed by Davidson and Cullen[9], Himmelblau[21], Tyrell[31], Geddes[51] and Gordon[63]. The diaphragm cell usually consists

of two chambers separated by a porous disc. The solute is able to diffuse through the sintered disc from a solution of high concentration to one of lower concentration. Provided the volume of the two chambers is sufficiently large and the mixing in the two chambers, either by convection or mechanical means, is sufficient to maintain a homogeneous concentration in each phase, then the transfer conditions across the disc may be assumed at steady state.

The problems which hamper the free diffusion method, such as convective mixing due to vibrations and interface formation, are overcome in the diaphragm cell. However, the diaphragm cell technique does not yield an absolute value for the diffusion coefficient as the effective thickness of the diaphragm and cross-sectional area of the pores is not known. In order to calibrate the cell, a gas-liquid system for which the diffusion coefficient is known must be used. As the calibration is a function of liquid viscosity, the calibration liquid must be similar to the one being studied. Some uncertainty exists as to the surface effects within the pores and how they are affected by changes in solvent or solution concentration. A further drawback of the diaphragm cell technique is the long time ($\sim$5 days) required for one determination. Maintaining constant conditions within the cell for this length of time may be very difficult when low temperatures are involved.

A steady state capillary cell method was developed by Ross and Hildebrand[64] for determining diffusion coefficients of dissolved gases. Their apparatus was constructed in much the same manner as a diaphragm cell, however, in place of the porous disc

they used a stainless steel plate through which was drilled a number of 1 m.m. holes. The gas-free solvent was introduced to the bottom portion of the cell until it formed a shallow layer above the plate. Solute gas was then introduced to the chamber above the plate. The solute pressure was maintained constant with a mercury U-tube arrangement and the amount of gas absorbed was measured from the rate at which mercury was added to maintain the constant pressure.

This apparatus gives excellent results. The only drawbacks are the long time required for a determination (several days) and the problem of maintaining a constant solute partial pressure above a volatile liquid solvent.

Haul and Puttbach[65] measured the diffusivity of hydrogen in liquid ammonia using an apparatus similar to that of Ross and Hildebrand[64].

A simple method for measuring molecular diffusion coefficients of dissolved gases has been devised by Malik and Hayduk[66]. The equipment consists of a single capillary tube connected to a large liquid reservoir. The gas is absorbed at the liquid interface in the capillary tube. The simplicity of their apparatus makes the method worthy of consideration for moderately soluble and highly soluble gases, however, it is not suitable for sparingly soluble gases.

(b) Mobile Interface Methods

Laboratory absorbers utilizing a mobile interface include wetted wall columns, laminar jets, single sphere absorbers, annular jets and rotating drum absorbers. The hydrodynamics of these absorbers are sufficiently well understood that realistic models

of the absorption process can be developed.

The wetted wall column has been used for a number of mass transfer studies and Himmelblau[21] has listed several papers concerning the use of this apparatus for diffusivity experiments. End effects and surface rippling must be carefully controlled and even in a well designed system they may be the cause of large errors in the calculated diffusion coefficient. Bourke and Lee[2] utilized a wetted wall column for their study of the ammonia-hydrogen exchange reaction. They reported that surface rippling could only be eliminated at very low ammonia flow rates. The flow rate for all their[2] tests corresponded to a Reynold's number $\left(\frac{4\Gamma_v}{\nu}\right)$ of 10.

The laminar jet absorber is a very flexible apparatus for performing both physical absorption and absorption with chemical reaction studies. This apparatus has been used extensively for determining molecular diffusion coefficients[21]. The interfacial area and physical absorption coefficient can be varied by changing the jet length and liquid flow rate. Interfacial areas may be varied from 0.3 cm^2 to 10 cm^2 and the diffusion times fall in the range 0.01 sec. to 0.1 sec.[7]. The laminar jet possesses an advantage over the wetted wall column and single sphere absorber, especially for liquids with high surface tension, in that surface wetting is not required. Entrance and exit effects are fairly well understood[20] and suitable correlations are available.

However, the laminar jet is very difficult to design for proper operation. It is not well suited for physical absorption studies involving slightly soluble gases as the small interfacial area and diffusion time result in a very low absorption rate which is very

difficult to measure. Also, fairly large volumetric liquid flow rates are required to maintain a stable jet.

Baird and Davidson[11,67] used an annular jet absorber to measure the molecular diffusivity of sparingly soluble gases in water. They state that surface rippling and stagnant end effects are not a problem. The absorber volume is small since the gas is absorbed on the internal surface of the jet thus temperature fluctuations do not affect the measured absorption rate to the same extent as observed for other absorbers. However, careful design of the nozzle appears to be critical and it would appear to be difficult to duplicate the behaviour of different nozzles.

A rotating drum absorber was used by Danckwerts and Kennedy[23] for measuring the physical and physio-chemical absorption rates of carbon dioxide in various aqueous solutions. This apparatus has the advantage that diffusion times can be easily varied (0.0075 sec. to 0.25 sec.) by changing the speed of rotation of the drum. Problems with gas entrainment and slippage between the liquid film and drum surface are the main drawbacks.

The single sphere absorber is similar in concept to the wetted wall column. It was first proposed by Lynn et al[8] and has since been used by a number of investigators[9,10,11,12] for determining molecular diffusion coefficients. The entrance and exit effects were reported to be small and fairly well understood[7]. Relatively high liquid flow rates with the absence of surface ripples were reported[5,9]. Interfacial areas of the order 10 cm.^{2} to 40 cm.^{2} are possible with corresponding diffusion times of 0.1 sec to

1.0 sec.. The interfacial areas and diffusion times associated with this absorber make the single sphere absorber desirable for physical absorption studies involving sparingly soluble gases.

B. Experimental Background on the Design of a Single Sphere Absorber

A single sphere absorber consists of a sphere over which a liquid flows in a laminar film. The liquid is introduced through an orifice onto the top pole of the sphere and is collected in a constant liquid level take-off tube situated directly below the sphere. The sphere is enclosed in a gas tight chamber which is in turn located in a constant temperature environment. The molecular diffusivity can be calculated from the measured rate of absorption of a gas into the liquid film on the sphere.

Various designs for the single sphere absorber and auxiliary equipment are presented in the literature. A number of these designs are summarized below.

The first investigators to use a single sphere or ball absorber were Lynn, Straatemeier and Kramers[8]. They supported a sphere on a vertical wire which extended through the liquid feed jet and take-off tube. The sphere used by the above authors was a steel ball bearing. Tests were conducted on spheres of radius 1.00, 1.50, 1.90 and 2.00 cm.. The single sphere was located in a cylindrical chamber formed from a glass pipe section. The liquid level in the take-off tube was controlled by a needle valve.

Davidson and Cullen[9] mounted a standard table tennis ball (3.78 cm. diameter) on a 1/8 inch stainless steel rod. The rod was centered in a mounting block which formed a portion of the liquid distributor (Chamber for distributing fluid evenly to jet). The

support rod passed through the liquid feed nozzle and terminated in the take-off tube. The liquid level in the take-off tube was maintained by a constant liquid level device (lute vessel). The chamber wall was constructed from a perspex cylinder. Temperature control of the absorber was maintained by controlling the temperature of the room.

The single sphere absorber design of Davidson and Cullen[9] was used by Ratcliff and Holdcroft[3], Ratcliff and Reid[10] and Baird and Davidson[11]. Baird and Davidson[11] slightly modified the original design of Davidson and Cullen[9] by reducing the volume of the absorber chamber. They[11] pointed out an error in the original data of Davidson and Cullen when slightly soluble gases were involved. The error was attributed to the effect of temperature variations on the specific volume of the gas phase.

Wild and Potter[6] modified the liquid feed jet from that of Davidson and Cullen's design but they maintained the basic design of extending the support rod through the liquid feed nozzle.

Goettler[4,5] attempted to use the same design as Davidson and Cullen[9] but was unable to obtain ripple free flow. He substituted a laminar jet as the liquid feed device. The laminar jet was found to give a more stable surface film.

All of the above mentioned investigators found that the surface film was very sensitive to vibrations of the apparatus. In each case, the absorber was mounted on a concrete pad which was in turn mounted on foam rubber vibration arrestors.

Goettler[4,5] found that when the design of Davidson and

Cullen[9] was used, the presence of surface rippling was dependent on the amount of gas trapped in the liquid distributor and on the design of the annular nozzle. When using a laminar jet feed system he noted a strong dependence between the surface ripples on the sphere and instability of the laminar jet. The laminar jet had an upper and lower limit for stable flow. The upper limit of flow, defined as a Reynold's number based on the jet diameter, was found to be approximately 3500 for each nozzle.

$$Re_j = \frac{4L}{\pi D_J \nu} = 3500 \qquad [3.1]$$

The lower limit of flow was observed by the breakup of the jet stream and was dependent on the nozzle diameter.

It should be noted that the above observations are based on experience gained with aqueous systems. Liquid was fed to the absorber from constant head tanks. Rotameters were used to measure the flow rate by all investigators except Goettler[4,5] who measured the time required to collect a known volume of the exit liquid.

A number of gas feed systems have been employed. Lynn et al[8] fed the gas directly from a cylinder, through a rotameter and saturator and into the absorber. The incoming gas flow rate was maintained at a larger value than the rate at which the gas was being absorbed. The excess gas flowed through a second rotameter and was discharged to the atmosphere. The outlet flow rate was approximately 5% of the feed rate. The continuous purging of the absorber prevented the accumulation of insoluble gaseous impurities in the system.

Davidson and Cullen[9] stored the dry absorption gas in an atmospheric balloon. The absorption rate was metered with a rotameter or soap film meter. The gas in the absorber was saturated with water prior to a run, but the incoming gas was not saturated during a run.

Wild and Potter[6] utilized a similar system to that of Davidson and Cullen[9], however they introduced water to the balloon to ensure a saturated gas feed.

C. Experimental Background on the Operation of a Single Sphere Absorber

A number of operating variables must be fixed prior to the operation of a single sphere absorber. The parameters which can be adjusted are liquid flow rate, absorber temperature, absorber pressure, sphere size, distance between the sphere and feed jet and distance between the base of the sphere and the stagnant liquid level in the take-off tube. To minimize the sensitivity to temperature fluctuations, the absorber volume should be small[11]. However, wall effects can be significant when the sphere diameter approaches the absorption chamber diameter. For example, Howkins and Davidson[68] observed the formation of a standing wave near the base of the sphere as gas phase was being circulated.

The operating conditions as employed by the various authors are presented in Table 2.

The conditions listed in Table 2 would indicate that a distance of 3.0 m.m. should be maintained between the sphere and liquid jet and that the distance between the sphere and take-off liquid level

TABLE 2

OPERATING PARAMETERS FOR SINGLE SPHERE ABSORBER

Author(s)	Liquid	Gas	Liquid Flow Rate $\left(\frac{c.c.}{sec.}\right)$	Sphere Radius (cm.)	Jet Length (m.m.)	Take-off Length (cm.)	Temperature °C
Lynn et al[8]	Water + 0.050% Teepol	SO_2	0.5 to 7.5	1.0 1.50 1.90 2.95	-	2.0	20
Davidson & Cullen (9)	Water	CO_2 H_2 O_2 Cl_2 NO	0.5 to 3.0	1.89	3	1.5	15 20 25 } ± 0.5
Ratcliff & Reid (10)	Water	Benzene	0.5 to 2.8	1.89	3	1.5	25 ± 0.1
Goettler[4]	Water	CO_2	0.3 to 4.5	1.89	3.5 to 6.0	2.0	25 ± 0.1

should be approximately 2.0 cm.. However, the magnitude of these parameters is dependent on the properties of the liquid and should be checked for each solvent.

D. Hydrodynamics of the Liquid Film

The flow of liquids over a solid surface in a thin film is a phenomena which has received a large amount of attention but which still defies a satisfactory understanding. The flow conditions at which the film surface is non rippling are still not well defined. Sherwood and Pigford[69] state that laminar flow without rippling occurs at Reynolds numbers below 4. Their observation was based on flow down a wetted wall column for which the Reynolds number is defined as:

$$Re = \frac{4\Gamma_v}{\nu} \qquad [3.2]$$

Bird, Stewart and Lightfoot[70] list the following limits for the Reynolds number as defined by equation [3.2].

$$Re < 4 \text{ to } 25 \qquad [3.3]$$

Kapitza[71] derived the Reynolds number for the onset of wavy flow to be

$$Re_i = 2.43 \left(\frac{\delta^3}{g \nu^4} \right)^{1/11} \qquad [3.4]$$

where the kinematic surface tension δ is given by the expression:

$$\delta = \frac{\sigma}{\rho} \qquad [3.5]$$

Mossot et al[72] state that surface waves are normally encountered

at Reynolds numbers above 20.

Benjamin[73] and Bennie[74] presented a detailed treatment of the conditions at which a liquid film becomes unstable. Their results indicated that vertical film flow is inherently unstable. The equation of Bennie[74] is

$$Re_i = \frac{5}{6} \cot \theta \qquad [3.6]$$

where θ is the angle of inclination of the plane from the horizontal plane. It can be seen from equation [3.6] that for values of θ greater than $\frac{\pi}{2}$, the Reynolds number is zero or negative (impossible).

The apparent disagreement of the various Reynolds numbers indicates the degree of uncertainty associated with the formation of wavy surfaces. Extensive reviews of the subject are given by Fulford[75] and Levich[76].

Reynolds numbers (equation [2.33]) corresponding to the maximum liquid flow rates presented in Table 2 are listed in Figure 3. No Reynolds number was calculated from the data of Lynn et al[8] as there is confusion as to which sphere the high liquid flow rate was applied to.

Equation [3.4], or Kapitza's equation predicts the Reynolds number for wave inception to be 21.5. It is apparent that the liquid flow rates utilized by the authors listed in Table 3 are well above the values for which surface ripples would be anticipated, no matter which of the Reynolds number criteria one chooses.

Table 3

REYNOLDS NUMBER FOR INCEPTION OF RIPPLING ON A SINGLE SPHERE

Author(s)	Liquid Flow Rate $\left(\frac{c.c.}{sec.}\right)$	Temperature	Reynolds Number
Davidson and Cullen[9]	3.0	25	113
Ratcliff and Reid[10]	3.0	25	113
Goettler[4]	4.5	25	170
	3.5[a]	25	132

a - flow rate at which dye streak tests indicated instability.

E. Entrance Effects

The single sphere absorber design utilized in this work was similar to that of Goettler[4,5]. The entrance correction for a laminar jet will therefore be discussed.

The surface of the laminar jet is fresh and will absorb solute gas. The amount of gas absorbed on the jet was reported by Goettler[4] to be significant. He noted a correction of between 2% and 4% of the total gas absorbed.

The amount of gas absorbed on the jet was calculated from the equation for physical absorption on an ideal jet[4,7,21]:

$$G_J = 4\sqrt{h_J L D}\,(C_i - C_o') \qquad [3.7]$$

Goettler[4] found that complete mixing of the liquid and dissolved gas occured at the sphere-jet junction. The bulk concentration of the liquid flowing over the sphere was therefore corrected for the gas absorbed on the jet.

$$C_o = \frac{G_J}{L} \qquad [3.8]$$

F. Exit Effects

The amount of solute absorbed on the support rod between the sphere and liquid take-off level is reported to be negligible compared to the amount of gas absorbed on the sphere. The small absorption rate on the take-off level has been attributed to the formation of a stagnant liquid layer on the rod[4,8,9,10]. The presence of a stagnant surface layer was first reported by Lynn et al[18] with regard to flow down a short wetted wall column. They

observed the height of the stagnant layer was inversely proportional to the liquid flow rate. The thickness of the film was slightly larger than the thickness of the normal film and a narrow horizontal band of ripples appeared at the top of the film. Light powder (lycopodium seed) which was blown on the surface of the film was observed to circulate around the film rather than be swept from the surface. Similar observations of stagnant layer formation on a wetted wall column have been reported by Roberts and Danckwerts[77], Nijsing and Kramers[78] and Wilkes and Nedderman[79].

Ratcliff and Reid[10] report that the stagnant film gradually built up from the take-off surface to some limiting height. They attributed the slow buildup to the accumulation of trace impurities of surface active agents which were present in the water supply. The stagnant film was observed from the presence of small particles circulating on the interface. The particles could be raised onto the sphere by increasing the level of the liquid in the take-off tube. Ratcliff and Reid[10] assumed that the velocity profile of the liquid film was full parabolic with zero velocity at the interface. The amount of absorption on the small area with zero surface velocity was therefore assumed to be negligible.

Goettler[4] also attributed the formation of a stagnant layer to the presence of surface active impurities which tend to concentrate on the interface of the support rod and take-off tube. He stated that the surface active agents cause a reduction in the surface tension which results in an upward force on the film due to the greater surface tension of the liquid on the sphere. A full para-

bolic velocity profile would therefore exist in the liquid film on the rod.

Goettler[4], Ratcliff and Reid[10] and Stewart[12] found the height of the stagnant liquid layer to be independent of the liquid flow rate. This independence has also been implied by Davidson and Cullen[9] who conducted all their experiments with a constant take-off height of 1.5 cm..

G. Interfacial Area Correction due to the Liquid Film

Goettler[4] and Ratcliff and Reid[10] applied a correction to the absorption model to account for the increase in the interfacial area of the sphere as a result of the liquid film. Goettler used an average correction which was based on the average liquid depth over the complete sphere. The correction is of the form

$$\frac{A_A}{A_s} = 1 + 2.58 \frac{\Delta^+}{R} \qquad [3.9]$$

where A_A = corrected interfacial area

A_s = surface area of the dry sphere

Δ^+ = depth of the liquid film at the sphere equator

The depth of the liquid film at the sphere equator was calculated from the following equation.

$$\Delta^+ = \left\{\frac{3\nu L}{2\pi R g}\right\}^{1/3} \qquad [3.10]$$

H. Diffusivity Data for Hydrogen Dissolved in Aliphatic Amines

No experimental molecular diffusion coefficients for hydrogen dissolved in any of the aliphatic amines considered in Part 1 of this study were available. The diffusivity of hydrogen and deuter-

ium in liquid ammonia was determined by Haul and Puttbach[65]. The diffusion coefficients were measured at a constant solute partial pressure of nine atmospheres over the temperature range -60°C to +10°C. The experimental data for hydrogen in ammonia, as presented by Haul and Puttbach, is listed in Table 4.

TABLE 4

MOLECULAR DIFFUSION COEFFICIENTS FOR HYDROGEN DISSOLVED IN LIQUID AMMONIA[65]

Temperature °C	Diffusion Coefficient $\frac{cm.^2}{sec.} \times 10^6$
8.0	222.0
3.2	190.5
-10.1	170.0
-22.2	141.4
-31.2	120.0
-45.2	93.0
-58.7	69.0

4. EXPERIMENTAL APPARATUS AND PROCEDURE

A. Description of Apparatus

A schematic diagram of the single sphere absorber is presented in Figure 2. Auxiliary equipment which includes:

(a) Refrigeration System

(b) Hydrogen Purification Unit

(c) Methylamine Purification Unit

(d) Vacuum System

is described in Chapter 4, Part 1 and will not be further discussed in this section.

The general flow diagram of the apparatus, as shown in Figure (2), was fashioned after the equipment used by previous investigators [4,5,9,10]. The design of the single sphere absorption chamber was similar in concept to the absorber of Goettler[4,5] in that a laminar jet was used for introducing methylamine onto the sphere. A number of modifications on the equipment used by the above authors were necessary due to the properties of methylamine.

The single sphere absorption chamber was enclosed in a refrigerated air bath to enable operation in the temperature range -30°C to -10°C. Methylamine was fed from the two feed tanks to the absorber under its own vapor pressure. The spent amine leaving the absorption chamber was collected in a dump tank which was immersed in the liquid nitrogen.

Pure methylamine was found to chemically attack lucite, hence glass sections were used when visual observations were necessary. A standard table tennis ball was deteriorated by the amine, so a steel sphere was used.

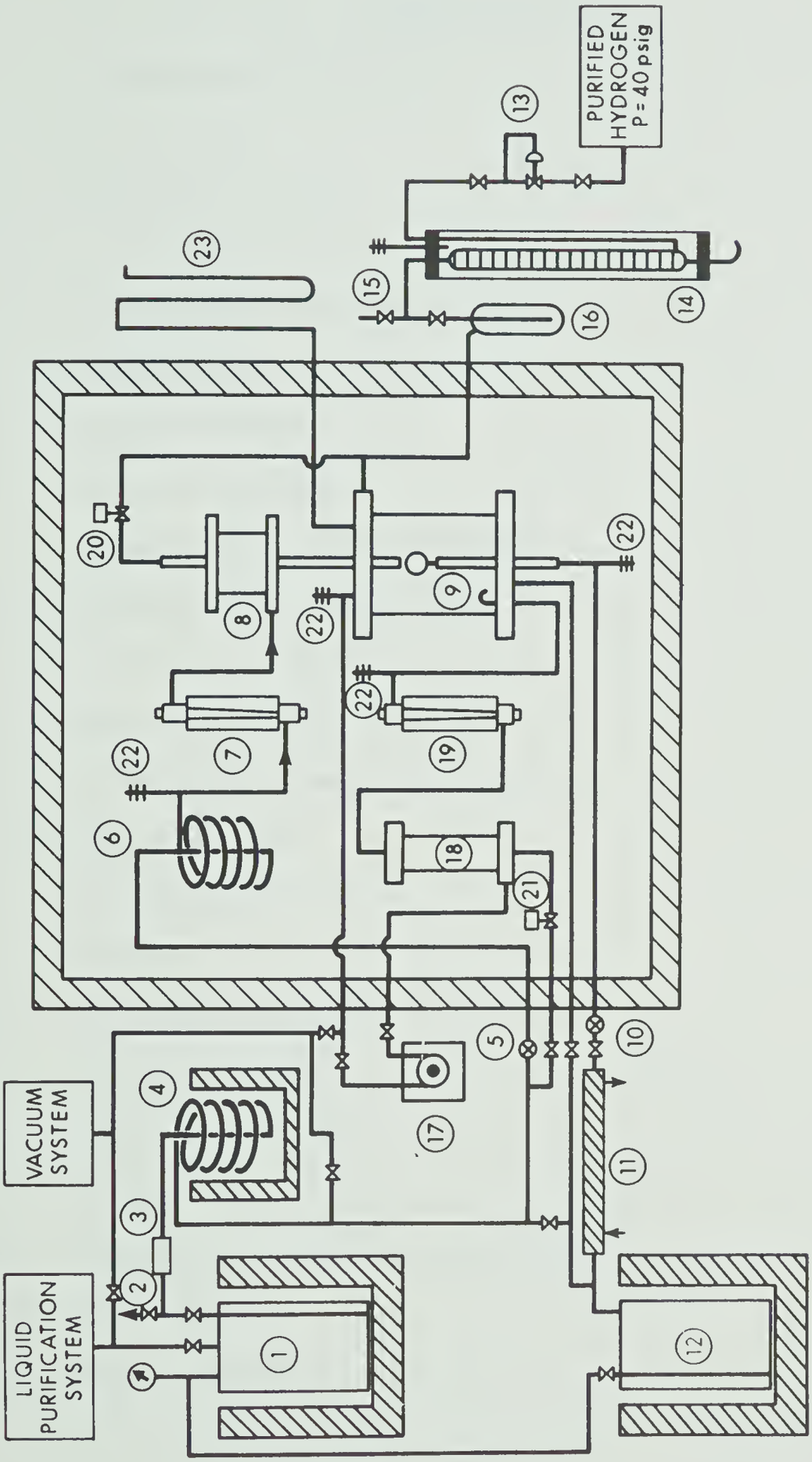


FIG. 2. SCHEMATIC DIAGRAM OF SINGLE SPHERE ABSORBER



SYMBOLS FOR FIGURE 2

1. Liquid Amine Feed Tank
2. Relief Valve
3. Glass Wool Filter
4. Liquid Feed Chiller
5. Liquid Feed Rate Control Valve
6. Liquid Feed Chiller
7. Liquid Rotameter
8. Liquid Distributor
9. Single Sphere Absorption Chamber
10. Take-off Level Control Valve
11. Liquid Outlet Chiller
12. Spent Liquid Amine Dump Tank
13. Hydrogen Low Pressure Regulator
14. Soap Film Meter
15. Hydrogen Vent Valve
16. Soap Trap
17. Hydrogen Circulator
18. Hydrogen Saturator
19. Hydrogen Rotameter
20. Solenoid Valve (Hydrogen Balance Line)
21. Solenoid Valve (Hydrogen Saturator)
22. Thermocouples
23. Mercury Manometer

1. Methylamine Feed Tanks

The methylamine feed tanks were two five liter pressure vessels which were connected in parallel to the inlet feed line to the absorber. The tanks were equipped with eductor tubes and connected by a vent line to ensure a balance in pressure. The vent line also served as an inlet line for feeding amine to the vessels. A measure relief valve was provided to protect against excessive pressure due to over filling.

Each tank was fabricated by welding end flanges on an 11-inch section of nominal 6-inch, schedule 80 pipe. One tank was constructed of mild steel while the other was type 316 stainless steel. They were permanently mounted in an insulated bath, as liquid nitrogen was used to freeze the methylamine when the tanks were being filled and when hydrogen was degassed from the methylamine in preparation for a run.

Methylamine was simultaneously fed from the two vessels under the force of its own vapor pressure.

2. Methylamine Feed System

The temperature of the liquid methylamine leaving the feed tanks was very nearly that of the room. A liquid chiller was therefore located immediately downstream of the feed tanks. This exchanger consisted of a twelve foot section of $\frac{1}{4}$ inch stainless steel tubing which was wrapped in a tight coil and immersed in a refrigerated bath. This bath was filled with "Varsol" and cooled by passing a stream of ethanol from the main refrigeration system through a second coil located in the bath.

The temperature of the methylamine leaving this coil was slightly warmer than the desired system temperature. A second cooling coil was located inside the constant temperature cold box. This coil was identical in design with the external coil but was not as efficient due to the surrounding air bath.

A packed glass wool filter was mounted on the outlet from the feed tanks. This filter was necessary to insure that no small particles became lodged in the fine metering valve.

The needle control valve was located immediately outside the cold box, between the two liquid chillers. Initial fluctuations in the flow rate occurred as the amine feed was being cooled, however, these soon dampened out.

3. Liquid Rotameter

The volumetric flow rate of liquid methylamine was measured with a "Brooks Full-View Rotameter", model 1110-2. The rotameter was calibrated for either a R-2-15-D tube and stainless steel float (sp. gr. float = 8.04) or a R-2-15-C tube and glass float (sp. gr. float = 2.20). The two rotameter tubes were calibrated with acetone at 20°C and were found to have a maximum flow rate of 0.600 $\frac{\text{c.c.}}{\text{sec.}}$ acetone (R-2-15-D) and 2.300 $\frac{\text{c.c.}}{\text{sec.}}$ (R-2-15-C). The calibration curves are presented in Tables D2-1 and D2-2, Appendix D2.

The volumetric flow rate of methylamine was initially calculated from the acetone calibration by applying the following correction[80].

$$Q_2 = Q_1 \left\{ \frac{(\text{Sp. gr. float} - \text{Sp. Gr. liq. 2})(\text{Sp. gr. liq. 1})}{(\text{Sp. gr. float} - \text{Sp. gr. liq. 1})(\text{Sp. gr. liq. 2})} \right\}^{\frac{1}{2}} \quad [4.1]$$

The subscript 1 refers to the acetone flow rate $\left(\frac{\text{c.c.}}{\text{sec.}} \text{ at } 20°C\right)$ and subscript 2 refers to the methylamine flow rate $\left(\frac{\text{c.c.}}{\text{sec.}} \text{ at the system temperature}\right)$.

The correction, as given by equation [4.1], was checked by measuring a series of flow rates for acetone at -20°C (R-2-15-D tube). The volumetric flow rate obtained by correcting the 20°C acetone calibration curve did not agree with the measured results except when the reading was in the top one third of the scale. The discrepancy was attributed to the change in viscosity of the acetone.

No mention of viscosity corrections was made in the "Brooks" manual[80], however, the Fischer and Porter Co.[81] have outlined the correction for the "Tri-Flat Variable-Area Flowmeter". The "Brooks" R-2-15-D and R-2-15-C tubes correspond to the "Fischer & Porter" 1/8-inch "Tri-Flat" tube. The viscosity correction, for the same acetone flow rate, was assumed to be equal for the "Brooks" and "Fischer & Porter" tubes.

The viscosity correction was handled in the following manner.

(1) The viscous influence number for acetone at 20°C was calculated.

$$N = \frac{404}{\mu_1}\{(\rho_f - \rho_1)\rho_1\}^{\frac{1}{2}} \qquad [4.2]$$

(2) From Fiqure (10), reference (81), the flow coefficient for acetone C_n was obtained for each of the n scale divisions on the "Fischer & Porter" tube. The acetone flow rate which corresponds to each scale division was calculated.

$$Q_{1,n} = \frac{76.8\ C_n}{\rho_1} \{(\rho_f - \rho_1)\rho_1\}^{\frac{1}{2}} \qquad [4.3]$$

(3) The same procedure was repeated for methylamine noting that a flow rate must be calculated for each scale division and for each degree of temperature in the range -10°C to -30°C. For a given temperature T_m, and the nth scale division the methylamine flow rate is:

$$Q_{2,n} = \frac{76.8\ C'_{n,m}}{\rho_2} \{(\rho_f - \rho_2)\rho_2\}^{\frac{1}{2}} \qquad [4.4]$$

where the prime indicates the flow coefficient is for methylamine.

(4) The viscosity correction factor corresponding to a methylamine temperature T_m and the nth scale reading was obtained from the equation:

$$F_{m,n} = \frac{Q_{2,n}}{Q_{1,n}} \qquad [4.5]$$

(5) A table of viscosity corrections, corresponding to the acetone flow rate $Q_{1,n}$ and methylamine temperature T_m, was therefore generated. The form of this table is shown in Figure 3. The actual corrections for the R-2-15-D and R-2-15-C rotameter are presented in Tables D2-3 and D2-4, Appendix D2, respectively.

A table of the form outlined in Figure 3 was read into the computer for the R-2-15-C tube and for the R-2-15-C tube. The cor-

FIGURE 3

ROTAMETER VISCOSITY CORRECTION TABLE

	$Q_{1,1}$	$Q_{1,2}$	$Q_{1,3} \cdots\cdots Q_{1,n}$
T_1	$F_{1,1}$	$F_{1,2}$	$F_{1,3} \cdots\cdots F_{1,n}$
T_2	$F_{2,1}$	$F_{2,2}$	$F_{2,3} \cdots\cdots F_{2,n}$
T_3	$F_{3,1}$	$F_{3,2}$	$F_{3,3} \cdots\cdots F_{3,n}$
.	.	.	. .
.	.	.	. .
.	.	.	. .
.	.	.	. .
T_m	$F_{m,1}$	$F_{m,2}$	$F_{m,3} \cdots\cdots F_{m,n}$

rection factor corresponding to a flow rate or temperature in the range of the table was obtained by linear interpolation.

The methylamine flow rate when the liquid temperature was T_x and the rotameter reading was such as to correspond to an acetone flow rate of $Q_{1,y}$ $\left(\frac{\text{c.c.}}{\text{sec.}} @ 20°C\right)$ was obtained from the equation:

$$Q_{2,y} = Q_{1,y} F_{x,y} \qquad [4.6]$$

The methylamine flow rate, as calculated from equation [4.6] agreed with the flow rate calculated from equation [4.1] when the rotameter reading was in the upper 1/3 of the tube.

Viscosity correction factors were calculated for acetone at -20°C, and they were found to predict the correct acetone flow rates at -20°C from the acetone calibration curve at +20°C.

4. Liquid Distributor

Liquid methylamine was fed to the laminar jet from a liquid distributor which was mounted on the approach tube to the

nozzle. The purpose of this vessel was to dampen any flow fluctuations which might occur in the feed lines and to provide additional residence time for temperature stability. The liquid distributor was also connected, through a solenoid valve, to the absorber. This connection allowed hydrogen which was displaced from the approach tube and liquid distributor during start-ups, to be fed back to the absorber. A small bore glass tube, which was part of the equalization line, was mounted on the top flange of the distributor. During normal operation of the absorber, the liquid level was maintained in this tube, hence, the absorption of hydrogen in the distributor was negligible.

The liquid distributor is shown in Figure 4. It was constructed of a nominal one inch "Q.V.F." glass pipe section sealed between two type 316 stainless steel flanges. "Swagelok" fittings were employed for all connections. Use of teflon ferrules on the ½-inch connector which connected the approach tube to the liquid distributor allowed for easy adjustment of the tube height.

5. Absorption Chamber

The single sphere absorption chamber (Figure 5) had the same basic construction as the liquid distributor. A glass "Q.V.F." pipe section was used for the chamber wall and stainless steel end flanges were fabricated to provide the necessary inlet and outlet ports. The original absorber wall was a seven inch section of nominal four inch glass pipe, however, this was later replaced by a five inch section of nominal 1½ inch glass pipe. Stainless steel adapter flanges were used to mate the small glass section with the

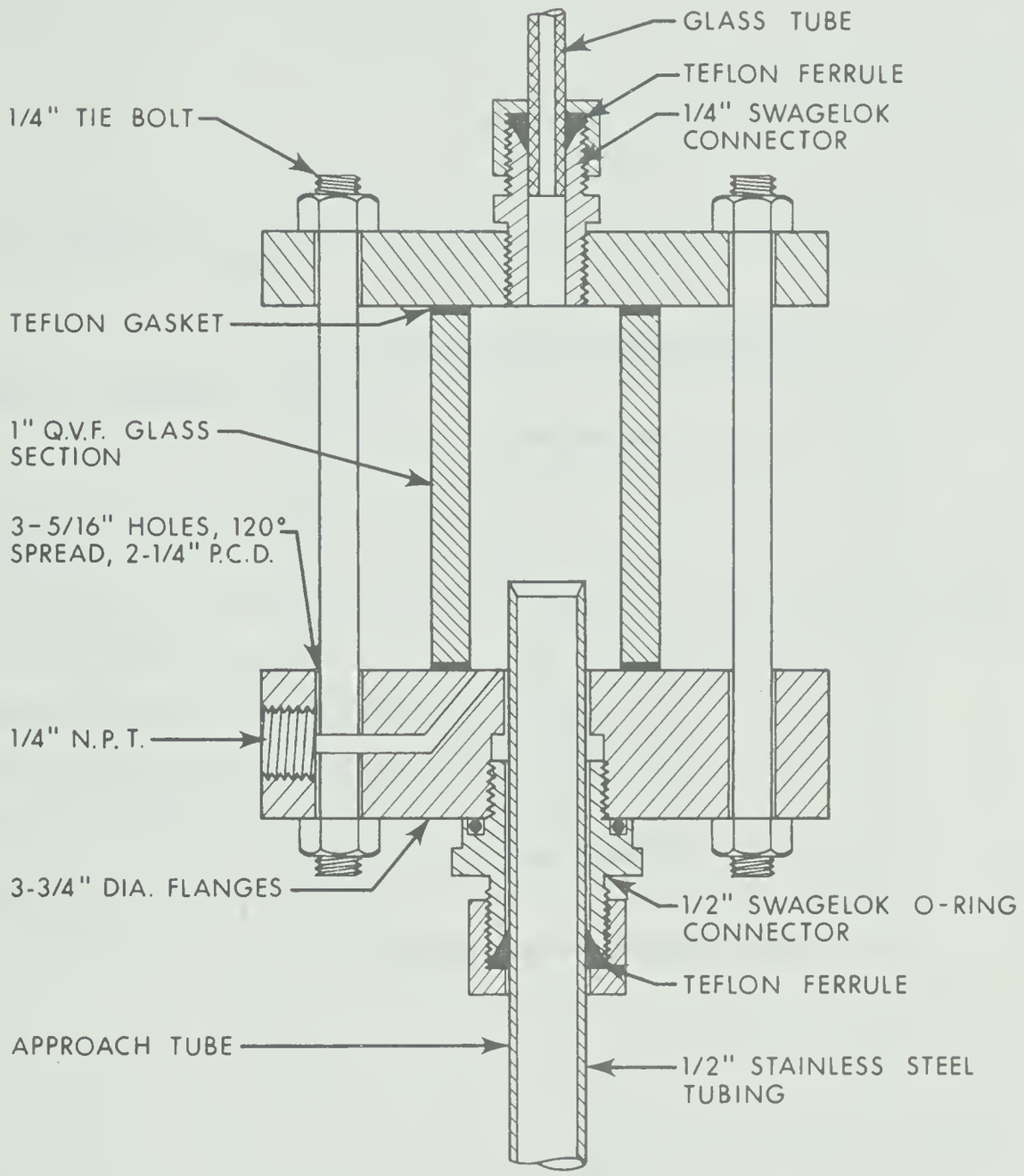


FIG. 4. LIQUID DISTRIBUTOR

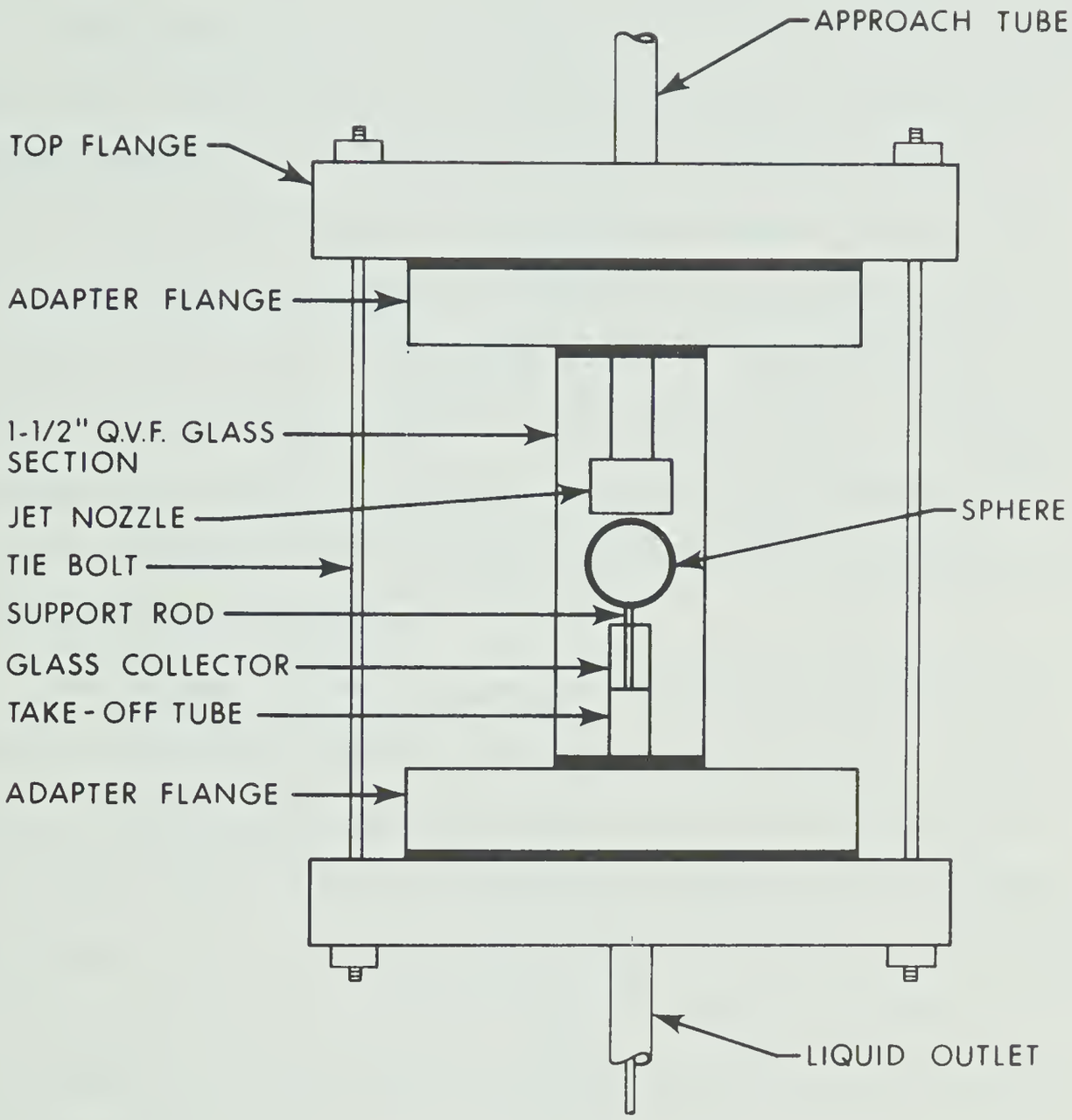
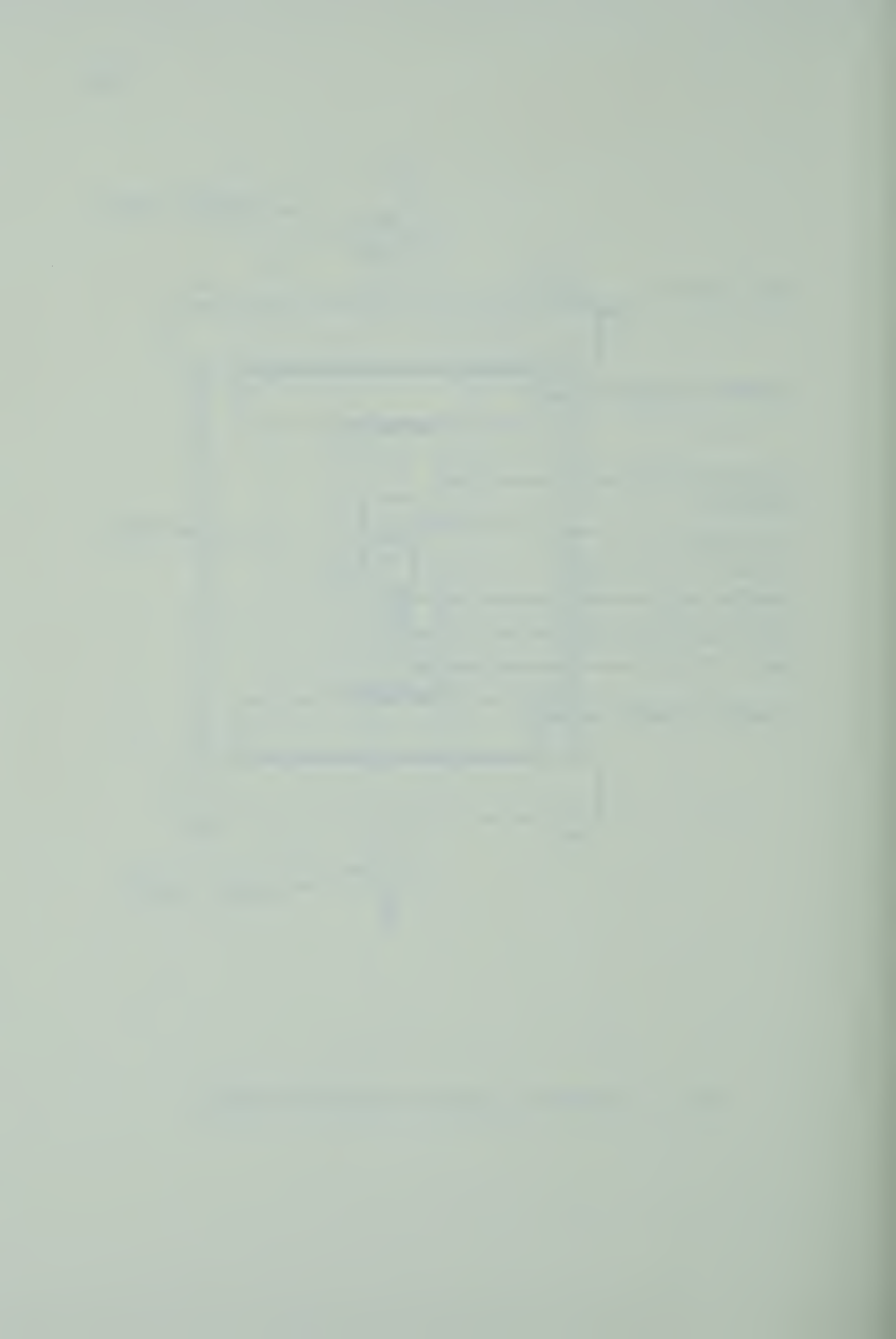


FIG. 5. SCHEMATIC DIAGRAM OF ABSORPTION CHAMBER



original stainless steel end flanges.

The spheres used in this study were 3/4 inch and 1 inch diameter steel ball bearings which had been softened by heat treating. The spheres were drilled to enable mounting on a 1/8 inch diameter shaft and both were fitted with a 1/16 inch diameter teflon disc on the top pole. The teflon disc was machined to conform with the contour of the sphere. The purpose of the disc was to mark the top pole of the sphere for alignment of the laminar jet. A small protrusion was originally tried as an alignment marker (Goettler[41]) however methylamine had a tendency to spray out from the protrusion and the design was abandoned.

The support rod was roughened to enhance wetting and was centered in the liquid take-off tube by two teflon spiders. The rod passed through the base of the take-off tube and was attached to the frame supporting the entire absorption apparatus by a threaded adjustment nut. An o-ring seal was used to seal the rod in the base of the take-off tube. The ball height, relative to the floor of the absorber could be varied by releasing the o-ring seal and turning the adjusting nut.

The take-off tube was fabricated from a ½ inch stainless steel tube on one end of which was welded a machined block (Figure 6). A ½ inch "Swagelok" connector was used to seal the glass collector tube to the top of the take-off tube. The height of the take-off tube could be varied by sliding it in the o-ring seal which provided the seal between the tube and flange.

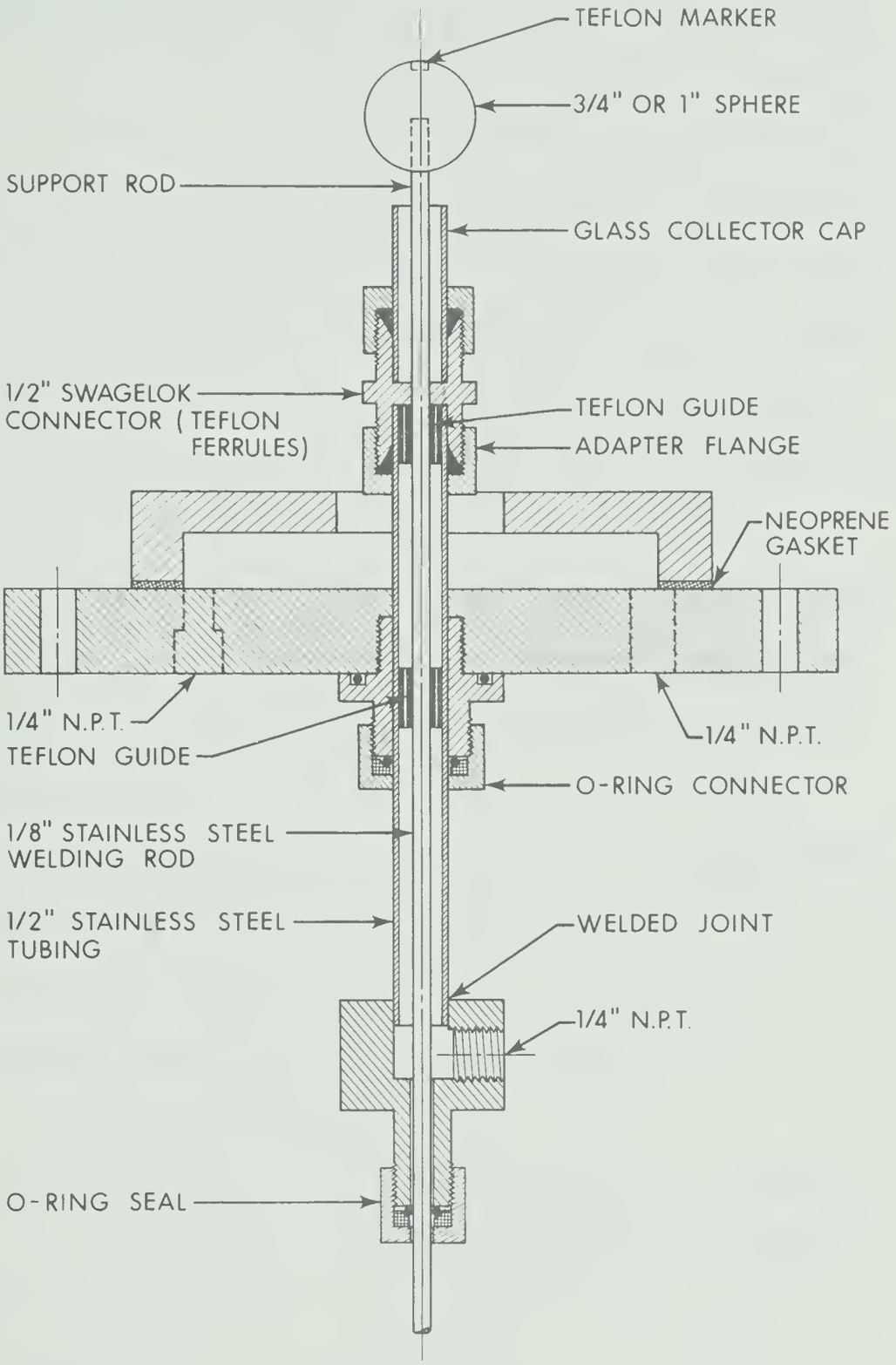


FIG. 6. ABSORBER BASE FLANGE AND TAKE-OFF TUBE

The laminar jet was designed in a similar manner to those of Goettler[4], Scriven[19,20] and Hatch[82]. The nozzle design was modified to incorporate the use of ruby watch jewels for the cylindrical throat sections. These jewels were relatively inexpensive, accurately sized and easily press fit into the nozzle caps. Their use overcame the problem of drill wander when drilling the small bore jet throats in the nozzle caps. A series of nozzles (0.40, 0.46, 0.50, 0.60 and 0.76 mm.) were built to cover the possible flow requirements of the study.

Centering of the laminar jet accurately over the teflon marker was performed with an eccentric mounted in the top flange of the absorber (Figure 7). Acetone was passed through the jet during the alignment procedure.

Teflon was initially used for all o-ring seals. Leaks formed after the system had been cooled and warmed a number of times, so all the teflon o-ring seals were replaced with Neoprene o-rings. The Neoprene seals were replaced on a regular basis and no further problems with leaks were encountered.

Lucite was originally used for the chamber wall and take-off tube collector cap, however, it underwent rapid chemical decomposition and was rejected.

6. Hydrogen Saturation System

Saturation of the hydrogen with methylamine was carried out by bubbling the hydrogen through a stagnant depth of methylamine. The saturation vessel was formed by sealing a nominal one inch

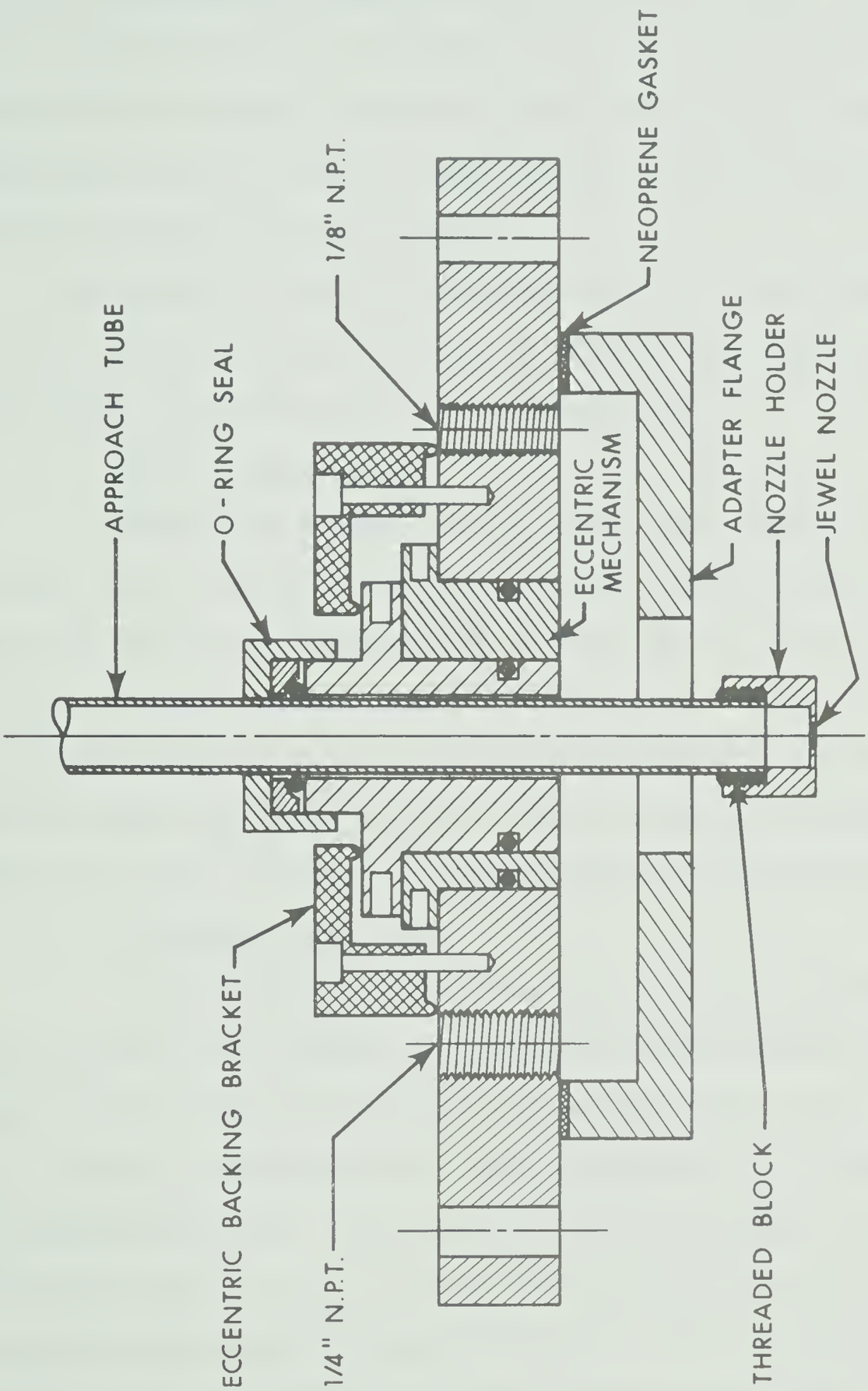


FIG. 7. ABSORBER TOP FLANGE AND LAMINAR JET



"Q.V.F." pipe section between two stainless steel flanges. Hydrogen was circulated through the absorber and saturator by a peristaltic pump which was located immediately outside the cold box. A rotameter was located in the flow loop, although it was not required for the physical absorption studies.

The peristaltic pump was equipped with latex or gum rubber tubing. A steel casing was used on the pump as methylamine diffused through the rubber and attacked the original lucite head.

7. Outlet Liquid Cooler

Methylamine passed from the single sphere chamber to a spent amine dump tank. The amine collector tank was located outside the cold box and problems were incurred due to the amine heating in the flow line. An external heat exchanger was therefore installed on this line. The cooler was fabricated by fitting a $\frac{1}{2}$ inch copper jacket over the $\frac{1}{4}$ inch flow line. A stream of refrigerant from the primary refrigeration loop was passed through this coil.

8. Spent Amine Dump Tank

Liquid methylamine which had passed through the absorber was collected, under vacuum, in a standard propane tank which had been modified to allow installation of the flow lines. The tank was located in an insulated bath which was kept full of liquid nitrogen during a run. The pressure in the tank changed slightly during the course of the run due to the release of dissolved hydrogen, however, no appreciable change in the control valve setting was required to maintain the liquid level in the take-off tube.

9. Hydrogen Feed System

Hydrogen was drawn from the supply cylinder and passed through the purification system on the solubility cell (See Part I) prior to having its pressure reduced to the desired value by a "Matheson model 70A" low pressure regulator. The hydrogen absorption rate was measured with a soap film meter which was constructed from a 50 c.c. burette with 0.10 c.c. graduations. (Initial efforts to use a smaller burette with finer graduations failed as the soap film was not stable at the low flow rates involved in this study). A soap trap and a vent valve were installed between the absorber and soap film meter. The vent valve was used when wetting the tube walls prior to a run.

10. Controlled Temperature Chamber

A controlled temperature chamber was constructed to house those components of the absorption apparatus which were required to be at the same temperature. The internal dimensions of the box were 18 inches deep by 42 inches wide by 54 inches high. The external and internal walls of the chamber were fabricated from ½ inch "K-board" and the space between the walls was insulated with a 4 inch layer of Styrofoam. The complete front wall of the box was removable. This door was equipped with a 36 inch square frost free window. An "Armaflex" foam rubber seal was installed between the front wall and main section.

The ethanol refrigerant was circualated through five copper coils which surrounded three sides of the box. The coils were

piped in parallel from common inlet and outlet manifolds.

A forced air blower was used to recirculate dry air through the box. The air was drawn from the base of the box and returned through two vents situated in the sides of the chamber. A purge of dry instrument air was continuously introduced to the chamber to maintain a slight positive pressure.

Two $1\frac{1}{2}$ inch copper pipes were sealed in the sides of the box to provide access ports for the flow lines. The void space around the lines was filled with putty.

The refrigeration cold box was mounted on a steel frame table. Ribbed-rubber vibration pads were installed beneath each table leg.

11. System Valves

The on-off valves utilized on the single sphere absorption apparatus were "Whitey" forged body valves. Two valve models were used, the IKS4-316 valve when a positive seal was imperative and the IVS4-316 model when the application was not critical. The IKS4 valves had "Kel-F" stem tips which required frequent attention as methylamine degraded this material after a long contact period.

The liquid feed and liquid outlet control valves were both "Whitey 2IRS4-316" micrometering control valve. These valves provided an almost linear response with regard to the number of turns of the stem. Excellent control was obtained over the complete flow range.

The solenoid valves were situated inside the cold box. They were both "Asco" midget size valves and were both equipped with explosion proof coils. The valve stem tips were replaced with latex rubber to enhance sealing.

A "Hoke Safety Cylinder Adapter", model 62208A spring relief valve was installed on the feed tanks. The original valve seat was Viton-A which was rapidly attacked by methylamine, hence Teflon seats were installed.

12. Temperature Measurement

The single sphere absorption apparatus was equipped with four thermocouples. The placement of these thermocouples is shown in Figure 2. All the thermocouples were of the copper-constantan type, and were sealed in 1/8 inch stainless steel sheaths. The thermocouples were mounted in the flow lines by standard "Swagelok" connectors which were equipped with teflon ferrules.

Each thermocouple was individually calibrated against a platinum resistance thermometer. The calibration curves were very nearly identical, hence the same correction was applied to each thermocouple. The calibration curve is presented in Figure D2-1, Appendix D2.

A "Leeds & Northrup" millivolt potentiometer, model number 8686, was used for the readout of all the thermocouples.

13. Pressure Measurement

A mercury manometer was used for measuring the system pressure. Some danger existed when mercury was used in an environment where ammonia might be present[83,84], however this danger is minimal at low system pressures[85].

B. Experimental Procedure

1. Methylamine Purification

The liquid methylamine was dried on contact with freshly cut lithium metal and degassed by vacuum distillation according to

the procedure outlined in Chapter 4, Part 1. The methylamine feed was regenerated following each experimental run, hence, fresh amine was only added to replace the liquid lost during the normal operation of the absorber.

2. Operation of the Single Sphere Absorber

The following startup and operating procedure was developed for the single sphere absorber.

(a) Methylamine was introduced to the hydrogen saturator and the system was charged with hydrogen.

(b) The peristaltic pump was started and hydrogen was circulated for approximately one half hour.

(c) The hydrogen circulator was stopped and the system temperature allowed to stabilize.

(d) The methylamine dump tank was immersed in liquid nitrogen.

(e) The solenoid valve between the liquid distributor and absorber was opened.

(f) Methylamine was introduced to the system. The flow rate was maintained at a greater value than the discharge rate from the nozzle, hence methylamine accumulated in the distributor.

(g) When the methylamine level appeared in the take-off tube, the ball valve between the absorber and dump tank was opened and the outlet control valve was set so as to maintain the liquid level in the take-off tube.

(h) When the level of the methylamine in the liquid distributor reached the glass tube above the distributor, the solenoid valve was closed and the feed control valve adjusted to maintain this level.

(i) The absorber pressure was brought to the desired value by either venting or adding hydrogen.

(j) With the hydrogen feed valve closed, the vent valve was cracked and hydrogen allowed to escape. A number of soap bubbles were generated in the soap film meter and carried up the meter tube by the force of the escaping hydrogen. Hydrogen was allowed to escape until the soap had wet the complete meter tube.

(k) The final adjustments on the amine feed rate and amine level in the take-off tube were then carried out.

(l) The hydrogen feed valve was then opened and the system pressure allowed to stabilize.

(m) Frequent measurements of the four system thermocouples were obtained during the start-up period and no hydrogen absorption measurements were taken until the temperatures had stabilized.

(n) The total time required for the system to stabilize was approximately 45 minutes. When the system was deemed to be at steady state, three soap films were formed in the soap film meter and the time required for the bottom film to sweep a given volume (5c.c. or 10c.c.) was recorded.

(o) The liquid in the take-off tube was continuously controlled at the desired height. A cathetometer was used to observe the level and to provide the reference mark.

(p) The liquid flow rate or take-off height could be changed during a run, however, at least 20 minutes was required for the system to stabilize after any change in the absorber conditions.

(q) Upon completion of a run the hydrogen feed valve was closed and the liquid methylamine was drained from the absorber flow lines and hydrogen saturator to the dump tank. The remaining methylamine in the feed tanks was also drained to the dump tank.

(r) The dump tank was then isolated from the absorber and a vacuum of at least five microns was drawn on the tank.

(s) When the desired vacuum was attained, the dump tank was isolated and allowed to warm.

(t) On the day following the run, the feed tanks were immersed in liquid nitrogen and a vacuum was applied to the tanks to check for any possible leaks. Methylamine was then fed, under its own vapor pressure, from the dump tank to the feed tank.

(u) When all the methylamine had been transferred to the feed tank, the dump tank was isolated and a vacuum was drawn on the feed tanks. Evacuation of the tanks continued until methylamine appeared in the diffusion pump cold trap.

(v) The feed tanks were then isolated and allowed to warm. Approximately eight hours was required for the tanks to attain room temperature in preparation for another run.

C. Data Reduction

The following section outlines the method used to reduce the experimental measurements to a molecular diffusion coefficient for hydrogen dissolved in methylamine. The experimental parameters which were measured during a single experimental run were:

(a) Temperature of methylamine entering the rotameter (T_L).

(b) Temperature of methylamine leaving the rotameter (T_A).

(c) Methylamine flow rate (L).

(d) Total absorber pressure (π).

(e) Volume flow rate of hydrogen entering the absorber (Q_H).

(f) Temperature of the hydrogen feed (T_H).

(g) Height of methylamine in the take-off tube (h_T).

(h) Barometric pressure (P_{bar}).

(i) Jet length (h_J).

The first seven parameters were recorded for each individual reading. The barometric pressure and jet length were assumed to be constant throughout the run.

The high depth of penetration model of Davidson and Cullen[9] was assumed to describe the physical absorption process occuring on the sphere. The form of this equation, as discussed in Chapter 2, is:

$$G_s = L(C_i - C_o)[1 - 0.7857 \exp(-3.414\ \alpha) - 0.1001 \exp(-26.21\ \alpha) - 0.03599 \exp(-70.43\ \alpha) - 0.01811 \exp(-136.5\ \alpha)] \quad [2.70]$$

where:

$$\alpha = 2 \times 1.68\pi \left(\frac{2\pi g}{3\nu}\right)^{1/3} \frac{R^{7/3}}{L^{4/3}} D \quad [2.71]$$

The ten term equation of Olbrich and Wild[28] (equation [2.72]) was found to agree with the above equation at the levels of saturation involved in this study. The simpler solution of Davidson and Cullen[9] was chosen to reduce the computation time required for the trial and error solution for the diffusion coefficient.

The solution of equation [2.70] for the molecular diffusion coefficient D was based on the following assumptions.

(a) The gas-liquid interface was saturated at all locations on the film so that:

$$C_i = \frac{2.016\ \rho_1}{M_1} \left\{\frac{1}{\frac{H_2}{P_2} - 1}\right\} \quad [4.7]$$

Henry's law coefficient (H_2) was calculated from the best fit polynomial as determined in Part 1 of this study. The liquid density (ρ_1) was calculated from equation [3.3] of Part 1

(b) The temperatures of the liquid and vapor phases in the absorber were equal to the temperature of the methylamine leaving the absorber (T_A). This assumption is valid if the heat of absorption is negligible.

(c) The hydrogen partial pressure was:

$$P_2 = \pi - P_1(1 - x_2) \simeq \pi - P_1 \qquad [4.8]$$

The vapor pressure of methylamine at the system temperature (T_A) was determined from equation [3.2], Part 1.

(d) The amount of hydrogen absorbed on the take-off rod and the stagnant liquid interface in the take-off tube was negligible.

(e) The rate of absorption of hydrogen on the laminar jet was equal to the rate predicted by the penetration theory solution for absorption on an ideal jet[4,7,21].

$$G_J = 4(C_i - C_o') \sqrt{h_J L D} \qquad [3.7]$$

The bulk concentration of hydrogen in the methylamine entering the absorber (C_o') was assumed to be negligible.

(f) Complete mixing occured at the jet-sphere junction. The bulk concentration of the liquid film on the sphere was:

$$C_o = \frac{G_J}{L} \qquad [3.8]$$

(g) The surface area available for absorption on the sphere was corrected for the increase in area due to the thickness of the film. The increase in area was calculated from the following equation.

$$\frac{A_A}{A_s} = \left(1 + \frac{2.58\ \Delta^+}{R}\right) \qquad [3.9]$$

The actual rate of absorption of hydrogen on the sphere (G_A) was related to the corrected absorption rates (G_s) by the relationship:

$$\frac{G_A}{A_A} = \frac{G_s}{A_s} \qquad [4.9]$$

Therefore:

$$G_s = G_A \left\{ \frac{1}{1 + \frac{2.58\ \Delta^+}{R}} \right\} \qquad [4.10]$$

(8) The mass flow rate of hydrogen entering the absorber, was calculated from the equation:

$$G_H = \left(\frac{2.016}{22414.6}\right)\left(\frac{273.15}{T_H}\right)\left(\frac{\pi}{1}\right) Q_H \qquad [4.11]$$

A number of individual determinations of the equilibrium temperature (T_A), liquid flow rate (L) and hydrogen absorption rate Q_H were used for calculating the diffusion coefficient.

The solution of equation [2.70] involved a trial and error search for the value of D which would yield the minimum deviation of the experimental absorption rates from those predicted by the equation. The molecular diffusion coefficient was taken to be the value of D for which the function

$$E = \sum_{k=1}^{N} \left| (G_s)_K - (L(C_i - C_o)\ f(\alpha))_K \right| \qquad [4.12]$$

$$f(\alpha) = 1 - 0.7857 \exp(-3.414\ \alpha) - 0.1001 \exp(-26.21\ \alpha) - 0.03599 \exp(-70.43\ \alpha) - 0.01811 \exp(-136.50\ \alpha) \qquad [4.13]$$

N = number of determinations.

is a minimum. It can be seen that all the terms in equation [4.12], except the liquid flow rate L and the interfacial concentration C_i, are functions of the diffusivity D.

The initial estimation of the diffusivity D was obtained from the low depth of penetration model (equation [2.67]) of Davidson and Cullen[9].

$$G_s' = (12 \times 1.68)^{1/2} \left(\frac{2\pi g}{3\nu}\right)^{1/6} D^{1/2} L^{1/3} R^{7/6} (C_i - C_o) \qquad [2.67]$$

Rearranging equation [2.67] for the sphere and equation [3.7] for the jet yields:

$$Z_s = \frac{G_s'}{\sqrt{D}\,(C_i - C_o)} = (12 \times 1.68)^{1/2} \left(\frac{2\pi g}{3\nu}\right)^{1/6} L^{1/3} R^{7/6} \qquad [4.14]$$

$$Z_j = \frac{G_J}{\sqrt{D}\,(C_i - C_o')} = 4\sqrt{h_J L} \qquad [4.15]$$

Assuming $C_o = C_o' \simeq 0$, the fraction of the total hydrogen entering the absorber which is absorbed on the sphere and jet respectively is:

$$F_s = \frac{Z_s}{Z_s + Z_J} \qquad [4.16]$$

$$F_J = 1 - F_s \qquad [4.17]$$

The amount of hydrogen absorbed on the sphere and jet respectively is:

$$G_s' = G_A = G_H F_s \qquad [4.18]$$

$$G_J = G_H F_J \qquad [4.19]$$

and the initial estimate of the diffusion coefficient D was calculated from the following equation:

$$D = \left\{ \frac{G_s'}{Z_s \left[C_i - \frac{G_J}{L} \right]} \right\}^2 \qquad [4.20]$$

The surface area correction to the hydrogen absorption rate was neglected in equation [4.20] due to the approximate nature of the estimate. The correction was however applied to the absorption rate when it was substituted in equation [4.12].

The interfacial concentration (C_i) and the total hydrogen absorption rate (G_H) which were substituted in equation [4.18] through equation [4.20] were average values for a given flow rate L. A value of D corresponding to each liquid flow rate was calculated and an average of these diffusion coefficients was taken as the initial estimate.

The value of the diffusion coefficient (D) which satisfied the constraint of equation [4.12] was obtained by an interval halving search routine. The value of D which satisfied equation [4.12] was substituted into equation [3.7] and a revised estimate of the amount of hydrogen absorbed on the jet (G_J) was calculated. The revised estimate of G_J was substituted into equation [3.8] to obtain a new estimate of the bulk phase concentration of the film at the top of the sphere. The revised estimate of the corrected hydrogen absorption rate on the sphere (G_s) was calculated form the following equation.

$$G_s = \frac{(G_H - G_J)}{\left\{1 + \frac{2.58\ \Delta^+}{R}\right\}} \qquad [4.21]$$

The revised parameters were again substituted in equation [4.12] and a new estimate of D obtained. This procedure was carried out until the consecutive estimates of D from equation [4.12] agreed to within one half of one percent.

The computer program which was developed for carrying out the above calculation routine has been listed elsewhere[86]. A sample calculation is presented in Appendix B2.

D. Results

The experimental determinations on the physical absorption rate of hydrogen in methylamine are reported in Tables A2-1 to A2-3 of Appendix A2. The data presented in Tables A2-1 and A2-3 were measured on the 3/4 inch and 1 inch sphere respectively. The data reported in Table A2-2 were measured by Kalra[87] on a 3/4 inch sphere.

The experimental data are plotted in Figures 8 to 12 as the measured total hydrogen absorption rate to the absorber (G_H) corrected to one atmosphere hydrogen partial pressure. The data reported were determined at temperatures within ±1°C of the average temperature stated on the graph. As the temperatures corresponding to the absorption rate measurements are not equal, some scatter of the points is caused by temperature differences. The data were plotted in this manner in order to indicate the degree of agreement of the experimental absorption rates with those predicted by the absorption

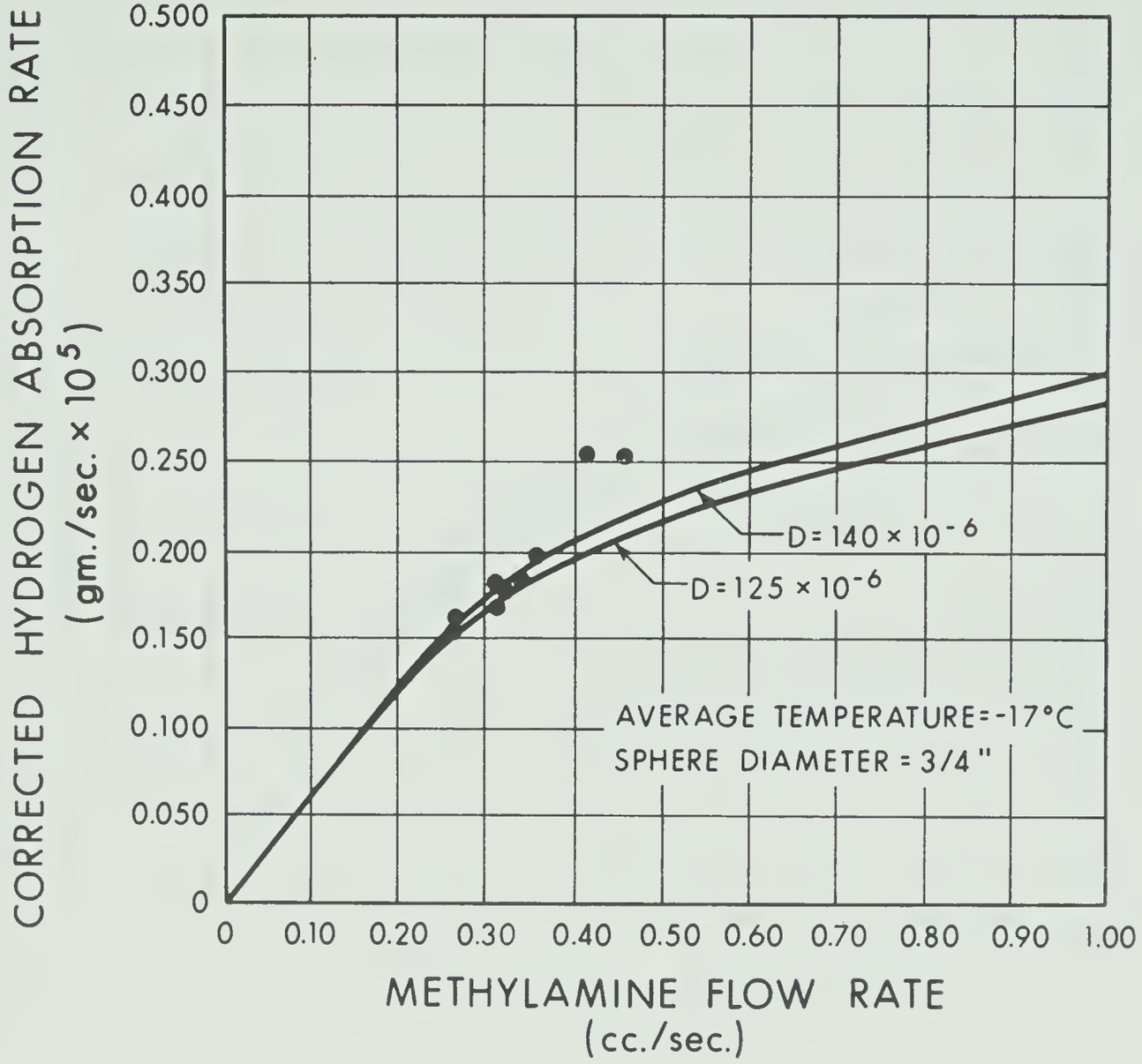


FIG. 8. RATE OF ABSORPTION OF HYDROGEN IN METHYLAMINE AT -17°C ON 3/4 INCH SPHERE



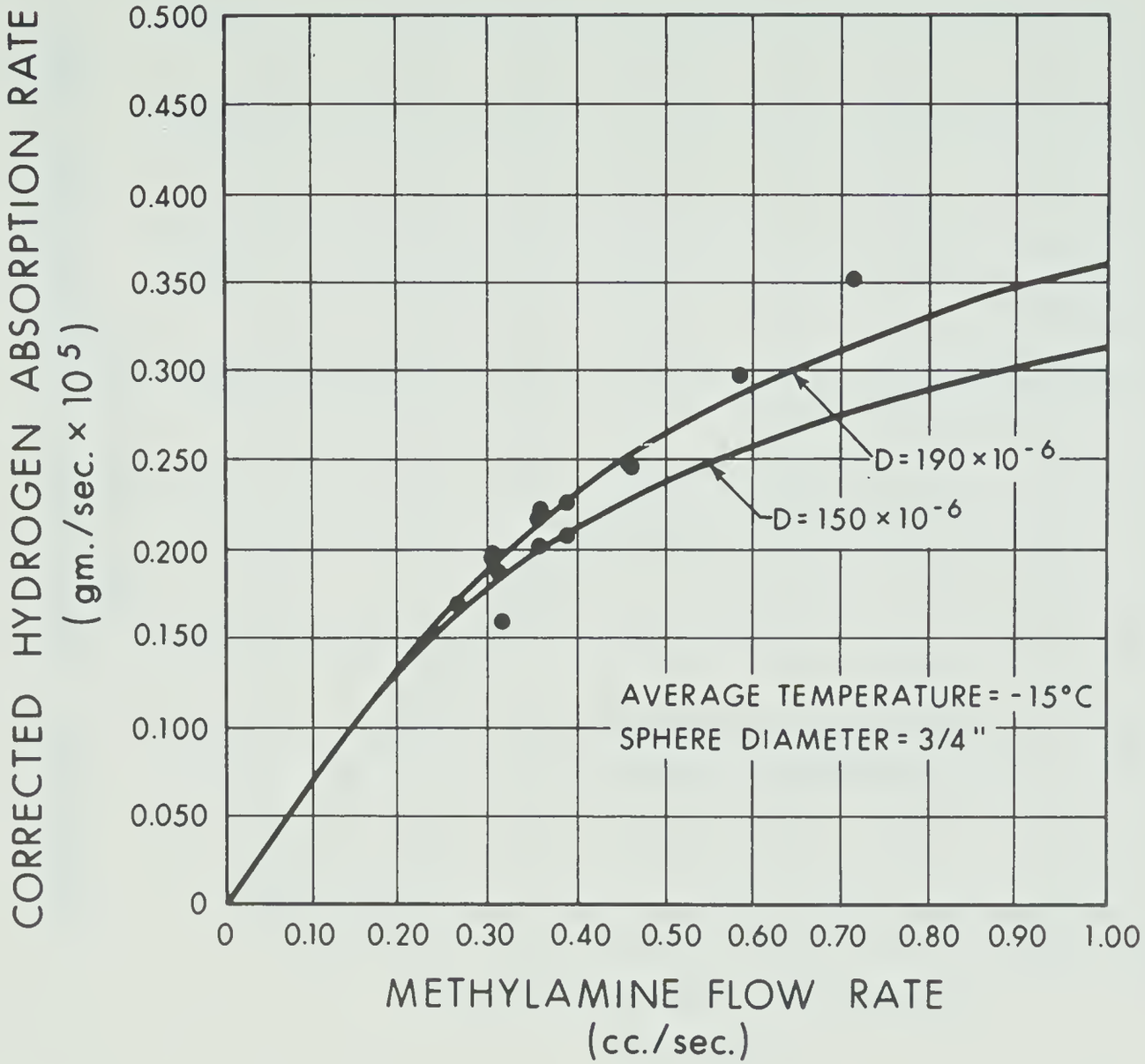


FIG. 9. RATE OF ABSORPTION OF HYDROGEN IN METHYLAMINE AT -15°C ON 3/4 INCH SPHERE



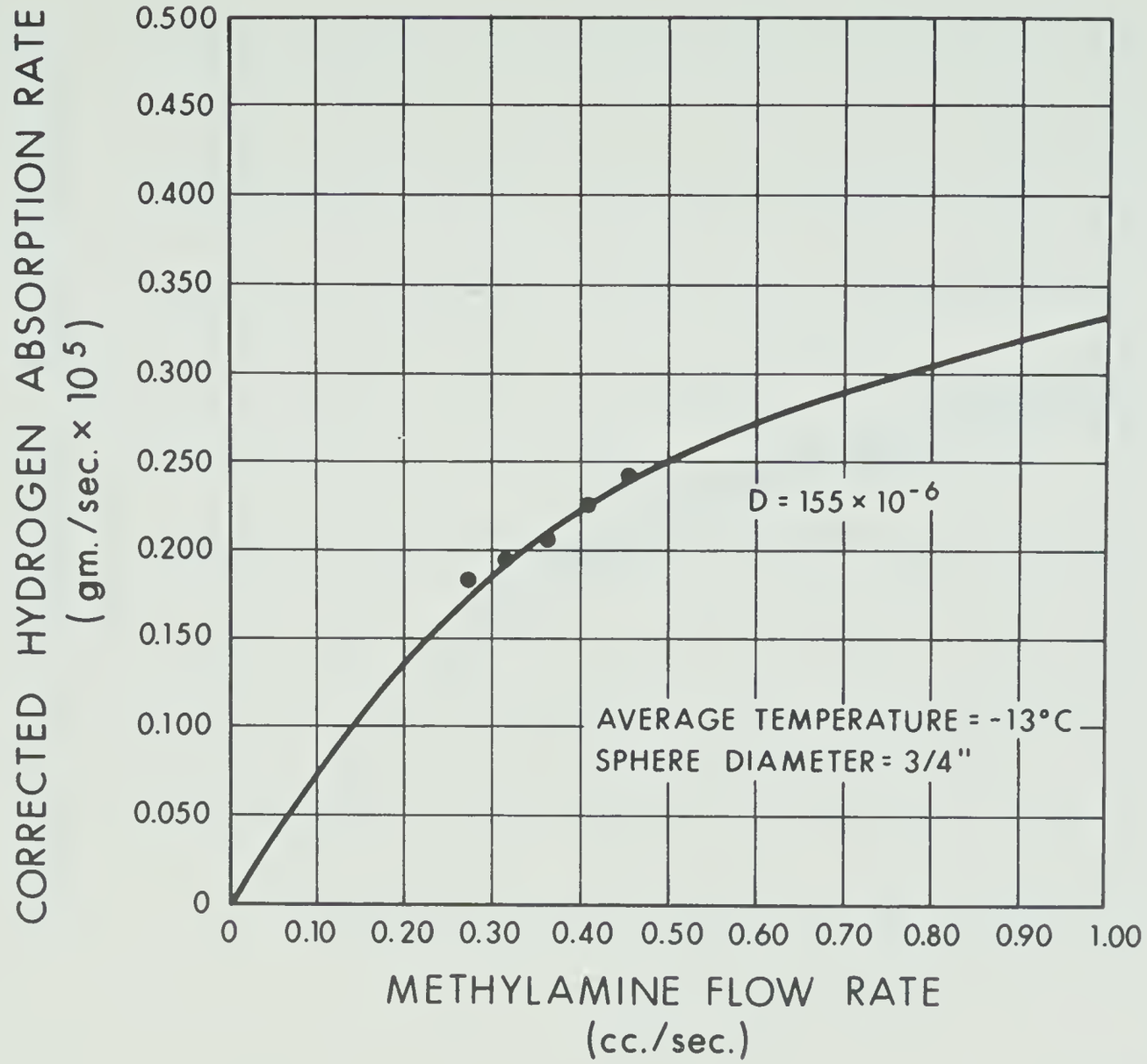


FIG. 10. RATE OF ABSORPTION OF HYDROGEN IN METHYLAMINE AT -13°C ON 3/4 INCH SPHERE



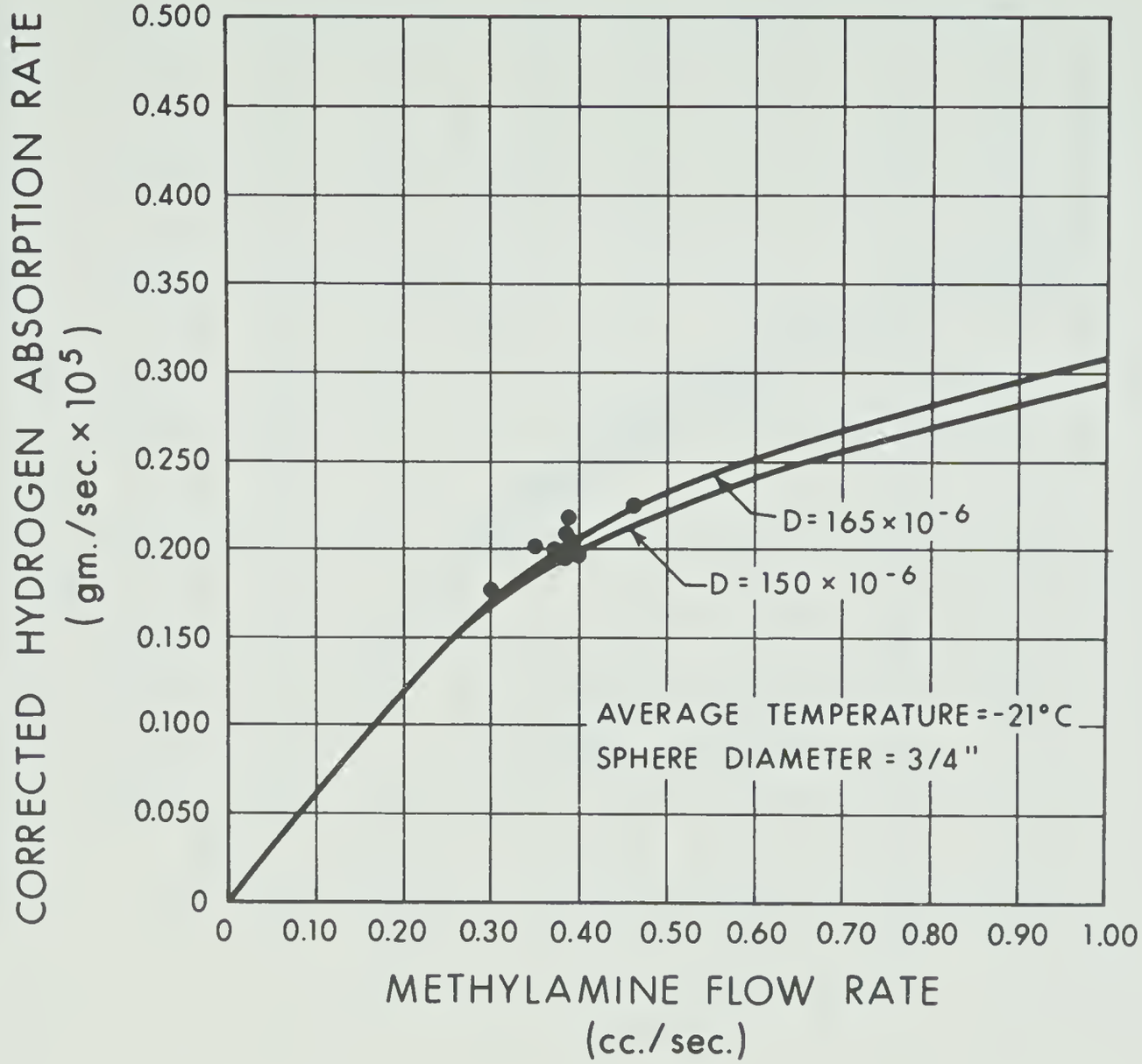


FIG. 11. RATE OF ABSORPTION OF HYDROGEN IN METHYLAMINE AT -21°C ON 3/4 INCH SPHERE (KALRA[87])

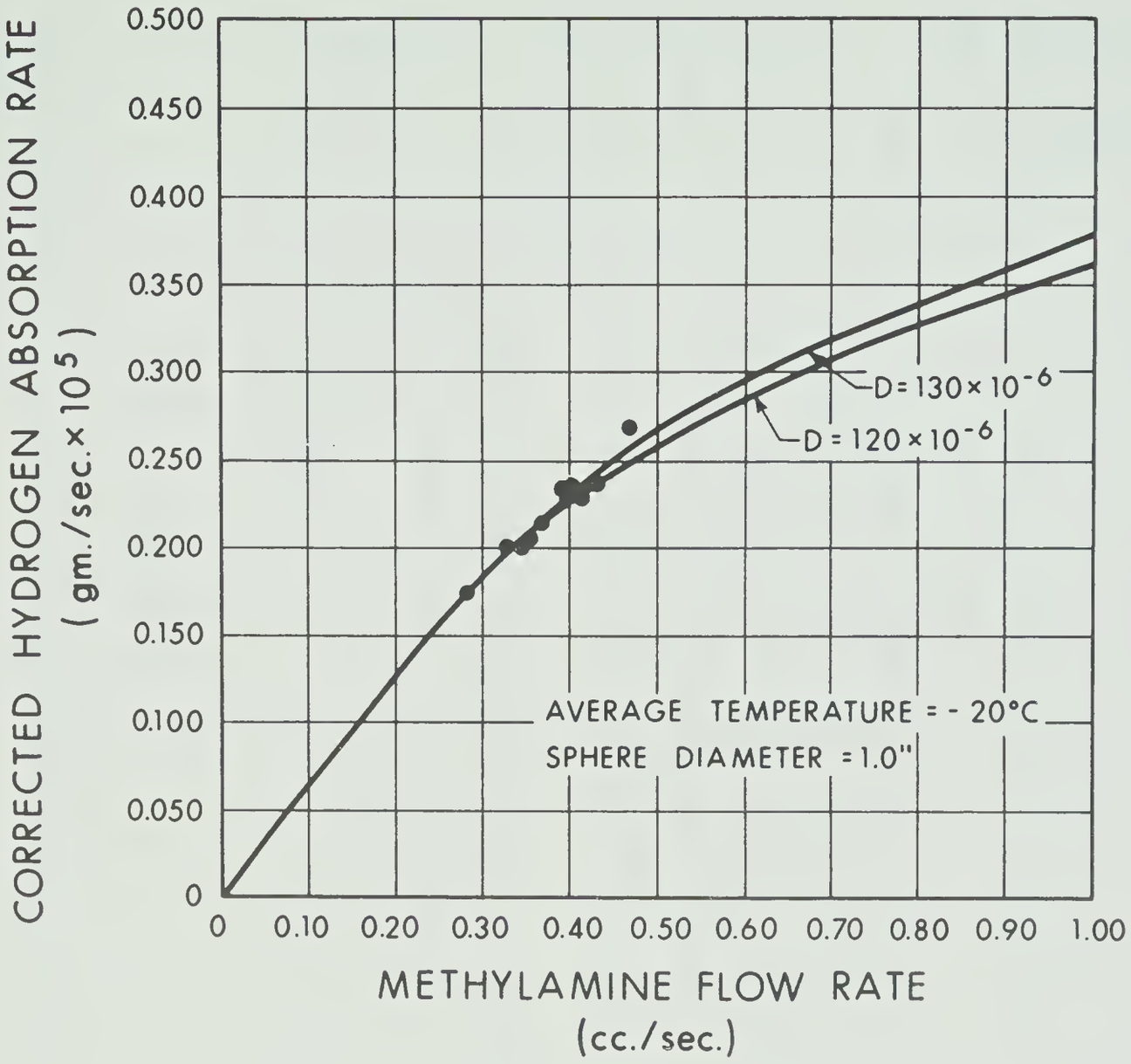


FIG. 12. RATE OF ABSORPTION OF HYDROGEN IN METHYLAMINE AT -20°C ON 1 INCH SPHERE



model.

The solid curves in Figures 8 to 12 were generated by a computer program which simulated the expected total hydrogen absorption rate (G_H) for given values of the liquid flow rate (L), diffusion coefficient (D) and temperature (T_A). This program was based on the absorption model for the sphere (equations [2.70] and [3.9]) and laminar jet (equations [3.7] and [3.8]).

The diffusivity of hydrogen in methylamine, as calculated from the physical absorption data, are listed in Tables A2-1 to A2-3. Diffusion coefficients are presented for each flow rate. In addition, a number of best fit diffusion coefficients (D_{AVG}), which were calculated using data for all liquid flow rates studied during a run, are presented.

The natural logarithm of the diffusion coefficients determined on the 1 inch sphere are plotted versus the reciprocal absolute temperature in Figure 13. The solid curve represents the line described by the group $\frac{D\mu_l}{T}$ when

$$\frac{D\mu_l}{T} = 1.570 \times 10^{-7} \qquad [4.22]$$

and the methylamine viscosity (μ_l) is calculated from equation [3.4] of Part 1.

The diffusivity of hydrogen in methylamine at -20°C, as obtained from Figure 13 is:

$$D = 122 \times 10^{-6} \frac{cm.^2}{sec.} \qquad [4.23]$$

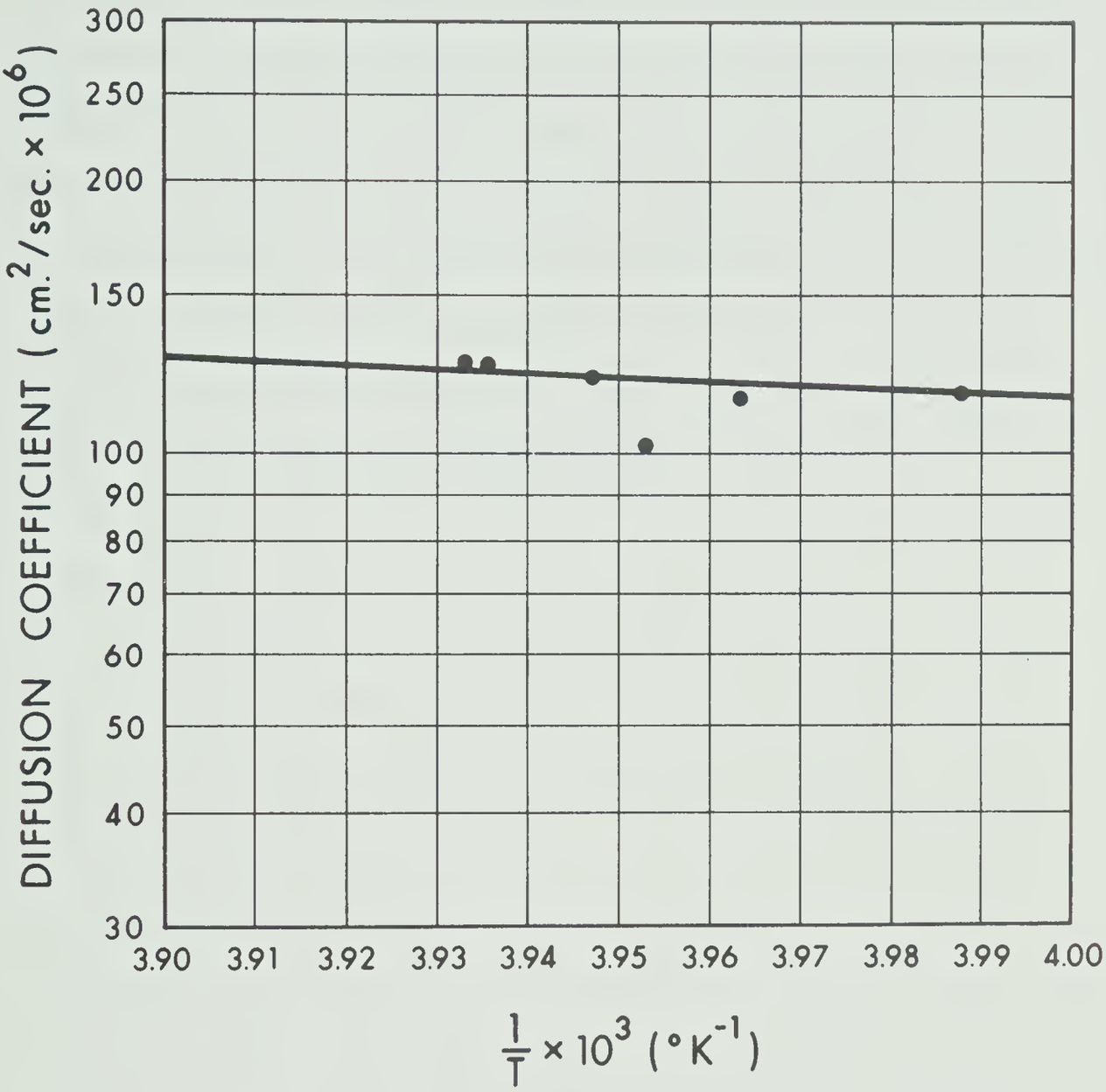


FIG. 13. EFFECT OF TEMPERATURE ON THE DIFFUSIVITY OF HYDROGEN IN METHYLAMINE

The diffusion coefficients, as determined on the 3/4 inch sphere, have not been plotted in the above form. The diffusion coefficients for the first set of 3/4 inch sphere determinations (Table A2-1) scatter considerably and tend to be higher than the values measured on the 1 inch sphere. The data presented in Table A2-2, which were taken after the data on the 1 inch sphere under what were thought to be improved operating conditions, also tend to scatter. However, values which were calculated for methylamine saturations of less than 90% are in the range $150 \times 10^{-6} \frac{cm.^2}{sec.}$ (±15%) for a temperature of about -21°C.

5. DISCUSSION OF RESULTS

A. Experimental Measurement of Diffusivity

The data presented in Figures 8 to 12 follow the general form of the absorption model up to liquid flow rates of approximately 0.45 $\frac{c.c.}{sec.}$. The absorption rates, as seen in Figure (9), tend to deviate significantly above this flow rate. The deviations are probably due to convective mixing in the laminar film although visual observations indicated that the surface film was smooth. A Reynold Number criterion, based on the data of previous investigators for water flowing over a sphere, predicts that the laminar film should be stable for methylamine flow rates up to approximately 1.0 $\frac{c.c.}{sec.}$.

Two correlation curves, corresponding to two values of the diffusion coefficient, are presented in Figures (8), (9), (11) and (12). The two curves were included in these figures to indicate the effect of a change in the hydrogen absorption rate on the calculated diffusion coefficient. It is apparent that for the liquid flow rates where the absorption data agree with the theoretical model ($L < 0.45 \frac{c.c.}{sec.}$), a small change in the measured absorption rate will cause a large change in the calculated diffusion coefficient. This is especially true for the determinations obtained on the 1 inch sphere.

The fact that the calculated diffusion coefficients are very sensitive to small changes in model parameters is confirmed by the error analysis presented in Appendix C2. This analysis indicates that as the percent saturation of the outlet liquid approaches

100%, the expected error in the calculated diffusion coefficient approaches infinity.

The initial 3/4 inch sphere determinations of the diffusion coefficient for hydrogen in methylamine are seen from Table A2-1 to be badly scattered. The large degree of uncertainty in the diffusion coefficients reflects the scatter in the measured absorption rates (Figures (8), (9), and (10)). The reproducibility of the data, both within any given run and between different runs, is poor. The low quality of this initial 3/4 inch data is thought to be due, in part, to operating difficulties (absorber temperature control, methylamine flow control, etc.)

The general range of values for the diffusion coefficients presented in Table A2-1 (3/4 inch sphere) appears to be greater than the diffusion coefficients for hydrogen in ammonia (Haul and Puttbach[65]). This is contrary to the relative values predicted by empirical correlations.

The Reynolds number criterion suggests that increased methylamine flow rates can be achieved by increasing the diameter of the sphere. Also, the relative magnitude of the end effects are reduced by increasing the sphere diameter as the fraction of hydrogen absorbed on the sphere is increased. A 1 inch sphere was therefore installed and a number of determinations obtained. The internal consistency and reproducibility of the runs was greatly improved (Table A2-3]. The physical absorption data reported in Figure (12) are consistent with the absorption model and much of the apparent scatter about the theoretical curve is due to temperature differences

for the measured absorption rates. However, the levels of saturation of the methylamine leaving the absorber are high and the reliability of the absorption model under these conditions is questionable.

The natural logarithm of the diffusion coefficients calculated from the 1 inch sphere determinations are plotted versus the reciprocal absolute temperature in Figure (13). The effect of temperature on the diffusion coefficients is consistent with the slope of the methylamine viscosity curve (equation [3.4], Part 1), however the experimental temperature range is so small that this result may only be fortuitous. The value of the diffusion coefficient at -20°C is 122 x 10^{-6} $\frac{cm.^2}{sec.}$ which is lower than the range of diffusivities calculated from the initial 3/4 inch sphere determinations.

A 3/4 inch sphere was again installed in the single sphere absorber to determine if the improved consistency of the 1 inch data was associated with the use of a 1 inch sphere or was due to an improvement in the operating characteristics of the overall absorber. It is seen from Table A2-2 that the reproducibility of the diffusion coefficients is better than that obtained during the initial 3/4 inch determinations. The internal consistency of each run is as good as the 1 inch sphere determinations, and if the runs obtained at high methylamine saturations are discarded the average value of the diffusion coefficient at -21°C is 150 x 10^{-6} $\frac{cm.^2}{sec.}$ (±15%). This value would indicate that the diffusivity of hydrogen in methylamine is very close to the value for the diffusivity of hydrogen in ammonia[65]. No effect of temperature could be observed for these determinations due to the very narrow temp-

erature range of the study.

B. Comparison of the Experimental Diffusion Coefficients with Estimated Values

The empirical correlations for predicting diffusion coefficients for gases dissolved in dilute solutions have been discussed in Chapter 2 of this thesis. It was pointed out that the reliability of the various correlations may be poor considering the temperatures employed in this study and the fact that the solute gas is hydrogen.

In order to ascertain the merit of the various correlations for predicting hydrogen diffusion coefficients in a non-aqueous solvent, the diffusivity of hydrogen in ammonia was estimated for three temperatures. The estimated diffusion coefficients were then compared with the experimental data of Haul and Puttbach[65].

The physical data required by the various empirical correlations are listed in Table 5. These data were extracted from Appendix D1 of Part 1.

TABLE 5

SELECTED PHYSICAL PROPERTIES OF HYDROGEN, AMMONIA AND METHYLAMINE

Component	$V \left[\frac{\text{c.c.}}{\text{gm. mole}}\right]$	$\Delta H \left[\frac{\text{cal.}}{\text{gm. mole}}\right]$	$\Delta H^* \left[\frac{\text{cal.}}{\text{gm.}}\right]$
Hydrogen	14.3	216	108
Ammonia	25.3	5581	327.4
Methylamine	45.4	6200	200.0

The "association parameter" required by the Wilke-Chang correlation[45] was assumed to equal unity for ammonia and methylamine.

The value of the "association parameter" would be expected to fall between 1.0 and 2.6 and should be a function of the molecular dipole moment and dielectric constant. However, there is not enough experimental data to justify choosing a value different from unity.

The diffusion coefficients for hydrogen in liquid ammonia, as predicted by the correlations of Wilke-Chang[45], Scheibel[46], Sitaraman et al[47], King et al[48] and Lusis and Ratcliff[49], are compared with the experimental data of Haul and Puttbach[65] in Table 6.

The percent errors in Table 6 were calculated from the equation

$$\% \text{ error} = \frac{\text{Dest.} - D(65)}{D(65)} \times 100 \qquad [5.1]$$

where Dest = estimated diffusion coefficient

$D(65)$ = measured diffusion coefficient

The predicted diffusion coefficients show poor agreement with the experimental values. The predicted values are low for all correlations except King et al[48]. This correlation may be expected to deviate as the group $\frac{D\mu}{T}$ predicted by the correlation is above the limit specified for application of the equation. The King et al[48] correlation is interesting however, as the predicted diffusion coefficient is very nearly twice the experimental value. The same factor of 2 was noted when this correlation was used to predict the diffusion coefficients for hydrogen dissolved in water.

The Wilke-Chang[45] "association parameter" for ammonia was calculated from the experimental diffusion coefficient and found to

TABLE 6

DIFFUSION COEFFICIENTS FOR HYDROGEN IN AMMONIA

T	μ	D(65)	Wilke-Chang		Scheibel		Sitaraman		King		Lusis-Ratcliff	
°C	c.p.	x 10^6	D x 10^6	% error	D x 10^6	% error	D x 10^6	% error	D x 10^6	% error	D x 10^6	% error
-10.08	0.195	170.0	83.4	-50.9	97.0	-42.9	77.8	-54.2	332	+95.3	135	-20.6
-22.15	0.222	141.4	69.9	-50.6	81.5	-42.4	66.0	-53.3	278	+96.6	113	-20.1
-31.20	0.247	120.0	60.5	-49.6	70.5	-41.2	57.8	-51.8	241	+100.8	97.9	-18.4

be 4.15. This value is above the "association parameter" for water which indicates that the deviation of the predicted diffusion coefficient from the experimental coefficient is due not only to the association of the solvent. The Wilke-Chang[45] correlation is poor when the solute gas is hydrogen.

Judging from the large discrepancy between the predicted and experimental diffusion coefficients in Table 6, the empirical correlations would not be expected to yield good estimates of the diffusion coefficients for hydrogen in methylamine. In order to obtain a realistic estimate of the diffusion coefficients, the values predicted by a particular correlation were corrected by the mean error of that correlation when it was applied to liquid ammonia.

Rearranging equation [5.1] yields:

$$D^{*}_{exp} = \frac{\text{Dest.}}{\left(1 + \frac{\%\ \text{error}}{100}\right)} = \frac{\text{Dest.}}{C} \qquad [5.2]$$

where D^{*}_{exp} is the corrected estimate.

The correction factor for each correlation is listed in Table 7.

TABLE 7

CORRECTION FACTORS FOR DIFFUSION COEFFICIENT CORRELATIONS

Correlation	Mean Error From Table 6	Correction Factor C
Wilke-Chang[45]	-50.6	.494
Scheibel[46]	-42.4	.576
Sitaraman et. al.[47]	-53.3	.467
King et. al[48]	+96.6	1.966
Lusis and Ratcliff[49]	-20.1	.799

The corrected estimates of the diffusivity of hydrogen in methylamine are listed in Table 8.

TABLE 8

ESTIMATED DIFFUSION COEFFICIENT FOR HYDROGEN IN METHYLAMINE

T	μ	Wilke-Chang	Scheibel	Sitaraman	King	Lusis and Ratcliff
C°	c.p.	D^*	D^*	D^*	D^*	D^*
-10	0.291	153	113	131	132	142
-20	0.326	132	97.4	113	113	122
-30	0.367	112	82.6	97.0	96.4	104

The corrected estimates of the diffusion coefficients for hydrogen dissolved in methylamine are very rough but they should indicate the magnitude of the actual diffusion coefficient in the temperature range of this study. The corrected Wilke-Chang[45] estimations of the diffusion coefficients would be expected to be high as the correction implies the same "association parameter" for ammonia and methylamine. The degree of association of the two solvents is not equal according to the solubility studies in Part 1.

The Lusis and Ratcliff[49] correlation should provide the best estimates of the diffusion coefficients for hydrogen in methylamine as this correlation gave the best estimate of the diffusivity of hydrogen in ammonia.

The diffusivity of hydrogen in methylamine at -20°C was determined from the 1 inch sphere studies to be:

$$D = 122 \times 10^{-6} \frac{cm.^2}{sec.} \qquad [4.23]$$

The fact that this value agrees with the diffusion coefficient predicted by the corrected Lusis and Ratcliff[49] correlation is fortuitous, however it does indicate that the measured diffusion coefficient is plausible.

The effect of temperature on the diffusion coefficients, as determined from Figure 13, is expressed by the following equation

$$\frac{D\mu}{T} = 1.570 \times 10^{-7} \qquad [4.22]$$

which relates the diffusion coefficient to the temperature and viscosity of the methylamine.

The absorption data measured by Kalra[87] on the 3/4 inch sphere yielded a value of the diffusion coefficient for hydrogen in methylamine at -21°C to be:

$$D = 150 \times 10^{-6} \frac{cm.^2}{sec.} \qquad [5.3]$$

An equation similar to equation [4.22] can be determined from the diffusion coefficient of Kalra[87]. The revised equation describing the effect of temperature on the diffusivity of hydrogen in methylamine is:

$$\frac{D\mu}{T} = 1.960 \times 10^{-7} \qquad [5.4]$$

Equations [4.22] and [5.4] were utilized for generating two curves describing the effect of temperature on the diffusivity of hydrogen in methylamine. The two curves, along with the dif-

fusivity data of Haul and Puttbach[65] for hydrogen dissolved in ammonia, are presented in Figure 14. Caution must be exercised when Figure 14 is used for obtaining a value of the diffusivity of hydrogen in methylamine.

C. Operating Problems

The accuracy of the measured diffusion coefficients for hydrogen dissolved in methylamine was found to be much less than the ±5% quoted by Davidson and Cullen (9) for their diffusivity studies involving water as the solvent. A number of factors which contribute to the poor quality of the data are outlined in the error analysis of Appendix C2. It should be noted from the error analysis that at the levels of methylamine saturation encountered in this study, the expected errors in the calculated diffusion coefficients are large. This is true even for consistent measurements (±1%) of the total rate of hydrogen entering the absorber (G_H). In addition, there are conditions which are not considered in the error analysis which can cause large errors in the measured data (convective mixing on the laminar film, hydrogen absorption on the support rod and equipment leaks). The purpose of this section is to discuss the most probable sources of errors in the experimental measurements.

1. Temperature Control

Slight changes in the absorber temperature appear to cause large variations in the measured absorption rate. It has been shown in the error analysis of Appendix C2 that a temperature variation of ±0.01°C over a 10 minute reading can cause a 3 percent change in the measured hydrogen absorption rate to the absorber.

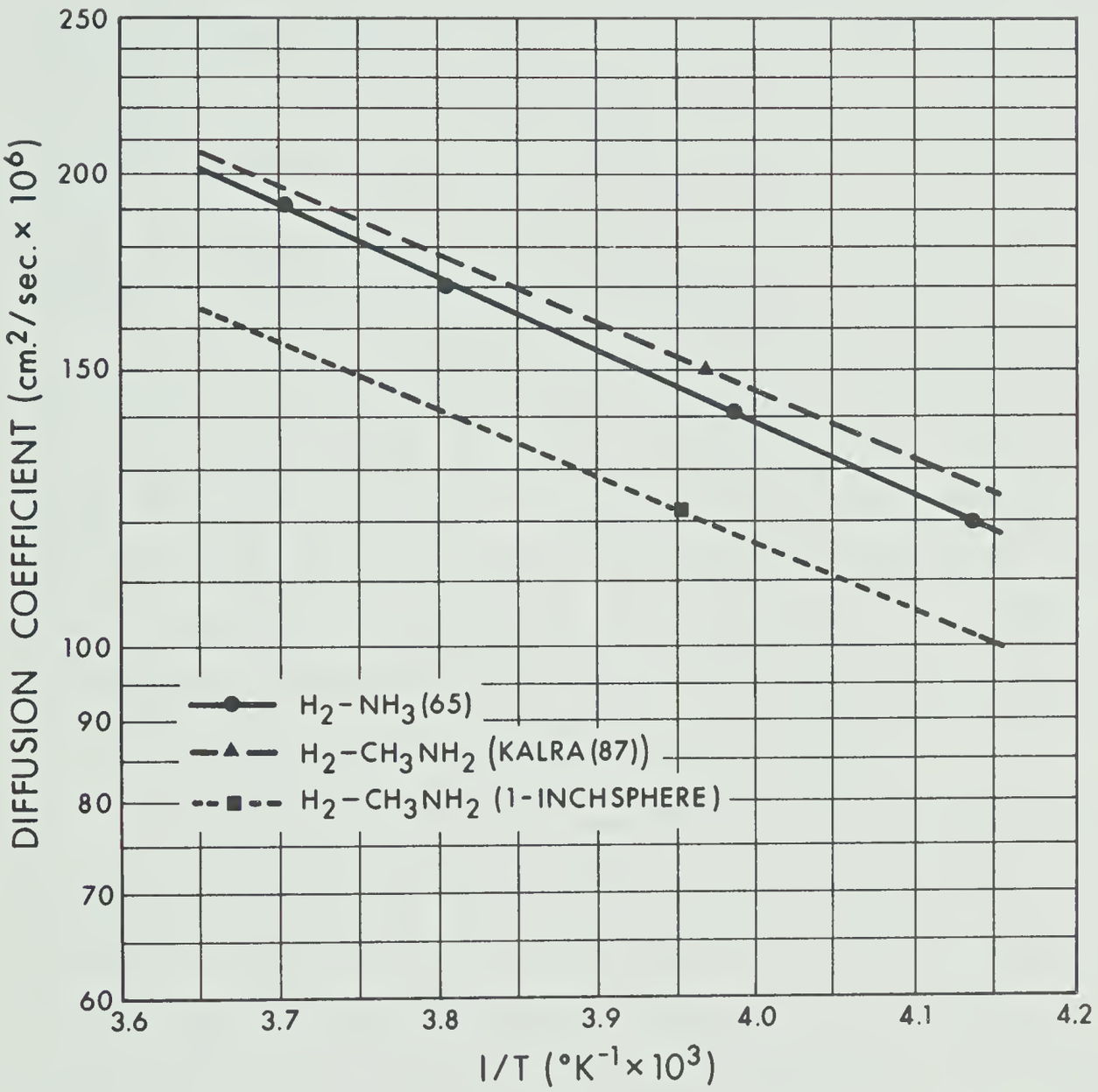


FIG. 14. EFFECT OF TEMPERATURE ON THE DIFFUSIVITY OF HYDROGEN IN AMMONIA AND METHYLAMINE

Unfortunately, ±0.01°C is the limit of the readability of the potentiometer used for the temperature measurements.

Considerable difficulties were encountered in attempting to control the box temperature within ±0.25°C over the complete run. The temperature would change when methylamine was introduced to the absorber at the start of a run, when the hydrogen circulator was used to pre-saturate the vapor phase and when the room temperature changed. The first two temperature changes were smoothed out by allowing the system to operate for approximately 45 minutes prior to recording the absorption rates. Variations in the room temperature were more difficult to handle as the chiller temperature on the refrigeration unit would follow the room temperature change. The maximum variation of temperature for the data of Kalra[87], as presented in Table A2-2, was 0.36°C in a total time of 60 minutes.

2. Measurement of the Methylamine Flow Rate

The liquid flow rate measurement was not entirely satisfactory. The fact that the rotameter was influenced by the viscosity of the fluid may have caused an error in the flow measurement, even though a viscosity correction was applied. A system which would enable flow calibration during a run would be a worthwhile addition.

3. Convective Mixing in the Spherical Film

The liquid film on the sphere appeared to have a glassy, smooth appearance at flow rates up to approximately 0.7 $\frac{c.c.}{sec.}$. Initial tests with acetone indicated that ripple free flow was possible at flow rates of approximately 1.10 $\frac{c.c.}{sec.}$, however, ripples

were present on the methylamine film at these flow rates.

Initial tests with acetone suggested that the laminar film was stable at higher volumetric flow rates on the 3/4 inch diameter sphere than on the 1 inch sphere. A Reynolds Number criterion would predict the opposite effect of sphere size on the flow rate for inception of surface ripples. Subsequent tests with methylamine did not confirm or disprove this observation as the upper limit for stable flow was very similar for both spheres.

The liquid film on the take-off rod was thought to be a good indicator of the presence of ripples on the sphere. Surface activity was much more apparent here than on the sphere and it was generally observed that when ripples were present on the take-off rod, they were also present on the sphere.

Ryan[88] undertook a study of the stability of a water film on a single sphere. This study suggested that visual observations are very insensitive as a means of observing ripples. A liquid film which appeared smooth to the observer was found to have surface ripples when photographed with a laser beam light source.

The dimensionless flow parameters for a number of runs are presented in Table 9. The parameters are based on the liquid flow conditions at the equator of the sphere.

The Reynolds Numbers for the flow of methylamine over the sphere, as presented in Table 9, are well below the values stated by previous investigators[4,9,10] for the inception of surface ripples (Table 3). The Reynolds Numbers are however, greater than the Reynolds number for the onset of wavy flow on a vertical plate or

TABLE 9

TYPICAL VALUES OF THE DIMENSIONLESS FLOW PARAMETERS

Date	Temperature °C	Sphere Radius (inches)	Liquid Flow Rate $\frac{c.c.}{sec.}$	Re	Fr	We	Bo
3/31/70	-18.9	3/4	0.703	112	2.33	0.149	0.064
4/17/70	-15.3	3/4	0.585	97	2.02	0.113	0.056
5/14/70	-12.7	3/4	0.456	78	1.62	0.076	0.047
5/7/70	-15.1	3/4	0.263	44	0.91	0.030	0.033
5/29/70	-19.1	1	0.468	56	1.16	0.047	0.040
7/16/70	-20.9	1	0.281	33	0.69	0.020	0.029

wetted wall column (references (69) through (76)). Therefore, the possibility of surface ripples cannot be precluded.

The Froude Number, Weber Number and Bond Number have been included in Table 9 for the purpose of comparison with other studies.

The reason that the total rate of hydrogen absorption (G_H) deviated from the theoretical model at flow rates above 0.45 $\frac{c.c.}{sec.}$ could be due to convective mixing in the spherical film.

Also, the fact that the reproducibility of the 3/4 inch sphere determinations, especially the data tabulated in Table A2-1, were poor could be attributed to different degrees of surface activity being present on the spherical liquid film. If the surface film was not stable for each run, there is no insurance that the degree of instability should be the same. The presence of convective mixing in the spherical liquid film could account for the difference in the magnitude of the diffusion coefficients calculated from the 1 inch sphere determinations compared to those calculated from the 3/4 inch sphere determinations of Kalra[87].

The agreement between the physical absorption data and the theoretical absorption curve, as presented in Figure (12) for the 1 inch sphere determinations, would suggest that the laminar film was stable during these runs.

It is of interest to note that the majority of the data in Figure (9) lie on two distinct correlation curves. The lower curve, which corresponds to a diffusion coefficient of 150×10^{-6} $\frac{cm.^2}{sec.}$ and a temperature of -15°C appears to agree with the 5/7/70 run

and one half of the 5/13/70 run. These runs were made with a laminar jet nozzle diameter of 0.040 cm. and 0.046 cm. respectively. The points which coincide with a value of D equal to $190 \times 10^{-6} \frac{cm.^2}{sec.}$ were obtained with laminar jet nozzle diameters of 0.050 cm. and 0.060 cm. It would appear that the liquid jet from the two largest nozzles may have been unstable and induced convective mixing in the laminar film on the sphere. Again, no surface waves were visible but this does not rule out their existence.

4. End Effects

The relative magnitude of the end effects are greater for the 3/4 inch sphere determinations than for the 1 inch sphere determinations. This is due to the larger surface area available for absorption on the 1 inch sphere which results in a greater fraction of the total hydrogen entering the absorber being absorbed on the spherical liquid film. Also, the percent saturation of the liquid at the base of the 1 inch sphere is greater than the saturation at the base of the 3/4 inch sphere, hence the driving force for absorption on the support rod for the 1 inch sphere is reduced.

End effects could be dominant factors if the amount of hydrogen absorbed on the laminar jet is different from the amount predicted by the ideal jet theory (equation [3.7]) or if a significant amount of hydrogen is absorbed on the support rod.

5. System Leaks

System leaks are a constant problem with equipment which is continually being cooled and heated, hence it is possible that

small leaks may have caused errors in the data. However a number of spot leak checks were performed on the equipment and the system was found to be gas tight.

6. Saturation of the Hydrogen Phase

The hydrogen phase was saturated with methylamine prior to a run and was assumed to remain saturated during the duration of the run. This assumption was checked by operating the hydrogen circulator during a run. The absorption rates which were measured before and after the operation of the circulator were compared and no observable change was noted. The hydrogen saturator was removed for several runs and the resulting absorption rates indicated that the vapor phase did not become saturated within the time required for the run. Consequently, percent saturations based on the measured hydrogen absorption rate, liquid flow rate and calculated interfacial concentration were observed to be in excess of 100%.

D. Operating Characteristics of the Absorber

1. Laminar Jet Stability

The laminar jet had an upper and lower limit of stability. The transition of the jet from smooth laminar flow to unstable flow conditions could be seen with the aid of a cathetometer. The upper limit of stability, which corresponded to a nozzle Reynolds Number (equation [3.1]) of approximately 3500, was observed by the change in the jet from a glass like rod appearance to an oscillating string appearance. The lower limit of stability was identified by the onset of unsteady or pulsing flow from the nozzle. The above observations are consistent with those of Goettler[4].

The jet length was varied from 1.35 m.m. to 3.50 m.m. with no apparent change in the operating characteristics of the nozzle. When the jet length was reduced below 1 m.m., a liquid film would form between the nozzle holder and sphere. The jet lengths utilized for the various runs are summarized in Tables A2-1 to A2-3, Appendix A2.

2. Liquid Take-Off Length

Several runs were conducted in an effort to determine the extent of the stagnant layer on the exposed support rod between the base of the sphere and the liquid level in the take-off tube. The data presented in Figure 15 suggests that the height of the stagnant layer is approximately 2.0 cm.. This height agrees with the value determined by Goettler[4], Lynn et al[8], Davidson and Cullen[9] and Ratcliff and Reid[10].

The stagnant layer could be observed for acetone by the slow circulation of small particles on the liquid film covering the support rod. These particles could be raised onto the sphere by raising the liquid level in the take-off tube. This observation is consistent with those of Goettler[4] and Ratcliff and Reid[10].

The liquid interface in the take-off tube was unstable at the start of a run but would settle out as the run progressed. The degree of surface activity was dependent on the internal diameter of the glass collector cap which was mounted on the take-off tube. A 1/4 inch internal diameter cap was used for several runs but it was impossible to obtain a non-active liquid interface with this cap.

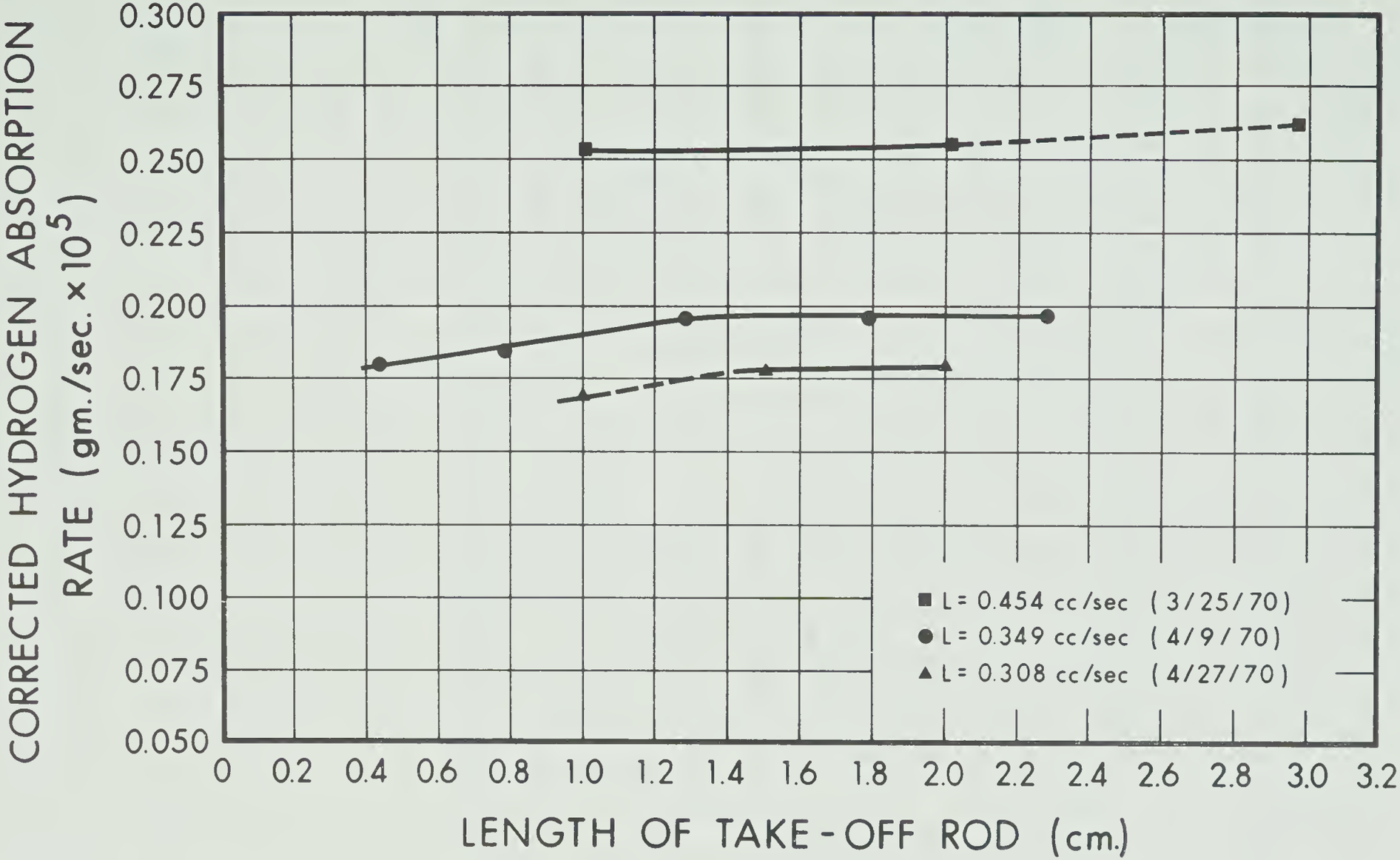


FIG. 15. EFFECT OF TAKE-OFF LENGTH ON HYDROGEN ABSORPTION RATE

Adequate control of the liquid level in the take-off tube could be maintained by using the "Whitey" needle valve. The control would become erratic however, if the liquid film on the sphere was not stable.

E. Materials of Construction for Handling Methylamine

The materials of construction which are capable of handling methylamine are somewhat limited. Lucite and Viton A are rapidly attacked and must be avoided. Kel-F slowly deteriorates on contact with methylamine, hence periodic replacement is necessary. Neoprene o-rings were observed to stretch after prolonged periods of contact, but they are suitable for short term usage. Gum rubber or latex tubing was suitable for use in the peristaltic pump which was used for circulating the hydrogen phase. However methylamine slowly diffused through the tubing so that a steel pump head was required. Teflon is not deteriorated by pure methylamine but sealing problems can occur at low temperatures due to hardening. Mild steel and stainless steel (type 304 or 316) are not affected by pure methylamine.

6. CONCLUSIONS AND RECOMMENDATIONS

A single sphere absorber was constructed for low temperature mass transfer studies involving gaseous hydrogen and liquid methylamine. The absorber was used for measuring the rate of physical absorption of hydrogen in pure methylamine. Diffusion coefficients were evaluated from the absorption data, however the reliability of the coefficients is somewhat questionable. The poor performance of the single sphere absorber, when utilized for hydrogen-methylamine studies can be attributed to two main factors.

(a) The hydrodynamic consideration of ripple free flow limits the liquid flow rate to a range where the analytical model describing the absorption process is approaching its useful limit of applicability.

(b) Due to the volatile nature of methylamine and the fact that hydrogen is only slightly soluble in methylamine, small variations in temperature have been shown to have a significant effect on the measured hydrogen absorption rate to the absorber (G_H). The error in the absorption rate is greatly propagated when the diffusion coefficient is calculated.

The initial absorption measurements on the 3/4 inch sphere are badly scattered, hence the diffusion coefficients calculated from the data are very inconsistent. The magnitude of the diffusion coefficients calculated from this data is greater than the diffusion coefficients for hydrogen in methylamine.

The absorption measurements on the 1 inch sphere are fairly consistent, however the levels of saturation of the methylamine leaving the absorber are above 90%. At these levels of saturation,

the absorption model has poor resolution characteristics in so far as calculation of the diffusion coefficients is concerned. The calculated diffusion coefficients agree well with the values predicted by the modified diffusivity estimation techniques. These data suggest that at a given temperature in the range of this study, the diffusivity of hydrogen in methylamine is less than the diffusivity of hydrogen in ammonia.

The diffusion coefficients calculated from the physical absorption measurements of Kalra[87] on the 3/4 inch sphere are somewhat scattered but are much more consistent than the diffusion coefficients calculated from the initial 3/4 inch sphere data. These data suggest that the diffusivity of hydrogen in methylamine is slightly greater than the diffusivity of hydrogen in ammonia.

At -20°C, the diffusion coefficient for hydrogen in methylamine is $122 \times 10^{-6} \frac{cm.^2}{sec.}$ from the 1 inch sphere measurements and $152 \times 10^{-6} \frac{cm.^2}{sec.}$ from the 3/4 inch sphere measurements. The corresponding value for hydrogen in ammonia at -20°C is $146 \times 10^{-6} \frac{cm.^2}{sec.}$. The above results indicate that the diffusivity data for hydrogen in ammonia are reasonable estimates of the diffusivity of hydrogen in methylamine.

A number of changes should be incorporated in the single sphere absorber design if further methylamine diffusivity studies are to be conducted. The reasons behind the majority of these changes are apparent from the error analysis of Appendix C2. Many of the modifications are desirable for the kinetic studies.

(a) Install a soap film meter with finer graduations. The volume measurement on the soap film meter contributes a substantial error (±1%) to the measurement of the total hydrogen absorption rate to the absorber (G_H).

(b) A more sensitive potentiometer should be used for measuring the thermocouple outputs. Small variations in temperature could be detected and suitable corrections applied.

(c) The calibration on the thermocouples should be refined to error limits of ±0.05°C.

(d) Solenoid valves should be installed between the absorber chamber and hydrogen saturator. The subsequent reduction in volume of the absorption system would almost halve the effect of temperature fluctuations on the hydrogen absorption rate.

(e) The laminar jet length should be minimized to reduce the absorption of hydrogen on the jet.

(f) A system should be installed for direct measurement of the liquid flow rate.

(g) The methylamine feed tanks could be replaced by a controlled volume feed pump based on the design of a motorized "Ruska" pump. This system would ensure a constant liquid feed rate and is suitable for feeding less volatile amines such as ethylamine or n-propylamine.

(h) A better system for alignment of the laminar jet should be incorporated The eccentric mechanism is satisfactory, however it is very difficult to see the alignment marker on the top of the sphere. The incorporation of flat absorber

walls, with one or more removable faces would allow direct access to the sphere and laminar jet. A mechanical measuring instrument could then be used to center the jet on the pole of the sphere.

(i) All of the system valving could be installed in the front panel of the cold box. This would prevent methylamine from vaporizing in any of the flow lines.

It should be noted that even with the above modifications, the accuracy of the measured diffusion coefficients on a 3/4 inch sphere would not be better than ±10% and the accuracy on the 1 inch sphere would be even less. This is true so long as the levels of methylamine saturation remain above approximately 80%.

The single sphere absorber design which was developed during this work is suitable for hydrogen deuteride exchange studies as the limitations of the apparatus for physical absorption studies would not adversely affect kinetic exchange studies.

(a) For chemical absorption occuring in the fast reaction regime, the rate of absorption is independent of the hydrodynamics of the system. This is true providing the surface area for absorption is not altered by surface ripples. Also, absorption can occur at very low flow rates as methylamine readily wets the sphere surface.

(b) As the hydrogen phase will be continually recirculated, small pressure fluctuations caused by temperature variations will affect only the hydrogen deuteride driving force. The

small changes in the driving force will cause negligible error in the measured exchange rate when they are averaged over the total time required for a run.

NOMENCLATURE

The nomenclature in use throughout this text is given in the following list. Special symbols are defined where they occur.

English Letter Symbols

a	Association parameter in Wilke-Chang correlation
A_1	Constant in equation [2.73]
A_2	Constant in equation [2.75]
Bo	Bond Number as defined by equation [2.37).
C	Concentration of the solute in the liquid phase $\left(\frac{\text{gm.}}{\text{c.c.}}\right)$
C_i	Concentration of solute at the interface $\left(\frac{\text{gm.}}{\text{c.c.}}\right)$
C_o	Concentration of solute in the bulk liquid phase $\left(\frac{\text{gm.}}{\text{c.c.}}\right)$
C_o'	Concentration of hydrogen in the bulk liquid phase leaving the nozzle $\left(\frac{\text{gm.}}{\text{c.c.}}\right)$
C_1	Constant in equation [2.76]
D	Diffusion coefficient of the dissolved solute $\left(\frac{\text{cm.}^2}{\text{sec.}}\right)$
D_J	Internal diameter of laminar jet throat (cm.)
E_d	Energy of activation for diffusion $\left(\frac{\text{cal.}}{\text{gm. mole}}\right)$
E_v	Energy of activation for viscosity $\left(\frac{\text{cal.}}{\text{gm. mole}}\right)$
F_J	Fraction of hydrogen absorbed on the jet.
F_s	Fraction of hydrogen absorbed on the sphere.
F_r	Froude Number as defined in equation [2.34]
g	Acceleration due to gravity $\left(\frac{\text{cm.}}{\text{sec.}^2}\right)$
G	Rate of absorption of the solute gas $\left(\frac{\text{gm.}}{\text{sec.}}\right)$
G_A	Actual rate of absorption of hydrogen in the spherical film $\left(\frac{\text{gm.}}{\text{sec.}}\right)$

G_H Total rate of absorption of hydrogen to the absorber $\left(\frac{gm.}{sec.}\right)$

G_J Rate of absorption of hydrogen on the surface of the jet $\left(\frac{gm.}{sec.}\right)$

G_s Corrected rate of absorption of hydrogen in the spherical film. $\left(\frac{gm.}{sec.}\right)$

G_s' Absorption rate of hydrogen on the sphere assuming low depth of penetration $\left(\frac{gm.}{sec.}\right)$

G° Instantaneous rate of physical absorption $\left(\frac{gm.}{sec.}\right)$

$\bar{G}^\circ$ Average rate of physical absorption $\left(\frac{gm.}{cm.^2\ sec.}\right)$

h_J Jet length (cm.)

h_T Take-off tube length (cm.)

H_2 Henry's Law Coefficient $\left(\frac{atm.}{mole\ frac.}\right)$

ΔH_1 Solvent latent heat of vaporization at N.B.P. $\left(\frac{cal.}{gm.\ mole}\right)$

ΔH_2 Solute latent heat of vaporization at N.B.P. $\left(\frac{cal.}{gm.\ mole}\right)$

ΔH_1^* Solvent latent heat of vaporization at N.B.P. $\left(\frac{cal.}{gm.}\right)$

ΔH_2^* Solute latent heat of vaporization at N.B.P. $\left(\frac{cal.}{gm.}\right)$

k_1 Kinetic velocity constant $(sec.^{-1})$

k_L Overall mass transfer coefficient $\left(\frac{cm.}{sec.}\right)$

k_L° Physical mass transfer coefficient $\left(\frac{cm.}{sec.}\right)$

K Modified kinetic equilibrium constant

K' Kinetic equilibrium constant

L Liquid volumetric flow rate $\left(\frac{cm.^3}{sec.}\right)$

M_1 Molecular weight of the solvent $\left(\frac{gm.}{gm.\ mole}\right)$

N Viscous influence number as defined in equation [4.2]

P_1 Vapor pressure of methylamine (atm.)

P_2 Hydrogen partial pressure (atm.)

P_{bar} Barometric pressure (atm.)

Q_1 Volumetric flow rate of acetone $\left(\frac{\text{c.c.}}{\text{sec.}} \text{ @ } 20°\text{C}\right)$

Q_2 Volumetric flow rate of methylamine as calculated in equation [4.1] $\left(\frac{\text{c.c.}}{\text{sec.}}\right)$

Q_H Volumetric flow rate of hydrogen entering the absorber $\left(\frac{\text{c.c.}}{\text{sec.}}\right)$

R Radius of the sphere (cm.)

Re Reynolds Number as defined by equation [2.33]

Re_J Jet Reynolds Number as defined in equation [3.1]

S Rate of surface renewal (sec.^{-1})

t Contact time (sec.)

t^* Total life of an element (diffusion time (sec.)

T Temperature (°K)

T_A Temperature of methylamine leaving the absorber (°C)

T_H Temperature of hydrogen entering the soap film meter (°C)

T_L Temperature of methylamine entering the rotameter (°C)

V_1 Solvent molar volume $\left(\frac{\text{c.c.}}{\text{gm. mole}}\right)$

V_2 Solute molar volume $\left(\frac{\text{c.c.}}{\text{gm. mole}}\right)$

V_o Liquid velocity at the interface $\left(\frac{\text{cm.}}{\text{sec.}}\right)$

V_o^+ Liquid velocity at the interface as determined at the sphere equator $\left(\frac{\text{cm.}}{\text{sec.}}\right)$

V_ψ Liquid velocity along a streamline $\left(\frac{\text{cm.}}{\text{sec.}}\right)$

$\bar{V}_\psi$ Average velocity of the liquid film $\left(\frac{\text{cm.}}{\text{sec.}}\right)$

We Weber Number as defined in equation [2.36]

x Distance from the liquid surface to a streamline (cm.)

x_2 Mole fraction dissolved hydrogen

y Dimensionless liquid depth $\left(\frac{x}{\Delta}\right)$

Z_s Reduced rate of absorption of hydrogen on the sphere

Z_J Reduced rate of absorption of hydrogen on the jet.

Greek Letter Symbols

α Angle of inclination of the radial line from the vertical plane

α Coefficient in the absorption model (equation [2.71])

Γ_v Liquid volumetric flow rate per unit length of wetted perimeter $\left(\frac{\text{c.c.}}{\text{cm. sec.}}\right)$

Δ Film thickness (cm.)

Δ^+ Film thickness at the equator (cm.)

μ_l Viscosity of methylamine (c.p.)

ν_l Kinematic viscosity of the liquid $\left(\frac{\text{cm.}^2}{\text{sec.}}\right)$

π Total absorber pressure (atm.)

ρ_l Density of methylamine $\left(\frac{\text{gm.}}{\text{c.c.}}\right)$

ρ_f Density of the float $\left(\frac{\text{gm.}}{\text{c.c.}}\right)$

σ Surface tension of methylamine $\left(\frac{\text{dyne}}{\text{cm.}^2}\right)$

ϕ Defined by equation [2.62] $\left(\frac{\text{sec.}}{\text{cm.}^2}\right)$

ψ Stream function

$\psi(t)$ Distribution function of surface ages

BIBLIOGRAPHY

(1) Bar-Eli, K., and Klein, F.S., J. Chem. Soc. (London), 36, 3083, (1962).

(2) Bourke, P.J., and Lee, J.C., Trans. Instn. Chem. Engrs., 39, 280, (1961).

(3) Ratcliff, M.A., and Holdcroft, J.G., Chem. Eng. Sci., 15, 100, (1961).

(4) Goettler, L.A., Ph. D. Dissertation, University of Delaware, 1967.

(5) Goettler, L.A., and Pigford, R.L., Tripartite Chemical Engineering Conference, Symposium on Mass Transfer with Chemical Reaction, September 23, 5, (1968).

(6) Wild, J.D., and Potter, O.E., Ibid, 34, (1968).

(7) Astarita, G., "Mass Transfer with Chemical Reaction", Elsevier Publishing Company, Amsterdam, 1967.

(8) Lynn, S., Straatemeier, J.R., and Kramers, H., Chem. Eng. Sci., 4, 63, (1955).

(9) Davidson, J.F., and Cullen, E.J., Trans. Instn. Chem. Engrs., 35, 51, (1957).

(10) Ratcliff, M.A., and Reid, K.J., Ibid, 39, 424, (1961).

(11) Baird, M.H.I., and Davidson, J.F., Chem. Eng. Sci., 17, 473, (1962).

(12) Stewart, G., Ph.D. Dissertation, University of Edinburgh, 1962.

(13) Astarita, G., Chem. Eng. Sci., 17, 708, (1962).

(14) Whitman, W.G., Chem. and Met. Eng., 29, No. 4, 146, (1923).

(15) Higbie, R.W., Trans. Am. Instn. Chem. Engrs., 31, 365, (1935).

(16) Emmert, R.E., and Pigford, R.L., Chem. Eng. Prog., 50, 87, (1954).

(17) Lynn, S., Straatemeier, J.R., and Kramers, H., Chem. Eng. Sci., 4, 49, (1955).

(18) Ibid, 4, 58, (1955).

(19) Scriven, L.E., and Pigford, R.L., A.I.Ch.E.J., 4, 382, (1958).

(20) Ibid, 5, 397, (1959).

(21) Himmelblau, D.M., Chem. Rev., 64, 527, (1964).

(22) Danckwerts,P.V., Ind. Eng. Chem., 43, 1460, (1951).

(23) Danckwerts, P.V., and Kennedy, A.M., Trans. Instn. Chem. Engrs. Supp., 32, S49, (1954).

(24) Toor, H.L., and Marchello, J.M., A.I.Ch.E.J., 4, 97, (1958).

(25) Perlmutter, D.D., Chem. Eng. Sci., 16, 287, (1961).

(26) Davies, J.T., "Mass Transfer and Interfacial Phenomena", Adv. in Chem. Eng., 4, 1, 1963.

(27) Nusselt, W., Ver. Deut. Ingr. Z., 60, 549, (1916).

(28) Olbrich, W.E., and Wild, J.D., Chem. Eng. Sci., 24, 25, (1969).

(29) Pigford, R.L., Ph.D. Dissertation, University of Illinois, 1941.

(30) Vyazovov, V.V., J. Tech. Phys. (U.S.S.R.), 10, 1519, (1940).

(31) Tyrell, H.J.V., "Diffusion and Heat Flow in Liquids", Butterworth & Co. (Publishers), Ltd., London, 1961.

(32) Crank, J., "The Mathematics of Diffusion", Claredon Press, Oxford, 1956.

(33) Glasstone, S., Laidler, K., and Eyring, H., "Theory of Rate Processes", McGraw-Hill Book Co., New York, 1941.

(34) Othmer, D.F., and Thakar, M.S., Ind. Eng. Chem., 45, 589, (1953).

(35) Othmer, D.F., Ind. Eng. Chem., 32, 841, (1940).

(36) Einstein, A., Ann. Phys., 17, 549, (1905).

(37) Einstein, A., "Investigations on the Theory of Brownian Movement", Dover Publications, New York, N.Y., 1956.

(38) Sutherland, G.B.B.M., Phil. Mag., 9, 781, (1905).

(39) Ree, R.H., Ree, T., and Eyring, H., Ind. Eng. Chem., 50, 1036, (1958).

(40) Ferrell, R.T., and Himmelblau, D.M., A.I.Ch.E.J., 13, 702, (1967).

(41) Bolles, W.L., and Fair, J.R., Ind. Eng. Chem., 61, 112, (1969).

(42) Reid, R.C.,and Sherwood, T.K., "The Properties of Gases and Liquids", McGraw-Hill Book Co., New York, 1966.

(43) Huq, A., and Wood, T., J. Chem. Eng. Data, 13, 256, (1968).

(44) Wilke, C.R., Prausnitz, J.M., Acrivos, A., Petersen, E.E., and Olander, D.R., Ind. Eng. Chem., 53, 925, (1961).

(45) Wilke, C.R., and Chang, Pin, A.I.Ch.E.J., 1, 264, (1955).

(46) Scheibel, E.G., Ind. Eng. Chem., 46, 2007, (1954).

(47) Sitaraman, R., Ibrahim, S.H., and Kuloor, N.R., J. Chem. Eng. Data, 8, 198, (1963).

(48) King, C.J., Hsueh, L., and Mao, Kao-Wen, J. Chem Eng. Data, 10, 348, (1965).

(49) Lusis, M.A., and Ratcliff, G.A., Can. J. Chem. Eng., 46, 385, (1968).

(50) Nakanishi, K., Voigt, E.M., and Hildebrand, J.H., J. Chem. Phys., 42, 1860, (1965).

(51) Geddes, A.L., in A. Weissberger (Ed.), "Techniques of Organic Chemistry", 2nd Ed., Vol. 1, pt. 1, p.p. 551, Interscience

Publishers, Inc., New York, 1949.

(52) Carlson, T., J. Am. Chem. Soc., 33, 1027, (1911).

(53) Tamman, G., and Jessen, V., Z. Anorg. Allgem. Chem., 179, 125, (1929).

(54) Hagenbach, A., Wied. Ann., 65, 673, (1898).

(55) Ringbom, A., Z. Anorg. Allgem. Chem., 238, 94, (1938).

(56) Smith, R.E., Friess, E.T., and Morales, M.F., J. Phys. Chem., 59, 382, (1955).

(57) Stefan, I., Sitzber. AKad. Wiss. Wien, Math.-naturw. Kl., Abt. II, 37, (1878).

(58) Wang, J.H., J. Am. Chem. Soc., 75, 2777, (1953).

(59) Witherspoon, P.A., and Saraf, D.N., J. Phys. Chem., 69, 3752, (1965).

(60) Taylor, G.I., Proc. Royal Soc. (London), A219, 186, (1953).

(61) Ibid, A225, 473, (1954).

(62) Northrop, J.H., and Anson, M.L., J. Gen. Physiol., 12, 543, (1928).

(63) Gordon, A.R., Ann. N.Y. Acad. Sci., 46, 285, (1945).

(64) Ross, M., and Hildebrand, J.H., J. Chem. Phys., 40, 2397, (1964).

(65) Haul, R., and Puttbach, E., Z. Naturforsch., 21a, 1914, (1969).

(66) Malik, V.K., and Hayduk, W., Can. J. Chem. Eng., 46, 462, (1969).

(67) Baird, M.H.I., and Davidson, J.F., Chem. Eng. Sci., 17, 467, (1962).

(68) Howkins, J.E., and Davidson, J.F., Chem. Eng. Sci., 7, 235, (1958).

(69) Sherwood, T.K., and Pigford, R.L., "Absorption and Extraction", McGraw-Hill Book Co., New York, 1952.

(70) Bird, R.B., Stewart, W.E., and Lightfoot, E.N., "Transport Phenomena", John Wiley & Sons, Inc., New York, 1963.

(71) Kapitza, P.L., "Collected Papers of Kapitza", Edited by Ter Haar, D., Vol. II, Pergamon Press, New York, 1965.

(72) Mossot, C., Irani, F., and Lightfoot, E.N., A.I.Ch.E.J., 12 445, (1966).

(73) Benjamin, T.B., J. Fluid Mech., 2, 554, (1957).

(74) Binnie, A.M., Ibid, 5, 561, (1959).

(75) Fulford, G.D., "Advances in Chemical Engineering", Edited by Drew, T.B., Hoopes, J.W., and Vermeulen, T., Vol. 5, p.p. 151-236, Academic Press, New York, 1964.

(76) Levich, V.G., "Physicochemical Hydrodynamics", Prentice-Hall, Englewood Cliffs, N.J., 1962.

(77) Roberts, D., and Danckwerts, P.V., Chem. Eng. Sci., 17, 961, (1962).

(78) Nijsing, R.A.T.O., and Kramers, H., Ibid, 8, 81, (1958).

(79) Wilkes, J.O., and Nedderman, R.M., Ibid, 17, 177, (1962).

(80) Brooks Technical Bulletin T-022, Brooks Instrument Division, Emerson Electric Co., Hatfield, Pennsylvania.

(81) Fischer & Porter Co., "Tri-Flat Variable-Area Flowmeters", Handbook 10A9010, Fischer & Porter Co., Warminster, Pennsylvania, 1962.

(82) Hatch Jr., T.F., and Pigford, R.L., Ind. Eng. Chem. Fund., 1, 209, (1962).

(83) Matheson Gas Data Book, 4th. Ed., The Matheson Company, Inc., Herst Litho Inc., New York, N.Y., (1966).

(84) "Methylamines, Storage and Handling", p.p. 10, Rohm and Haas Company, Independence Mall West, Philadelphia, Pa., 1965.

(85) Thodos, G., A.I.Ch.E.J., 10, 274, (1964).

(86) Moore, R.G., Lab Book, University of Alberta, 1970.

(87) Kalra, H., Private Communication, University of Alberta, Edmonton, Alberta

(88) Ryan, J.T., Private Communication, University of Alberta, Edmonton, Alberta.

APPENDIX A2

PHYSICAL ABSORPTION RESULTS

The experimental data on the physical rate of absorption of hydrogen in methylamine are summarized in Tables A2-1 to A2-3.

The data in Tables A2-1 and A2-2 were determined on the 3/4 inch sphere, and are included in separate tables as the data presented in Table A2-2 were determined by Kalra[87]. The data reported in Table A2-3 were measured on the 1 inch sphere.

All of the experimental parameters affecting the rate of absorption have been listed in each Table. The majority of symbols used in the column headings correspond to those used in the main text. The symbols which are not listed in the main text are:

G(atm) = Absorption rate of hydrogen corrected to one atmosphere hydrogen partial pressure

PS = Percent saturation of the methylamine leaving the absorber

standard error = standard error of the calculated outlet methylamine saturation

The standard error for all the determinations obtained under one set of absorption conditions was calculated from the following equations.

$$\text{standard error} = \left\{ \frac{\sum_{1}^{N} \{(PS)_K - (PS)_{avg}\}^2}{N - 1} \right\}^{\frac{1}{2}} \qquad [A2\text{-}1]$$

$$PS_{avg} = \frac{\sum_{1}^{N} (PS)_K}{N} \qquad [A2\text{-}2]$$

$$(PS)_K = \left(\frac{G_H}{L\ C_i} \right)_K \qquad [A2\text{-}3]$$

The figure number on which each determination appears in the main text has been noted in the last column of each table.

TABLE A2-1

PHYSICAL ABSORPTION RESULTS (3/4-inch SPHERE)

DATE	T_A °C	π atm.	L cc./sec.	h_T cm.	h_J cm.	D_J cm.	$G_H \times 10^5$ gm./sec.	$G(1\ atm.) \times 10^5$ gm./sec.	%	$D \times 10^6$ $cm.^2/sec.$	$D_{AVG.} \times 10^6$ $cm.^2/sec.$	Standard Error	Fig. No.
3/31/70	-18.9	1.351	.703	0.600	0.135	0.060	.2517	.3137	69.7	212		.70	
3/31/70	-19.2	1.351	.702	1.200	0.135	0.060	.2568	.3176	70.8	220		.44	
3/19/70	-18.7	1.355	.451	0.575	0.180	0.050	.1900	.2378	82.2	182		1.75	
4/9/70	-18.0	1.342	.349	0.435	0.135	0.060	.1373	.1797	79.5	118		.96	
4/9/70	-18.0	1.342	.349	0.785	0.135	0.060	.1408	.1839	81.4	127		1.98	
4/9/70	-18.0	1.342	.349	1.285	0.135	0.060	.1462	.1960	86.8	156		.29	
4/9/70	-18.0	1.342	.349	1.785	0.135	0.060	.1498	.1964	86.9	157		1.00	
4/9/70	-18.0	1.342	.349	2.285	0.135	0.060	.1507	.1969	87.2	158		.80	8
4/23/70	-17.8	1.340	.308	2.000	0.135	0.040	.1262	.1661	83.1	115		1.05	8
4/23/70	-17.7	1.340	.261	2.000	0.135	0.040	.1155	.1528	90.2	123	124	.82	8
4/23/70	-17.5	1.218	.337	2.000	0.135	0.040	.1362	.1810	82.8	127		3.99	8
3/23/70	-16.8	1.341	.480	0.570	0.180	0.050	.1863	.2556	81.4	191		1.60	
3/23/70	-16.8	1.341	.479	1.070	0.180	0.050	.1914	.2619	83.5	206		6.00	
3/25/70	-16.7	1.360	.454	1.070	0.180	0.050	.1887	.2528	85.1	203		.57	
3/25/70	-16.7	1.360	.454	2.070	0.180	0.050	.1902	.2555	85.9	210		.80	8
3/25/70	-16.7	1.358	.454	2.970	0.180	0.050	.1944	.2620	88.1	229		2.10	
4/21/70	-16.7	1.348	.318	2.000	0.135	0.040	.1286	.1753	84.1	124		3.76	
4/21/70	-16.7	1.348	.260	2.000	0.135	0.040	.1181	.1608	94.6	151		2.00	8
4/21/70	-16.7	1.348	.409	2.000	0.135	0.040	.1844	.2506	93.6	259		2.75	8
4/27/70	-16.7	1.352	.308	2.000	0.135	0.040	.1323	.1791	88.9	143		.004	8
4/27/70	-16.8	1.352	.307	1.500	0.135	0.040	.1315	.1773	88.3	139		.73	
4/27/70	-16.8	1.352	.308	1.000	0.135	0.040	.1241	.1682	83.5	116		.55	

TABLE A2-1 (continued)

DATE	T_A	π	L	h_T	h_J	D_J	G_H	G(1 atm.)	PS	D	$D_{AVG.}$	Standard	Fig.
							x 105	x 10^5		x 10^6	x 10^6	Error	No.
	^oC	atm.	cc./sec.	cm.	cm.	cm.	gm./sec.	gm./sec.	%	$cm.^2/sec.$	$cm.^2/sec.$		
5/4/70	-16.3	1.363	.309	2.000	0.135	0.040	.1431	.1943	95.7	202		.25	9
4/13/70	-15.4	1.363	.301	1.000	0.135	0.060	.1370	.1938	97.0	211		1.45	
4/13/70	-15.4	1.363	.301	1.500	0.135	0.060	.1389	.1956	98.0	228		.28	9
4/17/70	-15.3	1.352	.385	2.000	0.135	0.060	.1571	.2258	88.4	187		2.61	9
4/17/70	-15.3	1.352	.457	2.000	0.135	0.060	.1725	.2481	81.8	182	212	.28	9
4/17/70	-15.3	1.352	.585	2.000	0.135	0.060	.2067	.2972	76.6	209		.53	9
4/17/70	-15.3	1.352	.710	2.000	0.135	0.060	.2452	.3524	74.8	253		.63	9
5/7/70	-15.3	1.350	.388	2.000	0.100	0.040	.1442	.2086	80.9	143		2.05	9
5/7/70	-15.2	1.350	.310	2.000	0.100	0.040	.1283	.1860	90.2	152	150	1.54	9
5/7/70	-15.1	1.349	.263	2.000	0.100	0.040	.1156	.1688	96.4	171		.41	9
4/15/70	-15.2	1.359	.359	2.000	0.135	0.060	.1549	.2221	93.0	210		2.19	9
4/15/70	-15.2	1.359	.354	2.000	0.135	0.060	.1525	.2189	93.0	207	196	.25	9
4/15/70	-15.2	1.359	.457	2.000	0.135	0.060	.1735	.2487	81.9	182		.54	9
5/13/70	-14.5	1.359	.312	2.000	0.140	0.046	.1060	.1570	75.3	87.5		.41	9
5/13/70	-14.1	1.359	.359	2.000	0.140	0.046	.1331	.2012	83.3	140		1.06	9
5/14/70	-13.2	1.366	.361	2.000	0.140	0.046	.1312	.2061	84.3	145		1.60	10
5/14/70	-12.8	1.365	.316	2.000	0.140	0.046	.1213	.1941	90.4	156		1.70	10
5/14/70	-12.8	1.364	.272	2.000	0.140	0.046	.1134	.1822	98.6	209	154	1.07	10
5/14/70	-13.0	1.366	.408	2.000	0.140	0.046	.1424	.2257	81.5	154		.36	10
5/14/70	-12.7	1.364	.456	2.000	0.140	0.046	.1484	.2410	77.6	155		.51	10

TABLE A2-2

PHYSICAL ABSORPTION RESULTS OF KALRA (87) (3/4-inch SPHERE)

DATE	T_A	π	L	h	h_J	D_J	G	G(1 atm.)	PS	D	$D_{AVG.}$	Standard	Fig.
							$\times 10^6$	$\times 10^6$		$\times 10^6$	$\times 10^6$	Error	No.
	^oC	atm.	cc./sec.	cm.	cm.	cm.	gm./sec.	gm./sec.	%	$cm.^2/sec.$	$cm.^2/sec.$		
8/10/70	-22.0	1.346	.387	2.000	.1700	0.046	.1716	.1955	81.3	147		0.81	11
8/10/70	-21.8	1.346	.461	2.000	.1700	0.046	.1963	.2247	78.4	167		0.24	11
8/17/70	-20.8	1.337	.348	2.000	.1700	0.046	.1728	.2001	92.5	201		1.19	11
8/17/70	-20.7	1.337	.397	2.000	.1700	0.046	.1751	.2033	82.3	157		3.38	11
8/20/70	-21.7	1.343	.300	2.000	0.170	0.046	.1530	.1764	94.3	182		.32	11
8/20/70	-21.6	1.343	.371	2.000	0.170	0.046	.1712	.1979	85.6	162		1.16	11
8/24/70	-21.2	1.353	.393	0.660	0.170	0.046	.1785	.2061	83.8	164		.44	
8/24/70	-21.4	1.353	.391	1.160	0.170	0.046	.1721	.1975	80.8	146		.76	
8/24/70	-21.4	1.353	.394	1.660	0.170	0.046	.1748	.2009	81.7	152		(a)	11
8/27/70	-21.2	1.352	.393	2.000	0.170	0.046	.1690	.1958	79.5	140		1.13	11
8/27/70	-21.3	1.352	.393	1.000	0.170	0.046	.1664	.1924	78.3	134		.91	
9/02/70	-21.1	1.338	.394	0.615	0.170	0.046	.1694	.2002	81.1	148		.67	
9/09/70	-21.6	1.353	.390	1.500	0.170	0.046	.1804	.2064	84.8	168		0.09	11
9/09/70	-21.6	1.353	.390	0.720	0.170	0.046	.1740	.1987	81.8	150		0.24	
9/15/70	-22.5	1.354	0.387	2.000	0.170	0.046	0.1950	0.2173	90.8	213		0.08	11
9/15/70	-22.5	1.354	0.389	1.000	0.170	0.046	0.1892	0.2108	87.6	188		0.04	

(a) Data based on 1 determination.

TABLE A2-3

PHYSICAL ABSORPTION RESULTS (1-inch SPHERE)

DATE	T_A	π	L	h_T	h_J	D_J	G_H	G(1 atm.)	PS	D	$D_{AVG.}$	Standard	Fig.
	^oC	atm.	cc./sec.	cm.	cm.	cm.	x 10^5 gm./sec.	x 10^5 gm./sec.	%	x 10^6 $cm.^2/sec.$	x 10^6 $cm.^2/sec.$	Error	No.
7/18/70	-22.4	1.353	0.342	2.000	0.225	0.046	.1773	.1983	93.7	111	117	0.34	12
7/18/70	-22.4	1.353	0.430	2.000	0.225	0.046	.2118	.2369	89.0	120		0.10	12
7/16/70	-20.9	1.341	0.281	2.000	0.195	0.046	.1457	.1728	97.9	114		0.22	12
7/16/70	-20.9	1.341	0.327	2.000	0.195	0.046	.1692	.2003	97.9	136	115	0.65	12
7/16/70	-20.9	1.341	0.412	2.000	0.195	0.046	.1931	.2289	88.6	110		0.56	12
7/20/70	-20.2	1.345	0.352	2.000	0.225	0.046	.1690	.2036	91.4	102		0.01	12
7/22/70	-19.8	1.341	0.358	2.000	0.225	0.046	.1753	.2146	94.3	121		0.19	12
7/29/70	-19.0	1.338	0.398	2.000	0.225	0.046	.1826	.2309	90.7	115		1.62	12
7/29/70	-19.1	1.338	0.400	2.000	0.225	0.046	.1869	.2354	92.1	124	126	1.56	12
7/29/70	-19.1	1.338	0.468	2.000	0.225	0.046	.2131	.2687	89.8	137		.01	12
7/27/70	-18.9	1.345	0.392	2.000	0.225	0.046	.1861	.2338	93.0	127	128	.06	12
7/27/70	-18.9	1.345	0.390	2.000	0.225	0.046	.1860	.2337	93.4	129		.36	12

APPENDIX B2

SAMPLE CALCULATION

The following sample calculation was performed on the experimental determinations from the 7/29/70 run. Only those data which were obtained for a methylamine flow rate of 0.400 $\frac{c.c.}{sec.}$ are considered.

The experimental measurements are listed in Table B2-1. The second column in this table presents the elapsed time (minutes) from the start of the run to the time when the determination was recorded. The liquid flow rate (column 4) is listed as the actual rotameter reading. Four thermocouple outputs are recorded, however only thermocouple number 14 and thermocouple number 16 are used in the calculation. The temperature of the methylamine entering the liquid rotameter is measured by thermocouple number 14 and the temperature of the methylamine leaving the absorber is measured by thermocouple number 16. Columns 10 and 11 present the swept volume and time measurements from the soap film meter while column 12 lists the temperatures of the hydrogen entering the soap film meter.

The experimental determinations as presented in Table B2-2 are of the form required by the absorption model.

The experimental observations listed in Table B2-1 were transformed to the variables required by the absorption model according to the procedure outlined in Chapter IV. The sample calculation of the absorption variables listed in Table B2-2 is carried out in detail for the first determination (N = 1) and it is implied that the same procedure was followed for all the determinations.

TABLE B2-1

SINGLE SPHERE ABSORBER DATA SHEET

Date: 7/29/70

Barometric Pressure: 69.92 cm. Hg.

Barometric Temperature: 22.3°C

Ball Height: 71.600 cm.

Jet Length: 0.225 cm.

Feed Tank Pressure: 32 $\frac{lb_f}{in^2}$ (g)

Ball Diameter: 1"

Jet Size: 0.046 cm.

Determination Number	Real Time Min.	Liquid Height cm.	Liquid Flow Rate	System Pressure cm. Hg.	Thermocouple 13	14	15	16 m.v.	Volume Swept c.c.	Time Sec.	T_H °C
1	132.75	69.600	10.05	31.80	-.695	-.701	-.702	-.716	5.0	307.1	20.60
2	145.75	69.600	10.05	31.80	-.698	-.705	-.708	-.723	5.0	290.3	20.42
3	151.75	69.600	10.05	31.80	-.698	-.703	-.706	-.723	10.0	582.6	20.30
4	156.50	69.600	10.05	31.80	-.698	-.706	-.708	-.722	5.0	295.2	20.25
5	161.60	69.600	10.05	31.80	-.699	-.706	-.707	-.724	10.0	590.4	20.25
6	167.50	69.600	10.05	31.80	-.698	-.705	-.707	-.722	5.0	294.2	20.22
7	172.25	69.600	10.05	31.80	-.698	-.705	-.708	-.723	10.0	586.4	20.22
8	178.25	69.600	10.05	31.80	-.699	-.705	-.708	-.722	5.0	299.2	20.20
9	183.25	69.600	10.05	31.80	-.699	-.705	-.706	-.720	10.0	612.8	20.30
10	189.25	69.600	10.05	31.80	-.697	-.705	-.708	-.720	5.0	302.5	20.30

(1) Take-off Length

$$(h_t)_1 = \text{Ball height - Liquid height} \qquad [B2-1]$$

$$= 71.600 - 69.600$$

$$= 2.000 \text{ cm.}$$

All determinations which were utilized for evaluating the diffusion coefficient were obtained at a take-off height of 2.000 cm.

(2) Absorption Temperature $(T_A)_1$

$$(\varepsilon_s)_1 = \left\{\frac{\varepsilon_A + 0.0064}{0.9962}\right\} \qquad [D2-2]$$

$$= \frac{(-0.716 + 0.0064)}{0.9962}$$

$$= - 0.712 \text{ m.v.}$$

The temperature corresponding to a standard E.M.F. of -0.712 m.v. is read from the "Leeds and Northrup" thermocouple tables (copper-constantan) to be:

$$(T_A)_1 = -18.9°C \qquad [B2-2]$$

(3) Total Absorber Pressure $(\pi)_1$

$$(\pi)_1 = \left\{\frac{P_{abs} + P_{bar}}{76.0}\right\}$$

$$= \left\{\frac{31.80 + 69.92}{76.0}\right\}$$

$$(\pi)_1 = 1.338 \text{ atm.} \qquad [B2-3]$$

P_{abs} = absorber pressure as read on a Hg. manometer (cm. Hg.)

P_{bar} = barometric pressure (cm. Hg.)

(4) Hydrogen Partial Pressure $(P_1)_1$

The vapor pressure of methylamine is given by equation [3.2] of Part 1.

$$\ln P_1 = \frac{100.90554 - 5716.32506}{T} + 0.02248(T) - 15.30000 \ln(T)$$

where T = temperature (°K)

For $(T_A)_1 = -18.9°C = 254.2°K$

$$(P_1)_1 = 0.548 \text{ atm.} \qquad [B2\text{-}4]$$

The hydrogen partial pressure, as described by equation [4.8] is:

$$(P_2)_1 = (\pi)_1 - (P_1)_1 = 0.790 \text{ atm.} \qquad [B2\text{-}5]$$

(5) Henry's Law Coefficient

Henry's law coefficient is given by the best fit polynomial as presented in Table 4, Part 1.

$$\ln H_2 = 4.1403 + 1.66129\beta - 0.1160\beta^2$$

where:

$$\beta = \frac{1000.0}{T}$$

T = temperature (°K)

For $(T_A)_1 = -18.9°C = 254.2°K$

$$(H_2)_1 = 7190 \text{ atm.} \qquad [B2\text{-}6]$$

(6) Density of Methylamine

Equation [3.3], Part 1, describes the effect of temperature on the vapor pressure of methylamine.

$$\rho_1 = 0.90580 - 4.00947 \times 10^{-4}(T) - 1.45769 \times 10^{-6}(T)^2$$

where: T = temperature (°K)

For $(T_A)_1 = -18.9°C = 254.2°K$

$$(\rho_l)_1 = 0.7096 \frac{gm.}{c.c.} \qquad [B2\text{-}7]$$

(7) Viscosity of Methylamine

The viscosity of methylamine is obtained from equation [3.4] of Part I.

$$\ln \mu_l = \frac{741.817}{T} - 4.0524$$

μ_l = viscosity in centipoise

For $(T_A)_1 = -18.9°C = 2.54.2°K$

$$(\mu_l)_1 = 0.322 \text{ c.p.} \qquad [B2\text{-}8]$$

(8) Interfacial Concentration of Hydrogen

$$C_i = \frac{2.016\ \rho_l}{M_l} \left\{ \frac{1}{\frac{H_2}{P_2} - 1} \right\} \qquad [4.7]$$

$$(C_i)_1 = \frac{2.016 \times 0.7096}{31.07} \left\{ \frac{1}{\frac{7190}{0.790} - 1} \right\}$$

$$(C_i)_1 = 0.5059 \times 10^{-5} \frac{gm.}{c.c.} \qquad [B2\text{-}9]$$

(9) Total Rate of Absorption of Hydrogen into the Absorber

$$(G_H) = \frac{2.016}{22414.6} \left(\frac{273.15}{T_H} \right) \left(\frac{\pi}{1} \right) Q_H \qquad [4.11]$$

$$(G_H)_1 = \frac{2.016}{22414.6} \left\{ \frac{273.15}{273.15 + 20.60} \right\} \left\{ \frac{1.338}{1} \right\} \left\{ \frac{5.0}{307.1} \right\}$$

$$(G_H)_1 = 0.1808 \times 10^{-5} \frac{gm.}{sec.} \qquad [B2\text{-}10]$$

(10) Methylamine Volumetric Flow Rate

The equivalent flow rate of acetone at 20°C, which corresponds to the rotameter reading (RR) is given by equation [D2-1], Appendix D2.

$$Q_1 = -0.0745 + 0.4526 \times 10^{-1} (RR) - 0.6421 \times 10^{-4} (RR)^2$$

$$\text{For } (RR)_1 = 10.05$$

$$(Q_1)_1 = 0.3739 \left(\frac{\text{c.c.}}{\text{sec.}} \text{ acetone @ } 20°C\right) \qquad [B2\text{-}11]$$

The methylamine flow rate is obtained by applying the viscosity correction factor from Table D2-3, Appendix D2.

The temperature of the methylamine entering the liquid rotameter is obtained from thermocouple 14, Table B2-1.

$$\text{For } (\varepsilon_A) = -0.695 \text{ m.v.}$$

$$(\varepsilon_s) = -0.691 \text{ m.v.}$$

$$(T_L)_1 = -18.3°C \qquad [B2\text{-}12]$$

The portion of Table D2-3 which is required for converting an equivalent acetone flow rate of 0.3739 $\frac{\text{c.c.}}{\text{sec.}}$ to a methylamine flow rate at -18.3°C is reproduced below

	Flow rate (acetone @ 20°C)	
Temp.	0.2859	0.3751
-18°C	1.0773	1.0735
-19°C	1.0708	1.0683

The correction factor for 0.3739 $\frac{\text{c.c.}}{\text{sec.}}$ equivalent acetone flow rate at -18.3°C is obtained from the above table by linear interpolation for both the acetone flow rate and the temperature.

$$(F)_1 = 1.0688 \qquad [B2\text{-}13]$$

Therefore, the methylamine flow rate is:

$$L = Q_1 F_1 = 0.3739 \times 1.0688 = 0.400 \ \frac{c.c.}{sec.}$$

$$L = 0.400 \ \frac{c.c.}{sec.} \text{ methylamine} \qquad [B2\text{-}14]$$

(11) Percent Saturation of the Methylamine leaving the Absorber

$$PS = \frac{G_H}{L \ C_i} \times 100 \qquad [B2\text{-}15]$$

$$(PS)_1 = \left\{ \frac{0.1808 \times 10^{-5} \ \frac{gm.}{sec.}}{0.400 \ \frac{c.c.}{sec.} \times 0.5059 \times 10^{-5} \ \frac{gm.}{c.c.}} \right\} \times 100$$

$$= 89.3\% \qquad [B2\text{-}16]$$

The above calculations were performed for each of the ten determinations. The transformed variables are presented in Table B2-2.

(12) Calculate the Average Parameters for the Run

(a) Average Temperature

$$(T_A)_{avg} = \frac{\sum_1^{10} T_{A_i}}{10} = -19.1°C \qquad [B2\text{-}17]$$

(b) Average Interfacial Concentration

$$(C_i)_{avg} = \frac{\sum_1^{10} (C_i)_i}{10} = 0.5078 \times 10^{-5} \ \frac{gm.}{sec.} \qquad [B2\text{-}18]$$

TABLE B2-2

ABSORPTION VARIABLES

Det. No.		P_2	$C_i \times 10^5$	$G_H \times 10^5$	PS	L	T_A
	atm.	atm.	$\frac{gm.}{c.c.}$	$\frac{gm.}{sec.}$	%	$\frac{c.c.}{sec.}$	°C
1	1.338	0.790	0.5059	.1808	89.3	0.400	-18.9
2	1.338	0.795	.5083	.1914	94.2	0.400	-19.1
3	1.338	0.795	.5083	.1908	93.8	0.400	-19.1
4	1.338	0.795	.5080	.1883	92.7	0.400	-19.1
5	1.338	0.795	.5087	.1883	92.6	0.400	-19.1
6	1.338	0.795	.5080	.1890	93.0	0.400	-19.1
7	1.338	0.795	.5083	.1897	93.4	0.400	-19.1
8	1.338	0.795	.5080	.1858	91.5	0.400	-19.1
9	1.338	0.793	.5073	.1814	89.4	0.400	-19.1
10	1.338	0.793	.5073	.1837	90.6	0.400	-19.1

(c) Average Total Hydrogen Absorption Rate

$$(G_H)_{avg} = \frac{\sum_{1}^{10} (G_H)_i}{10} = 0.1869 \times 10^{-5} \frac{gm.}{sec.} \qquad [B2-19]$$

(d) Average Liquid Flow Rate

$$(L)_{avg} = \frac{\sum_{1}^{10} L_i}{10} = 0.400 \frac{c.c.}{sec.} \qquad [B2-20]$$

(e) Average Percent Saturation

$$(PS)_{avg} = \frac{\sum_{1}^{10} (PS)_i}{10} = 92.1\% \qquad [B2-21]$$

(13) Standard Error for the Run as Calculated From the Percent Saturation of the Individual Determinations

$$\sigma = \left\{ \frac{1}{N-1} \sum_{r=1}^{N} \delta_i^{\,2} \right\}^{\frac{1}{2}} \qquad [B2-22]$$

N = number of determinations

$$\delta_i = (PS)_i - (PS)_{avg}$$

From Table B2-2:

$$\delta_1 = (89.3 - 92.1) = -2.8$$

$$\delta_2 = (94.2 - 92.1) = +2.1$$

$$\delta_{10} = (90.6 - 92.1) = -1.5$$

The standard error for the run is:

$$\sigma = \left\{ \frac{1}{9} \sum_{1}^{10} \delta_i \right\}^{\frac{1}{2}} = 1.56 \qquad [B2\text{-}23]$$

Therefore, assuming the error distribution is normal, the probability that the percent saturation of a determination is in error by an amount no larger than 1.56 is 68.26%.

(14) Calculate the Initial Estimate of the Diffusion Coefficient

(a) Average Kinematic Viscosity

The density and viscosity of methylamine at -19.1°C were calculated according to the equations outlined in sections (6) and (7) respectively.

$$(\nu)_{avg} = \left(\frac{\mu}{\rho}\right)_{avg} = 4.538 \times 10^{-3} \frac{cm.^2}{sec.} \qquad [B2.24]$$

(b) Average Fraction of Hydrogen Absorbed on the Sphere: (Initial Estimate)

$$Z_s = (12 \times 1.68)^{\frac{1}{2}} \left(\frac{2\pi g}{3r}\right)^{1/6} L^{1/3} R^{7/6} \qquad [4.14]$$

$$(Z_s)_{avg} = 4.49 \left\{ \frac{2\pi\ 981.168}{3 \times 0.4538 \times 10^{-2}} \right\}^{1/6} \{0.400\}^{1/3} \{1.2700\}^{7/6}$$

$$= 38.341 \qquad [B2.25]$$

$$Z_J = 4.0(H_J\ L)^{\frac{1}{2}} \qquad [4.15]$$

$$(Z_J)_{avg} = 4.0(0.225 \times 0.400)^{\frac{1}{2}} = 1.20 \qquad [B2\text{-}26]$$

$$F_s = \frac{Z_s}{Z_s + Z_J} \qquad [4.16]$$

$$(F_s)_{avg} = \frac{38.341}{38.341 + 1.20}$$

$$= 0.970 \qquad [B2.27]$$

$$F_J = 1 - F_s \qquad [4.17]$$

$$(F_J)_{avg} = 0.030 \qquad [B2\text{-}28]$$

(c) Average Rate of Absorption of Hydrogen on the Sphere (Initial Estimate)

$$(G_A)_{avg} = (G_H)_{avg} \; (F_s)_{avg}$$

$$= (0.1869 \times 10^{-5})(0.970)$$

$$(G_A)_{avg} = 0.1812 \times 10^{-5} \frac{gm.}{sec.} \qquad [B2\text{-}29]$$

(d) Average Rate of Absorption of Hydrogen on the Jet (Initial Estimate)

$$(G_J)_{avg} = (G_H)_{avg} \; (F_J)_{avg}$$

$$= (0.1869 \times 10^{-5})(0.030)$$

$$(G_J)_{avg} = 0.0057 \times 10^{-5} \frac{gm.}{sec.} \qquad [B2\text{-}30]$$

(e) Average Bulk Concentration of the Methylamine Flowing Over the Sphere (Initial Estimate)

$$C_o = \frac{G_J}{L} \qquad [3.8]$$

$$(C_o)_{avg} = \frac{(G_J)_{avg}}{(L)_{avg}}$$

$$= \frac{0.0057 \times 10^{-5}}{0.400}$$

$$(C_o)_{avg} = 0.0142 \times 10^{-5} \frac{gm.}{c.c.} \qquad [B2\text{-}31]$$

(f) Average Driving Force for the Physical Absorption of Hydrogen (Initial Estimate)

$$(C_i - C_o)_{avg} = 0.5078 \times 10^{-5} - 0.0142 \times 10^{-5} \frac{gm.}{c.c.}$$

$$= 0.4936 \times 10^{-5} \frac{gm.}{c.c.} \qquad [B2\text{-}32]$$

(g) Initial Estimate of the Hydrogen Diffusion Coefficient

$$D_1^{(1)} = \left\{ \frac{(G_A)_{avg}}{(Z_s)_{avg} (C_i - C_o)_{avg}} \right\}^2$$

$$= \left\{ \frac{0.1812 \times 10^{-5}}{38.341 \times 0.4936 \times 10^{-5}} \right\}^2$$

$$D_1^{(1)} = 91.8 \times 10^{-6} \frac{cm.^2}{sec.} \qquad [B2\text{-}33]$$

(15) Trial and Error Solution of Equation [2.70] for the Diffusion Coefficient (Initial Estimate)

$$G = L(C - C_o)[1 - 0.7857 \exp(-3.414\ \alpha) - 0.1001 \exp(-26.21\ \alpha) - 0.03599 \exp(-70.43\ \alpha) - 0.01811 \exp(-136.5\ \alpha)] \qquad [2.70]$$

$$\alpha = 2 \times 1.68\ \pi \left(\frac{2\pi g}{3\nu} \right)^{1/3} \frac{R^{7/3}}{L^{4/3}}\ D \qquad [2.71]$$

In order to illustrate the trial and error solution of equation [2.70] for the diffusion coefficient D, the following calculations have been based on the average absorption variables as presented in

Section (12). The computer solution for equation [2.70] performed the following calculations for each determination, however the procedure is analogous and the increased complexity due to the use of all determinations is not warranted for illustration of the procedure.

(a) Average Film Thickness at the Equator

$$\Delta^{+} = \left\{\frac{3L\nu}{2\pi Rg}\right\}^{1/3} \qquad [3.10]$$

$$(\Delta^{+})_{avg} = \left\{\frac{3 \times 0.400 \times 0.4438 \times 10^{-2}}{\pi \times 1.2700 \times 981.168}\right\}^{1/3}$$

$$(\Delta^{+})_{avg} = 0.0088 \text{ cm.} \qquad [B2\text{-}34]$$

(b) Corrected Hydrogen Absorption Rate on the Sphere (Initial Estimate)

$$(G_s)_{avg} = \frac{(G_A)_{avg}}{ACOR} \qquad [B2\text{-}35]$$

where:

$$ACOR = 1 + \frac{2.58\ \Delta^{+}}{R} \qquad [3.9]$$

$$= 1 + \frac{2.58(0.0088)}{1.2700}$$

$$ACOR = 1.0179 \qquad [B2\text{-}36]$$

$$(G_s)_{avg} = \frac{0.1812 \times 10^{-5}}{1.0179}$$

$$(G_s)_{avg} = 0.1780 \times 10^{-5} \frac{gm.}{sec.} \qquad [B2\text{-}35]$$

(c) Calculate the Initial Estimate of "α"

From Section (14-g) $D_1^{(1)} = 91.8 \times 10^{-6}$ [B2-33]

$$\alpha_1^{(1)} = 2 \times 1.68\pi \left\{ \frac{2\pi \times 981.168}{3 \times 0.4538 \times 10^{-2}} \right\}^{1/3} \frac{(1.2700)^{7/3}}{(0.400)^{4/3}} (91.8 \times 10^{-6})$$

$$\alpha_1^{(1)} = 0.4410 \qquad [B2\text{-}36]$$

(d) Calculate the Hydrogen Absorption Rate From Equation [2.70]

$$G_{cal_1}^{(1)} = 0.400 \times 0.4936 \times 10^{-5}[1 - 0.7857 \exp(-3.414(0.4410)) - 0.1001 \exp(-26.21(0.4410)) - 0.03599 \exp(-70.43(0.4410)) - 0.01811 \exp(-136.5(0.4410))]$$

$$G_{cal_1}^{(1)} = 0.1974 \times 10^{-5}[1 - 0.7857(.22194) - 0.1001[9.5735 \times 10^{-6}) - 0.03599(3.261 \times 10^{-14} - 0.01811[7.273 \times 10^{-27}]]$$

$$G_{cal_1}^{(1)} = 0.1630 \times 10^{-5} \frac{gm.}{sec.} \qquad [B2\text{-}37]$$

(e) Calculate the Deviation Between the Measured and Calculated Absorption Rate

$$E_1^{(1)} = |(G_s)_{avg} - G_{cal}| \qquad [4.12]$$

$$= |0.1780 \times 10^{-5} - 0.1630 \times 10^{-5}|$$

$$E_1^{(1)} = \left|0.0150 \times 10^{-5} \frac{gm.}{sec.}\right| \qquad [B2\text{-}38]$$

(f) Increase the Estimated Value of the Diffusion Coefficient by a Fixed Increment

$$D_2^{(1)} = D_1^{(1)} + \Delta D \qquad [B2\text{-}39]$$

The first estimate of the increment is:

$$\Delta D = 0.10\ D_1^{(1)} \qquad [B2\text{-}40]$$

$$D_2^{(1)} = 91.8 \times 10^{-6} + 9.2 \times 10^{-6}$$

$$= 101.0 \times 10^{-6} \frac{cm.^2}{sec.} \qquad [B2\text{-}41]$$

(g) Calculate the Revised Hydrogen Absorption Rate from Equation [2.70] and Compare with the Measured Rate

$$\alpha_2^{(1)} = 0.4852 \qquad [B2\text{-}42]$$

$$G_{cal_2}^{(1)} = 0.1678 \times 10^{-5} \frac{gm.}{sec.} \qquad [B2\text{-}43]$$

$$E_2^{(1)} = 0.0102 \times 10^{-5} \frac{gm.}{sec.} \qquad [B2\text{-}44]$$

Since $E_2^{(1)} < E_1^{(1)}$, increase the estimated value of the diffusion coefficient by ΔD_1, and evaluate $E_3^{(1)}$. Continue this calculation until the deviation passes through a minimum. When the deviation crosses a minimum, reduce the increment by one half and reverse the sign of the increment. The estimated value of the diffusion coefficient is now reduced by subtracting one half the original increment and the deviation will again cross the minimum in a maximum of three iterations. When the minimum deviation is again crossed, ΔD is reduced by one half and its sign reversed. This procedure is continued until the magnitude of ΔD is such that:

$$\frac{\Delta D}{D_n^{(1)}} < 0.5 \times 10^{-4} \qquad [B2\text{-}45]$$

where $D_n^{(1)}$ is the last estimate of the diffusion coefficient.

The final estimate of the diffusion coefficient ($D_n^{(1)}$) is

assumed to be the solution of equation [2.70] corresponding to the initial estimate of the amount of hydrogen absorbed on the jet and sphere:

$$D_n^{(1)} = 124.0 \frac{cm.^2}{sec.} \qquad [B2\text{-}46]$$

$$G_{cal_n}^{(1)} = 0.1782 \times 10^{-5} \qquad [B2\text{-}47]$$

$$E_n^{(1)} = |0.1780 \times 10^{-5} - 0.1782 \times 10^{-5}| = 0.0002 \times 10^{-5} \qquad [B2\text{-}48]$$

(16) Trial and Error Solution of Equation [2.70] for the Diffusion Coefficient (Second Estimate

(a) Calculate the Amount of Hydrogen absorbed on the Jet

The diffusion coefficient, as evaluated in the previous section, is used to calculate the amount of hydrogen absorbed on the jet.

$$G_J = 4.0(C_i - C_o^1)\{h_J \; L \; D\}^{\frac{1}{2}} \qquad [3.7]$$

$$C_o^1 = 0 \qquad [B2\text{-}49]$$

Therefore $(G_J)_{avg} = 4.0(.5078 \times 10^{-5})(0.225 \times 0.400 \times 124.0 \times 10^{-6})^{\frac{1}{2}}$

$$= 6.7855 \times 10^{-8} \frac{gm.}{sec.} \qquad [B2\text{-}50]$$

(b) Average Bulk Concentration of the Methylamine Flowing Over The Sphere (Second Estimate)

$$C_o = \frac{G_J}{L} \qquad [3.8]$$

$$(C_o)_{avg} = \frac{6.7855 \times 10^{-8}}{0.400}$$

$$(C_o)_{avg} = 0.0170 \times 10^{-5} \frac{gm.}{c.c.} \quad [B2\text{-}51]$$

(c) Average Driving Force for the Physical Absorption of Hydrogen (Second Estimate)

$$(C_i - C_o) = 0.5078 \times 10^5 - 0.0170 \times 10^5$$

$$= 0.4908 \times 10^{-5} \frac{gm.}{c.c.} \quad [B2\text{-}52]$$

(d) Average Rate of Absorption on the Sphere (Second Estimate)

$$(G_A)_{avg} = (G_H)_{avg} - (G_J)_{avg}.$$

$$(G_A)_{avg} = 0.1869 \times 10^{-5} - 0.0068 \times 10^{-5}$$

$$(G_A)_{avg} = 0.1801 \times 10^{-5} \frac{gm.}{sec.} \quad [B2\text{-}53]$$

(e) Corrected Hydrogen Absorption Rate on the Sphere (Second Estimate)

$$(G_s)_{avg} = \frac{(G_A)_{avg}}{ACOR} \quad [B2\text{-}25]$$

$$= \frac{0.1801 \times 10^{-5}}{1.0179}$$

$$(G_s)_{avg} = 0.1769 \times 10^{-5} \frac{gm.}{sec.} \quad [B2\text{-}54]$$

Equation [2.70] is again solved for the diffusion coefficient by the interval halving search routine. The diffusion coefficient, as obtained in Section (15) ($D_n^{(1)}$), is used as the initial estimate of the solution for the revised set of absorption conditions. The minimum deviation between the measured and calculated hydrogen absorption rate occurs for a diffusion coefficient of:

$$D_n^{(2)} = 123.7 \times 10^{-6} \frac{cm.^2}{sec.} \quad [B2\text{-}55]$$

$$G_{cal_n}^{(2)} = 0.1771 \times 10^{-5} \frac{gm.}{sec.} \quad [B2\text{-}56]$$

$$E = |0.1769 \times 10^{-5} - 0.1771 \times 10^{-5}|$$

$$= 0.0002 \times 10^{-5} \frac{gm.}{sec.} \quad [B2\text{-}57]$$

(17) Compare the Diffusion Coefficients as Calculated in Sections (15) and (16)

$$PD = \left| \frac{D_n^{(m)} - D_{(n)}^{(m-1)}}{D_n^{(m)}} \right| \times 100 \quad [B2\text{-}58]$$

$$PD = \left| \frac{123.7 \times 10^{-6} - 124.0 \times 10^{-6}}{123.7 \times 10^{-6}} \right| \times 100 = 0.25\% \quad [B2\text{-}59]$$

If PD is less than 0.50% the diffusion coefficient, as calculated from the revised set of absorption conditions (Section (16)) is assumed to be the diffusion coefficient of hydrogen in methylamine at the average temperature of the run.

If PD is greater than 0.50%, the calculations in Section (16) are repeated until two successive estimates of the diffusion coefficient agree within 0.05%.

Since, for the preceeding sample calculation,

$$PD = 0.25\% \quad (B2\text{-}59]$$

the diffusion coefficient for hydrogen dissolved in methylamine at -19.1°C is:

$$D = 123.7 \times 10^{-6} \frac{cm.^2}{sec.} \quad [B2\text{-}60]$$

APPENDIX C2

ERROR ANALYSIS

A. Theoretical

Equation [2.70] was assumed to describe the relationship between the molecular diffusion coefficients for hydrogen in methylamine and the experimental absorption rates measured in this study. The effect of the propagation of errors on the calculated diffusion coefficient will therefore be evaluated on the basis of this equation.

$$G_s = L(C_i - C_o)[1 - 0.7857 \exp(-3.414\ \alpha) - 0.1001 \exp(-26.21\ \alpha)...] \qquad [2.70]$$

$$\alpha = 2 \times 1.68\pi \left(\frac{2\pi g}{3\nu}\right)^{1/3} \frac{R^{7/3}}{L^{4/3}} D \qquad [2.71]$$

The last two terms in equation [2.70] have been dropped as they are negligible at the methylamine saturations involved in this study.

In order to simplify the writing of equation [2.70], the following form is used throughout this analysis.

$$G_s = L(C_i - C_o)\ f(\alpha) \qquad [C2\text{-}1]$$

where $f(\alpha) = 1 - 0.7857 \exp(-3.414\ \alpha) - 0.1001 \exp(-26.21\ \alpha)$ [C2-2]

It can be seen from equations [2.70] and [2.71] that:

$$G_s = f[L, (C_i - C_o), D, \nu] \qquad [C2\text{-}3]$$

hence the equation describing the propagation of errors is of the form:

$$\Delta G_s = \left(\frac{\partial G_s}{\partial L}\right) \Delta L + \left(\frac{\partial G_s}{\partial (C_i - C_o)}\right) \Delta (C_i - C_o) + \left(\frac{\partial G_s}{\partial D}\right) \Delta D + \left(\frac{\partial G_s}{\partial \nu}\right) \Delta \nu \qquad [C2\text{-}4]$$

Evaluating the partial derivatives from equation [2.70] yields:

$$\frac{\partial G_s}{\partial L} = (C_i - C_o)\, f(\alpha) + L(C_i - C_o)[-0.7857(-3.414)\, \exp(-3.414\, \alpha)$$

$$-0.1001(-26.21)\, \exp(-26.21\, \alpha)\, \frac{\partial \alpha}{\partial L}$$

$$= (C_i - C_o)\, f(\alpha) + L(C_i - C_o)[2.6824\, \exp(-3.414\, \alpha)$$

$$+ 2.6234\, \exp(-26.21\, \alpha)]\, \frac{\partial \alpha}{\partial L} \qquad [C2\text{-}5]$$

Since $2.6824\, \exp(-3.414\, \alpha) >> 2.6234\, \exp(-26.21\, \alpha)$

equation [C2-5] becomes:

$$\frac{\partial G_s}{\partial L} = (C_i - C_o)\, f(\alpha) + L(C_i - C_o)[2.6824\, \exp(-3.414\, \alpha)]\, \frac{\partial \alpha}{\partial L} \qquad [C2\text{-}6]$$

The remaining derivatives are obtained in a similar manner.

$$\frac{\partial G_s}{\partial (C_i - C_o)} = L\, f(\alpha) \qquad [C2\text{-}7]$$

$$\frac{\partial G_s}{\partial D} = L(C_i - C_o)[2.6824\, \exp(-3.414\, \alpha)]\, \frac{\partial \alpha}{\partial D} \qquad [C2\text{-}8]$$

$$\frac{\partial G_s}{\partial \nu} = L(C_i - C_o)[2.6824\, \exp(-3.414\, \alpha)]\, \frac{\partial \alpha}{\partial \nu} \qquad [C2\text{-}9]$$

The partial derivatives of α are obtained from equation [2.71].

$$\frac{\partial \alpha}{\partial L} = -\frac{4}{3}\left(\frac{\alpha}{L}\right) \qquad [C2\text{-}10]$$

$$\frac{\partial \alpha}{\partial D} = \frac{\alpha}{D} \qquad [C2\text{-}11]$$

$$\frac{\partial \alpha}{\partial \nu} = -\frac{2}{3}\,\frac{\alpha}{\nu} \qquad [C2\text{-}12]$$

Substituting equations [C2-6] to [C2-12] into equation [C2-4] yields:

$$\Delta G_s = G_s \left| \frac{\Delta L}{L} + \frac{\Delta (C_i - C_o)}{(C_i - C_o)} + \frac{2.6824\ \alpha \exp(-3.414\ \alpha)}{f(\alpha)} \left\{ \frac{4}{3} \frac{\Delta L}{L} + \frac{\Delta D}{D} + \frac{2}{3} \frac{\Delta \nu}{\nu} \right\} \right| \qquad [C2\text{-}13]$$

Rearrangine equation [C2-13] in terms of the error in the diffusion coefficient results in the desired equation.

$$\frac{\Delta D}{D} = \frac{f(\alpha)}{2.6824\ \alpha \exp(-3.414\ \alpha)} \left| \frac{\Delta G_s}{G_s} + \frac{\Delta L}{L} + \frac{\Delta (C_i - C_o)}{(C_i - C_o)} \right| + \frac{4}{3} \frac{\Delta L}{L} + \frac{2}{3} \frac{\Delta \nu}{\nu} \qquad [C2\text{-}14]$$

As the percent saturation of the methylamine leaving the absorber approaches 100%;

$$f(\alpha) \rightarrow 1 \qquad [C2\text{-}15]$$

$$\exp(-3.414\ \alpha) \rightarrow 0 \qquad [C2\text{-}16]$$

It can be seen from equation [C2-14] that the expected error in the diffusion coefficient becomes very large as substitution of equation [C2-15] and [C2-16] into equation [C2-14] yields:

$$\frac{\Delta D}{D} \rightarrow \infty \qquad [C2\text{-}17]$$

Therefore, the saturation of the methylamine leaving the absorber must be maintained at as low a level as possible in order to obtain some degree of precision in the diffusion coefficient.

An estimation of the magnitude of the terms in equation [C-14] is required before a numerical solution of this equation can be obtained.

1. Total Hydrogen Absorption Rate to the Absorber

The total hydrogen absorption rate is described by equation

[4.11].

$$G_H = \frac{2.016}{22414.6}\left\{\frac{273.15}{T_H}\right\}\left\{\frac{\pi}{1}\right\} Q_H \qquad [4.11]$$

Therefore:

$$\Delta G_H = G_H \left\{\frac{\Delta\pi}{\pi} + \frac{\Delta T_H}{T_H} + \frac{\Delta Q_H}{Q_H}\right\} \qquad [C2\text{-}18]$$

The hydrogen volumetric flow rate, Q_H, is calculated from the soap film meter readings.

$$Q_H = \frac{V_{SFM}}{t} \qquad [C2\text{-}19]$$

V_{SFM} = Volume swept by the soap film

t = time for soap film to sweep volume V.

$$\therefore \Delta Q_H = Q_H \left\{\frac{\Delta V_{SFM}}{V_{SFM}} + \frac{\Delta t}{t}\right\} \qquad [C2\text{-}20]$$

Substituting equation [C2-20] into equation [C2-18] results in the equation for the expected error in the total hydrogen absorption rate.

$$\frac{\Delta G_H}{G_H} = \left\{\frac{\Delta\pi}{\pi} + \frac{\Delta T_H}{T_H} + \frac{\Delta V_{SFM}}{V_{SFM}} + \frac{\Delta t}{t}\right\} \qquad [C2\text{-}21]$$

2. Hydrogen Absorption Rate on the Sphere

Under ideal absorber conditions (no fluctuations in the absorber temperature, pressure, or liquid take-off level) the rate of absorption of hydrogen on the spherical liquid film is equal to the total rate of absorption of hydrogen to the absorber less the rate of absorption of hydrogen on the laminar jet. As temperature

and liquid take-off levels do fluctuate during an actual run, their effect on the amount of hydrogen absorbed on the sphere must be considered. The total absorber pressure may be assumed to be constant within the limits of accuracy of the hydrogen regulator.

The total rate of absorption of hydrogen to the absorber can be described by the following equation:

$$G_H = G_A + G_J + G_{Temp} + G_{TL} \qquad [C2\text{-}22]$$

G_A = hydrogen absorption rate on the sphere

G_J = hydrogen absorption rate on the jet

G_{Temp} = hydrogen absorption rate due to a change of the absorber temperature

G_{TL} = hydrogen absorption rate due to a change of the liquid take-off level.

The absorption rates G_{Temp} and G_{TL} are assumed to have a mean value of zero, hence only the expected error due to their presence is considered. (Otherwise they are a systematic error for which corrections can be applied).

The expected error in the hydrogen absorption rate to the sphere is seen from equation [C2-22] to be:

$$\Delta G_A + \Delta G_H + \Delta G_J + \Delta G_{Temp} + \Delta G_{TL} \qquad [C2\text{-}23]$$

a) Absorption Rate on the Jet

The rate of absorption of hydrogen on an ideal jet is given by equation [3.7].

$$G_J = 4.0(C_i - C'_o)\{h_J\ L\ D\}^{\frac{1}{2}} \qquad [3.7]$$

where $C_o' = 0$.

The expected error in the absorption rate on the jet is:

$$\Delta G_J = G_J \left\{ \frac{\Delta C_i}{C_i} + \frac{1}{2} \left| \frac{\Delta h_J}{h_J} + \frac{\Delta L}{L} + \frac{\Delta D}{D} \right| \right\} \qquad [C2\text{-}24]$$

b) Error in the Hydrogen Absorption Rate to the Sphere Due to Fluctuations in the Absorber Temperature or Liquid Take-Off Level.

A change in the absorber temperature will cause a change in the methylamine vapor pressure and to a lesser degree, a change in the density of the hydrogen gas contained in the absorber. As hydrogen is fed into the absorber to maintain a constant total pressure (π), any change in the absorber pressure is interpreted from the soap film measurements, as a change in the hydrogen absorption rate.

A slight variation of the liquid level in the take-off tube will result in a change in the absorber volume. Hydrogen will again be introduced or the saturated hydrogen phase will be expelled from the absorber in order to maintain a constant absorber pressure π. This transfer of hydrogen is interpreted as a change in the absorption rate.

The effect of a change in the absorber temperature or liquid take-off level can be determined from the equation describing the hydrogen partial pressure in the absorber.

$$P_2 = \pi - P_1 \qquad [4.8]$$

If hydrogen is assumed to be an ideal gas, the hydrogen partial pressure is related to the number of moles of hydrogen in the ab-

sorber by the ideal gas law.

$$P_2 = \frac{n R_G T_A}{V} \qquad [C2\text{-}25]$$

where R_G = ideal gas constant = $82.06 \frac{\text{c.c. atm.}}{\text{gm. mole } ^\circ K}$

n = number of moles of hydrogen

Substituting equation [C2-25] into equation [4.8] yields the following equation:

$$\frac{n R_G T_A}{V} = \pi - P_1 \qquad [C2\text{-}26]$$

The change in the hydrogen absorption rate due to a change in the absorber temperature or liquid take-off height is given by the following expression.

$$G_{Temp} + G_{TL} = 2.016 \left(\frac{\partial n}{\partial t}\right)_\pi \qquad [C2\text{-}27]$$

where t = time (seconds).

The partial derivative in equation [C2-27] is obtained from equation [C2-26] to be:

$$R_G \left(\frac{\partial n}{\partial t}\right) = \frac{(\pi - P_1)}{T_A} \left(\frac{\partial V}{\partial t}\right)_\pi - \frac{V}{T_A^2} (\pi - P_1) \left(\frac{\partial T_A'}{\partial t}\right)_\pi - \frac{V}{T_A} \left(\frac{\partial P_1}{\partial t}\right)_\pi \qquad [C2\text{-}28]$$

Since

$$\left(\frac{\partial P_1}{\partial t}\right) = \left(\frac{\partial P_1}{\partial T_A'}\right)_\pi \left(\frac{\partial T_A'}{\partial t}\right)_\pi \qquad [C2\text{-}29]$$

equation [C2-28] can be written as:

$$\left(\frac{\partial n}{\partial t}\right) = \frac{P_2}{T_A R_G}\left(\frac{\partial V}{\partial t}\right)_\pi - \frac{V}{R_G T_A^2}\left\{P_2 - T_A\left(\frac{\partial P_1}{\partial T_A'}\right)_\pi\right\}\left(\frac{\partial T_A'}{\partial t}\right)_\pi \qquad [C2\text{-}30]$$

A prime is used on the partial derivatives involving temperature in order to distinguish the temperature variations which may occur during a reading (governed by the sensitivity of the potentiometer used to measured the thermocouple e.m.f.) from the limits of uncertainty of the thermocouple calibration.

Substituting equation [C2-30] into equation [C2-27] yields the following two equations which describe the effect of a liquid level change and a temperature change respectively.

$$\Delta G_{TL} = \frac{2.016\ P_2}{T_A R_G}\left(\frac{\partial V}{\partial t}\right)_\pi \qquad (C2\text{-}31]$$

$$G_{Temp} = \frac{2.016\ V}{R_G T_A^2}\left\{P_2 - T_A\left(\frac{\partial P_1}{\partial T_A'}\right)_\pi\right\}\left(\frac{\partial T_A'}{\partial t}\right) \qquad [C2\text{-}32]$$

The change in the total absorber volume due to a change in the liquid take-off height (Δh_{TL}) is:

$$\Delta V = \frac{\pi d^2}{4}\Delta h_{TL} \qquad [C2\text{-}33]$$

where d = internal diameter of the glass collector

Δh_{TL} = change in height of the take-off level (cm.) (positive as level drops and negative as the level rises).

As the level change occurs over the time required for a determination (t), the partial derivative in equation [C2-31] may be approximated by the following expression.

$$\left(\frac{\partial V}{\partial t}\right)_{\pi} \simeq \left(\frac{\Delta V}{t}\right)_{\pi} = \frac{\pi d^2}{4}\left(\frac{\Delta h_{TL}}{t}\right)_{\pi} \qquad [C2\text{-}34]$$

Substituting equation [C2-34] into equation [C2-31] yields the desired equation for the effect of a change in the liquid take-off level on the measured hydrogen absorption rate.

$$\Delta G_{TL} = \frac{2.016}{R_G} \times \frac{\pi d^2}{4} \times \frac{P_2}{T_A} \times \left(\frac{\Delta h_{TL}}{t}\right) \qquad [C2\text{-}35]$$

The vapor pressure of methylamine is given by equation [3.2] of Part 1.

$$\ln P_1 = \frac{100.90554 - 5716.32506}{T_A} + 0.02248\ T_A - 15.3000 \ln T_A$$

Therefore:

$$\frac{1}{P_1}\frac{\partial P_1}{\partial T_A} = \frac{5716.32}{T_A^2} + 0.02248 - \frac{15.300}{T_A} \qquad [C2\text{-}36]$$

Substituting equation [C2-36] into equation [C2-32] results in the desired equation describing the effect of a temperature change on the absorption rate.

$$\Delta G_{Temp} = \frac{-2.016}{R_G}\frac{V}{T_A^2}\left\{P_2 - P_1\left[\frac{5716.32}{T_A} + 0.02248\ T_A - 15.30\right]\right\}\left\{\left(\frac{\Delta T'_A}{t}\right)_{\pi}\right\} \qquad [C2\text{-}37]$$

The partial derivative of the absorber temperature with respect to time was calculated from the approximation:

$$\left(\frac{\partial T'_A}{\partial t}\right) \simeq \left(\frac{\Delta T'_A}{t}\right) \qquad [C2\text{-}38]$$

It should be noted that absorption rate error due to a change in the absorber temperature or liquid level can be considered a systematic error if the change in temperature or liquid level is greater than the limits of the reading accuracy. In this case, equations [C2-35] and [C2-37] can be used to correct the measured absorption rate.

It should also be noted that the total absorber pressure (π) has been assumed constant for the above calculations. This is true if hydrogen is being fed to the absorber to maintain the pressure, however, it is a less accurate assumption if the absorber pressure rises above the hydrogen regulator setting. When this happens, the regulator shuts off and the hydrogen phase from the absorber will flow back through the soap film meter and into the hydrogen feed lines. As the volume of these lines is small, sufficient hydrogen phase may not be expelled from the absorber to maintain the pressure. Hence, a slight pressure increase will be noted. This case was neglected, however, as a pressure increase will back out the soap film and no absorption rates can be measured.

c) Absorption Rate on the Sphere

The expected error in the hydrogen absorption rate to the sphere is obtained by substituting equations [C2-21], [C2-24], [C2-35] and [C2-37] into equation [C2-23].

$$\Delta G_A = G_H\left\{\frac{\Delta\pi}{\pi} + \frac{\Delta T_H}{T_H} + \frac{\Delta V}{V} + \frac{\Delta t}{t}\right\} + G_J\left[\frac{\Delta C_i}{C_i} + \frac{1}{2}\left[\frac{\Delta h_J}{h_J} + \frac{\Delta L}{L} + \frac{\Delta D}{D}\right]\right]$$

$$+ \frac{2.016}{R_G} \times \frac{\pi d^2}{4} \times \frac{P_2}{T_A}\left[\frac{\Delta h_{TL}}{t}\right]$$

$$+ \frac{2.016}{R_G} \frac{V}{T_A^2} \left\{ P_2 - P_1 \left[\frac{5716.32}{T_A} + 0.02248\, T_A - 15.30 \right] \right\} \left(\frac{\Delta T'_A}{t} \right)_\pi$$

[C2-39]

The negative sign in equation [C2-37] was dropped as the errors are cumulative.

3. Corrected Hydrogen Absorption Rate on the Sphere

The absorption rate of hydrogen onto the sphere is corrected for the increased absorption area due to the film thickness prior to being substituted into equation [2.70].

$$G_s = \frac{G_A}{ACOR} \qquad [B2-35]$$

where:

$$ACOR = 1 + \frac{2.58\, \Delta^+}{R} \qquad [3.9]$$

and

$$\Delta^+ = \left\{ \frac{3\, L\, V}{2\pi\, R\, g} \right\}^{1/3} \qquad [3.10]$$

It can be shown from the above equations that the expected error in the corrected absorption rate is:

$$\frac{\Delta G_s}{G_s} = \frac{\Delta G_A}{G_A} + \frac{\left\{ \frac{2.58\, \Delta^+}{3R_s} \left\{ \frac{\Delta L}{L} + \frac{\Delta \nu}{\nu} \right\} \right\}}{ACOR} \qquad [C2-40]$$

4. Bulk Concentration of the Methylamine Flowing Over the Sphere

The bulk concentration of hydrogen in the methylamine flowing over is given by equation [3.8].

$$C_o = \frac{G_J}{L} \qquad [3.8]$$

The estimated error in the bulk phase concentration is therefore:

$$\frac{\Delta C_o}{C_o} = \frac{\Delta G_J}{G_J} + \frac{\Delta L}{L} \qquad [C2\text{-}41]$$

5. Interfacial Concentration of Hydrogen

The interfacial concentration of hydrogen is given by equation [4.7].

$$C_i = \frac{2.016\ \rho_1}{M_1} \left\{ \frac{1}{\frac{H_2}{P_2} - 1} \right\} \qquad [4.7]$$

The hydrogen partial pressure is calculated by subtracting the amine vapor pressure from the total absorber pressure.

$$P_2 = \pi - P_1 \qquad [4.8]$$

It can be seen from equations [4.7] and [4.8] that:

$$C_i = f(\rho_1, H_2, P_1, \pi, T_A) \qquad [C2\text{-}42]$$

$$\therefore \Delta C_i = \left(\frac{\partial C_i}{\partial \rho_1}\right) \Delta\rho_1 + \left(\frac{\partial C_i}{\partial H_2}\right) \Delta H_2 + \left(\frac{\partial C_i}{\partial P_1}\right) \Delta P_1 + \left(\frac{\partial C_i}{\partial \pi}\right) \Delta\pi + \left(\frac{\partial C_i}{\partial T_A}\right) \Delta T_A \qquad [C2\text{-}43]$$

Equation [4.7] can be simplified by noting that

$$\frac{H_2}{P_2} = \frac{H_2}{\pi - P_1} >> 1 \qquad [C2\text{-}44]$$

Therefore:

$$C_i = \frac{2.016\ \rho_1}{M_1} \frac{\pi - P_1}{H_2} \qquad [C2\text{-}45]$$

Equation [C2-43], upon substitution of the partial derivatives, is of the form

$$\Delta C_i = C_i \left\{ \frac{\Delta \rho_1}{\rho_1} + \frac{\Delta H_2}{H_2} + \frac{\Delta P_1}{(\pi - P_1)} + \frac{\Delta \pi}{(\pi - P_1)} \right\} + \left[\frac{\partial C_i}{\partial T_A} \right] \Delta T_A \qquad [C2\text{-}46]$$

where:

$$\frac{\partial C_i}{\partial T_A} = C_i \left[\frac{1}{\rho_1} \frac{\partial \rho_1}{\partial T_A} - \frac{1}{(\pi - P_1)} \frac{\partial P_1}{\partial T_A} + \frac{1}{H_2} \frac{\partial H_2}{\partial T_A} \right] \qquad [C2\text{-}47]$$

The density of methylamine is described by equation [3.3] of Part 1.

$$\rho_1 = 0.90580 - 4.00947 \times 10^{-4} T_A - 1.45769 \times 10^{-6} (T_A)^2$$

$$\frac{\partial \rho_1}{\partial T_A} = -4.01 \times 10^{-4} - 2.92 \times 10^{-6} T_A \qquad [C2\text{-}48]$$

The partial derivative of the methylamine vapor pressure with respect to temperature is given by equation [C2-36].

$$\therefore \frac{1}{P_1} \frac{\partial P_1}{\partial T_A} = \frac{5716.32}{T_A^2} + 0.02248 - \frac{15.30}{T_A} \qquad [C2\text{-}35]$$

The equation for Henry's Law coefficient is presented in Table 4, Part 1.

$$\ln H_2 = 4.1403 + \frac{1661.2}{T} - \frac{0.1160 \times 10^6}{T^2}$$

$$\therefore \frac{1}{H_2} \frac{\partial H_2}{\partial T} = \frac{-1661.2}{T_A^2} + \frac{2.320 \times 10^5}{T_A^3} \qquad [C2\text{-}49]$$

Substituting equations [C2-36], [C2-48] and [C2-49] into equation [C2-47] yields:

$$\frac{\partial C_i}{\partial T_A} = C_i \left\{ \frac{1}{\rho_1} (-4.01 \times 10^{-4} - 2.92 \times 10^{-6} T_A) \right.$$

$$\left. + \frac{P_1}{P_2} \left[\frac{5716.32}{T_A^2} + 0.02248 - \frac{15.30}{T_A} \right] + \left[-\frac{1661.2}{T_A^2} + \frac{2.320 \times 10^5}{T_A^3} \right] \right\} \quad [C2\text{-}50]$$

The expected error in the driving force is therefore:

$$\Delta(C_i - C_o) = \Delta C_i + \Delta C_o \quad [C2\text{-}38]$$

which is calculated from equations [C2-41], [C2-46] and [C2-50].

$$\Delta(C_i - C_o) = C_o \left[\frac{\Delta G_J}{G_J} + \frac{\Delta L}{L} \right] + C_i \left\{ \frac{\Delta \rho_i}{\rho_1} + \frac{\Delta H_2}{H_2} + \frac{\Delta P_1}{(\pi - P_1)} + \frac{\Delta \pi}{(\pi - P_1)} + \right.$$

$$\left[\frac{1}{\rho_1} (-4.01 \times 10^{-4} - 2.92 \times 10^{-6} T_A) + \frac{P_1}{P_2} \left[\frac{5716.32}{T_A^2} + 0.02248 - \frac{15.30}{T_A} \right] \right.$$

$$\left. \left. + \left[-\frac{1661.2}{T_A^2} + \frac{2.320 \times 10^5}{T_A^3} \right] \right] \Delta T_A \right\} \quad [C2\text{-}51]$$

B. Estimation of the Expected Error in the Diffusion Coefficient For the 7/29/70 Run.

The expected error in the diffusion coefficient which was evaluated from the 7/29/70 run (Appendix B2) is calculated in the following section. The calculation is based on the mean absorption conditions for the run. The conditions, as obtained from Appendix B2, are listed below. The estimated error is listed for the experimental measurements and calculated parameters.

α = 0.61003

$f(\alpha)$ = 0.9021

$e(-3.414\ \alpha)$ = 0.1246

$G_H = 0.1869 \times 10^{-5} \frac{gm.}{sec.}$

$G_A = 0.1801 \times 10^{-5} \frac{gm.}{sec.}$

$G_J = 0.0068 \times 10^{-5} \frac{gm.}{sec.}$

$C_i = 0.5078 \times 10^{-5} \frac{gm.}{sec.}$

$C_o = 0.170 \times 10^{-5} \frac{gm.}{sec.}$

$\Delta^+ = 0.0088$ cm.

$R = 1.270$ cm.

ACOR $= 1.0179$

$T_H = 20.3°C = 293.5°K$

$V_{SFM} = 10.0$ c.c.

$t = 595$ sec.

$T_A = -19.1°C = 254.1°K$

$\pi = 1.338$ atm.

$P_1 = 0.543$ atm.

$P_2 = 0.795$ atm.

$L = 0.400 \frac{c.c.}{sec.}$

$\rho_1 = 0.7099 \frac{gm.}{c.c.}$

$\nu_1 = 4.538 \times 10^{-3} \frac{cm.^2}{sec.}$

$\Delta h_{TL} = 0.010$ cm.

$H_2 = 7206$

$h_J = 0.225$ cm.

$h_{TL} = 2.000$ cm.

$d = 1'' = 1.270$ cm.

$\Delta T_H = \pm 0.1°C$

$\Delta V_{SFM} = \pm 0.10$ c.c.

$\Delta t = \pm 0.2$ sec.

$\Delta T_A = \pm 0.1°C$

$\Delta T'_A = \frac{0.001 \text{ m.v.}}{0.036 \text{ m.v.}} (1°C) = 0.03°C$

$\Delta\pi = \pm 0.10$ cm. Hg. $= 0.0013$ atm.

$\frac{\Delta P_1}{P_1} = 0.005 \qquad \Delta P_1 = 0.0027$ atm.

$\frac{\Delta L}{L} = 0.01$

$\frac{\Delta \rho_1}{\rho_1} = 0.05$

$\frac{\Delta \nu_1}{\nu_1} = 0.01$

$\frac{\Delta H_2}{H_2} = 0.01$

$\Delta h_J = 0.010$ cm.

1. Total Hydrogen Absorption Rate to the Absorber

$$\frac{\Delta G_H}{G_H} = \left\{ \frac{\Delta\pi}{\pi} + \frac{\Delta T_H}{T_H} + \frac{\Delta V_{SFM}}{V_{SFM}} + \frac{\Delta t}{t} \right\} \qquad [C2\text{-}21]$$

$$= \left\{ \frac{0.0013}{1.338} + \frac{0.1}{293.5} + \frac{0.1}{10} + \frac{0.2}{595} \right\}$$

$$= \{0.00097 + 0.00034 + 0.010 + 0.00033\}$$

$$= 0.01164$$

$$\therefore \Delta G_H = 0.1869 \times 10^{-5} \times 0.01164 = 0.2175 \times 10^{-7} \frac{gm.}{sec.}$$

The dominant term in the estimated error for the total hydrogen absorption rate is the volume measurement from the soap film measurement.

2. Interfacial Concentration

$$\Delta C_i = C_i \left\{ \frac{\Delta \rho_1}{\rho_1} + \frac{\Delta H_2}{H_2} + \frac{\Delta P_1}{P_2} + \frac{\Delta \pi}{P_2} \right\} + \left(\frac{\partial C_i}{\partial T_A} \right) \Delta T_A \qquad [C2\text{-}46]$$

$$\frac{\partial C_i}{\partial T_A} = C_i \left| \frac{1}{\rho_1} (-4.01 \times 10^{-4} - 2.92 \times 10^{-6} T_A) \right.$$

$$\left. + \frac{P_1}{P_2} \left(\frac{5716.32}{T_A^2} + 0.02248 - \frac{15.30}{T_A} \right) + \left(- \frac{1661.2}{T_A^2} + \frac{2.320 \times 10^5}{T_A^3} \right) \right| \qquad [C2\text{-}50]$$

$$\frac{\partial C_i}{\partial T_A} = C_i \, [-0.000016 + 0.0347 - 0.0116]$$

$$= C_i \, [.0231]$$

$$\therefore \Delta C_i = C_i \, [0.005 + 0.010 + 0.0034 + 0.0016 + (0.0231)(0.10)]$$

$$= C_i \, [0.0223]$$

$$\therefore \frac{\Delta C_i}{C_i} = 0.0223$$

$$\Delta C_i = 0.5078 \times 10^{-5} \, [0.0223]$$

$$= 0.1133 \times 10^{-6} \frac{gm.}{sec.}$$

3. Hydrogen Absorption Rate on the Jet

$$\Delta G_J = G_J \left[\frac{\Delta C_i}{C_i} + \frac{1}{2}\left\{\frac{\Delta h_J}{h_J} + \frac{\Delta L}{L} + \frac{\Delta D}{D}\right\}\right] \qquad [C2\text{-}24]$$

$$= G_J \left\{0.0223 + \frac{1}{2}\left[0.0444 + 0.01 + \frac{\Delta D}{D}\right]\right\}$$

$$= G_J \left[0.0495 + \frac{1}{2}\frac{\Delta D}{D}\right]$$

$$\Delta G_J = 0.3366 \times 10^{-8} + 0.0034 \times 10^{-5} \frac{\Delta D}{D}$$

$$\frac{\Delta G_J}{G_H} = 0.0019 + 0.0189 \frac{\Delta D}{D}$$

4. Hydrogen Absorption Rate due to a Change in the Take-off Level

$$\Delta G_{TL} = \frac{2.016}{R_G} \times \frac{\pi d^2}{4} \times \frac{P_2}{T_A}\left(\frac{\Delta h_{TL}}{t}\right) \qquad [C2\text{-}35]$$

$$= 0.0175 \times \frac{0.795}{254.1}\left(\frac{0.010}{595}\right)$$

$$= 0.9201 \times 10^{-9}$$

$$\frac{\Delta G_{TL}}{G_H} = 0.0005$$

5. Hydrogen Absorption Rate due to a Change in the Absorber Temperature

$$\Delta G_{Temp} = \frac{2.016}{R_G}\frac{V}{T_A^2}\left\{P_2 - P_1\left[\frac{5716.32}{T_A} + 0.02248\, T_A - 15.30\right]\right\}\left\{\frac{\Delta T'_A}{t}\right\}_{\pi} \qquad [C2\text{-}37]$$

$$= 0.1522 \times 10^{-3}\,[0.795 - 7.0096]\left[\frac{0.03}{595}\right]$$

$$\Delta G_{Temp} = 0.4769 \times 10^{-7} \frac{gm.}{sec.}$$

$$\frac{\Delta G_{Temp}}{G_H} = 0.0265$$

6. Hydrogen Absorption Rate to the Sphere

$$\Delta G_A = \Delta G_H + \Delta G_J + \Delta G_{TL} + \Delta G_{Temp} \qquad [C2\text{-}23]$$

$$= 0.2175 \times 10^{-7} + 0.0337 \times 10^{-7} + 0.0034 \times 10^{-5} \frac{\Delta D}{D}$$

$$+ 0.0092 \times 10^{-7} + 0.4769 \times 10^{-7}$$

$$\therefore \Delta G_A = 0.7373 \times 10^{-7} + 0.0034 \times 10^{-5} \frac{\Delta D}{D}$$

7. Corrected Hydrogen Absorption Rate on the Sphere

$$\frac{\Delta G_s}{G_s} = \frac{\Delta G_A}{G_A} + \frac{\frac{2.58\ \Delta^+}{3R}\left[\frac{\Delta L}{L} + \frac{\Delta \nu}{\nu}\right]}{ACOR} \qquad [C2\text{-}40]$$

$$\frac{\Delta G_s}{G_s} = \frac{0.7373 \times 10^{-7}}{0.1801 \times 10^{-5}} + \frac{0.0034 \times 10^{-5} \frac{\Delta D}{D}}{0.1801 \times 10^{-5}} + 0.0001$$

$$= 0.0409 + 0.0189 \frac{\Delta D}{D} + 0.0001$$

$$= 0.0410 + 0.0189 \frac{\Delta D}{D}$$

8. Corrected Hydrogen Driving Force

$$\Delta C_o = C_o \left[\frac{\Delta G_J}{G_J} + \frac{\Delta L}{L}\right] \qquad [C2\text{-}41]$$

$$= C_o \left[0.0495 + \frac{\Delta D}{2D} + 0.01\right]$$

$$\Delta C_o = 0.0170 \times 10^{-5} \left[0.0595 + \frac{\Delta D}{2D}\right]$$

$$= .1012 \times 10^{-7} + .8500 \times 10^{-7} \frac{\Delta D}{D}$$

$$\therefore \Delta(C_i - C_o) = \Delta C_i + \Delta C_o \qquad [C2\text{-}38]$$

$$\Delta(C_i - C_o) = 0.1133 \times 10^{-6} + 0.0101 \times 10^{-6} + 0.8500 \times 10^{-7} \frac{\Delta D}{D}$$

$$= 0.1234 \times 10^{-6} + 0.8500 \times 10^{-7} \frac{\Delta D}{D} \frac{gm.}{sec.}$$

$$\frac{\Delta(C_i - C_o)}{(C_i - C_o)} = \frac{0.1234 \times 10^{-6} + 0.8500 \times 10^{-7} \frac{\Delta D}{D}}{(0.5078 - 0.0170) \times 10^{-5}}$$

$$= 0.0251 + 0.0173 \frac{\Delta D}{D}$$

9. Estimated Error in the Diffusion Coefficient

$$\frac{\Delta D}{D} = \frac{f(\alpha)}{2.6824\ \alpha\ e(-3.414\ \alpha)} \left[\frac{\Delta G_s}{G_s} + \frac{\Delta L}{L} + \frac{\Delta(C_i - C_o)}{(C_i - C_o)}\right] + \frac{4}{3}\frac{\Delta L}{L} + \frac{2}{3}\frac{\Delta \nu}{\nu} \qquad [C2\text{-}14]$$

$$= \frac{0.9021}{2.6824\ (0.6103)(0.1246)} \left[0.0410 + 0.0189 \frac{\Delta D}{D} + 0.01 + 0.0251 + \right.$$

$$\left. 0.0173 \frac{\Delta D}{D}\right] + \frac{4}{3}(0.01 + \frac{2}{3}(0.01)$$

$$\frac{\Delta D}{D} = 4.4225 \left[0.0761 + 0.03620 \frac{\Delta D}{D}\right] + 0.02$$

$$\frac{\Delta D}{D} = 0.4244$$

It is apparent from the above analysis that the errors associated with the experimental measurements are greatly magnified in the value of the diffusion coefficient which is evaluated from those measurements. The largest source of error is the absorber temperature fluctuations which, due to the volatile nature of methylamine, cause a significant change in the hydrogen absorption rate.

It is of interest to estimate the error associated with a 3/4 inch sphere run. Consider the 8/24/70 run of Kalra[87] (Table A2-2)

for which it can be shown that:

$$L = 0.394 \frac{c.c.}{sec.}$$

$$D = 134 \times 10^{-6} \frac{cm.^2}{sec.}$$

$$\alpha = 0.345$$

$$f(\alpha) = 0.7583$$

$$\exp(-3.414\ \alpha) = 0.3076$$

If the expected error in the corrected hydrogen absorption rate, hydrogen driving force, methylamine flow rate and methylamine kinimatic viscosity are assumed to equal the values calculated for the 7/29/70 run (1 inch sphere), then:

$$\frac{\Delta D}{D} = \frac{0.7583}{2.6824\ (0.345)(0.3076)} \left| 0.0761 + 0.03620 \frac{\Delta D}{D} \right| + 0.02$$

$$= 2.6639\ \ 0.0761 + 0.03620 \frac{\Delta D}{D} + 0.02$$

$$\frac{\Delta D}{D} = 0.2464$$

This expected error in the diffusion coefficient is considerably reduced, however, it is still substantial.

In order to increase the accuracy of the evaluated diffusion coefficient, it is necessary to:

(1) Use a soap film meter which has finer graduations. This requires a small bore tube for which it is difficult to maintain a stable soap film at the flow rates considered in this study.

(2) Measure the methylamine flow rate for each run by using a direct weighing technique. (The calibrated accuracy of rotameter is ±1%.)

(3) Reduce the volume of the absorber to as small a value as possible. This will reduce the temperature effect on the hydrogen absorption rate to the absorber.

The above modifications will increase the accuracy of the diffusion coefficient to a certain extent. However, as long as hydrodynamic considerations limit the methylamine flow rate to such a degree that the liquid phase is nearly saturated, then good accuracy (±5%) is not possible.

APPENDIX D2

CALIBRATION SECTION

The calibration curves for the "Brooks" R-2-15-D and R-2-15-C rotameter tubes are shown in Tables D2-1 and D2-2. Both calibrations were carried out at room temperature by measuring the time required to collect a measured volume of acetone. The data reported in Tables D2-1 and D2-2 were fit by a Forsythe polynomial fitting routine to yield an equation of the form:

$$Q_1 = C_o + C_1(RR) + C2(RR)^2 + C3(RR)^3 \qquad [D2\text{-}1]$$

Q_1 = Acetone flow rate $\frac{c.c.}{sec.}$

RR = Rotameter reading

The determined coefficients of equation (D2-1] are:

TUBE	C_o	C_1	C_2	C_3
R-2-15-D	-0.744598×10^{-1}	0.452570×10^{-1}	-0.642143×10^{-4}	
R-2-15-C	-0.689329×10^{-1}	0.245837×10^{-1}	-0.391080×10^{-4}	-0.277973×10^{-6}

The viscosity correction tables for calculating the methylamine flow rate ($L \frac{c.c.}{sec.}$) from the acetone calibration are presented in Table D2-3 for the R-2-15-D tube and Table D2-4 for the R-2-15-C tube.

A single thermocouple calibration correction was applied to all four thermocouples which were located in the single sphere absorption apparatus. Each thermocouple was calibrated against a platinum resistance thermometer. The deviation between the standard E.M.F. (m.v.) corresponding to the temperature registered by the resistance thermometer and the E.M.F. output from the thermocouple

being calibrated were measured. All deviations are plotted versus the standard E.M.F. in Figure D2-1. Deviation data for a fifth thermocouple (number 11) are included in the plot as this thermocouple was made from the same batch of wire.

The straight line in Figure D2-1 is described by the equation

$$\varepsilon_s = \frac{\{\varepsilon_A + 0.0064\}}{0.9962} \qquad [D2\text{-}2]$$

where: ε_s = standard or tabulated E.M.F. (m.v.).

ε_A = E.M.F. output from the thermocouple (m.v.)

Standard E.M.F. versus temperature data were read into the computer in tabular form. A measured thermocouple output (ε_A) was converted to a standard E.M.F. by equation (D2-2] and this value was used to obtain the calibrated temperature.

TABLE D2-1

CALIBRATION OF BROOKS ROTAMETER TUBE R-2-15-D

Calibration Fluid: Acetone

Calibration Temperature: 20.0°C

Density of Acetone @ 20°C = 0.7894 $\frac{gm.}{c.c.}$

Float Material: 316 Stainless Steel

Rotameter Reading	Calibrated Flow Rate c.c./sec.
3.00	0.066
4.00	0.108
5.00	0.150
6.00	0.194
7.00	0.238
8.00	0.284
8.05	0.286
9.00	0.329
10.00	0.373
11.00	0.415
11.95	0.457
12.00	0.459
12.95	0.500
13.00	0.501
14.00	0.547
14.50	0.569
15.00	0.590

TABLE D2-2

CALIBRATION OF BROOKS ROTAMETER TUBE R-2-15-C

Calibration Fluid: Acetone

Calibration Temperature: 20.7°C

Density of Acetone @ 20°C: 0.7892 $\frac{gm.}{c.c.}$

Float Material: Glass

Rotameter Reading % Linear	Calibrated Flow Rate $\frac{c.c.}{sec.}$
10	0.173
20	0.411
30	0.640
40	0.869
50	1.098
70	1.556
96	2.177

TABLE D2-3

VISCOSITY CORRECTION FACTOR TABLE (R-2-15-D)

TEMP	FLOW RATE												
	0.0567	0.1139	0.1355	0.2253	0.3751	0.5635	0.7764	0.9710	1.1737	1.4059	1.6010	1.8710	2.4141
-10.00	1.2002	1.1647	1.1463	1.1213	1.1163	1.1017	1.0950	1.0904	1.0913	1.0932	1.0926	1.0884	1.0878
-11.00	1.1848	1.1545	1.1409	1.1161	1.1052	1.0993	1.0914	1.0967	1.0859	1.0905	1.0876	1.0852	1.0843
-12.00	1.1725	1.1456	1.1325	1.1109	1.1004	1.0955	1.0874	1.0925	1.0853	1.0873	1.0876	1.0821	1.0815
-13.00	1.1603	1.1363	1.1241	1.1057	1.0962	1.0913	1.0833	1.0882	1.0825	1.0840	1.0856	1.0790	1.0732
-14.00	1.1482	1.1330	1.1157	1.1005	1.0921	1.0879	1.0792	1.0840	1.0799	1.0809	1.0836	1.0759	1.0749
-15.00	1.1362	1.1193	1.1074	1.0953	1.0879	1.0841	1.0751	1.0797	1.0773	1.0775	1.0816	1.0727	1.0714
-16.00	1.1241	1.1105	1.0990	1.0901	1.0837	1.0803	1.0711	1.0754	1.0746	1.0743	1.0796	1.0697	1.0634
-17.00	1.1109	1.1002	1.0907	1.0838	1.0787	1.0760	1.0682	1.0718	1.0714	1.0710	1.0758	1.0672	1.0661
-18.00	1.0973	1.0904	1.0823	1.0773	1.0735	1.0715	1.0657	1.0684	1.0681	1.0678	1.0713	1.0650	1.0642
-19.00	1.0837	1.0786	1.0740	1.0708	1.0683	1.0673	1.0633	1.0650	1.0648	1.0645	1.0669	1.0628	1.0622
-20.00	1.0702	1.0670	1.0657	1.0642	1.0631	1.0625	1.0609	1.0616	1.0615	1.0614	1.0624	1.0606	1.0602
-21.00	1.0567	1.0571	1.0575	1.0577	1.0579	1.0583	1.0583	1.0582	1.0582	1.0582	1.0580	1.0584	1.0584
-22.00	1.0423	1.0469	1.0495	1.0512	1.0521	1.0527	1.0543	1.0551	1.0549	1.0554	1.0549	1.0559	1.0565
-23.00	1.0273	1.0368	1.0417	1.0448	1.0459	1.0469	1.0493	1.0521	1.0516	1.0528	1.0525	1.0533	1.0545
-24.00	1.0124	1.0268	1.0339	1.0383	1.0397	1.0410	1.0443	1.0491	1.0484	1.0502	1.0501	1.0507	1.0527
-25.00	0.9975	1.0170	1.0261	1.0318	1.0335	1.0352	1.0393	1.0462	1.0451	1.0476	1.0477	1.0481	1.0508
-26.00	0.9826	1.0071	1.0183	1.0255	1.0274	1.0294	1.0343	1.0432	1.0419	1.0450	1.0453	1.0455	1.0489
-27.00	0.9678	0.9969	1.0107	1.0191	1.0217	1.0243	1.0296	1.0403	1.0386	1.0419	1.0425	1.0427	1.0464
-28.00	0.9530	0.9864	1.0030	1.0127	1.0157	1.0193	1.0252	1.0373	1.0354	1.0392	1.0391	1.0395	1.0433
-29.00	0.9383	0.9758	0.9953	1.0064	1.0113	1.0156	1.0209	1.0296	1.0322	1.0345	1.0358	1.0347	1.0401
-30.00	0.9236	0.9654	0.9877	1.0000	1.0069	1.0119	1.0164	1.0233	1.0290	1.0309	1.0325	1.0300	1.0370

TABLE D2-4

VISCOSITY CORRECTION FACTOR TABLE (R-2-15-C)

TEMP	FLOW RATE												
	0.0209	0.0250	0.0401	0.0858	0.1174	0.1704	0.2743	0.3541	0.4391	0.5326	0.6154	0.7219	0.8583
-10.00	1.2855	1.2654	1.2504	1.1952	1.1316	1.1585	1.1517	1.1450	1.1360	1.1354	1.1261	1.1223	1.1256
-11.00	1.2686	1.2509	1.2371	1.1845	1.1737	1.1619	1.1460	1.1388	1.1325	1.1319	1.1226	1.1256	1.1220
-12.00	1.2518	1.2362	1.2234	1.1778	1.1652	1.1551	1.1403	1.1246	1.1290	1.1273	1.1190	1.1219	1.1183
-13.00	1.2351	1.2212	1.2101	1.1691	1.1580	1.1485	1.1346	1.1294	1.1236	1.1228	1.1155	1.1182	1.1147
-14.00	1.2184	1.2073	1.1967	1.1604	1.1502	1.1418	1.1290	1.1243	1.1192	1.1183	1.1120	1.1145	1.1110
-15.00	1.2017	1.1930	1.1833	1.1518	1.1424	1.1351	1.1233	1.1192	1.1148	1.1138	1.1085	1.1108	1.1074
-16.00	1.1851	1.1786	1.1700	1.1432	1.1346	1.1285	1.1177	1.1140	1.1104	1.1093	1.1049	1.1072	1.1038
-17.00	1.1685	1.1643	1.1567	1.1347	1.1268	1.1219	1.1121	1.1088	1.1060	1.1048	1.1015	1.1036	1.1002
-18.00	1.1520	1.1500	1.1434	1.1261	1.1191	1.1153	1.1065	1.1038	1.1017	1.1004	1.0980	1.0999	1.0967
-19.00	1.1356	1.1358	1.1302	1.1176	1.1113	1.1082	1.1009	1.0986	1.0971	1.0959	1.0943	1.0960	1.0930
-20.00	1.1194	1.1191	1.1152	1.1091	1.1039	1.0999	1.0946	1.0931	1.0923	1.0912	1.0900	1.0912	1.0891
-21.00	1.1032	1.1030	1.1003	1.0958	1.0928	1.0916	1.0885	1.0876	1.0871	1.0865	1.0858	1.0865	1.0852
-22.00	1.0871	1.0871	1.0856	1.0846	1.0833	1.0834	1.0824	1.0821	1.0819	1.0818	1.0815	1.0818	1.0814
-23.00	1.0711	1.0711	1.0709	1.0736	1.0743	1.0752	1.0764	1.0767	1.0769	1.0771	1.0773	1.0771	1.0775
-24.00	1.0551	1.0553	1.0577	1.0632	1.0659	1.0671	1.0703	1.0712	1.0719	1.0724	1.0731	1.0724	1.0737
-25.00	1.0391	1.0395	1.0454	1.0527	1.0562	1.0589	1.0643	1.0659	1.0669	1.0673	1.0689	1.0673	1.0699
-26.00	1.0233	1.0237	1.0329	1.0421	1.0481	1.0503	1.0583	1.0604	1.0620	1.0632	1.0648	1.0621	1.0661
-27.00	1.0075	1.0081	1.0153	1.0316	1.0382	1.0429	1.0523	1.0551	1.0573	1.0594	1.0607	1.0595	1.0623
-28.00	0.9917	0.9925	1.0000	1.0211	1.0304	1.0347	1.0463	1.0497	1.0521	1.0542	1.0565	1.0539	1.0585
-29.00	0.9760	0.9769	0.9849	1.0107	1.0215	1.0267	1.0404	1.0444	1.0472	1.0495	1.0524	1.0493	1.0548
-30.00	0.9605	0.9615	0.9733	1.0003	1.0127	1.0183	1.0344	1.0392	1.0423	1.0448	1.0483	1.0448	1.0510

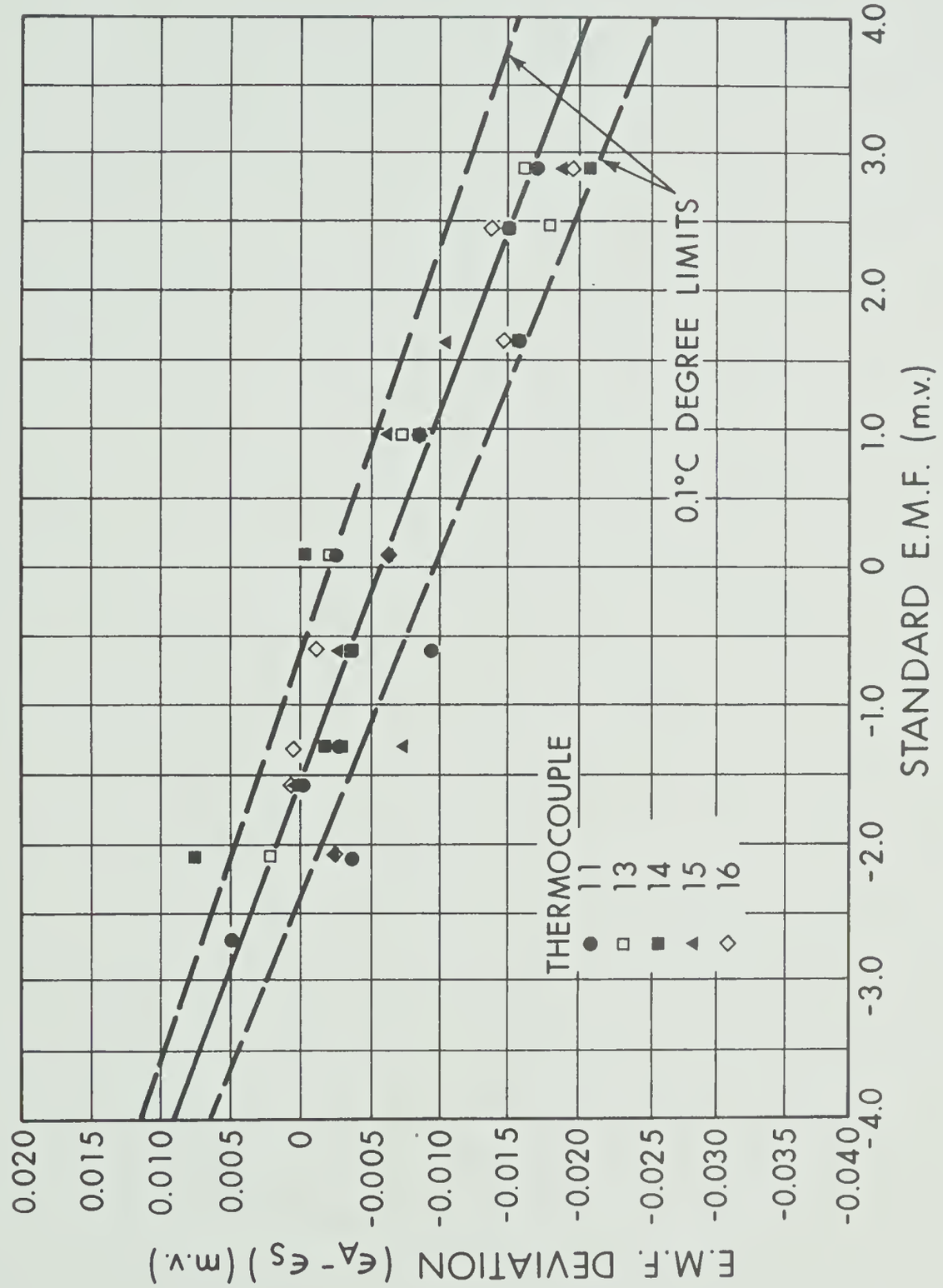


FIG. D2-1 CALIBRATION CURVE FOR THE SYSTEM THERMOCOUPLES

B29985